ACTA UNIVERSITATIS SZEGEDIENSIS

ACTA MINERALOGICA—PETROGRAPHICA

TOMUS XX. FASC. 2.

DONNEL FOSTER HEWETT MEMORIAL VOLUME

SZEGED, HUNGARIA
1972

Redigit
GYULA GRASSELLY

Edit
Institutum Mineralogicum, Geochimicum et Petrographicum
Universitatis Szegediensis de Attila József nominatae
Szeged, Táncsics Mihály u. 2.

Nota
Acta Miner. Petr., Szeged

Szerkeszti
GRASSELLY GYULA

Kiadja
a József Attila Tudományegyetem Ásványtani, Geokémiai és Kőzettani Intézete
Szeged, Táncsics Mihály u. 2.

Kiadványunk címének rövidítése
Acta Miner. Petr., Szeged

Felelős kiadó: Dr. Grasselly Gyula
72-3438 — Szegedi Nyomda

DONNEL FOSTER HEWETT
1881—1971

Acta Mineralogica-Petrographica, Szeged XX/2, 187-189, 1972

MEMORIAL OF DONNEL FOSTER HEWETT (JUNE 24, 1881-FEBRUARY 5, 1971)

MICHAEL FLEISCHER

D. F. HEWETT, widely recognized as one of the world's leaders in research on manganese deposits, died at Palo Alto, California, at the age of 89. Although seriously ill for some time, he had continued his work until a few weeks before his death. His publications on manganese (see appended bibliography) span a period of 59 years, reflecting a lifetime of productive interest.

FOSTER, as he was known to his friends, was born at Irwin, Pennsylvania. His father was a successful mining engineer and it was natural that he studied chemistry, metallurgy, and mining at Lehigh University, graduating with high honors in 1902 with the degree of Bachelor of Metallurgy. HEWETT remained at Lehigh for another year as assistant in the geology department, where he was strongly influenced by Professor JOSEPH BARRELL. From 1903 to 1909, he was mining engineer for the Pittsburgh Testing Laboratories. During these years he examined and reported on many mines; he was the first to recognize the value of the large vanadium deposit at Mina Ragra, Peru; the new calcium vanadates hewettite and metahewettite (from this locality) were named in his honor.

In 1909 and 1910, HEWETT was enrolled as a graduate student at Yale University; his thesis and the award of the Ph. D. degree were delayed until 1924.

In 1911 he joined the U. S. Geological Survey, where he remained until his death. His extensive contributions in many areas of geologic research included outstanding work on the structural geology of the Great Basin, the association of dolomitization with ore deposits, and the recognition of the large bastnaesite deposits at Mountain Pass, California, but his main interest from World War I on was in manganese deposits. He visited nearly every deposit in the United States, as well as some in Cuba, and had read nearly everything ever published on the world's deposits.

As Chief of the Section of Metalliferous Geology of the U. S. Geological Survey from 1935 to 1944, HEWETT planned and directed an extensive program of studies of strategic minerals, including manganese. He was responsible not only for field studies of deposits in the United States, Mexico, and Cuba, but vigorously promoted laboratory studies of their mineralogy and geochemistry.

In 1951 he reached the statutory retirement age of 70, but fortunately was continued indefinitely as a full-time employee by special presidential order; his bibliography for the years that followed bear witness to his undiminished vigor, enthusiasm, and capacity to generate new ideas. Perhaps even more important than his own publications was the impact he had on his associates, and especially on the

young geologists under his direction, in whom he took great interest and to whom he was always a source of inspiration and ideas.

HEWETT served as president of the Society of Economic Geologists in 1936 and as vice-president of the Geological Society of America in 1935 and 1945. He received the Penrose Medal of the Society of Economic Geologists in 1956 and the Penrose Medal of the Geological Society of America in 1964, and was awarded the honorary D. Sc. by Lehigh University in 1942. He was elected to the National Academy of Sciences in 1937.

FOSTER was married in January, 1909 to MARY AMELIA HAMILTON; their home was a delightful haven to their friends for sixty-two years. MRS. HEWETT died in August, 1971.

The appended bibliography lists Hewett's publications on manganese; in all he published about 100 papers.

---

1 The production of manganese and manganiferous ores in 1912, U. S. Geol. Survey, Mineral Resources of the United States, pt. *1*, 203—221 (1913).

2 The production of manganese and manganiferous ores in 1914, U. S. Geol. Survey, Mineral Resources of the United States, pt. *1*, 165—181 (1915).

3 Manganese and manganiferous ores in 1915. U. S. Geol. Survey, Mineral Resources of the United States, pt. *1*, 29—43 (1916).

4 Some manganese mines in Virginia and Maryland. U. S. Geol. Survey Bull. *640-C*, 37—71 (1916).

5 The significance of manganese in American steel metallurgy. Am. Inst. Mining Engineers Bull. *855—856* (1917).

6 Manganese and manganiferous ores in 1916, U. S. Geol. Survey, Mineral Resources of the United States, pt. *1*, 20 pp. (1918).

7 (and G. W. STOSE, F. J. KATZ, and H. D. MISER), Possibilities for manganese ore on certain undeveloped tracts in the Shenandoah Valley, Virginia. U. S. Geol. Survey Bull. *660*, 271—296 (1918).

8 (with E. C. HARDER), Recent studies of domestic manganese deposits, Am. Inst. Mining Engineers, 895—901 (1919).

9 Manganese and manganiferous ores in 1917. U. S. Geol. Survey, Mineral Resources of the United States, pt. *1*, 665—696 (1919).

10 Manganese and manganiferous ores in 1918. U. S. Geol. Survey, Mineral Resources of the United States, pt. *1*, 607—656 (1919).

11 (and E. V. SHANNON), Orientite, a new hydrous silicate of manganese, and calcium from Cuba. Am. Jour. Sci. *1*, 491—506 (1921).

12 Manganese deposits near Bromide, Oklahoma. U. S. Geol. Survey Bull. *725-E*, 311—329 (1921).

13 A manganese deposit of Pleistocene age in Bannock County, Idaho. U. S. Geol. Survey Bull. *795-H*, 211—218 (1928).

14 (and O. N. ROVE), Occurrences and relations of alabandite. Econ. Geol. *25*, 36—56 (1930).

15 Genesis of iron-manganese concretions in central South Dakota: Wash. Acad. Sci., Jour. *20*, 243 (1930).

16 (with B. N. WEBBER), Bedded deposits of manganese oxides near Las Vegas, Nevada. Nevada Univ. Bull. *25* (6) 17 pp. 1931.

17 Manganese in sediments, *in* TWENHOFEL, W. H., Treatise on Sedimentation, 562—581 (1932).

18 Sedimentary manganese deposits: Ore deposits of the Western States (LINDGREN Volume), Am. Inst. Mining Met. Engineers, 488—491 (1933).

19 (and J. T. PARDEE), Manganese in western hydrothermal ore deposits: Ore Deposits of the Western States (LINDGREN Volume) Am. Inst. Mining Met. Engineers, 671—682 (1933).

20 (and W. T. SCHALLER), Braunite from Mason County, Texas: Am. Mineralogist *22*, 785—789 (1937).

21 Helvite from the Butte district, Montana. Am. Mineralogist *22*, 803—804 (1937).

22 (with H. D. MISER), The unweathered manganese deposits of the Batesville district, Arkansas. Econ. Geol. *32*, 1069 (1938) (abs.).
23 (with H. D. MISER), Manganese carbonate in the Batesville district, Arkansas. U. S. Geol. Survey Bull. *921-A*, 1—97 (1941).
24 (and M. D. CRITTENDEN, LOUIS PAVLIDES, and G. L. DEHUFF, JR.), Manganese deposits of the United States, Symposium sobre yacimientos de manganeso, Internatl. Geol. Congress, Mexico City, 1956, t. *3*, 169—230.
25 (and FLEISCHER, MICHAEL), Deposits of the manganese oxides. Econ. Geol. *55*, 1—55 (1960).
26 (and CHESTERMAN, C. W. and TROXEL, B. W.), Tephroite in California manganese deposits. Econ. Geol. *56*, 39—58 (1961).
27 Manganese is a clue to deep base and precious metals. Mining World *25*, 26—28 (1963).
28 (and FLEISCHER, MICHAEL; Conklin, Nancy) Deposits of the manganese oxides: Supplement. Econ. Geol. *58*, 1—51 (1963).
29 Veins of hypogene manganese oxide minerals in the southwestern United States. Econ. Geol. *59*, 1429—1472 (1964).
30 Stratified deposits of the oxides and carbonates of manganese. Econ. Geol. *61*, 431—461 (1966).
31 (and RADTKE, A. S.), Silver-bearing black calcite in Western mining districts. Econ. Geol. *62*, 1—21 (1967).
32 (with RADTKE, A. S. and TAYLOR, C. M.), Aurorite, argentian todorokite, and hydrous silver-bearing lead manganese oxide. Econ. Geol. *62*, 186—206 (1967).
33 Silver in veins of hypogene manganese oxides. U. S. Geol. Survey Circ. *553*, 1—9 (1968).
34 (and OLIVARES, R. S.), High-potassium cryptomelane from Tarapaca Province, Chile. Am. Mineralogist *53*, 1551—1557 (1968).
35 (and CORNWALL, H. R. and ERD, R. C.), Hypogene veins of gibbsite, pyrolusite, and lithiophorite in Nye County, Nevada. Econ. Geol. *63*, 360—371 (1968).
36 Coronadite- modes of occurrence and origin. Econ. Geol. *66*, 164—177 (1971).
37 Manganite, hausmannite, braunite: features and mode of origin. Econ. Geol. *67*, 83—102 (1972).
Manuscript received, December 20, 1971.

Dr. Michael Fleischer
U. S. Geological Survey
Washington, D. C. 20242
U. S. A.

Acta Mineralogica-Petrographica, Szeged, XX/2, 191—207, 1972.

THE CARBONIFEROUS AND PERMIAN OF HUNGARY

by

K. BALOGH and A. BARABÁS

I. STRATIGRAPHY

Lower Carboniferous

1. Safely-dated Lower Carboniferous in Hungary is known only in a narrow belt between the Velence granite mass and Lake Balaton, in the footwall of the Devonian crystalline limestone blocks of the Szabadbattyán—Polgárdi zone [A. FÖLDVÁRI 1952*a*, *b*; J. KISS 1951; G. KOLOSVÁRY 1951]. The base of this Lower Carboniferous has not been uncovered as of yet. The relevant statements of A. FÖLDVÁRI, however, have been confirmed by the careful analyses of recent drilling materials [Cs. DETRE 1970, 1971; S. MIHÁLY 1971; M. MONOSTORI 1971]. This has to be emphasized because in recent years several workers, relying on erroneous determinations, have attempted to assign both the crystalline limestones and their tectonic footwall to the Upper Carboniferous [E. NAGY 1971; GY. MAJOROS 1971; M. SIDÓ 1971]. A starting point for the development of these ideas has been the isolated position of the Transdanubian occurrence, as the nearest, paleontologically dated Lower Carboniferous within the Carpathian arch can be found as far away as the Bihor Mountains and the Southern Carpathians [K. BALOGH 1964, pp. 602—603].

The Lower Carboniferous at Szabadbattyán consists of dark shales alternating with sandstones and limestones. The limestones show a purely marine facies, abunding in blue and green algae, crinoids and brachiopods. On the basis of their positive *(Table 1)* and negative features (e. g. the total absence of Westphalian *fusulinids* and Middle Visean *koninckopores)* they can be assigned convincingly to the Upper Visean [M. MONOSTORI 1971].

The normal stratigraphic hanging wall of these Upper Visean strata is not known either. For, the Upper Visean strata are in a tectonic contact with the partly ankeritized, crystalline limestones overlying them. Consequently, these should be annexed to the pre-Carboniferous phyllite sequence of the Balaton Region. In reality, in Borehole Sz-9 quartz-phyllites of 18 m thickness overlie the 167 m-thick crystalline limestones including, themselves, an interbedded breccia layer of quartz-phyllite.

2. On the basis of geological considerations, the author ascribed earlier [K. BALOGH 1964, pp. 561—565] a Lower Carboniferous age to the tripartite sequence of the Uppony block as well. As shown by J. ORAVECZ (1965), the microfossils of the siliceous schists of the uppermost member, however are reminiscent of the Silurian schists of the Balaton Highland. The presence of *acritarchs* has not been confirmed by F. GÓCZÁN's informative investigations [1971]. M. HAJÓS' efforts [1971] to detect *conodonts* were similarly unsuccesful. Accordingly, though the Carboniferous age of the Uppony sequence has turned out to be uncertain, yet it has been impossible to warrant convincingly its assignment to the Silurian.

TABLE 1

The biostratigraphically interpretable forms of the Upper Viséan at Szabadbattyán

Species	Tournaian	Viséan	Namurian	Middle Carboniferous
FORAMINIFERA*				
Parathurammina cf. *stellata* LIPOVA	———	———	——	
P. cf. *sulcimanovi* LIPOVA	———	———	——	
Tuberitina cf. *reitlingerae* (M.-MACLAY)		———	——	
Pachysphaera aff. *dervillei* CONIL et LYS		———		
Diplosphaerina aff. *inaequalis* (DERVILLE)		———		
Palaeotextularia cf. *consobrina* LIPOVA				
Tetrataxis aff. *pressulus* MALAKHOVA	———	———	———	
T. cf. *paraminimus* VISSARIONOVA	———	———	———	
Howchinia aff. *exilis* (VISSARIONOVA)	———	———	——	
H. aff. *declivis* (LEBED.)	———	———	——	
Archaediscus cf. *krestovniki* RAUSER		———	——	
A. cf. *krestovniki redita* CONIL et LYS				
A. cf. *karreri* BRADY		———	—	
A. cf. *moelleri* RAUSER		——	—	
A. cf. *convexus* GROZD. et LEBEDEVA		———	—	
A. cf. *kakjubensis* RAUSER		———	—	
Endothyra cf. *prisca* RAUSER et REITL.		———		
E. cf. *bradyi* MIKHAJLOV		———		
E. cf. *omphalota samarica* RAUSER		———		
E. cf. *amplis* SHLYKOVA		———		
E. cf. *similis* RAUSER et REITLINGER		———		
E. aff. *similis elegia* MALAKHOVA		———		
Janischewkina aff. *typica* MIKHAJLOV		———		
Bradyina cf. *rotula* (EICHWALD)		———	—	
B. ex gr. *cribrostomata* RAUSER et REITL.		———	—	
B. cf. *modica* LEBEDEVA				
Eostaffella cf. *vasta* ROZOVSKAJA		———		
E. cf. *ikensis* VISSARIONOVA		———	—	
E. cf. *mosquensis* VISSARIONOVA		———	—	
E. cf. *parastruvii* RAUSER		———	—	
Mediocris cf. *mediocris* (VISSARIONOVA)		———		
M. cf. *breviscula* (GAMELINA)		———		
Pseudoendothyra aff. *struvii supressa* (SHLYKOVA)		———		
TABULATA**				
Syringopora lata PHILLIPS	———	———	———	
Chaetetes sp.	———	———	———	———
RUGOSA**				
Hapsiphyllum battyánense KOLOSVÁRY	- - - - -	- - - - -	- - - - -	
Amplexus sp.	———	———	———	
Dibunophyllum turbinatum (M'COY)		——	——	
Palaeosmilia murchisoni M. EDWARDS et HAÎME		———	——	
HETEROCORALLA**				
Heterophyllia mirabilis (DUNCAN)		——		
BRACHIOPODA***				
Gigantoproductus ? *transdanubicus* (FÖLDVÁRI)		- - - - -	- - - - -	
Productus sp.	- - - - -	- - - - -	- - - - -	- - - - -
aff. *Unispirifer* sp.				
aff. *Dictyoclostus* sp.				

* Determined by MONOSTORI, M. [1971].
** Determined by MIHÁLY, S. [1971].
*** Determined by DETRE, Cs. [1970, 1971].

Middle and Upper Carboniferous

The higher members of the Carboniferous in Hungary are represented by continental and marine facies.

a) Continental facies

At present the continental facies is known to occur in three places: *1.* the Tokaj Mountains, *2.* between Lake Balaton and the Velence Mountains (at Füle village) and *3.* the northern foreland of the Villány Mountains.

i. The Tokaj's Upper Carboniferous is exposed at Vilyvitány and it has been cut through in 226 m thickness in Borehole Felsőregmec-1. It joins the 500- to 600-m-thick Permo-Carboniferous sequence of the Czechoslovak Zemplin Mountains comprising meta-anthracite seams and Ottweilian floral elements and, in the upper part, some ash-flow-tuff-like quartz-porphyry intercalations as well. According to the data of drilling, this coarse-detrital Carboniferous sequence overlies crystalline schists or their Lower Paleozoic mantle, respectively. The meta-anthracitic lenses and vegetal remnants (fossil plant remnants) of the intersected sandstones and of the upper part of the schists represent certainly the Stephanian Stage [G. PANTÓ 1965, 1966, pp. 25—28].

ii. As discovered recently, the so-called "conglomerate-and-phyllite sequence of Füle" belongs to the Westfalian Stage [Á. B.-STUHL 1971; E. NAGY 1971; GY. MAJOROS 1971] rather than to the Upper Permian or the Lower Carboniferous [GY. WEIN 1969, p. 410]. Unfortunately, the rocks underlying this sequence of some 600 m thickness, uncovered by Borehole Polgárdi-2, has not been explored as of yet. Consequently, the relation of the sequence to the Visean of Szabadbattyán has remained unsettled.

The sequence consists of 15 microcycles of red breccias, conglomerates and sandstones which, however, turn grey in depth. Claystones and phyllites, if any, occur very seldom even in the upper strata. At 250 m depth Á. B.-STUHL [1971] found a sporomorph assemblage of Westfalian age *(Table 2)*. Most of the pebbles of the sequence are consituted by quartzite, quartz- and sericite-phyllites [G. TELEKI 1941, p. 314]. Accordingly, they indicate a continental formation accumulated on the denuded surface (paleorelief) of overwhelmingly Upper Paleozoic roks as a result of Sudetic overthrusts.

iii. The exploration of the continental Upper Carboniferous of the Villány and Mecsek Mountains is also a new discovery. Phytofossiliferous Upper Carboniferous sandstone pebbles were first shown to occur in the Miocene basal conglomerates of the northern margin of the Mecsek Mountains [G. ANDREÁNSZKY in: I. SOÓS—Á. JÁMBOR 1960] *(Table 3)*. The mother rock of the pebbles was identified first in Borehole Téseny-2 [I. BARANYI—Á. JÁMBOR 1962], then it was explosed by five more boreholes in a SE dipping position [Á. JÁMBOR 1969]. The sequence was found to be in contact with crystalline schists along a tectonic line in the north and to consist of light grey sandstones partly gravelly and of black sericitic schists partly sandy. Its facies is identical with that of the South Carpathian and Croatian Upper Carboniferous (Baia Noua, Secul, Lupac, resp. Slemenski Jarak, Ruc, Cipluh). Thereafter two additional boreholes were sunk at the foot of the Villány Mountains [E. NAGY 1971, p. 654]. According to L. R.-BARANYAI [in: R. HETÉNYI—M. FÖLDI—L. R.-BARANYAI 1971], these represent two different parts of the Middle and Upper Carboniferous without the hiatus between the two parts of profile being precisely definable. The footwall of the sequence has not been reached here either, yet the material of Borehole Bogádmindszent-1 with its 1105 m thickness represents the deeper, Borehole Siklósbodony-1 (round 630 m) the higher parts of the profile.

The Middle Garboniferous Sporomorpha in Hungary

Forms	Continental facies			Marine facies
	Polg. —2* 230 m	Bmsz. —1** 509—514 m	Sbod. —1** 779—798 m	Nagyvisnyó Railway 1**
Calamospora liquida f. major KOSANKE	+			
C. liquida f. *minor* KOSANKE	+			
C. breviradiata KOSANKE	+			
C. pallida (LOOSE) S. W. & B.			+	
Punctatisporites sabulosus IBRAHIM	+			
P. punctatus IBRAHIM	+			
P. obscurus KOSANKE	+			
Granulatisporites piriformis LOOSE	+			
G. microgranifer IBRAHIM	+			+
G. parvus IBRAHIM	+			
G. sp.				+
Laevigatisporites giganteus DYB. & JACH.	+			
Verrucosisporites sp.				+
Crassispora (Planisporites) kosankei (R. POT. & KREMP) BHARDVAJ				+
C. (P.) ovalis BHARDVAJ				+
Raistrickia aculeata KOSANKE				+
R. superba (IBRAHIM) S. W. & B.				+
R. sp.				+
Reticulatisporites sp.				+
Apiculatisporites raistricki DYB. & JACH.	+			
Anapiculatisporites spinosus (KOSANKE)			+	
Tuberculatisporites regularis DYB. & JACH.	+			
T. gigantomodatus DYB. & JACH.	+			
Conbaculatisporites sp.			+	
Canaliculatisporites spongiatus DYB. & JACH.	+	?		
Cristatisporites n. sp.		+	+	
Leiotriletes sphaerotriangulus R. POT. & KREMP	+			
L. adnatus KOSANKE	+			
Converrucosisporites sp.			+	
Converrucitriletes armatus DYB. & JACH.	+			
C. verrucosus DYB. & JACH.	+			
Triquitrites tribullatus (IBRAHIM) R. POT. & KREMP				+
T. trigallerus (NEVES) nov. comb.				+
T. tricuspis R. POT. & KREMP	+			
Tripartites cf. *confragosus* JACH. var. *cumareus* GÓCZÁN				+
cf. Neoraistrickia drybrookensis SULLIVAN				+
Savitrisporites asperatus SULLIVAN				+
S. concavus MARSHALL & SMITH				+

Forms	Continental facies			Marine
	Polg. —2* 230 m	Bmsz. —1** 509—514 m	Sbod. —1** 779—798 m	Nagyvisnyó Railway 1**
S. nux (BUTTERWORTH & WILLIAMS) SULLIVAN				+
Lycospora punctata KOSANKE	+			
L. parva KOSANKE	+			
L. spinosa BOHÁCOVÁ	+			
L. pellucida (WICHER) S. W. & B.				+
L. pusilla (IBRAHIM) S. W. & B.				+
L. torquifer (LOOSE) R. POT. & KREMP				+
L. triangulata BHARDVAJ				+
Densosporites granulosus KOSANKE				+
D. loricatus (LOOSE) S. W. & B.				+
D. parvus HOFFM., STAPL. & MALL.				+
D. ruhus KOSANKE				+
D. sinuosus KOSANKE				+
D. sp.	+			+
Verrucososporites obscurus R. POT. & KREMP	+			
V. verrucosus ALPERN	+			
Granulatosporites fabaeformis DYB. & JACH.	+			
G. granulatus DYB. & JACH.	+			
Latosporites latus R. POT. & KREMP	+			
Cirratriradiates arcuatus GUENNEL				+
Florinites ovatus DYB. & JACH.	+			+
F. sp. 1				+
F. sp. 2				+
Alisporites sp.	+			
Potonieisporites sp.				+

* Determined by BARABÁS-STUHL, Á. [1971].
** Determined by GÓCZÁN, F. [1971].

The Bogádmindszent sequence is constituted by coarse and fine conglomerates, coarse and fine sandstones, arcoses, siltstones and sandy, silty and calcareous shales. The grain size of the strata, as a rule, decreases down the profile and it is only in the lowermost 40 m that a coarsening is observable again. The sequence consists of 30 microcycles grading into one another without any sharp boundary. Between 648 and 1290 m several seams and stringers of freshwater metaanthracite of 20 to 60 cm thickness can be observed. The presence of carbonaceous shale pebbles in the higher-seated coarse conglomerate material testifies to occasional interruptions of the sedimentation by erosional episodes. According to its sporomorphs *(Table 2)* and the macroflora recovered from 20 levels *(Table 3)*, the sequence can be dated as Westfalian. The same can be said about the topmost strata, where, at 310 m depth, poorly preserved representatives of *Licospora, Savitrisporites, Cirratriradiates* and *Florinites* could still be observed.

The detrital rocks of Borehole Siklósbodony-1 differ in composition from those of Bogádmindszent. The pebbles are overwhelmingly metamorphites. No granite pebble is present, the pebbles of quartz-porphyry are scarce. The strata below 980 m are of greyish-green colour. Between 980 and 570 m, however, more and more red-brown intercalations are observable, so that this 410 m-thick member grades into the red Lower Permian strata conformably overlying it. The scant sporomorphs deriving from the middle of this interval *(Table 2)* do not exclude the possibility of a Stephanian age.

Otherwise, the Bogádmindszent sequence includes, at 784.5—785 m depth, a carbodiabase sill and, at 1100—1200 m, it is intervowen by a netlace of quartz, quartz-feldspar and quartz-carbonate streaks.

TABLE 3

Macroflora of the Middle Carboniferous in Hungary

Species	Boulders from North-Mecsek*	Bmsz—1 502—1195 m**
EQUISETINAE		
Sphenophyllum erosum LINDL & HUTT.	?	
S. schlotheimi BRONGN.	+	
Annularia sp.		+
Calamites sp.	+	+
FILICINAE		
Pecopteris volkmanni SAUVEUR		+
P. pennaeformis BRONGN.		+
P. (Daclitykitheca) dentata BRONGN.		+
P. cf. *miltoni* ARTIS		+
P. cf. *punctata* CORSIN		+
P. sp.	+	+
Neuropteris cf. *schlehani* STUR		+
N. microphylla BRONGN.	+	
N. gigantea STERNBERG	+	
N. articulata BRONGN.	+	
N. sp.		+
Alethopteris grandini BORNGN.		+
A. davreuxi (BRONGN.) GOEPP.		+
A. cf. *friedeli* BERTR.		+
A. sp.		+
PTERIDOSPERMAE		
Lepidopteris cf. *rigida* (KURZ) SCH.	+	

* Determinated by ANDREÁNSZKY, G. [in SOÓS, I.—JÁMBOR, Á. 1960].
** Determinated by FÖLDI, M. [1971].

b) Marine facies

Marine Middle to Upper Carboniferous sediments have for a long time been known to occur in the northern Bükk Mountains and were last described in detail by K. BALOGH [1964]. Unfortunately, the formations underlying this continuous geosynclinal-type sequence explored in about 1500 m thickness are unknown. If the Uppony sequence, which was earlier considered to be a representative of the Lower Carboniferous, was assigned, in accordance with J. ORAVECZ [1965] to the Silurian, a Lower Carboniferous of Szabadbattyán facies had to be supposed to be hidden in depths. The possibility of a Sudetic unconformity, however, cannot be completely rejected in this case, either.

Attaining a thickness of about 1100 m, the member of the Bükk's Carboniferous seems to span the Namurian-Bashkirian-Lower Moscovian interval. It consists of a monotonous sequence of dark shales and sandstones containing at the top both *brachiopods* and the fusulinid *Hemifusulina moelleri* RAUSER. The Upper Moscovian and Uralian are characterized by the alternation of dark limestone lenses with shales including sporadically interbedded massive quartz-conglomerates and sandstones. At the top the dark shales are replaced by variegated ones, so that the grading into a lagoonal Lower Permian of variegated facies locks very plausible. The facies reminds of the Hochwipfel and Auernig Beds of the Carnian Alps, it spans the interval Upper Moscovian – Uralian distinguished with the aid of *fusulinids*. In addition, the Upper Moscovian contains hosts of *calcareous algae, smaller foraminifera, corals, brachiopods, molluscs* and *trilobites* [K. BALOGH 1961, 1964, M. HERAK—V. DEVIDÉ 1963, SZ. E. ROZOVSZKAJA 1962, 1963, GY. RAKUSZ 1932, Z. SCHRÉTER 1948, 1963]. Let us admit, however, that the Uralian has so far been rather poorly identified and only in the southern limb of the northern Bükk anticline *(Pseudofusulina pseudojaponica* DUTKEVICH, *Quasifusulina, Triticites.)*

The continuation of the Bükk's marine Middle and Upper Carboniferous in the Carpathian Region may be searched for mainly in the magnesitic Carboniferous of the Slovak Metalliferous Mountains. Farther south, traces of marine facies are allegedly known to occur in the eastern Great Hungarian Plain, being represented there by dark shales and sandstones recovered from some boreholes [K. SZEPESHÁZY]. They appear, however, in form of yellowish-white limestone pebbles in the 956.5—959.5 m interval of Borehole Karád-1 south of Lake Balaton [K. BALOGH 1964. p. 339]. Although these seem to belong to Tertiary conglomerates, yet they form an important link, proved by *Triticides* and *Daixina*, with the Middle and Upper Carboniferous of the Southern Alps and Dinarides.

Permian

The Permian of Hungary is similarly represented by both continental and marine facies.

a) Continental Permian

The thickest sequence, including the Rotliegend, is known to occur in the western Mecsek and at the northern margin of the Villány Mountains. Elsewhere, sedimentation was restricted to the Late Permian time only. The sediments are accompained by eruptions of quartz-porphyry whose erosion products play a considerable role in both parts of the Permian. The individual sequences are characterized by a recurring rhythmicity of varying size.

1. The almost 2.5-km-thick red Lower Permian of the Mecsek Mountains *(Fig. 1)* begins — above Precambrian granitoids rejuvenated in Early Carboniferous time — with 340 m of coarse sediment. The pebbles of these consist of granite, crystalline schist, Carboniferous sandstone, Silurian shale and porphyrite. Above the talus-like basal strata follow four microcycles which can be divided into a number of rhythms. The top of this member contains, beside *Pecopteris* sp. and *Voltzites* sp., Lower Permian *sporomorphs (Table 4, Column 1)*.

These presumably fluviatile sediments are overlain by 30 to 150 m of quartz-porphyry lava. Above this, the fluviatile facies reappears, though with torrential features this time. This member can be split up into two cycles separated by erosion surface from each other. Most of the pebbles consist of porphyrites and quartz-porphyry. The grain size, however, shows a gradual decrease within the second cycle.

The upper part of the Mecsek's Lower Permian is constituted by lacustrial sediments linked through the medium of 150 of transitional sediment with the older fluviatile ones. The transitional member consists of an alternation of sandstones of graded bedding with thinly laminated (foliaceous) siltstones cemented by dolomite. One limestone intercalation could also be identified. The finer-grained strata contain the phyllopod *Lioestheria lallyensis* DEPÉRET et MAZAREN.

The transitional member is overlain by 700 to 900 m of red-brown siltstone with locally associated red dolomitic marls. Characterized by fine bedding, micro-crossbedding ripple marks, bioglyphs and dessication marks and cycles of 10 to 30 m thickness, the sequence appears to have been deposited in a non-agitated environment. Because of the absence of common salt accumulations, a shallowwater sea environment is hardly conceivable. In this respect, the phyllopods (*Limnadia* sp.) recovered from the sedimentary sequence do not give any information.

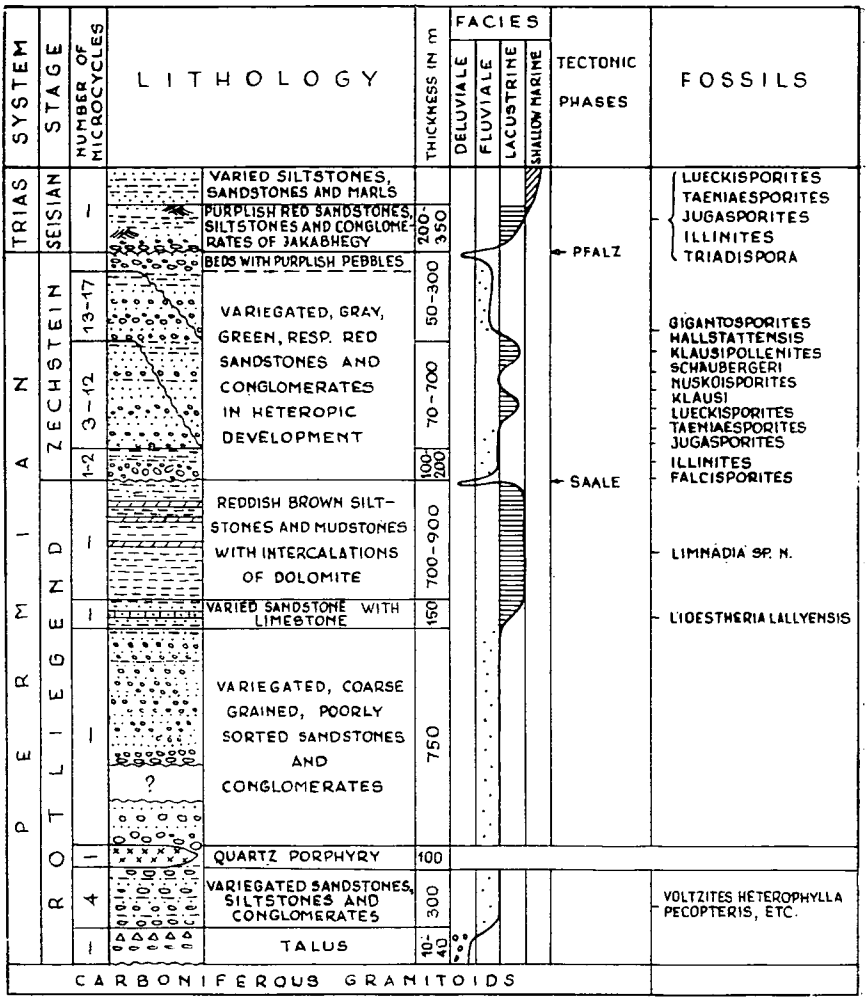

Fig. 1. Ideal profile of the Permian of the Western Mecsek.
Compiled by MR. and MRS. BARABÁS, Á. JÁMBOR and O. TŐZSÉR

As opposed to this asymmetrical megacycle, the Mecsek's Upper Permian exhibits a new and symmetrical megacycle of fluviatile nature. The total thickness of its four members increases from 200 m in the west up to 1200 m in the east (i.e. towards the centre of the basin). The merit of deciphering the intricate facial conditions belongs to Á. B.-STUHL [1969].

At the base, the Lower Permian siltstone sequence is overlain with a sharp unconformity by a very diversified, though overwhelmingly red-coloured, sequence of coarse- to fine-grained sediments. The second member consists of finer, fluviatile and lacustrial sediments which on the basin margins are variegated, in the basin centre grey. The third member shows the same development, but the colour is inversely distributed: turning red towards the centre of the basin. This member

TABLE 4

Sporomorpha from the Permian and Early Trias of the Mecsek Mountains after BARABÁS-STUHL, Á. [1967]

Species	Early Permian	Later Permian			Early Trias
	Sandstone				
	underlaying the quartz-porphyry	of varied colour	of gray colour	of green and red colour	of Jakabhegy
Nuskoisporites klausi GREBE		+	+	+	
Jugasporites schaubergeroides KLAUS		+	+	+	
J. delasaucei LESCHIK	+	+	+	+	+
Limitisporites sp.	+	+	+	+	+
Gigantosporites hallstattensis KLAUS		+			
Gardenasporites sp.	+	+	+	+	
Lueckisporites virkkiae POT. & KLAUS				+	
L. microgranulatus KLAUS	+	+	+	+	+
Taeniaesporites alatus KLAUS	+	+	+	+	
T. labdacus KLAUS		+	+	+	
T. sp.					+
Klausipollenites schaubergeri (POT. et KLAUS) JANSONIUS		+	+	+	
Falcisporites zapfei LESCHIK		+	+	+	+
Platysaccus papilionis POT. & KLAUS			+	+	+
Converrusisporites eggeri KLAUS	+	+	+	+	
Cordaitina sp.	+				
Lophotriletes sp.	+				
Illinites melanocorpus KLAUS					+
Triadispora sp.					+
Allisporites sp.					+

is rich in *silicified wood trunks [Baiera digitata* HEER, *Baieroxylon implexum* (ZIMMERMANN) GREGUSS, *Dadoxylon schrollianum* (GOEPPERT), *D. transdanubicum* SIMONCSICS, *D. rhodeanum* (GOEPPERT), *Araucarioxylon* sp., *Platyspiroxylon parenchymatosum* GREGUSS, *Voltzites hungarica* HEER, *V. boeckhiana* HEER, *Carpolithes geinitzi* HEER*]* and *phyllopods [Eoestheria dawsoni* (JONES), *Eoleaia leaiformis* RAYMOND [in VÁRSZEGI K. 1961]. The afore-mentioned "horizons", repeatedly intertonguing, are overlain by a relatively thin final layer of "sandstone with purple gravels" showing, again, a coarser grain size. This formation is undoubtedly separated by an unconformity from the Jakabhegy Sandstone Formation assigned recently to the Lower Trias, on account of its sporomorphs *(Table 4)*, lithological characteristics and overlapping transgression. The presence of an unconformity is emphasized by the basal conglomerates of the Jakabhegy Formation.

2. The Permian of the Villány Mountains is similar to that of the Mecsek, but is known only from boreholes (as a result of drilling). From the Lower Permian so far only the coarse-grained basal member developing gradually from the Stephanian (Siklósbodony-1) and the top of the siltstone sequence (Turony-1) are known. No trace of Lower Permian volcanism is available *(Fig. 2)*.

In the Upper Permian two heteropical facies occur in a juxtaposition. For, the purely sedimentary, Mecsek-type sequences of the western basin portion (Turony-1) show an intertonguing with the products of the large quartz-porphyry volcano of Bisse-Vokány in the east. And it is then that the Jakabhegy Sandstone

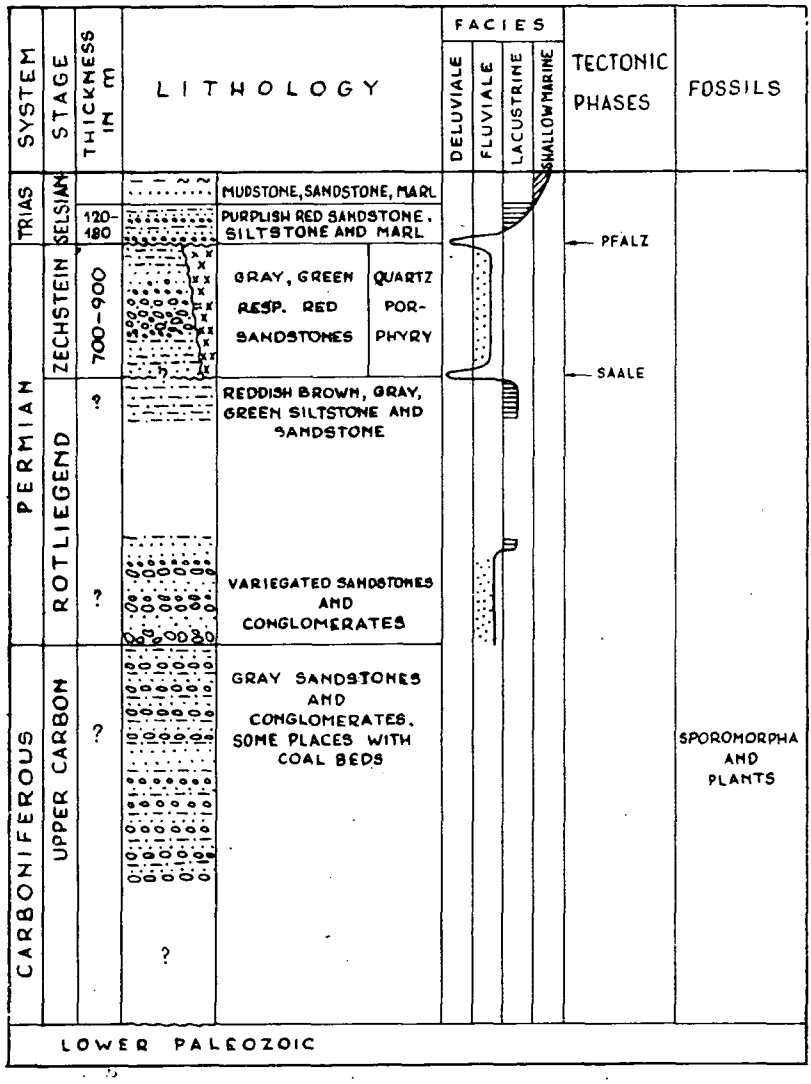

Fig. 2. Ideal profile of the Later Palaeozoic of the Villány Mountains. Compiled by MRS. BARABÁS, M. KASSAI, MRS. M. KOVÁCS and T. SZEDERKÉNYI

transgresses over both facies, extending eastwards beyond the limit of the Upper Permian area similarly way as in the Mecsek Mountains.

3. On the southeastern side of the Balaton Highland a continental Upper Permian is exposed in several places, being further traceable along the strike underground as shown by drilling *(Fig. 3).*

The basal conglomerates rest on a Silurian quartzphyllite sequence, being overlain by a rhythmical alternation of red, grey and variegated sandstones, siltstones and clays. The pebbles of the basal conglomerates are constituted by quartz, quartz-porphyry, phyllite and metamorphic sandstones. The sandstones contain, beside quartz and muscovite, some rock debris and feldspar as well. The coarser fluviatile deposits turn upwards gradually finer, grading into lacustrial sediments partly green in colour. These last-mentioned rocks include thin coal stringers, red dolomite lenses and even traces of gypsum.

The total thickness increases from 200 in the SW to 800 m in the NE. In a close connection with this the Upper Permian is separated by a slight angular disconformity and basal conglomerates from the purely marine Lower Trias transgressing over the SW part of the area (Kővágóőrs-Zánka). However, farther NE, i.e. closer to the basin centre, there is a transition in lithology between the two systems. Finally, the continental facies in the southern foreland of the Vértes Mountains grades into a gypsum-bearing, lagoonal-marine facies which was connected with the sea trough to the south of it.

However, the Upper Permian of the northern margin of the Bakony Mountains is again of purely continental facies. In Borehole Alsószalmavár-1, between the Lower Triassic and slightly metamorphosed Devonian (?) schists, it attains round

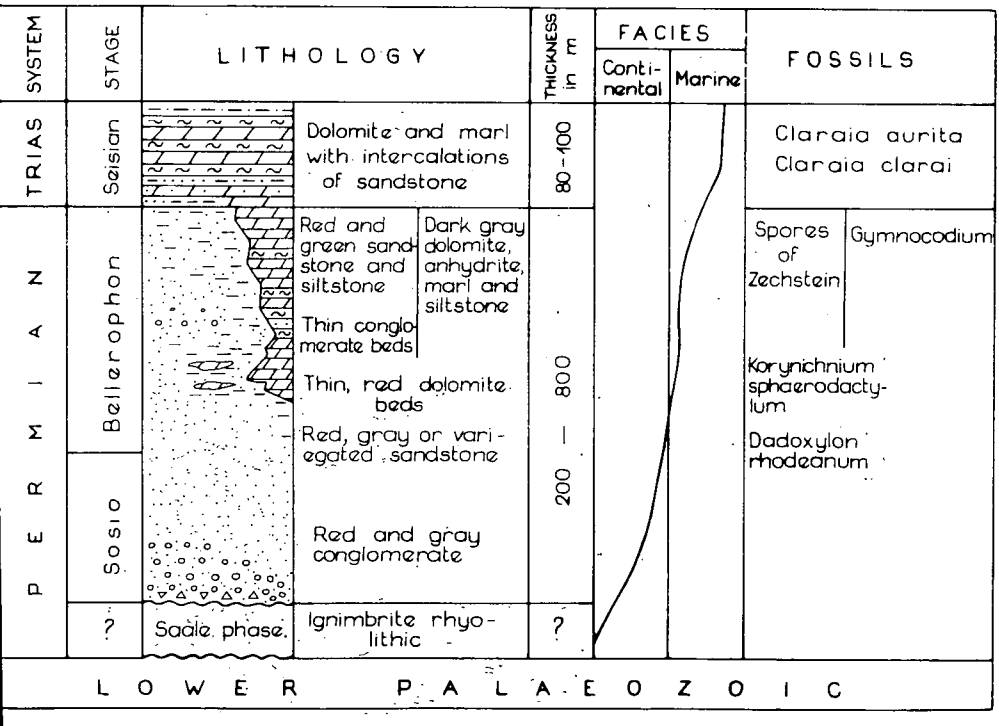

Fig. 3. Ideal profile of the Permian of the Balaton Region. Compiled by GY. MAJOROS

400 m in thickness [E. KORPÁS—Á. JÁMBOR—E. NAGY 1970; Cs. DETRE—E. NAGY 1971].

The *sporomorphs* of the Upper Permian of the Balaton Highland are for the most part identical with those of the Mecsek's Upper Permian [Á. B.-STUHL 1961]. In addition, however, *Araucarioxylon* sp., *Platyspiroxylon* sp., *Dadoxylon rhodeanum* (GOEPPERT), tracks and burrows of *worms* and *crustaceans* as well as foot-prints of *reptiles* [*Korynichnium sphaerodactylum* (PABST)] can also be observed [GY. MAJOROS, 1964; GY. MAJOROS in: J. FÜLÖP 1969. p. 8; A. KASZAP, 1968; P. GREGUSS, 1967].

4. The continental Upper Permian occupies large areas other than the Zemplén-Tokaj and Bihar Mountains in the southern Great Hungarian Plain as well. Overlying crystalline schists and Carboniferous granitoids, its strata have been uncovered by drilling in the vicinity of Érsekcsanád, Kunbaja, Ásotthalom and Nagykőrös [G. CSIKY, 1963; K. SZEPESHÁZY, 1962; A. BÉRCZI—MAKK, 1971]. The red conglomerates and arcoses at Nagykőrös grade upwards into gypsum-bearing beds which are difficult to separate from the Lower Trias. In the Zemplén Mountains and at Battonya and Kelebia the red sediments are accompained by quartz-porphyry tuffs and intrusions whose radiometric age at the last two localities is estimated at 250±20 M. Y. and 230±20 M. Y., respectively.

b) Marine Permian

Marine Permian deposits occur amidst the afore-listed continental occurrences in the Bükk Mountains. The basal member of their sequence attaining a total thickness of 400 to 500 m begins above the Uralian Stage with variegated sandstones, shales and lagoonal dolomites. These grade up in the profils into dark, bituminous limestone and dolomite facies abunding in Indo-Armenian to Dinarian microfloral elements and micro- and macrofossils [K. BALOGH 1961, 1964]. The continuation of this facies is still uncertain. Its connection with the South Alpine and Dinarian occurrences, however, can be supposed to be traceable, as shown by I. SZABÓ's observations, via the Boreholes of Bugyi, Tabajd-5, Táska, Dinnyés and Dióskál, i.e. virtually along the southern side of Lake Balaton.

Nota bene, at Bugyi, Gymnocodium-bearing Permian limestones occur in Eocene conglomerates. In the lithological log of Borehole Tabajd-5 the Lower Paleozoic schists are overlain by red conglomerates, sandstones and siltsones totalling 300 to 400 m in thickness. These agree in lithology and facies with the continental Permian of the Balaton Highland. The red siltstones, however, are overlain by yet another 350-m-thick sequence consisting of grey gypsum- an anhydrite-bearing sandstones, marls, siltstones and dolomites. According to Á. B.-STUHL, among the *sporomorphs* there are genuine Upper Permian forms such as *Nuskoisporites dulhuntyi* (POT et KLAUS), *Pityisporites zapfei* POT. et KLAUS, *P. delasaucei* (POT. et KLAUS), and *Klausipollenites schaubergeri* (POT. et KLAUS) JANSONIUS. The massive dolomite beds contain calcareous algae *(Gymnocodium bellerophontis* (ROTHPLETZ) PIA, *Permocalculus tenellus* (PIA)) and smaller foraminifera *(Glomospira* sp., *Climacammina* sp., *Ammodiscus* sp.). The transition into the Lower Trias is indicated by the appearance of sandy, marly and, finally, pure limestones. The last-mentioned member of 68 m thickness already contains small *gastropods, pseudomonotids, pectinids* and *lingulae.* At Táska, the Upper Permian is constituted by a thick dolomite complex.

II. MAGMATISM, TECTONIC PHASES, PALEOGEOGRAPHY

1. In addition to the already-mentioned Lower and Upper Permian quartz-porphyry bodies whose removed detrital material is so largely involved in the construction of sedimentary sequences, those granite bodies should also be referred which on the basis of their features and radiometric data may be assigned, with good reason, to the Carboniferous. Among them the granites of migmatic nature,

seemingly synorogenic, should be considered older, the batholitic, i.e. post-orogenic, ones younger.

The former, which are known to occur in Transdanubia and in the more southern part of the Great Hungarian Plain (Mágocs, Nyugat-Szenterzsébet, Pécs, Mórágy—Fazekasboda, Soltvadkert, Kecskemét, Cegléd, Algyő and Battonya), seem to be connected with the Breton phase. The latter occurring in the Velence Mountains in exposure and at Ságvár, Buzsák and Gelse underground, can be brought into connection with the Sudetic phase. It should be emphasized, however, that long-lasting magmatic processes are dealt with, as manifested by both the fluctuation of radiometric data and the occurrence of subsequent quartz-porphyry volcanism. At any rate, the frequency of igneous bodies testifies to vivid crustal activities to have taken place in Variscan time in what is now Hungary.

2. Because of the deficiency of information, intra-Carboniferous sedimentation breaks and unconformities cannot be located with complete accuracy as of yet. Nonetheless, the heaviest tectonic movements should be placed at the boundary between the Devonian and Carboniferous and Lower and Middle Carboniferous, respectively. This is confirmed, on the one hand, by the suddently increasing epi-metamorphism of the pre-Carboniferous formations, on the other hand, by the retrograde metamorphism (315—330 M. Y. old) of Precambrian crystalline rocks along planes of subsequent movements. The period of these northerly overthrustings, however, died with the Sudetic phase. (Movements of northerly trend can be observed in the SE dipping Lower Paleozoic of the Szendrő-Uppony Mountains as well as at Szabadbattyán, where the Visean shales are tectonically "overridden" by the Devonian crystalline limestones.) The post-Sudetic phases, however, brought about only synorogenic uplifts and subsidences. The resulting fractures, however, have not caused any considerable change in the original arrangement of the strata. This is the reason why both the main facies of Hungary's Upper Paleozoic are connected with the Alpide structures rather than Variscide ones (e.g. the Bükk's Upper Paleozoic was folded together with the Trias).

3. After the Breton phase the Hungarian territory of the Variscicum became a denudation area, except for a small central belt pointing towards Nötsch in the Gailtal (Austria). After the Sudetic phase, however, larger intramontane basins were formed here. At the same time, the sea transgressed in the central, "Dinaric", sea-trough in NE direction as far away as the Gemerides.

Essentially, the same conditions persisted in post-Carboniferous time as well. Of course, the boundaries of certain basins were changed and also new areas of sedimentation were brought about. The sedimentation of the "Dinaric" sea-trough had not been interrupted since the beginning of the Middle Carboniferous and it was not until the Carboniferous-Permian boundary that lagoons could develop. The continental realm proved to be much more sensitive to crustal movements. There are two continental areas (Villány and western Mecsek Mountains), where sedimentation began in the Middle Carboniferous and the earliest Permian, respectively. In other places sedimentation was restricted to Late Permian time. The boundaries of the megacycles of Southern Transdanubia's Permian coincide with the Saale and Pfalz phases. This should be emphasized, as these phases are just slightly manifested or totally absent in the more northern areas or the Great Hungarian Plain. In the central, "Dinaric", belt the Upper Permian grades directly into the Lower Trias.

Consequantly, the paleogeographic setting *(Fig. 4)* must have been totally different from that proposed earlier [1963] by V. I. SLAVIN.

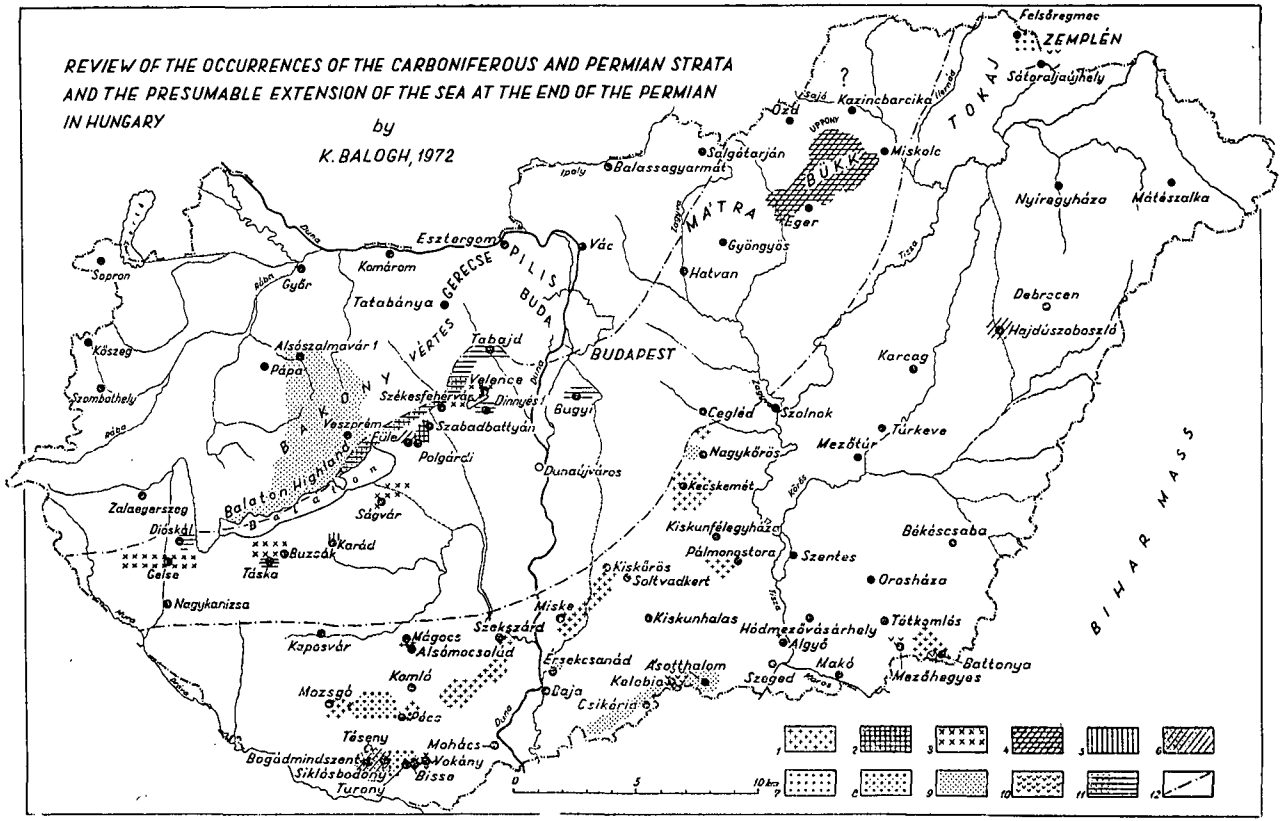

Fig. 4.

1: Migmatic granites (Breton phase?). — *2:* Early Carboniferous in marine facies. — *3:* Granite plutons (Sudetic phase?). — *4:* Marine sedimentary series, uninterrupted from the earliest Middle Carboniferous to the Latest Permian. — *5:* Later Carboniferous, purely marine. — *6:* Middle and Later Carboniferous in continental and marine facies. — *7:* Continental „Permocarboniferous". — *8:* Continental Early and Later Permian. — *9:* Later Permian, transgressing over Early Palaeozoic. *10:* Quartz porphyry and quartz porphyry tuff. *11:* Later Permian in continental—lagoonal, respective in continental—marine facies. — *12:* Later Permian shoreline

REFERENCES

ANDREÁNSZKY, G. [1962]: Calamites-Rest vom Bányahegy bei Füle (West-Ungarn). — Acta Univ. Szeged. Acta Biol. N. ser. *6*. pp. 1—4.

BALOGH, K. [1961]: Das Mesozoikum Nordungarns. — Ann. Inst. Geol. Hung. *49*. 2. pp. 365—379.

BALOGH, K. [1964]: Die geologischen Bildungen des Bükk-Gebirges. — Ann. Inst. Geol. Publ. Hung. *48*. 2. pp. 243—719.

BALOGH, K. [1969]: A Földtani Intézet száz éve — rétegtani síkon. — In: 100 éves a Magyar Állami Földtani Intézet. — Budapest. pp. 102—131.

BARABÁS, A., BARANYI, I., JÁMBOR, Á. [1965]: A Mecsek és a Villányi hegység harmadkor előtti alaphegység térképe. — Geofizikai Évkönyv *1*.

BARABÁS-STUHL, Á. [1969]: Gliederung der oberpermischen Ablagerungen des Mecsekgebirges auf Grund ihrer zyklischen Ausbildung. — Földtani Közl. *99*. 1. pp. 66—80.

BARABÁS-STUHL, Á. [1971]: Palynological Studie on the Late Paleozoic of Borehole Polgárdi-2, Transdanubia, Hungary. — Őslénytani Viták (Discussiones Palaeontologicae). *18*. pp. 21—50. Budapest.

BARANYI, I., JÁMBOR, Á. [1962]: A komplex geofizikai kutatások eredményeinek felhasználása a DK-Dunántúl területén az alaphegység kutatásában. — Magyar Geofizika. *3*. 3—4. pp. 165—176.

BÉRCZI-MAKK, A. [1971]: Extension of the subsurface graben-and-horst range of the Bácska into the Öttömös area, South Hungary. — Földtani Közl. *101*. 1. pp. 26—33.

CSIKY, G. [1963]: A Duna—Tisza köze mélyszerkezeti és ősföldrajzi viszonyai a szénhidrogén kutatások tükrében. — Földrajzi Közlem. *1963*. 1. pp. 19—36.

DETRE, CS. [1970]: The Revision of Kansuella transdanubica Földvári, 1952. — Őslényt. Viták. *16*. pp. 51—55.

DETRE, CS. [1971]: Revision of the Brachiopods from the Carboniferous of Szabadbattyán, Transdanubia, Hungary. — Őslényt. Viták *18*. pp. 77—88.

FORGÓ, L., MOLDVAY, L., STEFANOVITS, P., WEIN, GY. [1966]: Magyarázó Magyarország 200 000-es földtani térképsorozatához. L-34-XIII. Pécs. — Budapest.

FÖLDVÁRI, A. [1952a]: A szabadbattyáni ólomérc és kövületes karbonaelőfordulás. — MTA. Műsz. Tud. Oszt. Közlem. *5*. 3. pp. 25—53.

FÖLDVÁRI, A. [1952b]: Lead Ores and Fossiliferous Dinantian (Lower Carboniferous) at Szabadbattyán. — Acta Geologica *1*. pp. 11—36. Budapest.

FÜLÖP, J. (Red.) [1969]: Földtani Kirándulás a Dunántúli Középhegységben. — pp. 1—60. Budapest.

GÓCZÁN, F. [1971a]: Informative stratigraphisch-palynologische Untersuchungen an karbonischen Ablagerungen in Ungarn. — Jahresber. Ung. Geol. Anst. *1969*. pp. 719—727.

GÓCZÁN, F. [1971b]: Contributions to the Study of the Microplankton of the Silurian Siliceous Shales at Alsóörs. — Őslényt. Viták *18*. pp. 13—20.

GREGUSS, P. [1961]: Permische Fossile Hölzer aus Ungarn. — Palaeontographica Abt. B. *109*. pp. 131—196.

GREGUSS, P. [1967]: Fossil Gymnosperm woods in Hungary. — Budapest. 136 p. (Mit 86 Tafeln).

HAJÓS, M. [1971]: Versuche zum Aufschließen von Conodonten aus paläozoischen Gesteinsproben. — Jahresber. d. Ung. Geol. Anst. *1969*. pp. 719—721.

HERAK, M., KOCHANSKY, V. [1963]: Jungpaläozoische Kalkalgen aus dem Bükk-Gebirge (Nordungarn). — Geol. Hung. Ser. Pal. *28*. pp. 45—77.

HETÉNYI, R., FÖLDI, M., R. BARANYAI, L. [1971]: A délbaranyai karbon alaphegység vizsgálata. — Manuscript.

JÁMBOR, Á. [1969]: Carboniferous deposits in the area between the Mecsek and Villány Mountains. — Jahresber. Ung. Geol. Anst. *1967*. pp. 215—222.

KASSAI, M. [1968]: A jakabhegyi homokkő fácies- és korkérdései — Inauguraldissertation. Miskolc. Manuscript.

KASSAI, M. [1971]: A Villányi-hegység északi előterének permi képződményei. — Pécs. Manuscript.

KASZAP, A. [1968]: Korynichnium sphaerodactylum (Pabst) Einzelfährte im Perm von Balatonrendes (Transdanubien). — Földtani Közl. *98*. pp. 429—433.

KISS, J. [1951]: Les conditions géologiques et metallogenetiques du Mont Szár de Szabadbattyán. — Földtani Közl. *81*. 7—9. pp. 264—274.

KOLOSVÁRY, G. [1951a]: The permo-carboniferous corals of Hungary. — Földtani Közl. *81*. pp. 1—48, 171—185.

KOLOSVÁRY, G. [1951b]: The Lower-Carboniferous Corals from Hungary. — Földtani Közl. *81*. 7—9. pp. 276—283.

KORPÁS, L., JÁMBOR, Á., NAGY, E. [1970]: Az Alsószalmavár-1. sz. fúrás rétegsorozata — Ung. Geol. Anst. Budapest. Handschrift.

LÁNYI, J., NYITRAI, T., SZABÓ, M., SZABADVÁRY, L. [1969]: Komplex geofizikai kutatás a Dunántúli Középhegységben és peremvidékén. — Bericht von MÁELGI über 1968. pp. 37—46.

MAJOROS, GY. [1964]: Őshüllő lábnyom a balatonrendesi permből. — Földtani Közl. *94.* pp. 243—245.

MAJOROS, GY. [1971]: Forschungen im Bereich des Jungpaläozoikums NO vom Balaton. — Jahresber. Ung. Geol. Anst. *1969.* pp. 675—676.

MIHÁLY, S. [1971]: Revision of the Lower Carboniferous Coral Fauna from the Bituminous Limestones of Kőszárhegy Hill at Szabadbattyán, Transdanubia, Hungary. — Őslényt. Viták *18.* pp. 51—76.

MONOSTORI, M. [1971]: Jelentés a szabadbattyáni fúrásokban harántolt karbon bitumenes mészkőösszlet mikrofácies vizsgálatáról. — ELTE, Paläontologisches Inst. Budapest. Manuscript.

NAGY, E. [1971]: Magyarország permnél idősebb paleozóikumának átfogó földtani vizsgálata. — Jahresber. Ung. Geol. Anst. *1969.* pp. 653—656.

ORAVECZ, J. [1965]: Szilur kőzetkavicsok földtörténeti szerepe törmelékes összleteinkben. — Über die erdgeschichtliche Rolle silurischer Gesteinschotter in den klastischen Schichtkomplexen Ungarns. — Földtani Közl. *95.* 4. pp. 402—405.

PANTÓ, G. [1965]: Pre-Tertiary formations of the Tokaj Mts (Hungary). — Jahresber. Ung. Geol. Anst. *1963.* pp. 227—241.

PANTÓ, G. [1966]: In: Magyarázó Magyarország 200 000-es földtani térképsorozatához. M-34-XXXIV. Sátoraljaújhely. — Budapest. pp. 25—30.

RAKUSZ, GY. [1932]: Die oberkarbonischen Fossilien von Dobsina (Dobšina) und Nagyvisnyó. — Geol. Hung. Ser. Pal. *8.* pp. 1—223.

ROZOVSZKAJA, SZ. E. [1960]: Znacsenije fuzulinid dlja korrelacii verhne-paleozojszkih otlozsenij po materialom Ruszszkoj platformü i Vengrii. — Bjull. Moszkovszk. obscs. iszpüt. prirodü. Otd. geol. *35.* 3. pp. 172—173.

ROZOVSZKAJA, SZ. E. [1963]: Fuzulinidü gor Bjukk (Vengrija). Geol. Hung. Ser. Pal. *28.* pp. 3—43.

SCHRÉTER, Z. [1948]: Trilobiten aus dem Bükk-Gebirge. — Földtani Közl. *78.* pp. 25—39.

SCHRÉTER, Z. [1960]: Die geologischen Verhältnisse des Bükkgebirges. — Karszt- és Barlangkutatás. *1.* Budapest. pp. 7—36.

SCHRÉTER, Z. [1963]: A Bükkhegység felső-permi Brachiopodái. — Oberpermische Brachiopoden des Bükk-Gebirges (Nordungarn). — Geol. Hung. Ser. Pal. 28. pp. 79—179.

SIDÓ, M. [1971]: Beitrag zur Mikropaläontologie des Paläozoikums in Ungarn (Silur—Devon—Karbon). — Jahresber. Ung. Geol. Anst. *1969.* pp. 703—705.

SIMONCSICS, P. [1955]: Verkieselte permische Stammenreste von dem Mecsek-Gebirge. — Acta Univ. Szeged. Acta Biol. *1.* pp. 46—62.

SLAVIN, V. I. [1963]: Triasovye i jurskie otloženija Vostočnych Karpat i Pannonskogo Massiva. — Gosgeoltechizdat. Moskwa. 171 p.

SOMOGYI, J. [1965]: Über die Rippelmarken des unterpermischen Komplexes im Mecsek Gebirge. — Földtani Közl. *95,* pp. 37—39.

SOÓS, J., JÁMBOR, Á. [1960]: Oberkarbonische Pflanzenreste aus den Helvetschottern des Mecsekgebirges (Südungarn). — Földtani Közl. *90.* pp. 456—458.

STUHL, Á. [1961]: Ergebnisse von Sporenuntersuchungen an den Permablagerungen des Balatonhochlandes. — Földtani Közl. *91.* pp. 405—412.

SZABÓ, I. [1965]: Geologische Auswertung der Angaben über die Schrägschichtung des Oberperms und Unterseis im Mecsekgebirge (Südungarn). — Földtani Közl. *95.* pp. 40—46.

SZEPESHÁZY, K. [1962]: Contributions to the subsurface geology of the Nagykőrös—Kecskemét area. — Földtani Közl. *92.* 1. pp. 40—52.

SZEPESHÁZY, K. [1969]: Petrographische Angaben zur Kenntnis des Battonyaer Granits. — Jahresber. Ung. Geol. Anst. *1967.* pp. 227—267.

TELEKI, G. [1941]: Das Paleozoikum der Umgegend von Polgárdi. — Jahresber. Ung. Geol. Anst. *1936—38.* pp. 311—328.

VÁRSZEGI, K. [1961]: Remains of Phyllopods from the Permian of the Mecsek Mountains. — Földtani Közl. *91.* pp. 226—227.

VIRÁGH, K., VINCZE, J. [1967]: Specific features of the formation of the Uranium ore occurence, Mecsek Mts, Hungary. — Földtani Közl. *97.* 1. pp. 39—59.

WEIN, GY. [1969]: Tectonic Review of the Neogene-Covered Areas of Hungary. — Acta Geol. *13*. Budapest. pp. 399—437.
WÉBER, B. [1964]: Neue oberkarbonische Schotter mit Pflanzenresten aus den Helvetschichten des Westlichen Mecsek. Földtani Közl. *94*. pp. 378—381.

Manuscript received, June 20, 1972

DR. ANDOS BARABÁS
Mecsek Ore Mines
39-es dandár út 19.
Pécs, Hungary

Prof. DR. KÁLMÁN BALOGH
Institute of geology
Attila József University
Szeged, Táncsics M. u. 2. Hungary

Acta Mineralogica-Petrographica, Szeged, XX/2, 209—216, 1972.

GEOCHEMICAL CONTROLS ON MANGANESE DISTRIBUTION IN AMPHIBOLITE-GRADE METAMORPHIC ROCKS*

R. K. CORMICK, D. A. CRERAR and H. L. BARNES

The geochemical distribution of manganese in metamorphic rocks is explicable in terms of crystal field theory by comparison with other transition metals. We shall apply this theory to interpret crystal chemical controls on manganese fractionation as shown by distribution coefficient values for 13 mineral pairs. Among these, the silicate pair, clinopyroxene/amphibole is used as a detailed example.

Recent applications of crystal field theory to trace element distribution in metamorphic rocks, such as by SCHWARTZ [1967] or BURNS [1970], have provided explanations of crystal chemical mechanisms for fractionation phenomena which previously were limited only to thermodynamic considerations. In general, crystal field theory is based on electrostatic interactions between a metal ion and its neighboring anions or, more specifically, ligands. For a specific number and geometry of coordinating ligands, an electrostatic field of unique symmetry and intensity is produced which affects the d-orbital electrons of the metal ion. The differential effect of this crystal field on the energies of these bonding electrons is quantitatively described as crystal field stabilization energy, or simply "CFSE".

Silicates are predominantly ionic structures to which crystal field theory is particularly applicable. Most transition metals occur in silicates on sites with octahedral coordination. However, the ligand fields may cause some site distortion for the metals from the ideal octahedral symmetry to a somewhat more tetrahedral, perhaps trigonal, or even monoclinic symmetry. The corresponding change in CFSE may have a noticeable effect on transition metal ion distribution among competitive sites. Fortunately, most site distortions are consistent for any given type of silicate crystal structure. Besides the effects of distortion, a size factor may also operate on transition metal ion distribution. Site sizes and cationic radii vary with the nature of surrounding ligands and the crystal structure. Using average metal-oxygen bond distances to express site size, we find that larger transition metal ions (relative to a major host cation such as Mg^{2+} or Ca^{2+} in ferromagnesian silicates) will prefer coordination sites with larger average dimensions. Conversely, though, CFSE is greater in sites with smaller average dimensions, Thus, transition metal ions which possess a stabilization energy as a result of their electronic configurations, should prefer the smallest site which will accommodate their ionic radii. These competing factors, along with site distortion effects, determine the transition metal distribution between different sites of a single phase and also between sites of coexisting phases.

* Lecture delivered at the technical session of the Commission on Manganese (IAGOD) during the XXIV IGC, 23 August, 1972, Montreal, Canada.

Consider, for example, the effects of site distortion, site size and CFSE on the distribution of Mn^{2+}, relative to Fe^{2+}, Mg^{2+} and Ca^{2+}, in coexisting clinopyroxenes and amphiboles *(Tables 1 to 3)*. Within the octahedral layer of the clinopyroxenes, there are two crystallographically distinct cation sites designated M_1 and M_2. For M_1, which approximates a regular octahedron, the average metal-oxygen distance is 2.12 Å [CLARK, APPLEMAN, and PAPIKE, 1969]. The M_2 site is highly distorted and metal-oxygen distances, although much greater than for M_1, range from 2.34 to 2.75 Å depending on the resident cation. The Mn^{2+} ion, due to its electron configuration, possesses no CFSE and has a relatively large ionic radius. Consequently, it strongly prefers the M_2 sites. The Mg^{2+} and Ca^{2+} ions which have no d-electrons, and thus no CFSE, also are distributed according to size; the smaller Mg^{2+} ions prefer M_1 sites while the larger Ca^{2+} ions prefer the M_2 sites. Ferrous iron has a relatively small effective ionic radius of 0.86 Å *(Table 1)* and should prefer the M_1 site; however, the stabilization energy for Fe^{2+} is often slightly higher for the distorted M_2 site so that it is preferred. These relations are summarized in *Table 2*.

TABLE 1

Crystal chemical properties of the important metal ions

Ion	Ionic Radius (Å)[1]	d-electrons	CFSE
Na^+	1.24	0	0
Ca^{2+}	1.20	0	0
Mg^{2+}	0.80	0	0
Mn^{2+}	0.91	5	0
Fe^{2+}	0.86	6	+
Fe^{3+}	0.73	5	0

[1] From WHITTAKER and MUNTUS (1970) based on radius ratio criteria.

TABLE 2

Clinopyroxene site preferences

Ion	Site Preference	Criteria
Mg^{2+}	$M_1 \gg M_2$	Size
Fe^{2+}	$M_1 \cong M_2$	CFSE, Site Distortion[2]
Mn^{2+}	$Mn < M_2$	Size
Ca^{2+}	$M_1 \ll M_2$	Size

[1] For site sizes based on average metal-oxygen distances: $M_1 = 2.12$ Å and $M_2 = 2.34$ to 2.75 Å.
[2] Most other transition metal ions will distribute according to these criteria.

In the general amphibole structure, there are four distinct cation sites *(Table 3)*. The relatively undistorted octahedral M_1, M_2 and M_3 sites are small, having average metal-oxygen distances of 2.075, 2.065 and 2.080 Å respectively [PAPIKE, *et al.*, 1969], and accommodate the smaller cations including Mg^{2+} and Fe^{2+}. The larger M_4 site (see *Table 3*) with distorted sixto eight-fold coordination prefers the larger cations such as Mn^{2+}, Ca^{2+}, Na^+ and sometimes Fe^{2+}. Ferrous iron, however, should distribute between M_4 and the smaller M_1, M_2 and M_3 sites much the same as between the clinopyroxene M_2 and M_1. This is because the basic structures are very similar and the amphibole M_4 site is almost equal in size to the M_2 of the clinopyroxene.

TABLE 3

Amphibole site preferences

Ion	Site preference	Criteria
Mg^{2+}	$M_2 \gtrsim M_1 \sim M_3 \gg M_4$[1]	Size
Fe^{2+}	$M_1 \succ M_3 \sim M_4 \succ M_2$	CFSE, Site distortion
	or $M_3 \sim M_1 \gtrsim M_2 \gg M_4$[2]	CFSE, Site distortion
Mn^{2+}	$M_4 \gg M_3 \sim M_1 \cong M_2$	Size
Ca^{2+}	$M_4 \gg M_1, M_2, M_3$	Size
Na^{+}	$M_4 \gg M_1, M_2, M_3$	Size

[1] For site sizes based on average metal-oxygen distances, $M_1 = 2.075$; $M_2 = 2.065$; $M_3 = 2,080$; and $M_4 = 2.30$ to 2.75 Å.
[2] If Fe^{2+} is not concentrated in the M_1 site, it is very depleted (See text).

When Mn^{2+} is compared to other transition metal ions, all of which are sensitive to crystal field parameters (except Fe^{3+}), manganese appears anomalous in its distribution among sites in clinopyroxene and amphibole. The reason is that it responds only to size criteria. (The exception, Fe^{3+}, is an extremely small ion (0.73 Å) compared to Mn^{2+} (0.91 Å) and does not compete for the same sites.) Consequently, Mn^{2+} ions can be expected to predominate in the amphibole M_4 and clinopyroxene M_2 sites by about equal proportions. However, in some amphiboles, such as actinolite or hornblende, the M_4 site is considerably more distorted, contracting its size and leaving the clinopyroxene M_2, or even M_1, sites more attractive. The effects of these minor size variations among potential sites is illustrated by the observed Mn^{2+} distribution between clinopyroxenes and amphiboles (some examples are given later in this paper). Size differences between the smaller, more

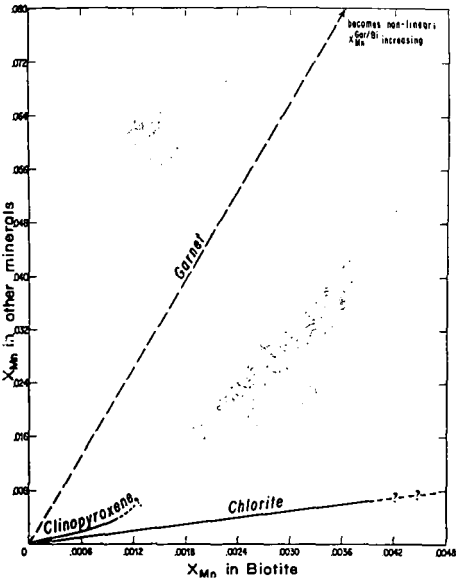

Fig. 1. Distribution of Mn between biotite and garnet, clinopyroxene, and chlorite. Concentrations are in atomic percent.

cramped sites of coexisting phases become important only if Mn^{2+} concentration in the environment is greater than can be accommodated in the primary sites. The clinopyroxene M_2 site, being significantly larger than the amphibole M_1, M_2 and M_3 sites, will preferentially accept the excess Mn^{2+} ions — producing an even greater fractionation towards clinopyroxene with increasing Mn concentration. In other words, an enrichment of manganese in clinopyroxene relative to amphibole greatly in excess of 1:1 correlates with a manganese-rich environment.

Ferrous iron (and other transition metal ions) sensitive to site distortion and crystal field effects, in addition to size criteria, can be expected to display a more complex distribution pattern between different clinopyroxenes and amphiboles. For example, acute distortion of the M_4 site of a particular amphibole may sufficiently affect the crystal field parameters to make this site more attractive for Fe^{2+} ions than the clinopyroxene M_2 site; alternatively, the presence of considerable Mn^{2+} in the clinopyroxene M_2 and amphibole M_4 sites could be enough to make the smaller sites more amenable to Fe^{2+} occupancy (see *Table 3*). We begin to see, then, how the very different crystal chemical behaviors of Mn^{2+} and other transition metal ions affect their distribution patterns in many ferromagnesian rock-forming silicates.

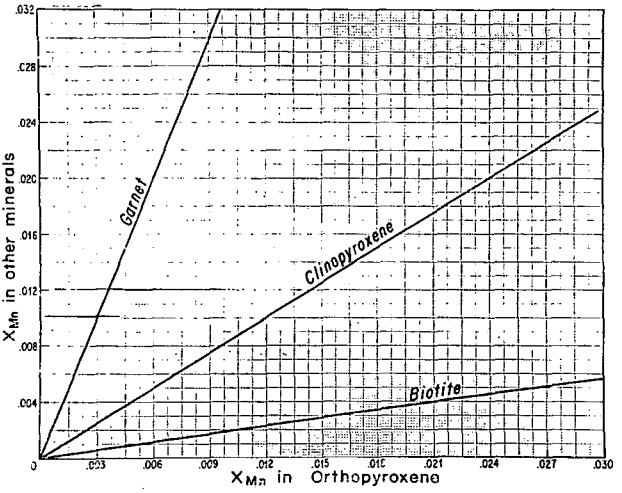

Fig. 2. Distribution of Mn between orthopyroxene and garnet, clinopyroxene, and biotite. Concentrations are in atomic percent.

Trace element distribution between coexisting phases is conveniently expressed by the distribution coefficient, K_D, which is the slope of a curve, near its origin, defined by the equation:

$$K_D = X_i^A / X_i^B$$

where, X_i^A is the atomic fraction of element i in mineral A

X_i^B is the atomic fraction of the same element i in coexisting mineral B.

For equilibrium between the two minerals, the data points should lie either on a straight line (ideal mixing) or a smooth curve (non-ideal mixing). In the ferromagnesian silicates, major cations competing for the same coordination sites are Ca^{2+},

Mg^{2+}, Fe^{2+} and Mn^{2+}. Other cations, usually present in trace amounts, do not noticeably affect Mn^{2+} distribution. Thus, rewriting K_D in terms of Mn^{2+} and competing ions:

$$K_D = X^A_{Mn}/X^B_{Mn}$$
$$= \frac{(Mn/Mn+Fe+Mg+Ca)^A}{(Mn/Mn+Fe+Mg+Ca)^B}$$

where the metals are divalent ions. The data used for calculation of average K_D values are from a variety of sources as given in Appendix 1. Most were available as chemical analyses of coexisting phases; equilibrium conditions stated by the authors were accepted unless the data failed to produce either a straight line or smooth curve, whereupon the data were rejected. Except for the mineral pair garnet/biotite for which the values are especially inconsistent, scatter in the data is about 20%. Distribution curves for Mn^{2+} are presented for 13 silicate mineral pairs common to protore assemblages surrounding metamorphic manganese deposits in *Figures 1*, *2* and *3*. The results suggest an increasing affinity for Mn^{2+} through the sequence biotite-chlorite-hornblende-actinolite-clinopyroxene, cummingtonite-orthopyroxene-garnet. Theoretical evaluations of manganese distribution in similar silicates by BURNS [1970] and WHITE [1971] add further support to this observation. Average numerical K_D values taken from the curves are tabulated in an appendix to this paper.

Several studies have implied a temperature-dependence of Mn^{2+} distribution between mineral pairs. Although such a *"geothermometer"* has been used with some success for Fe^{2+}, the available data do not show that Mn^{2+} distribution correlates well with temperature. It is conceivable that a manganese geothermometer the more promising examples is garnet/biotite partitioning, but more work is needed to verify the temperature dependency.

There is clear evidence that manganese content decreases with increasing temperature in both garnet and biotite. In garnet, for example, higher temperatures

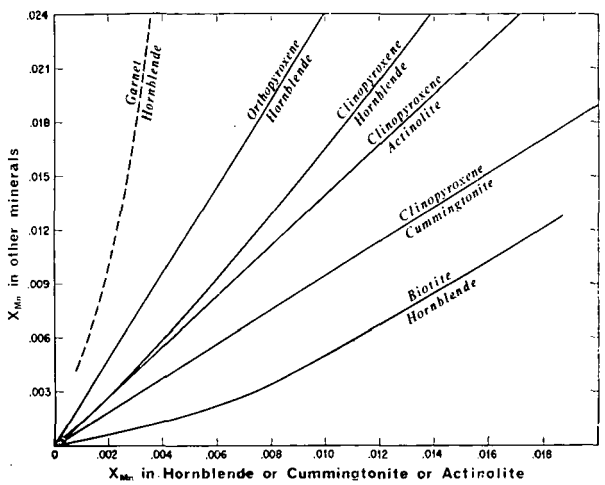

Fig. 3. Distribution of Mn between mineral pairs. Concentrations, in atomic percent, are given on the ordinate for Mn in garnet, orthopyroxene, clinopyroxene, and biotite, and on the abscissa for hornblende, cummingtonite, and actinolite for respective mineral pairs.

shrink cation sites to cause a decrease in manganese content [MIYASHIRO, 1953; LAMBERT, 1959; ENGEL and ENGEL, 1960; STURT, 1962]. In fact, STURT found that Mn-content of garnets was a very sensitive index of metamorphic grade throughout a section of pelitic schists. Although SEN and CHAKRABORTY [1968] found an opposite correlation with temperature, they attribute this to disequilibrium and inhomogeneity but other variables may also affect the Mn content of silicates. SAXENA [1968] cautions that high manganese concentrations in garnet contribute to diadochic Ca^{2+} effects — leading to somewhat unpredictable K_D values. Similar to that of garnet, there is apparently a coincident decrease in manganese content in biotite with increasing temperature. This decreases the temperature dependence of K_D for garnet/biotite but suggests an important, yet imperfectly known, function of temperature of manganese content in garnet and biotite. Other functional relations between K_D and temperature for the remaining mineral pairs presented in this paper cannot be resolved without much more detailed data than now available. These include metamorphic grade, temperatures, and concentrations of elements competing for manganese-containing sites.

In summary, a clearer chemical understanding of causes of manganese distribution in ferromagnesian silicates, relative to other transition metals, has become possible through the use of crystal field theory. Values of K_D for Mn^{2+} in 13 coexisting silicate pairs suggest two important relationships: *(1)* manganese distribution is affected by temperature and *(2)* manganese partitioning is sensitive to total manganese concentration. A *"manganese geothermometer"* based on distribution coefficients cannot be reliably evaluated until considerably more data are available. There is a distinct correlation, however, between total manganese content in the host rock and manganese distribution in coexisting silicates, so that we may soon be able to predict the minimum concentration levels at which formation of primary manganese silicates, such as rhodonite, will begin in metamorphic assemblages.

REFERENCES

ATHERTON, M. P. [1968]: The variation in garnet, biotite and chlorite composition in medium grade pelitic rocks from the Dalradian, Scotland, with particular reference to the zonation in garnet: Contr. Miner. and Petrol. *18*, 347—371.

BLACKBURN, W. H. [1968]: The spatial extent of chemical equilibrium in some high-grade metamorphic rocks from Grenville of Southeastern Ontario: Contr. Miner. and Petrol. *19*, 72—92.

BUDDINGTON, A. F. [1964]: Distribution of MnO between coexisting ilmenite and magnetite: in Advancing Frontiers in Geology and Geophysics: Subramanian, A. P., Ed. Ind. Geophys. Union, Hyderabad, India.

BURNS, R. G. [1970]: Mineralogical Applications of Crystal Field Theory, Cambridge Univ. Press.

BURNS, R. G. [1970]: Site preferences of transition metal ions in silicate crystal structures: Chem. Geol. *5*, 275—283.

CLARK, J. R., APPLEMAN, D. E. and PAPIKE, J. J. [1969]: Crystal-chemical characterization of clinopyroxenes based on eight new structure refinements: Crystal Chemistry and Phase Petrology, M.S.A. Spec. Paper 2, Ed. J. J. Papike, pp. 31—50.

CLIFFORD, T. N. [1960]: Spessartine and magnesium biotite in coticule-bearing rocks from Mill Hollow, Alstead Township, N. H., U.S.A. — A contribution to the petrology of metamorphosed manganiferous sediments — N. Jb. Min. Abh. *94*, (II), 1369—1400.

ENGEL, A. E. and ENGEL, C. G. [1962]: Progressive metamorphism and granitization of the major paragneiss, northwest Adirondack Mtns., New York: Geol. Soc. America, Buddington Vol., 37—82.

GORBATSCHEV, ROLAND [1968]: Distribution of elements between cordierite, biotite, and garnet: N. Jb. Miner. Abh. *110* (1) 57—80.

KRETZ, RALPH [1959]: Chemical study of garnet, biotite and hornblende from gneisses of southwestern Quebec, with emphasis on distribution of elements in co-existing minerals: J. Geol. *67*, 371—402.
KRETZ, RALPH [1960]: The distribution of certain elements among coexisting calcic pyroxenes, calcic amphiboles and biotites in skarns: Geochim. Cosmochim. Acta *20*, 161—191.
KRETZ, RALPH [1961]: Some applications of thermodynamics to coexisting minerals of variable composition. Examples: Orthopyroxene-Clinopyroxene and Orthopyroxene-Garnet: J. Geol. *69* (4), 361—387.
KRETZ, RALPH [1963]: Distribution of magnesium and iron between orthopyroxene and calcic pyroxene in natural mineral assemblages: J. Geol. *71*, 773—784.
KRETZ, RALPH [1964]: Analysis of equilibrium in garnet-biotite-sillimanite gneisses from Quebec: J. Petrol. *5*, 1—20.
LAMBERT, R. ST. J. [1959]: The mineralogy and metamorphism of the Moine schists of the Morar and Knoydart districts of Inverness-shine: Roy. Soc. Edin. Trans. *63* (3) 553—588.
LEELANANDAM, C. [1967]: Chemical study of pyroxenes from the charnockitic rocks of Kondapalli (Andhra Pradesh), India, with emphasis on the distribution of elements in coexisting pyroxenes: Min. Mag. *36*, 153—179.
MATEJOVSKA, O. [1970]: Composition of coexisting garnet and biotite from some granulites of Moldanubicum, Czechoslovakia: N. Jahrb. Miner. Monatsh. *6*, 249—262.
MIYASHIRO, A. [1953]: Progressive metamorphism of calcium-rich rocks of the Gosaisyo-Takanuki district, Abukuma, Japan: Jap. Jour. Geol. Geog. *23*, 81—107.
MUELLER, R. F. [1961]: Analysis of relations among Mg Fe and Mn in certain metamorphic minerals: Geochimica et Cosmochimica Acta *25*, 267—296.
PAPIKE, J. J., ROSS, M. and CLARK, J. R. [1969]: Crystal-chemical characterization of clinoamphiboles: Crystal Chemistry and Phase Petrology, M. S. A. Spec. Paper 2, Ed. J. J. Papike, pp. 117—136.
RAY, S. and SEN, S. K. [1970]: Partitioning of major exchangeable cations among orthopyroxene, calcic pyroxene and hornblende in basic granulites from Madras: N. Jb. Miner. Abh. *114*, 61—88.
SAXENA, S. K. [1966]: Distribution of elements between coexisting biotite and hornblende in metamorphic caledonides, lying to the west and northwest of Trondheim, Norway: Neues Jahrb. Min. Monatsh. *3*, 67—80.
SAXENA, S. K. [1968]: Chemical study of phase equilibria in charnockites, Varberg, Sweden: Amer. Min. *53*, 1674—1695.
SAXENA, S. K. [1968]: Distribution of elements among coexisting minerals and the nature of solid solution in garnet: Am. Min. *53*, 994—1014.
SAXENA, S. K. [1968]: Crystal-chemical aspects of distribution of elements among certain coexisting rock-forming silicates: N. Jb. Miner., Abh. *108*, 292—323.
SAXENA, S. K. [1968]: Nature of mixing in ferromagnesian silicates and the significance of the distribution coefficient: Neues. Jahrb. Miner. Monats. *8*, 275—286.
SAXENA, S. K. [1968]: Distribution of elements between coexisting minerals and the nature of solid solution in garnet: Amer. Min *53*, 994—1015.
SAXENA, S. K. [1969]: Distribution of elements in coexisting minerals and the problem of chemical disequilibrium in metamorphosed basic rocks: Contr. Miner. and Petrol. *20*, 177—197.
SCHWARCZ, HENRY P. [1967]: The effect of crystal field stabilization on the distribution of transition metals between metamorphic minerals: Geochimica et Cosmochimica Acta *31*, 503—517.
SEN, S. K. and CHAKRABORTY, K. R. [1968]: Magnesium-iron exchange equilibrium in garnet biotite and metamorphic grade: N. Jb. Miner. Abh. *108*, 181—207.
STURT, BRIAN [1962]: The composition of garnets from pelitic schists in relation to the grade of regional metamorphism: J. of Petrology *3*, Part 2, 181—191.
WHITE, W. B. [1971]: Electronic properties of minerals: Lecture Notes, Dept. of Geosciences, Pennsylvania State Univ.
WYNNE-EDWARDS, H. R. and HAY, P. W. [1963]: Coexisting cordierite and garnet in regionally metamorphosed rocks from the Westport area, Ontario: Can. Min. *7*, 453—478.

Manuscript received, June 15, 1972.

R. K. CORMICK, B. A. CRERAR
and H. L. BARNES
Ore Deposits Research Section, The Pennsylvania State University, 208 Deike Building, University Park, Pennsylvania 16802, U. S. A.

APPENDIX 1

Distribution Coefficient Data (primarily for the amphibolite facies)

Mineral Pair	K_D	Qualifying Remarks	Sources of Data
Garnet/Biotite	22 (X^{Bi}_{Mn} reaches max. at. 015)	considerable scatter in data; some T, X dependence	KRETZ [1959, 1964]; WYNNE-EDWARDS & HAY [1963]; GORBATSCHEV [1968]; SEN & CHAKRABORTY [1968]; BLACKBURN [1968]; MATEJOVSKA [1970], CLIFFORD [1960]
Hornblende/ Biotite	3.0 (at low ΣMn) 1.5 (at higher ΣMn)	data slim but good; some T, X dependence	KRETZ [1959, 1960]; MOXHAM [1964]; SAXENA [1968, 1969]
Chlorite/Biotite	1.6 (different from original source due to recalculations)	very little good data; T, X dependence uncertain	ATHERTON [1968]
Clinopyroxene/ Biotite	3.1 (increasing but not definite)	not enough data to substantiate results	KRETZ [1960]: SAXENA [1969]
Orthopyroxene/ Biotite	5.25 (linear)	not enough data to resolve P, T, X dependence	SAXENA [1969]
Garnet/ Orthopyroxene	3.3 (linear)	good data, but only from one area	KRETZ [1961]
Orthopyroxene/ Clinopyroxene	1.2 (linear)	differs from sources due to recalculation	SAXENA [1968]; BURNS [1970] MUELLER [1961]; RAY & SEN [1970]; SAXENA [1969]; KRETZ [1963]; LEELANANDAM [1967]
Garnet/ Hornblende	5?	data is scarce and poor; line only dashed and approximated	KRETZ [1959]; SAXENA [1968]
Clinopyroxene/ Hornblende	1.3 (at low ΣMn) 1.4 (at higher ΣMn)	data suggests compositional dependence	SAXENA [1968*a*, *b*, 1969]; KRETZ [1960]; RAY & SEN [1970]
Orthopyroxene/ Hornblende	2.4 (essentially linear)	more scatter; data probably quite good	SAXENA [1968*a*, *b*, 1969]; RAY & SEN [1970]
Cummingtonite/ Clinopyroxene	1.05 (linear)	very little data; probably good though	MUELLER [1961]
Clinopyroxene/ Actinolite	1.4 (linear)	may be non-linear but not enough data	MUELLER [1961]
Ilmenite/ Magnetite	8 (linear)	only one source; limited ΣMn range	BUDDINGTON [1964]

Acta Mineralogica-Petrographica, Szeged, XX/2, 217—226, 1972

ORGANIC CONTROLS ON THE SEDIMENTARY GEOCHEMISTRY OF MANGANESE*

D. A. CRERAR, R. K. CORMICK and H. L. BARNES

The sedimentary behavior of the element Mn is influenced by a wide variety of organic reactions and processes. In this discussion, we shall trace the sedimentary cycle of Mn, noting at each step some of the more important of these organic controls. To provide the necessary background, we first review the predominant inorganic controls on Mn solubility.

During weathering, Mn is leached typically after the mobile alkalis and alkaline earths, and just before or directly with the relatively immobile metals Fe and Al. This sequence is illustrated on the first figure which gives the solubilities of quartz and the simple oxides of Mn, Fe, and Al as a function of pH. The Mn curve has been calculated for three separate values of Eh. Note that Mn solubility exceeds that of Fe and Al by six or seven orders of magnitude for any given Eh and acid pH. Raising soil acidity markedly increases leaching capability and metal oxide solubility. Similarly, solubility is far greater in reducing than in oxidizing environments. Compare the position of the Mn oxide curves at the different Eh values shown. At any one pH, Mn solubility will increase by seven orders of magnitude on reducing Eh from 0.7 to 0.3 volts. Note that Al solubility changes only with acidity, not Eh.

Obviously, any agent capable of acidifying and/or reducing a weathering zone will increase mobility of Fe and Mn. Simplified reactions are given on the second figure. With the free electrons on the left side, these reactions indicate reductions. The hydrogen ion for such reactions is commonly contributed in nature by the organic oxy-acids of sulfur, nitrogen, phosphorus and carbon dioxide.

$$(1) \quad Al(OH)_3(C) + 3H^+ \rightarrow Al^{3+} + 3H_2O$$

$$(2) \quad Fe(OH)_3(\text{amorph.}) + e^- + 3H^+ \rightarrow Fe^{2+} + 3H_2O$$

$$(3) \quad MnOOH(C) + 3H^+ + e^- \rightarrow Mn^{2+} + 2H_2O$$

$$(4) \quad 2H_2O + CH_2O \rightarrow HCO_3^- + 5H^+ + 5e^-$$

Fig. 2. Solvation reactions involving Al, Fe and Mn oxyhydroxides and simple carbohydrates in weathering environments

In addition to these simple inorganic controls on Mn solubility, there are even more important organic reactions. Take, for example, simple organic decay reactions such as number *4* on this figure. Here, the decay of one mole of the simplified

* Lecture delivered at the technical session of the Commission on Manganese (IAGOD) during the XXIV IGC, 25 August, 1972, Montreal, Canada.

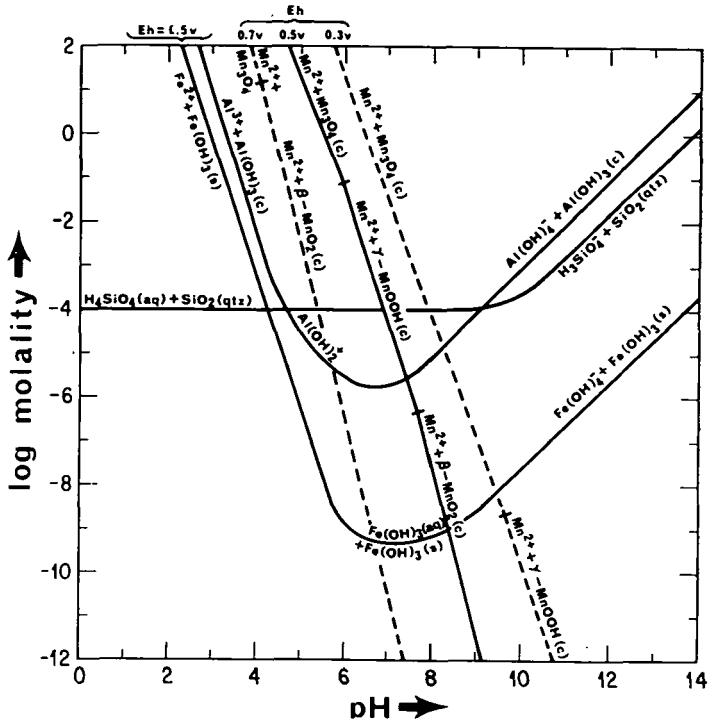

Fig. 1. Solubilities of Fe, Al, and Mn oxyhydroxides in weathering environments as a function of pH. Mn solubilities contoured in Eh.

carbohydrate, CH_2O, produces a sufficient number of electrons to reduce and dissolve five moles of manganite, and sufficient hydrogen ion to dissolve almost two moles. With more realistic complex hydrocarbons, this efficiency is dramatically increased. Organic decay, such as reaction *4*, is catalytically accelerated by simple oxidizing bacteria which thereby indirectly increase Mn dissolution. It is also possible that Mn-specific soil bacteria might directly solubilize the element in much the same manner as those known to corrode Fe. PERKINS and NOVIELLI [1962] for example, have isolated a Mn-specific soil bacterium capable of leaching most of the element from manganiferous rocks.

In densely vegetated regions, a significant quantity of Mn may be mobilized by simple plant accumulation and decay. Much of the Mn held within plant tissue may be returned to the soil in an immediately water-soluble form. LEVANIDOV [1957] for example, has found that birch leaves of the Southern Ural Steppes annually deposit about 2 Kg Mn per acre, some 50% of this being water-soluble. In such organic-rich weathering environments, both soluble and insoluble Mn complexes may form with many of the common organic constituents of soils. Chemical processes involved here include surface adsorption, ion exchange, chelation, and the formation of protective colloids. Organic reactants include amino and fatty acids, polysaccharides, amino sugars, porphyrins, and humic and carboxylic acids. In *figure 3* we have outlined a generalized humic acid reaction scheme first proposed by ONG, SWANSON and BISQUE [1970]. In part *A* of the reaction Mn^{2+} ions are

bound chemically to suitable organic ligands. Physical aging of the resultant complex and the possible adsorption of additional Mn^{2+} ions result in the flocculation and eventual precipitation of Mn humates shown by steps *B* and *C*.

$$\text{ORGANIC ACID} + 2Mn^{2+} \xrightarrow[\text{(chelation)}]{A} \text{Mn-ORGANIC COMPLEX (hydrophilic)} + Mn^{2+}$$

$$\text{Mn-ORGANIC COMPLEX (hydrophobic)} \xrightleftharpoons{B} \text{Mn-ORGANIC COMPLEX (hydrophobic)} \xrightarrow{C} \text{Mn-HUMATES} \downarrow$$

Fig. 3. Manganese and humic acid reaction mechanism

K	$Mn^{2+} + L^- = MnL^+$
$10^{3.9}$	DIGALLIC (TANNIC) ACID
$10^{2.16}$	GALLIC ACID
$10^{2.15}$ / $10^{3.7}$	FULVIC ACID
$10^{2.55}$	OXALIC ACID
$10^{3.29}$	MALONIC ACID

Fig. 4. Equilibrium constants for organic Mn complexes. $Mn^{2+} + L = MnL^+$

Compiled data on Mn organic complexes of geological interest are summarized in *figure 4*. These complexes form by reaction with the indicated organic acids, all of which occur in natural surface waters. Note that numerical values of all complexing constants are relatively high, showing a strong tendency towards complex formation. The fact that all constants agree to within an order of magnitude probably indicates similar bonding mechanisms by phenol, amide or carboxyl functional groups, and permits generalizing these data to high molecular weight organic compounds. Consequently, we may use these data to approximate soubility of naturally occuring organic Mn complexes in general. The results are shown in *figure 5* which compares concentrations of organic complexes and simple inorganic Mn ions in surface waters. Mn solubilities are plotted for typical conditions at Eh = 0.5 V and total carbonate = 10^{-3} m; total soluble organic concentrations of 10^{-2}, 10^{-4}, and 10^{-6} m have been used as estimates of the range expected in natural waters. When organic concentrations approach saturation levels of 10^{-2} to 10^{-4} molal characteristic of humate-rich soils, bogs and swamps, organic complexing may exceed other dissolution mechanisms by as much as several orders of magnitude. Add to this the further possibility of Mn transport by poly-nuclear and multi-ligand complexes or suspended organic colloids, and the pre-eminence of organic agents in weathering Mn from rocks becomes quite apparent.

With this chemical background, let us take a brief look at Mn behavior in certain soil types. Because acidity, total organic content, and rate of organic decay are predominant weathering controls, it is not surprising to find characteristically high Mn mobility in the humate-rich podzols and tundras of the northern temperature and subarctic climatic zones, as shown in *figure 6a*. Bog, lake, and stream-bed deposits

of both Fe and Mn are thus common in these regions and are not, as a rule, found under other climate conditions.

In tropical and subtropical humid climates, chemical weathering is greatly accelerated and soil profiles frequently exceed 100 m in depth. See *figure 6b*. Here however, total organic content is diluted by the actual bulk of soil. In addition, true laterites and bauxites do not support dense vegetation as soil fertility is reduced by effective leaching of essential alkali and alkaline-earth nutrients. As a rule then, Mn mobility is reduced, while Fe and Al commonly remain *in situ*. Residual Mn deposits, though not as common as bauxites and laterites, do form under tropical conditions. In general, the element may be leached or accumulated, thereby acting as a sensitive indicator of subtle variations in Eh, pH or total organic content.

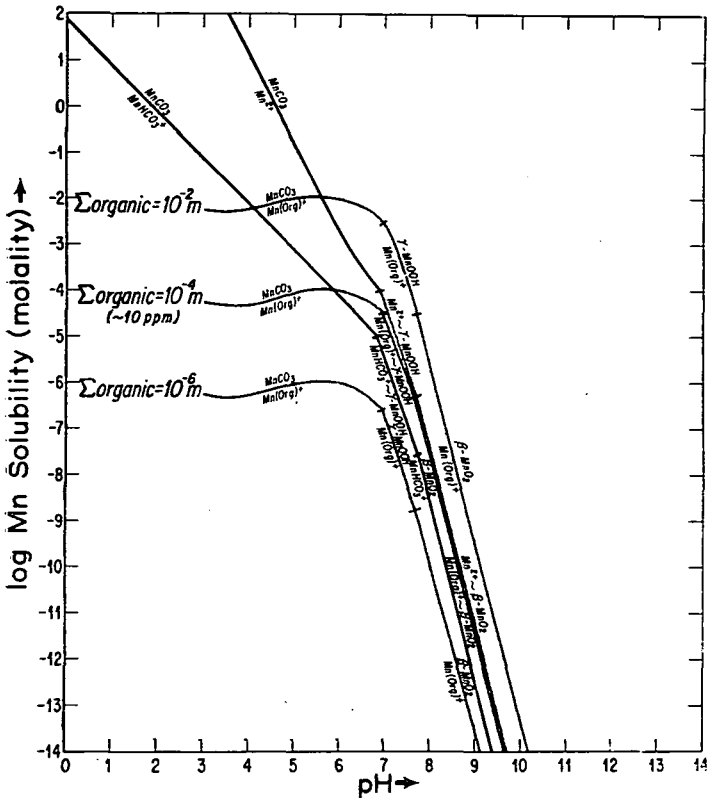

Fig. 5. Typical inorganic and organic complexing of manganese at 25°C. Eh. 0,5 *v*, and total carbonate activity at 10^{-3} molal.

In the arid regions illustrated by *figure 6c*, organic activity is minimized and Mn mobility is limited by simple inorganic mechanisms. Consequently, most Fe and Al remains in place and Mn only migrates locally resulting in surface deposits such as "desert varnish". An estimated 75% of Southern California desert bedrock is coated with a thin layer of amorphous material of this type, compositionally similar to marine Mn nodules [ENGEL and SHARP, 1963].

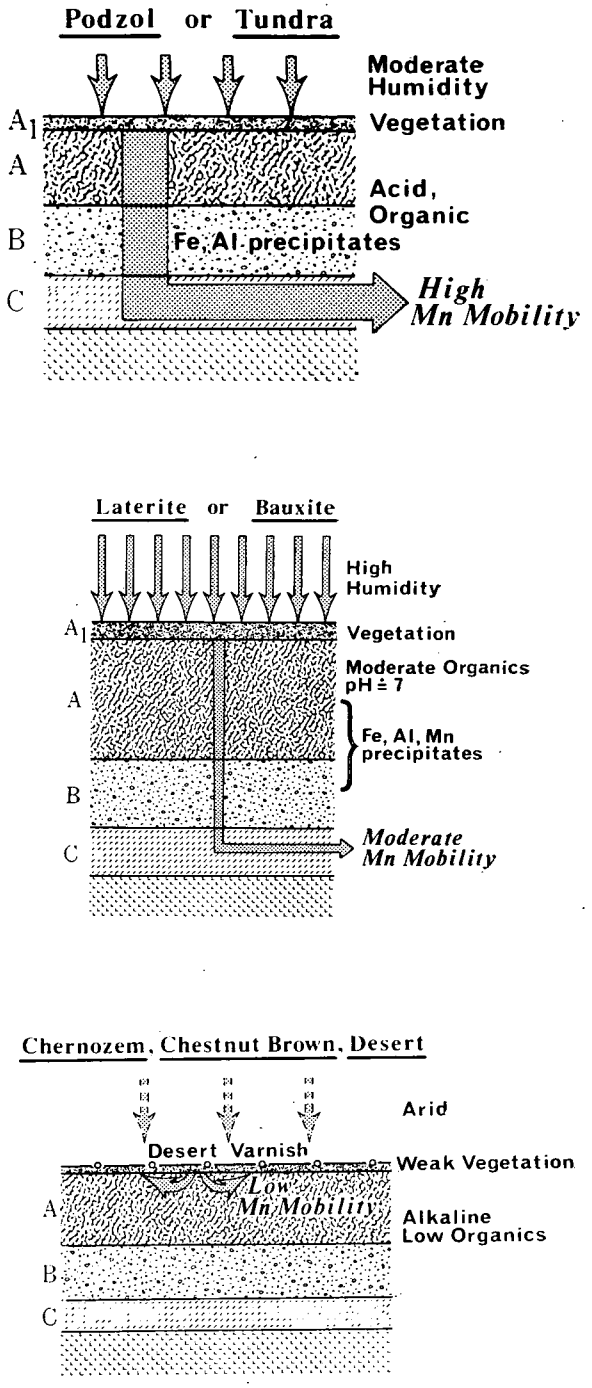

Fig. 6a, b, c. Manganese mobility in generalized soil profiles

Let us now combine these aspects of Mn behavior, considering their effect during transportational and depositional stages of the sedimentary cycle. Despite the fact that natural waters are nearly always undersaturated with respect to inorganic Mn species, there is good reason to believe that important concentrations may be transported as soluble or particulate organics. STRAKHOV [1967] for example, has found that over 50% of the total Mn dissolved in the Dneper R. travels as soluble humic acid compounds or complexes. He also finds that much of the Mn particulate fraction is associated with suspended organics. The situation is similar in the open oceans. Here, approximately 10% of the total Mn in seawater is colloidal or particulate, and only about 78% exists as simple inorganic ions. An additional 12% is complexed organically, or is at least, chemically associated with a sub-colloidal organic fraction [GOLDBERG and ARRHENIUS, 1958, RONA *et al,* 1962, HOOD and SLOWEY, 1964, SLOWEY, 1966, HOOD, 1967, SAXBY 1969]. The observed decrease in organic association on approaching marine environments, indicates that settling basins enroute to terminal marine outlets act as filters, effectively scavenging the larger, predominantly organic species.

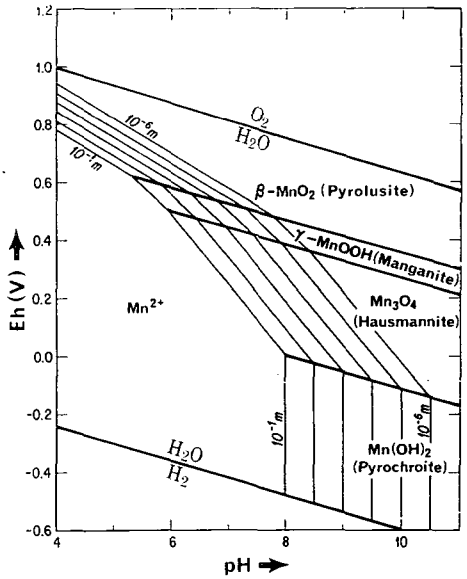

Fig. 7. Eh-pH diagram for system Mn-H_2O at 25°C, 1 atm. pressure. Contours represent Mn^{2+} molality.

Within any single depositional basin, marine or continental, sedimentary accumulation of Mn is primarily controlled by the effects of acidity and oxidation potential whether Mn is transported in inorganic or organic forms. *Figure 7* presents the Eh-pH relationships of common stable Mn oxyhydroxides. Note that solubility of any one phase given by the contours separating that phase from the Mn^{2+} ion field, decreases exponentially with increasing Eh and pH. Mn is thus most mobile in acid, reducing environments. Given two neighboring environments, one acid and/or reducing, the other basic and/or oxidizing, Mn will migrate from the former to the latter.

Precisely such a mechanism is provided during diagenesis on modern ocean floors, where the decay of buried organic detritus creates acid, reducing conditions at depth within the sediment. Refer to reaction *4, figure 2. Figure 8* presents a generalized chemical profile drawn from measurements on sediments in the Atlantic, Arctic, and Pacific Oceans [VAN DER WEIJDEN *et al.*, 1970, LI *et al.*, 1969, LYNN and BONATTI, 1965, BEZRUKOV, 1960, STRAKHOV, 1966, PRESLEY *et al.*, 1967]. Dissolved Mn and CO_2 increase with depth, Mn reaching a maximum while Eh and pH show a correlative decrease. The increased CO_2 at depth represents oxidation products of organic decay. Total Mn, constituting precipitated mineral phases, increases towards the surface. Assuming a roughly constant rate of Mn deposition, this data demonstrates that there must be an upward diagenetic migration of the element. Recent experimental studies support this conclusion [SHANKS, 1972]. Such a diagenetic migration can account for the large-scale surface accumulations of Mn characteristic of virtually all modern ocean basins.

An interesting corollary here is that too high an "active" or oxidizable sedimentary carbon content will effectively dissolve Mn right out of a deposit. Thus the thickness of marine surface oxidizing zones and associated Mn crusts correlates negatively with total oxidizable carbon in carbon-rich environments [PRICE and CALVERT, 1970, STRAKHOV, 1966, LYNN and BONATTI, 1965]. Oxidizing crusts of near-shore carbon-rich sediments are generally much thinner than deep-water equivalents where carbon has been previously oxidized during the long descent, or has been filtered out near river mouths. Similarly, highly organic stagnant conditions are capable of quantitatively leaching Mn from bottom sediments. For example, MANHEIM [1961, 1964, 1965] has shown that Mn migrates laterally away from stagnant reducing deeps of the Baltic Sea, forming oxide accumulations only in peripheral aerated regions. In the Black Sea, organic bottom waters and sediments are so reducing that, despite high dissolved concentrations of Mn, the metal will not accumulate as oxide crusts or concretions. Instead, Mn is carried as dis-

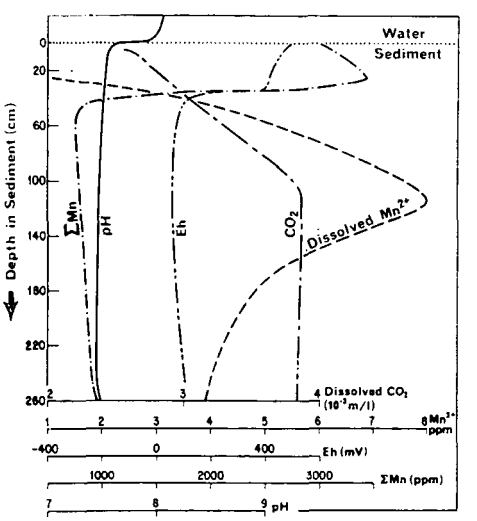

Fig. 8. Generalized geochemical profile of a marine sediment showing dissolved and total Mn variation with depth, Eh, pH and dissolved CO_2.

solved species in all but the uppermost aerated levels of sea water. STRAKHOV [1966] has estimated that 10^8 metric tons of dissolved Mn are borne by the lower, reducing waters of the Black Sea.

Similar diagenetic behavior occurs in manganiferous lake deposits, with the qualification that here the catalytic effects of Mn-specific bacteria vastly accelerates reaction times. PERFIL'EV and co-workers [1965] have found that lacustrine Fe—Mn ores commonly develop the layering shown in *figure 9*. An uppermost Mn-oxide zone is underlain by a similar Fe oxide crust. Im the lowermost reducing zone, total Mn and Fe are impoverished, but pore solutions commonly contain relatively high dissolved concentrations of both metals. Bacterial strains specific to either Fe or Mn occupy each of the three zones, oxidizing or reducing the metals as a necessary metabolic function. The net effect again is an accelerated upward migration of both Fe and Mn during diagenetic stages of sedimentation.

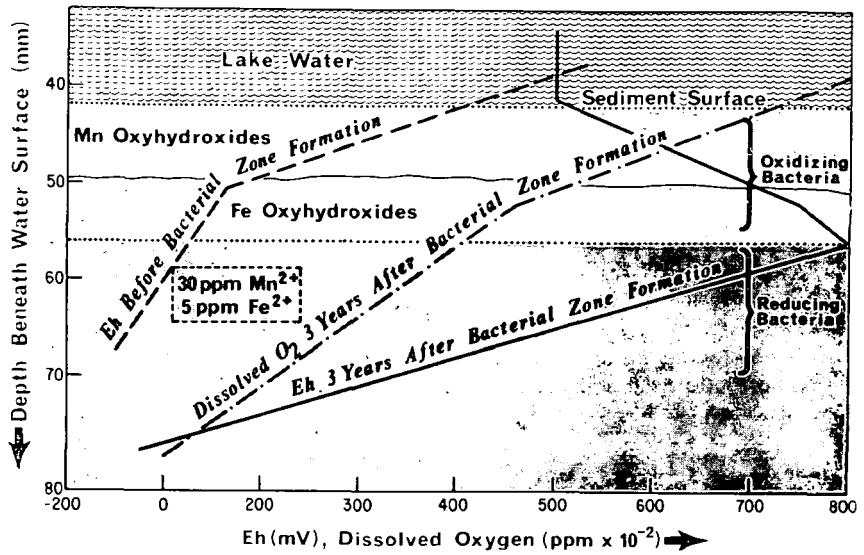

Fig. 9. Generalized geochemical profile of a lacustrine sediment showing Mn distribution, dissolved O_2, and Eh.

Interestingly enough, no comparable Mn-specific bacteria have yet been discovered in the marine environment despite the many similarities between continental and marine deposits. Such strains should be investigated, particularly in view of the current interest in marine Mn nodules. However, several preliminary investigations to date have produced only limited or negative results [GOLDBERG, 1961, GRAHAM, 1959, GRAHAM and COOPER, 1959].

In lacustrine, as in marine environments, a little bit of carbon goes a long way. Should total oxidizable carbon exceed specific limits, Mn mobility increases to the point where it is effectively washed away. STRAKHOV [1966] has proposed a theory relating the origin of Mn and Fe deposits to lateral variations in chemistry during the three major stages of lacustrine evolution. See *figure 10*. In youngest, oligotrophic lakes, waters are fresh, Eh and pH high, and total oxidizable carbon low. Ultrafine particles and suspensions are carried by waves out to quietest and deepest

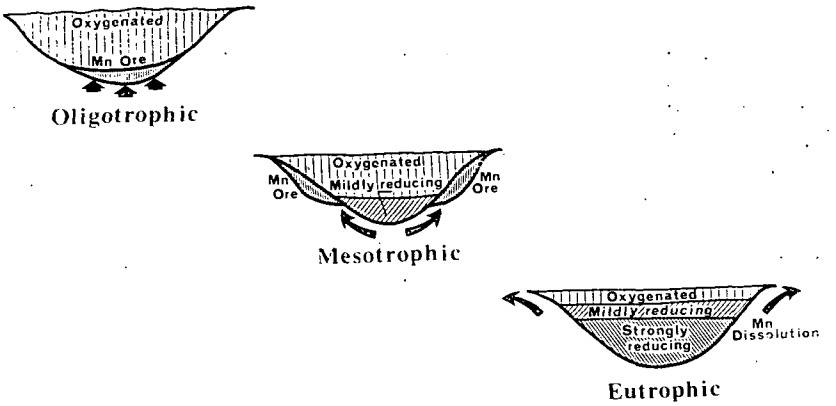

Fig. 10. Mn accumulation versus lacustrine evolution. Arrows indicate direction of diagenetic Mn migration.

reaches, where ferromanganese deposits readily accumulate. With increasing age and eutrophication, both Mn and Fe migrate to the margins of the reduced zone near aerated lake outlets.

In closing, we emphasize again that organic processes exert major and often predominant controls on the geochemical distribution of Mn at every phase of the sedimentary cycle. Inanimate processes include the formation of Mn-organic complexes, often outweighing inorganic ion concentrations by orders of magnitude in many soil and surface-water environments. Life forms such as bacteria contribute directly to the diagenetic behavior of Mn in lake deposits. Primary chemical variables such as Eh and pH are typically controlled by bacterially induced decay reactions of buried organic materials. The influence of organic processes on Mn behavior extends from weathering to depositional environments and must be given due weight in any consideration of Mn geochemistry.

REFERENCES

BEZRUKOV, P. L. [1960]: Sedimentation in the north-western part of the Pacific Ocean. Internat. Geol. Cong. 21, Copenhagen, 1960, Repts. pt. *10*, pp. 39—49.

ENGEL, C. G. and SHARP, R. P. [1958]: Chemical data on desert varnish. Bull. Geol. Soc. Amer. *69*, 487—518.

GOLDBERG, E. D. and ARRHENIUS, G. [1958]: Chemistry of Pacific pelagic sediments. Geochim. Cosmochim. Acta *13*, 153—212.

GOLDBERG, E. D. [1961]: Chemistry in the oceans. In Oceanography, ed. M. Sears, Amer. Assoc. Adv. Sci., pub. *67*, 583—597.

GRAHAM, J. [1959]: Metabolically induced precipitation of elements from sea water. Sci., *129*, 1428—1429.

GRAHAM, J. W. and COOPER, S. C. [1959]: Biological origin of manganese rich deposits of the sea floor. Nature *183*, 1050—1051.

HOOD, D. W. [1967]: Organic-inorganic interactions in the aquatic environment. Geol. Soc. Am. Ann. Meetings. Abs. p. 103, Spc. Pap. 115.

HOOD, D. W. and SLOWEY, J. F. [1964]: Texas A and M progress report, Proj. 276, AEC contract number AT-(40-1)-2799.

LEVANIDOV, L. YA [1957]: Manganese in the geochemical landscape of the South Ural forest-steppe. Uchenye Zapiski Chelabinsk, Otdel. Geograf. Obshchestva, SSSR V. *1957*, 137—143.

LI, Y. H., BISCHOFF, J., MATHIEU, G. [1969]: The migration of manganese in the Arctic Basin sediment. Earth Planet. Sci. Lett., *7*, 265—270.

LYNN, D. C. and BONATTI, E. [1965]: Mobility of Mn in diagenesis of deep sea sediments. Mar. Geol., *3*, 457—474.
MANHEIM, F. T. [1961]: A geochemical profile in the Baltic Sea. Geochim. Cosmochim. Acta *25*, 52—70.
MANHEIM, F. T. [1964]: Recent manganese deposits in the Baltic Sea. Program Geol. Soc. Amer. Ann. Met., 1964. p. 127.
MANHEIM, F. T. [1965]: Manganese-iron accumulation in the shallow-water environment. Narragansett Marine Lab., Occasional Publ. *3*, 217—276.
ONG, L. H., SWANSON, V. E., and BISQUE, R. E. [1970]: Natural organic acids as agents of chemical weathering. USGS Prof. Pap. *700-C*, 130—137.
PERFIL'EV, B. V., GABE, D. R., GAL'PERINA, A. M., RABINOVICH, V. A., SAPOTNITSKII, A. A., SHERMAN, É. É., TROSHANOV, É. P., [1965]: Applied capillary microscopy. The role of microorganisms in the formation of iron-manganese deposits. 122 pp., Consultants Bureau, N. Y.
PERKINS, E. C. and NOVIELLI, F. [1962]: Bacterial leaching of Mn ores. U. S. Bur. Mines. Rep. of Invest. *6102*, 11 pp.
PRESLEY, B. J., BROOKS, R. R., and KAPLAN, I. R. [1967]: Manganese and related elements in the interstitial water of marine sediments. Sci. *158*, 906—910.
PRICE' N. B. and CALVERT, S. E. [1970]: Compositional variation in Pacific Ocean ferromanganese nodules and its relationship to sediment accumulation rates. Marine Geol. *9*, 145—171.
RONA, E., HOOD, D. W., MUSE, L. and BUGLIO, B. [1962]: Activation analysis of manganese and zinc in sea water. Limnology and Oceanography *7*, 201—206.
SAXBY, J. D. [1969]: Metal organic chemistry of the geochemical cycle. Rev. Pure and Appl. Chem. *19*, 131—150.
SHANKS, W. C. [1972]: Experimental study of iron and manganese migration in marine sediments. Abst. GSA, Cordilleran Sect., 68th Ann. Meeting, V. 4., No. 3, Feb. 1972.
SLOWEY, J. F. [1966]: The distribution of copper, manganese and zinc in the ocean using neutron activation analysis. Texas A. and M. University, College Station, Univ. Microfilms, number 66-6532, 115 pp.
STRAKHOV, N. W. [1966]: Types of manganese accumulation in present-day basins: their significance in understanding of manganese mineralization. Internat. Geol. Rev., *8*, 1172—1196.
STRAKHOV, N. M. [1967]: Principles of lithogenesis. Ist Eng. Ed., V. 1, Oliver and Boyd, Edinburgh.
VAN DER WEIJDEN, C. H., SCHUILING, R. D., and DAS ,H. A. [1970]: Some geochemical characteristics of sediments from The North Atlantic Ocean. Marine Geol. *9*, 81—99.

Manuscript received, June 15, 1972.

D. A. CRERAR, R. K. CORMICK
and H. L. BARNES
Ore Deposits Research Section, The Pennsylvania State University, 208 Deike Building, University Park, Pennsylvania 16802, U. S. A.

Acta Mineralogica-Petrographica, Szeged, XX/2, 227—240, 1972.

THERMAL STABILITY AND OXIDATION OF Mn_3O_4*

GY. GRASSELLY

ABSTRACT. On the basis of thermal, X-ray, and infra-red investigations, it was found that Mn_3O_4 heated in air within the thermal stability range of Mn_2O_3 will be slowly oxidized to α-Mn_2O_3 if it is pure; however, oxidation will be initiated and accelerated by the presence of other manganese oxides and also by ferric oxide. If the possibility of oxidation is excluded, as in N_2 or CO_2 atmosphere, the Mn_3O_4 remains unchanged during prolonged heating in the temperature range cited above. However, Mn_2O_3 heated in a CO_2 atmosphere in its own thermal stability range will be decomposed into Mn_3O_4 and even more MnO appears as a new phase. These experimental facts presumably may be used in interpreting the formation of manganese oxide assemblages in different metamorphic processes.

INTRODUCTION

Thermal properties of artificial and natural manganese oxides, oxide hydrates, and manganese carbonate, as well as their transformations with increasing temperature were studied by several authors. The main results of these investigations were reviewed by SUPRIYA ROY [1972] in his paper about metamorphic manganese deposits.

It is well known — and therefore authors will not be cited here — that heated in air, different modifications of MnO_2 transform at about 560 °C into α-Mn_2O_3, which in turn transforms by further increase of temperature, according to some authors at 870 °C, according to others at 950 °C, into low temperature (tetragonal) Mn_3O_4. It is also known that at 1050 °C [D. H. DASGUPTA, 1965] or at 1160 ± 5 °C [J. J. VAN HOOK and M. L. KEITH, 1958] high temperature modification of Mn_3O_4 forms.

The study of solubility and oxidation of different manganese compounds, in the first line of manganese carbonate, as a function of pH and Eh of aqueous solutions is of great importance for interpreting the conditions of formation of supergene manganese oxide deposits. Similar importance is, however, to be attributed to studying thermal properties and transformations of manganese oxides from the point of view of formation of metamorphic manganese deposits.

As generally known, Mn_3O_4 is the stable oxide of manganese at higher temperatures above about 940 °C, i.e. the different manganese oxides and oxide hydrates transform into Mn_3O_4 at that temperature. Less data are found, however, in the related literature concerning the range of temperature and the conditions in which

* Lecture delivered at the technical session of the Commission on Manganese (IAGOD) during the XXIV IGC, 23 August, 1972, Montreal, Canada

the stability of Mn_3O_4 really exists. As the authors dealing with the metamorphism of manganese deposits point out, both chemical and mineral composition of the mineral assemblage formed during the metamorphism are strongly influenced by f_{CO_2} and f_{O_2} as well as by temperature and pressure and by the initial chemical and mineral composition of the metamorphized sediment.

The question arises, therefore, whether the Mn_3O_4 corresponding to hausmannite, at temperatures lower than its temperature of formation, shows changes to be taken into consideration in interpreting the formation of metamorphic manganese deposits.

OXIDATION OF Mn_3O_4

Oxidation in aqueous medium

References concerning oxidation of Mn_3O_4 in aqueous, slightly acidic media are to be found in the paper of several authors, such as MOTOAKI SATO [1955] and O. BRICKER [1966]. According to BRICKER during prolonged oxidation in slightly acidic aqueous medium the cinnamon brown colour of Mn_3O_4 became darker and, though the X-ray pattern remained the same as characteristic for Mn_3O_4, the grade of oxidation of the product proved to be $MnO_{1.44}$. BRICKER and HUEBNER [1969] similarly suppose that, during the oxidation mentioned above, γ-Mn_2O_3 was formed, the X-ray pattern of which cannot be distinguished from that of hausmannite.

Unpublished results [1964] of the present author support the above statements with the addition that, in strongly acidic medium and at higher temperatures, the oxidation of Mn_3O_4 does not end at the grade of oxidation $MnO_{1.5}$ corresponding to Mn_2O_3, but approaches that of MnO_2. According to our investigations, the same situation is found to be valid in the case of α-Mn_2O_3 treated with strongly acidic solutions at higher temperatures.

In strongly acidic medium (pH = 1) and at higher temperatures (40—60 °C) the oxidation was very intensive, and the grade of oxidation of the Mn_3O_4 treated reached $MnO_{1.437}$ after 3 hours, rose to $MnO_{1.659}$ after 10 hours and to $MnO_{1.70}$ after 24 hours. The water content increased almost linearly with the grade of oxidation from 0.57% to 3.86% after 5 hours and to 4.37% after 24 hours. The oxidation at pH = 1 and 25 °C is also definite, but its rate is lower; the grade of oxidation of Mn_3O_4 was $MnO_{1.44}$ after 24 hours treatment, and the water content reached 3.56%. A similar behaviour was found with α-Mn_2O_3, however, with a slower increase in grade of oxidation and water content.

The progress in time of the oxidation of Mn_3O_4 treated at 60 °C in a solution of pH = 1 could be well followed by IR-spectroscopic investigation of the products. While the spectrum of the sample treated 3 hours corresponded to that of Mn_3O_4, after 9 hours, and even more after 24 hours treatment, the spectra of the samples ceased to show the characteristics of Mn_3O_4; neither did the characteristic absorption bands of α-Mn_2O_3 appear, the spectrum resembled much more to the IR-spectrum of a cryptomelane species from Urkut (Hungary) or to that of an artificial γ-MnO_2.

Oxidation at higher temperatures

Oxidation of Mn_3O_4 between 250—550 °C in nitrogen-oxigen mixture (0—100% oxigen) is mentioned by H. R. OSWALD and M. J. WAMPETICH [1967]. According to these authors, in the oxidation of the small hausmannite grains an oxide of

Mn_5O_8 ($MnO_{1.60}$) composition is formed as a transitional step, which transforms into α-Mn_2O_3 above 550 °C.

The author [GY. GRASSELLY and É. KLIVÉNYI, 1956*a*, 1956*b*] called the attention to the fact, supported also by the present investigations and the results of the authors mentioned above that, though Mn_3O_4 is really the stable oxide of manganese above 940 °C, however, heated in air in the temperature range of stability of α-Mn_2O_3, it is oxidized into α-Mn_2O_3 in the presence of other manganese oxides.

The dependence on temperature and time of the oxidation of Mn_3O_4 into α-Mn_2O_3 can be especially well followed by thermal investigations. The initial temperature of oxidation, the beginning of the decomposition into Mn_3O_4 of the α-Mn_2O_3 formed during the former oxidation and the end of this retransformation, as well as the increase and the decrease in weight due to these changes can be especially well read from the TGA curves. Knowing the grade of oxidation, i.e. the composition of the starting material, the grade of oxidation belonging to different temperatures can be calculated from the data of TGA curves.

RESULTS OF THERMAL INVESTIGATIONS

Thermal investigations were performed with ERDEY-PAUL'K's "Derivatograph"; the heating rate was 10 °C/min. The instrument permits to record T, TGA, DTGA and DTA curves contemporaneously. From these, TGA curves obtained with uniform heating are presented in *Figs. 1* and *2*, while *Fig. 3* shows TGA curves during prolonged heating at constant temperature 650—670 °C.

In *Fig. 1*, curves *A*, *B* and *C* are TGA curves of the same Mn_3O_4 sample obtained by heating over 1000 °C, but with different rates of cooling of the products. In the case of curve, *A*, the sample was cooled slowly in a closed furnace after several hours ignition at 1050 °C; for curve *B* the cooling period was shorter than for curve *A*, while in the case of curve *C* it occurred in a comparatively short time. The rate of oxidation decreased in the order of the curves *A*, *B*, *C*: the slower the cooling of the Mn_3O_4 formed by ignition above 1000 °C was, the higher the quantities of Mn_3O_4 transformed into α-Mn_2O_3 between 600—800 °C; resulting an increase in weight which can be seen from the TGA curve. It can also be stated that the less the admixture of α-Mn_2O_3 to the Mn_3O_4 is, the higher the temperatures at which the oxidation starts: in curve *A* already at 500 °C, in curve *B* at 600 °C and in curve *C* at about 700 °C. As starting material for further investigations, this Mn_3O_4 sample was used.

The question may arise, how the oxidation of Mn_3O_4 is influenced by other manganese compounds present.

The answer to this question can be found in the TGA curves shown in *Fig. 1*, *2* and *3*.

In *Fig. 1*, beside the TGA curves of the Mn_3O_4 samples mentioned above those of Mn_3O_4 samples containing 1% of β-MnO_2, γ-MnO_2 and η-MnO_2, respectively, are presented, with the starting temperature of oxidation. The grade of oxidation calculated from the TGA curves at 650—660 °C is also given, as well as that for the temperature 870—880 °C at which the decomposition of α-Mn_2O_3 formed by oxidation of Mn_3O_4 begins.

On the basis of TGA curves of *Fig. 1* the following statements can be made:

a) While in the TGA curve of the comparatively pure Mn_3O_4 only oxidation of negligible degree can be seen, the oxidation of Mn_3O_4 to α-Mn_2O_3 in the thermal

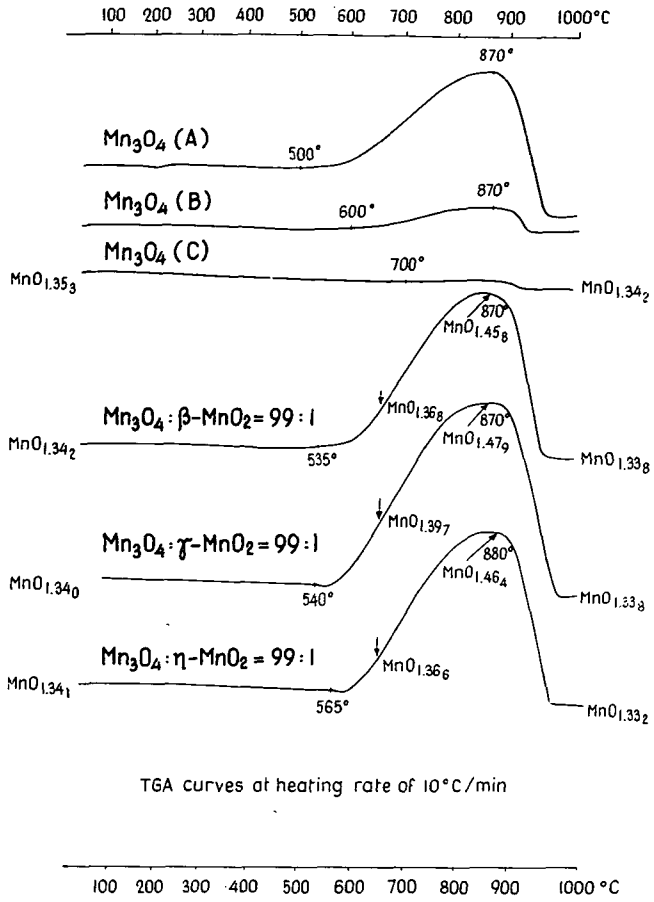

Fig. 1. TGA curves of Mn_3O_4 and mixtures of Mn_3O_4 with MnO_2-modifications heated in air with 10 °C/min rate (see the text)

stability range of the latter is significantly accelerated by adding 1% MnO_2-modification to the Mn_3O_4.

b) The starting temperature of the oxidation seems to be influenced by the character of the MnO_2; the oxidation starts at a substantially lower temperature — depending on the MnO_2-modification present — than that of pure Mn_3O_4.

c) The most intensive effect on the oxidation of Mn_3O_4 was exerted by γ-MnO_2.

d) With the heating rate 10 °C/min used the product at 870—880 °C approximates fairly well the composition $MnO_{1.50}$ corresponding to α-Mn_2O_3, though to reach this composition a more prolonged heating would be necessary.

Thus, with the heating rate mentioned the predominant part of the Mn_3O_4 was oxidized to α-Mn_2O_3 up to 870 °C.

e) At this temperature the transformation of the Mn_2O_3 into Mn_3O_4 begins. As can be seen from the TGA curves, this process is faster (the corresponding section of the curve is steeper) than the preceeding oxidation. The transformation

into Mn_3O_4 occurs between 870—970 °C, the rate of the reaction being the highest at about 940—950 °C. The composition of the resulting Mn_3O_4 (after rapid cooling) is near to the ideal $MnO_{1.33}$.

In *Fig. 2* beside the TGA curves of the starting Mn_3O_4 and of α-Mn_2O_3 teh curves of different mixtures of both materials, as well as those of samples containign 1% manganite and Fe_2O_3, respectively, are shown. Similarly as in *Fig. 1*, the starting temperatures of oxidation and the grades of oxidation reached at 650—660 °C and about 860—870 °C are indicated.

The TGA curves of *Fig. 2* permit the following statements:

a) By comparing the TGA curve of pure Mn_3O_4 with those of the mixtures it can be seen that the oxidation of Mn_3O_4 is significantly accelerated by the presence of other manganese oxides in the temperature range 500—870 °C.

b) The starting temperature of oxidation depends on quality and quantity of the material added to Mn_3O_4. In the presence of 50% α-Mn_2O_3 the oxidation begins at about 460 °C, with 1% α-Mn_2O_3 at about 490 °C, while in the presence

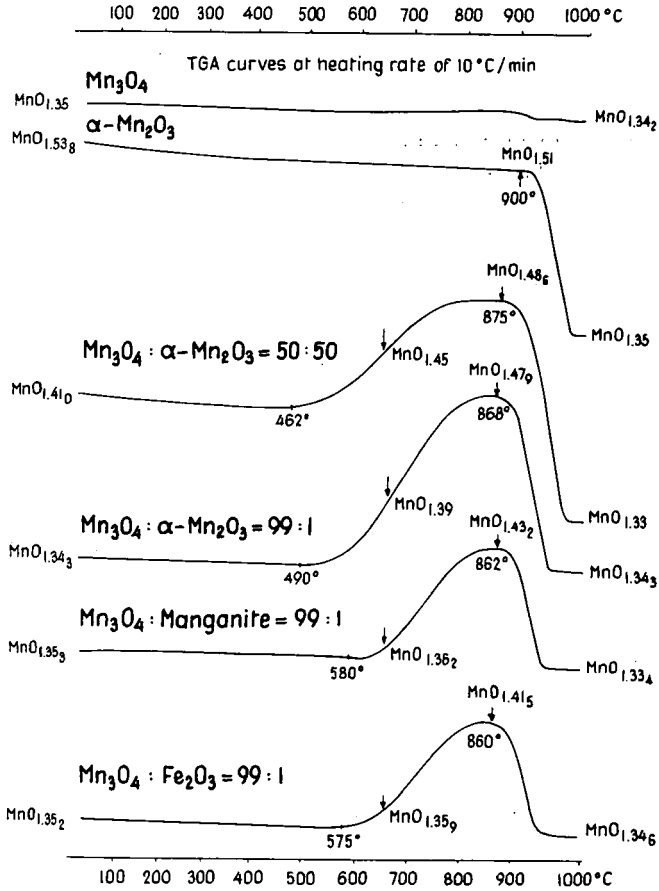

Fig. 2. TGA curves of Mn_3O_4, Mn_2O_3 and mixtures of Mn_3O_4 — α-Mn_2O_3, Mn_3O_4 — manganite and Mn_3O_4 — Fe_2O_3 heated in air (see the text)

of manganite and Fe_2O_3 the starting temperature of oxidation is between 570—580 °C.

c) The most intensive effect on the oxidation of Mn_3O_4 is exerted by α-Mn_2O_3, the oxidation being more intensive than in presence of other compounds, MnO_2 included.

d) With the given heating rate the oxidation terminates at 860—870 °C and the grade of oxidation at this temperature is more or less near to the composition of Mn_2O_3 depending on the material added. At the same temperature the retransformation into Mn_3O_4 begins.

e) The composition of the Mn_3O_4 formed as endproduct (with rapid cooling) is near to the ideal also in this case

In *Fig. 3* TGA curves of Mn_3O_4 samples containing γ-MnO_2 (curve *A*) and α-Mn_2O_3 (curves *B*, *C*, *D*) in the concentrations indicated as well as those of comparatively pure Mn_3O_4 samples, rapidly cooled after heating, (curves *E*, *F*) are presented.

Up to the temperature indicated (500 °C, 660—670 °C and 650 °C, respectively) the heating rate was 10 °C/min, then the heating was pursued at the same temperature for 3 hours. On the TGA curves the composition calculated from the increase in weight at the given temperature is indicated (inrespective of the material being not monophase) as well as the composition (grade of oxidation) reached after 1, 2 and 3 hours.

From the TGA curves of *Fig. 3* the following conclusions can be drawn:

a) In DTA and TGA investigations with the heating rate generally used (here 10 °C/min), the possible oxidation may be overlooked *(Fig. 1,* curve *C)* because no significant changes can be observed neither in the DTA nor in the TGA curves. This is comprehensible, namely the oxidation of Mn_3O_4 to α-Mn_2O_3 is not an instantaneous reaction, the rate of which being possible influenced by several factors. Therefore, even if no oxidation is observed in the usual DTA-TGA investigation, by heating the sample at a given temperature for a shorter or longer time the fact of the oxidation will become evident.

Curves *E* and *F* of *Fig. 3* are TGA curves of two relatively pure Mn_3O_4 samples heated at 650 °C for 3 hours. DTA and TGA curves of these samples with normal heating rate showed practically no changes. At the same time heating the samples at 650 °C, the oxidation begins and after 3 hours the grade of oxidation of both Mn_3O_4 samples reaches approximately the value $MnO_{1.46}$, though it is perceivable that the oxidation has not been finished during the time.

b) The initiating and accelerating effect exerted on the oxidation of Mn_3O_4 by other manganese oxides can be well observed by comparing the curves *A* to *D* and *E*, *F*. The Mn_3O_4, the oxidation of which begins only slowly at 650 °C and which reaches the grade of oxidation $MnO_{1.38}$ after 1 hour in pure state, with admixture of 1 % of other manganese oxides will exceed this value at the moment of reaching the temperature 650—660 °C and after 1 hour the grade of oxidation will be almost stabilized with the value $MnO_{1.48}$.

c) According to *Fig. 2* the oxidation of the mixture 99 % Mn_3O_4 — 1 % α-Mn_2O_3 starts at 490—500 °C. This temperature does not belong to the thermal stability range of α-Mn_2O_3, being under the lower limit of the latter. The oxidation of the mixture begins, however, at this temperature (curve *D*), though the process is slow and the grade of oxidation rises only to $MnO_{1.39}$ after 3 hours. Heating the sample for a suitable period of time would evidently lead to complete oxidation of the Mn_3O_4 even at 500 °C.

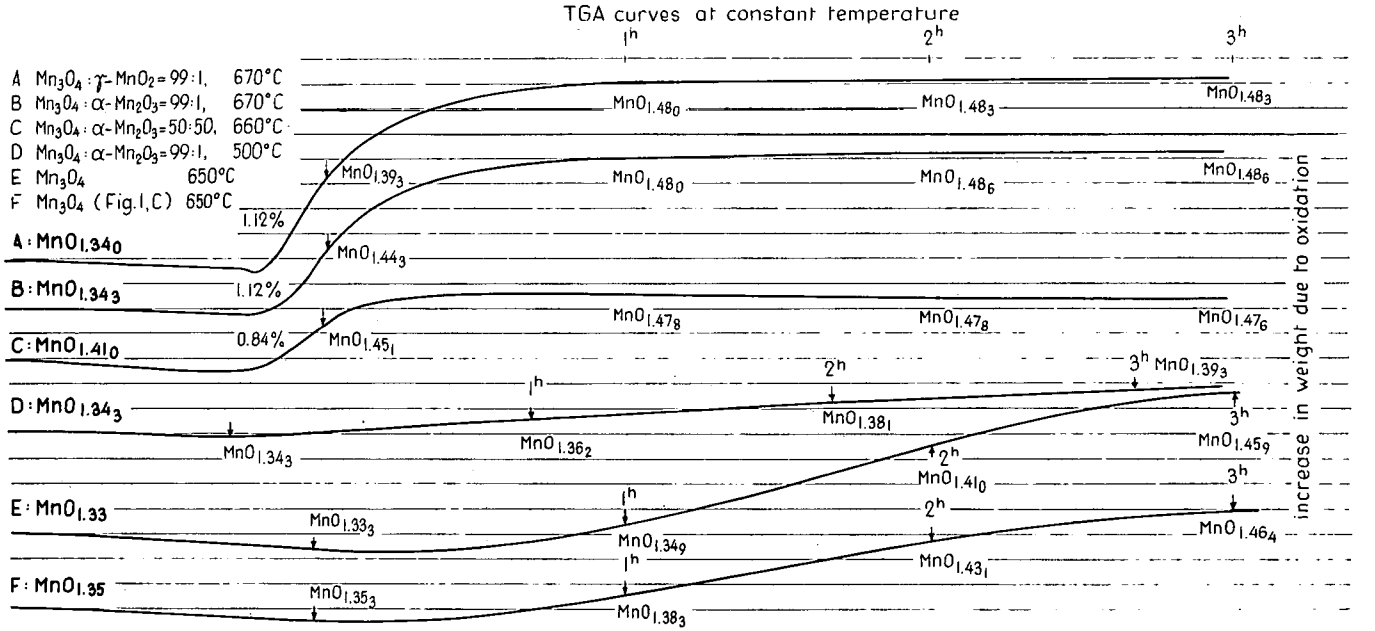

Fig. 3. TGA curves of Mn_3O_4 — γ-MnO_2, Mn_3O_4 — α-Mn_2O_3 and Mn_3O_4 samples during prolonged heating at constant temperature (see the text).

RESULTS OF INFRARED SPECTROSCOPIC AND X-RAY INVESTIGATIONS

The oxidation of Mn_3O_4 in air between 500 and 800 °C as well as that accelerated by other manganese oxides of higher valency is supported by qualitative investigations with IR-spectroscopy and X-ray, too.

IR-spectra were recorded with a Zeiss UR-20 spectrophotometer in the spectral range 400—800 cm^{-1}. X-ray patterns were obtained with an X-ray diffractometer DRON-1 with Fe K_α radiation (30 kV, 10 mA). Both in the IR-spectra and in the X-ray patterns the evanescence of the characteristics of Mn_3O_4 and the coming into prominence of the bands of α-Mn_2O_3 can be well followed in its dependence on the time of heating.

As can be seen from the X-ray patterns, the intensity of the reflexions characteristic for Mn_3O_4 begins to decrease in the samples heated to 660 °C, then with prolonged heating the reflexions of α-Mn_2O_3 become more and more dominant, though the presence of some Mn_3O_4 can be observed even after heating for 3 hours. The oxidation of Mn_3O_4 to α-Mn_2O_3 could not be considered as complete on the basis of TGA curves.

TABLE 1

d(Å)-*values of the starting material 99 %* Mn_3O_4—*1 %* α-Mn_2O_3 *and those of sample heated to 660 °C, after 1 hour and 3 hours*

d(Å)	Phase	I_{estim}			
		starting material	samples heated at 660 °C for		
			0^h	1^h	3^h
4.88	Mn_3O_4	m	m	—	—
3.84	α-Mn_2O_3	—	w	s	s
3.07	Mn_3O_4	m	m	—	—
2.86	Mn_3O_4	m	w	—	—
2.76	Mn_3O_4	vs	s	vw	—
2.74	α-Mn_2O_3	—	s	vs	vs
2.47	Mn_3O_4	vs	s	w	vw
2.35	α-Mn_2O_3 Mn_3O_4	m	m	m	m
2.02	Mn_3O_4	m	m	—	m
1.98	α-Mn_2O_3	—	w	m	m
1.84	α-Mn_2O_3	—	w	m	m
1.78	Mn_3O_4	—	m	—	—

The IR-spectra are also in full accordance with the results of TGA and X-ray investigations.

Comparing curves *3* to *6* of *Fig. 4*, it is evident that, while the absorption band at 670 cm^{-1} characteristic for α-Mn_2O_3 appears already in the spectrum of the sample heated to 670 °C and rapidly cooled, this band becomes more and more intensive after 1 hour and 3 hours treatment; curve *4* is more similar to the spectrum of the starting mixture, the characteristics of α-Mn_2O_3 become more and more conspicuous in curves *5* and *6*.

The same is valid in the case of the 50—50 % mixture. The starting mixture shows the characteristics of both components. The IR-spectra of the samples heated

TABLE 2

d(Å)-*values of the starting material 50% Mn_3O_4 — 50% α-Mn_2O_3 and those of sample heated to 660 °C, after 1 hour and 3 hours heating in air*

d(Å)	Phase	I_{estim}			
		starting material	samples heated at 660 °C for		
			0^h	1^h	3^h
4.88	Mn_3O_4	m	vw	vw	vw
3.84	α-Mn_2O_3	m	s	s	s
3.07	Mn_3O_4	m	vw	—	—
2.86	Mn_3O_4	w	vw	—	—
2.76	Mn_3O_4	vs	m	—	—
2.72	α-Mn_2O_3	vs	vs	vs	vs
2.47	Mn_3O_4 / Mn_3O_4	vs	m	vw	vw
2.35	α-Mn_2O_3	m	m	s	s
2.02	Mn_3O_4	m	vw	—	—
1.98	α-Mn_2O_3	m	m	s	s
1.84	α-Mn_2O_3	m	m	s	s
1.78	Mn_3O_4	m	vw	—	—

to 660 °C (curve *8*), and those of samples treated at that temperature for 1 and 3 hours (curves *9* and *10*) become more and more similar to the IR-spectrum characteristic for α-Mn_2O_3 (curve *2*).

BEHAVIOUR OF Mn_3O_4 AT HIGHER TEMPERATURES IN CO_2 AND N_2 ATMOSPHERE

To obtain further information on the behaviour of Mn_3O_4, the behaviour of the starting materials consisting of Mn_3O_4 and α-Mn_2O_3, as well as different mixtures of both was investigated in CO_2 and N_2 atmosphere, too, after heating the samples at 670 °C in the atmosphere indicated for 2 or 3 hours and then cooling in CO_2 or N_2 stream. We intend to continue these investigations in the future.

Some results are presented in *Fig. 5*. On the left of *Fig. 5* the IR-spectra of Mn_3O_4 and α-Mn_2O_3 as starting materials and of different mixtures of both, as well as the spectra of the products obtained from α-Mn_2O_3 by heating at 670 °C or 2 hours are to be seen.

The Mn_3O_4 heated in CO_2 stream at 670 °C for 2 hours shows no changes, its spectrum is nearer to that of ideal Mn_3O_4 than the spectrum of the starting aterial. In contrary heating α-Mn_2O_3 and mixtures containing α-Mn_2O_3 in CO_2 tream at the given temperature more substantial changes are observed. The spectrum haracteristic for α-Mn_2O_3 disappears and it is substituted by that characteristic or Mn_3O_4. While by heating in air between 600 and 800 °C the Mn_3O_4 was oxidized into α-Mn_2O_3, during heating in CO_2 atmosphere the Mn_3O_4 remains unchanged and α-Mn_2O_3 transforms into Mn_3O_4. It is to be remarked that the endproducts obtained by heating both α-Mn_2O_3 and its mixtures in CO_2 stream are heterogenous according to X-ray investigations; with reflexions of the dominating Mn_3O_4 as a rest those of α-Mn_2O_3 are to be seen; even MnO appears as a new phase, especially

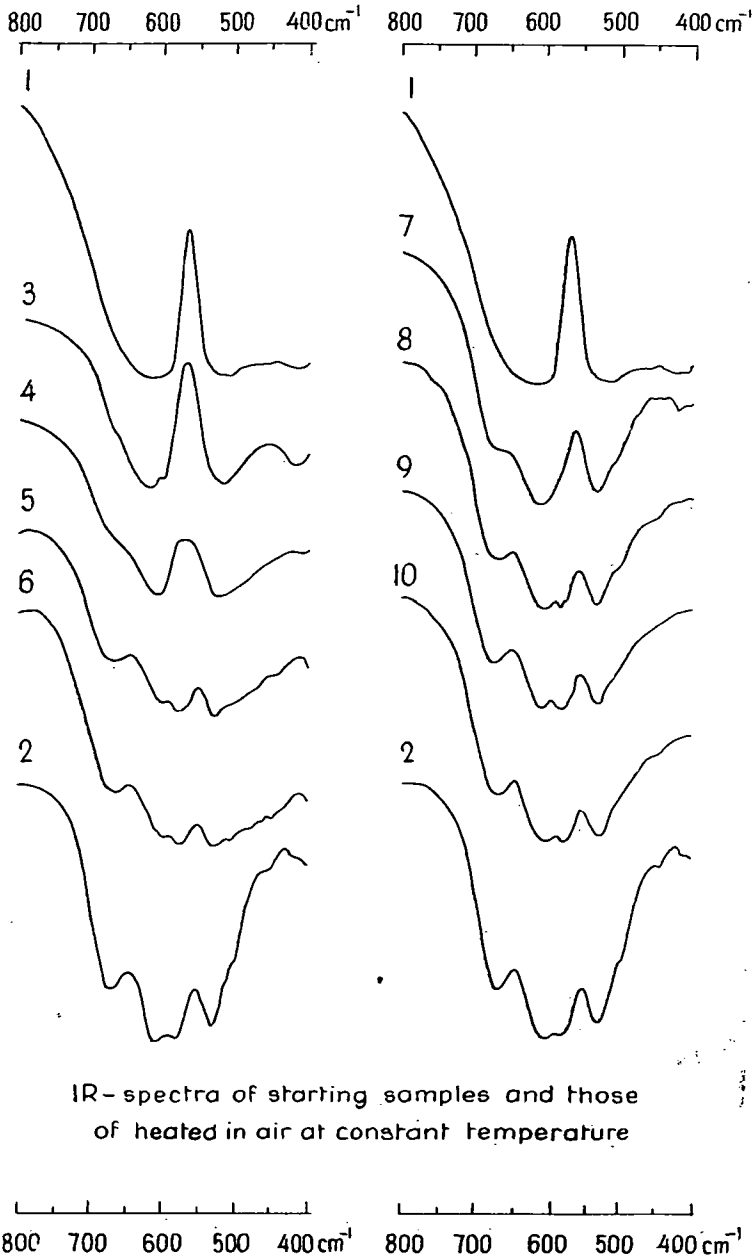

Fig. 4. IR-spectra of the starting materials and of samples heated to 660—670 °C in air: *1.* Mn_3O_4, *2.* α-Mn_2O_3, *3.* 99 % Mn_3O_4 — 1 % α-Mn_2O_3, *4.* The same as *3*, heated to 670 °C, *5—6.* The same sample heated at 670 °C for 1 hour and 3 hours, respectively. *7.* 50 % Mn_3O_4 — 50 % α-Mn_2O_3, *8.* The same as *7*, heated to 660 °C, *9—10.* The same sample heated at 660 °C for 1 hour and 3 hours, respectively.

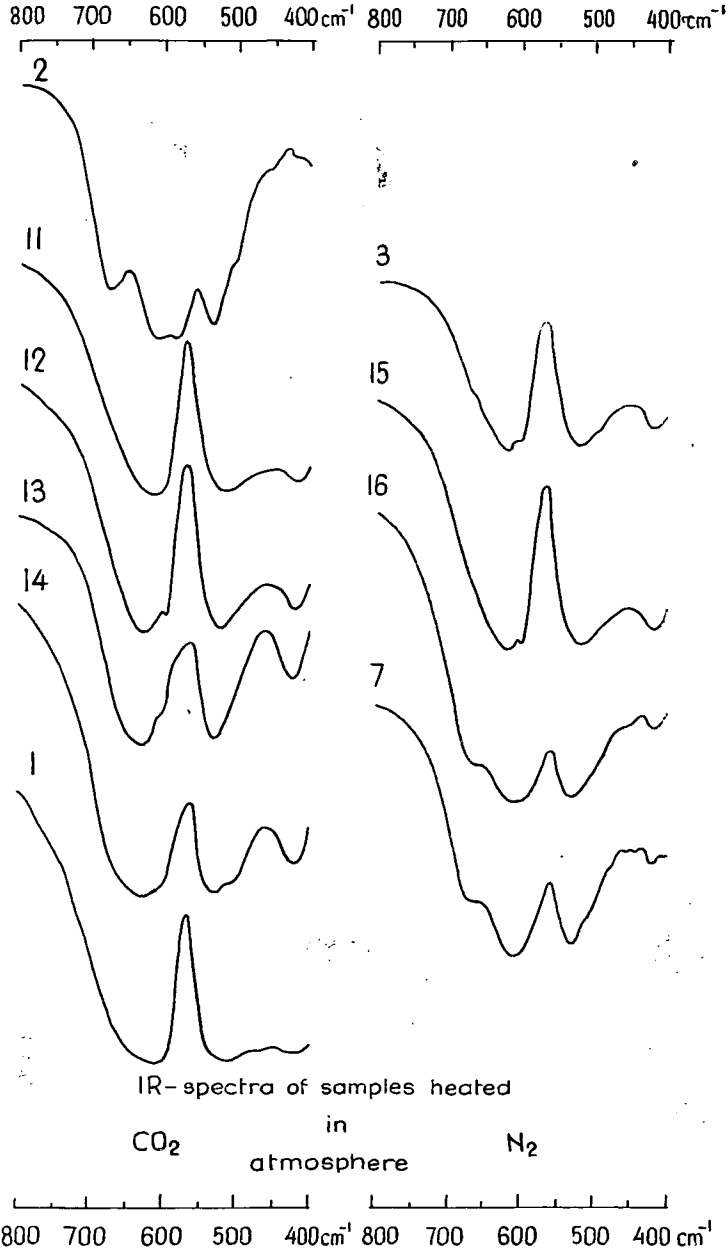

Fig. 5. IR-spectra of different starting materials and of samples heated to 660—670 °C in CO_2 or N_2 atmosphere:
Untreated samples: *1.* Mn_3O_4, *2.* α-Mn_2O_3, *3.* 99% Mn_3O_4 — 1% α-Mn_2O_3, *7.* 50% Mn_3O_4 — 50% α-Mn_2O_3;
Samples heated in CO_2 atmosphere:
11. Mn_3O_4, *12.* 75% Mn_3O_4 — 25% α-Mn_2O_3, *13.* α-Mn_2O_3, *14.* 25 % Mn_3O_4 — 75% α-Mn_2O_3;
Samples heated in N_2 atmosphere:
15. 99% Mn_3O_4 — 1% α-Mn_2O_3, *16.* 50% Mn_3O_4 — 50% α-Mn_2O_3.

TABLE 3

d-values of samples heated at 670 °C in CO_2 atmosphere for 2 hours

d(Å)	Phase	α-Mn_2O_3	75% Mn_3O_4 25% Mn_2O_3	25% Mn_3O_4 75% Mn_2O_3	Mn_3O_4
4.88	Mn_3O_4	m	m	w	m
3.84	α-Mn_2O_3	—	—	m	—
3.07	Mn_3O_4	s	s	m	m
2.86	Mn_3O_4	w	w	vw	vw
2.74	Mn_3O_4	vs	vs	s	vs
2.72	α-Mn_2O_3	—	—	vs	—
2.56	MnO	s	vw	vw	—
2.47	Mn_3O_4	vs	vs	vs	vs
2.35	Mn_3O_4 α-Mn_2O_3	w	w	w	w
2.22	MnO	vs	vw	w	—
2.02	Mn_3O_4	w	m	w	w
1.98	α-Mn_2O_3	—	—	w	—
1.82	Mn_3O_4	vw	vw	w	vw
1.78	Mn_3O_4	w	w	w	—
Composition of the samples	at the start	$MnO_{1.53}$	$MnO_{1.38}$	$MnO_{1.46}$	$MnO_{1.35}$
	after heating	$MnO_{1.24}$	$MnO_{1.33}$	$MnO_{1.37}$	$MnO_{1.25}$

TABLE

d-values of samples heated in N_2 atmosphere at 670 °C for 3 hours

d(Å)	Phase	50% Mn_3O_4 + 50% Mn_2O_3		99% Mn_3O_4 + 1% Mn_2O_3	
		before treatment	after treatment	before treatment	after treatment
4.88	Mn_3O_4	m	m	m	m
3.84	α-Mn_2O_3	m	m	—	—
3.07	Mn_3O_4	m	m	m	m
2.86	Mn_3O_4	w	w	m	w
2.76	Mn_3O_4	vs	s	vs	s
2.74	α-Mn_2O_3	vs	vs	—	—
2.47	Mn_3O_4	vs	vs	vs	vs
2.35	Mn_3O_4 α-Mn_2O_3	m	m	m	w
2.02	Mn_3O_4	m	w	m	w
1.98	α-Mn_2O_3	m	w	—	vw
1.84	α-Mn_2O_3	m	w	—	—
1.78	Mn_3O_4	m	w	—	w
Composition of the samples		$MnO_{1.39}$	$MnO_{1.40}$	$MnO_{1.34_3}$	$MnO_{1.31_8}$

markedly in the X-ray pattern of α-Mn_2O_3 heated in CO_2 stream at 670 °C for 2 hours. With weaker intensity the reflexion of MnO can be observed in the X-ray patterns of the treated mixtures, too.

By comparing curves *15* and *16* of *Fig. 5* with curves *3* and *7* it can be stated, in accordance with the results of X-ray investigations, as well as with the chemical composition that in N_2 atmosphere no changes occurred in the mixtures; both the Mn_3O_4 and the Mn_2O_3 component remained unchanged.

SUMMARY

Summarizing the results obtained from the IR-spectra and X-ray patterns and those of the thermal investigations, the following may be established concerning the oxidation and stability of Mn_3O_4 in the temperature range of the thermal stability of the Mn_2O_3:

A. In air

1. Though the DTA and TGA investigation of pure Mn_3O_4 at the generally used heating rate (10 °C/min) does not or only hardly point to oxidation, a slow oxidation of pure Mn_3O_4 is proved by TGA curves taken at constant temperatures during prolonged heating (or by slow heating rate). The composition of a Mn_3O_4 sample after heating at 670 °C for 3 hours proved to be $MnO_{1.46}$.

2. The presence of other manganese compounds (MnO_2 modifications, manganite, Mn_2O_3) or that of Fe_2O_3, in an amount as low as 1 per cent, exerts a significant influence on the oxidation of Mn_3O_4:

a) The oxidation of Mn_3O_4 is initiated and accelerated by the presence of other manganese oxides; the composition of a Mn_3O_4 sample containing other manganese oxide and heated at 660—670 °C reached the value $MnO_{1.48}$ after 1 hour, whereas the composition of a pure Mn_3O_4 sample in the same conditions proved to be only $MnO_{1.35}$.

b) The starting temperature of the oxidation of Mn_3O_4 is lowered by the presence of other manganese oxides and, depending on their quality and quantity, the oxidation starts at 460—560 °C.

c) The most intensive effect on the oxidation of Mn_3O_4 is exerted by Mn_2O_3.

B. In CO_2 atmosphere

1. The Mn_3O_4, also in presence of other manganese oxides, remains unchanged even after prolonged heating.

2. On the contrary, the Mn_2O_3 heated in CO_2 decomposes, even MnO appears as a new phase. In mixtures the Mn_2O_3 shows a similar behaviour and in the IR-spectra as well as in X-ray patterns of samples heated the characteristics of Mn_3O_4 are dominating beside weak traces of MnO and Mn_2O_3.

C. In N_2 atmosphere

Heating in nitrogen atmosphere both Mn_3O_4 and Mn_2O_3 as well as their mixtures remain unchanged as it is proved by the IR-spectra and X-ray patterns.

Thus, in the temperature range of the thermal stability of the Mn_2O_3:

a) if a possibility of oxidation exists, the Mn_3O_4 will be oxidized into Mn_2O_3, slower or faster;

b) if the possibility of oxidation is excluded, both the Mn_3O_4 and Mn_2O_3 remain unchanged, and

c) if the thermal effect is associated with CO_2 atmosphere, the Mn_3O_4 remains unchanged, the Mn_2O_3 will be, however, transformed into Mn_3O_4, and even, MnO appears as a new phase.

It seems that the experimental facts summarized above may be used in interpreting the formation of manganese oxide assemblages in different metamorphic processes.

REFERENCES

BRICKER, O. [1966]: Some stability relations in the system Mn—O_2—H_2O at 25° and one atmosphere pressure. Amer. Miner., *50*, 1296—1354.

DASGUPTA, D. R. [1965]: Oriented transformation of manganite during heat treatment. Miner. Mag., *35*, 131—139.

GRASSELLY, Gy. [1956*a*]: Remarks on the determination of the composition of MnO_2—Mn_2O_3—Mn_3O_4 systems. Acta Miner. Petr., Szeged, *9*, 41—46.

GRASSELLY, Gy. and É. KLIVÉNYI [1956*b*]: On the stability of Mn_3O_4. Acta Miner. Petr., Szeged, *9*, 33—40.

HOOK, H. J. VAN and M. L. KEITH [1958]: The system Fe_3O_4—Mn_3O_4. Amer. Miner., *43*, 69—83.

HÜEBNER, STEPHEN [1969]: Stability of rodochrosite. Amer. Miner., *54*, 457—481.

OSWALD, H. R. and M. J. WAMPETICH [1967]: Die Kristallstrukturen von Mn_5O_8 und $Cd_2Mn_3O_8$. Helv. Chim. Acta *50*, (7), 2023—2034.

ROY, SUPRIYA [1972]: Metamorphism of sedimentary manganese deposits. Acta Miner. Petr., Szeged, *20/2*, xxx—xxx.

SATO, MOTOAKI [1960]: Oxidation of sulfide ore bodies. 1. Geochemical environments in terms of Eh and pH. Econ. Geol., *55*,

Manuscript received, August 12, 1972.

PROF. DR. GYULA GRASSELLY
Institute of Mineralogy, Geochemistry and Petrography, Attila József University, Táncsics M. u. 2., Szeged, Hungary

Acta Mineralogica-Petrographica, Szeged, XX/2, 241—253, 1972

CHARACTERIZATION OF INSOLUBLE ORGANIC SUBSTANCE OF SEDIMENTS BY THERMAL AND INFRARED INVESTIGATION

GY. GRASSELLY, M. AGÓCS and K. NAGY

INTRODUCTION

According to FORSMAN and HUNT [1958] three different types of the kerogen, in organic solvents insoluble organic matter of the sediments, may be distinguished. Two of these types, except the coaly type kerogen, may be considered as an important step toward oil formation. The investigation of the horizontal and vertical distribution of these kerogen types as well as recording of this distribution on geological sections presumably contributes to indicate and outline the sediments to be considered as mother rock.

The total organic carbon (C_{org}) content of the sediments investigated is fairly low. It changes between 0.14 and 0.83 per cent on the basis of investigation of several cores from different borings. The very low organic matter content also resulted in that only a low grade enrichment of organic material could be obtained by the izolation method generally used.

Concerning the characterization of the insoluble organic matter of the sediments — taking into account the low grade enrichment, too — the question arose first of all whether it would be possible to distinguish by a simple method the insoluble organic matter of coaly character and that showing probably kerogen-like properties.

The question may be presumably answered by infrared spectroscopic and derivatographic investigations.

PREPARATION AND CHARACTERIZATION OF THE SAMPLES

The samples are originated from the boring cores of the Lower Pannonian sediments of the southern part of the Hungarian Great Plain. The samples are mostly of marly, lime-marly character with more or less dolomite and Mg-limestone, respectively.

The soluble organic content of the samples ground below 0,06 mm grain size was extracted in Soxhlet-extractor and after removing the carbonates the silicates of the samples were decomposed by hydrofluoric acid-treatment and removed by repeated washing and centrifugation. The process was continued by sodium carbonate treatment followed by repeated washing and centrifugation. The humic acids were removed from several samples by digestion with 0,5 N NaOH on water-bath.

The total organic carbon content of the samples was determined by DR. KASCHKA (Ernst—Moiitz—Arndt University, Department of Geology, Greifs-

wald, GDR). Further, the chloroform-soluble organic material (Bitumen A) was also determined and the bitumen coefficient of the samples calculated on the basis of the following equation:

$$\text{bitumen coefficient} = \frac{\text{Bitumen A \%}}{C_{org}\% \cdot 1{,}7},$$

where 1,7 is the factor to recalculate the C_{org} content to organic material according to Rodionova.

To support the identification of insoluble organic substance concentrated the infrared spectroscopic and thermal investigation of different coaly organic materials was also carried out.

TABLE 1

*Samples of investigation, their location and depth as well as the C_{org}%,** Bitumen A% and the bitumen coefficient*

Sample №	Location and depth (m) of boring		C_{org}%	Bit. A%	Bit. koeff.
S-1	Kelebia	545,4—645,5	0,39	0,03	4,69
S-5	Kelebia	842,4—842,5	0,58	0,11	11,43
S-6	Kelebia	898,4—899,4	0,14	0,12	49,16
S-7	Kelebia	947,3—947,8	0,58	0,08	7,75
S-8	Kelebia	1000,5—1001,5	0,43	0,09	12,19
S-9	Kelebia	1052,5—1053,0	0,52	0,23	26,47
S-10	Kelebia	1085,0—1085,4	0,66	0,13	11,25
S-12	Ásotthalom	987,0—987,2	0,43	0,14	19,45
S-14	Ásotthalom	1079,2—1079,5	0,27	0,05	10,43
S-16	Kkdorozsma	2155,0—2156,0	0,46	0,05	6,28
O-21	Pföldvár	1474,0—1477,0	0,58	0,14	13,97
O-22	Pföldvár	1526,0—1529,0	0,39	—	—
O-24	Pföldvár	1397,0—1400,0	0,43	0,27	36,98
O-28	Pföldvár	1383,0—1386,0	0,46	0,17	22,05
O-33	Pföldvár	1819,0—1820,0	0,54	0,12	12,61
O-40	Pföldvár	1978,0—1979,0	0,50	0,16	19,17
O-46	Pföldvár	1774,0—1775,0	0,50	0,06	7,53
O-48	Pföldvár	1747,5—1751,5	0,23	—	—
O-49	Pföldvár	1715,0—1718,0	0,54	0,26	28,47
O-50	Pföldvár	1778,0—1779,5	0,47	0,15	19,00
O-51	Pföldvár	1780,0—1784,0	0,50	0,46	54,47
O-53	Pszőlős	1690,0—1691,5	0,29	0,11	22,65
O-54	Pszőlős	1702,0—1704,0	0,31	0,21	39,24
O-56	Pszőlős	1764,0—1769,0	0,36	0,—	—
O-57	Pszőlős	1769,0—1773,0	0,35	0,22	38,13
O-66	Pszőlős	1773,0—1777,5	0,51	0,03	3,91
O-67	Pszőlős	1556,0—1562,0	0,39	0,08	12,27
O-71	Pszőlős	1040,0—1046,0	0,45	0,05	6,84
O-73	Pszőlős	1770,0—1774,0	—	—	—
O-80	Battonya	1004,0—1009,5	—	—	—
O-94	Pszőlős	1770,0—1771,5	—	—	—

** C_{org} means the total organic carbon content determined by combustion above 1000 °C in oxygen stream.

INFRARED SPECTROSCOPIC INVESTIGATION

Many authors have dealt with infrared spectroscopic investigation of different organic materials as this method proved to be very useful in identifying the functional groups of organic substances of different kind.

The infrared spectra of the comparison material and the samples investigated were taken by a Unicam SP 200 type spectrophotometer in the range of 650—5000 cm^{-1} vawe number.

The intensive absorption bands in the spectrum of the Estonian kukersite at 2.900, 1.700 and 1.460 cm^{-1} point to the dominating character of aliphatic structure.

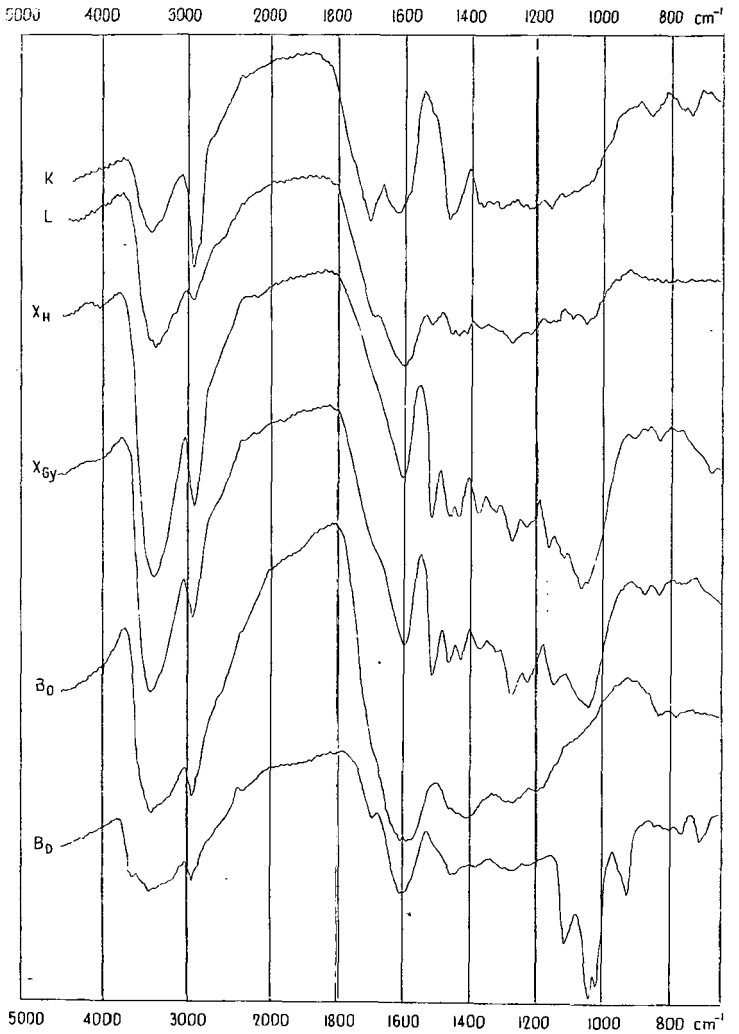

Fig.1. Infrared spectra of materials for comparison. K = kukersite (Estonian SSR), L = lignite, K_H = xilite (Herend, Hungary), X_{Gy} = xilite (Gyöngyös-Visonta, Hungary), B_O = brown coal (Orosz-lány, Hungary), B_D = brown coal (Dorog, Hungary).

While investigating the Green River oil-shale kerogen FORSMAN and HUNT [1958] from the significant intensity of bands at 2.857 and 1.449 cm^{-1} also found in this kerogen the presence of less aromatic and more aliphatic structure. The absorption band at 1.613 cm^{-1} may be attributed to a C=C bonding or to conjugated carbonyl-groups, according to KINNEY and SCHWARTZ [1957]. Investigating the infrared spectrum of the Green River oil-shale kerogen, ROBINSON [1969] attributed the intensive bands at 2.900 cm^{-1} and 1.460 cm^{-1} to methyl- and methylen-groups and interpreted the strong absorption in the range 1.680—1.720 cm^{-1} by the presence of carbonyl-groups. According to CALIKOWSKI and GONDEK [1968] the intensive absorption bands at 2.926 cm^{-1}, 2.853 cm^{-1} and 1.470 cm^{-1} point to methylen-groups whereas the bands at 2.926 cm^{-1} and 1.383 cm^{-1} to methyl-groups.

In the infrared spectrum of xilite samples shown in *Fig. 1* the significant absorption at 1.520 cm^{-1}, 1.600 cm^{-1} and 2.900 cm^{-1} indicate that they are mostly of aromatic structure with aliphatic side-chains. The bands between 1.000—1.500 cm^{-1}

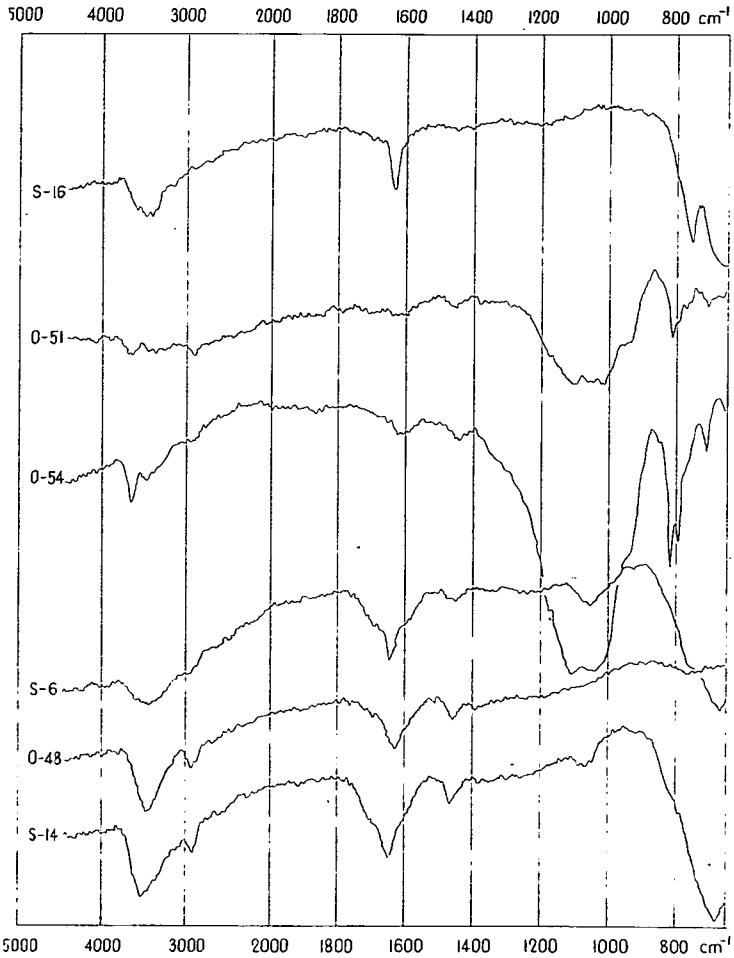

Fig. 2. Infrared spectra of samples belonging to Group I

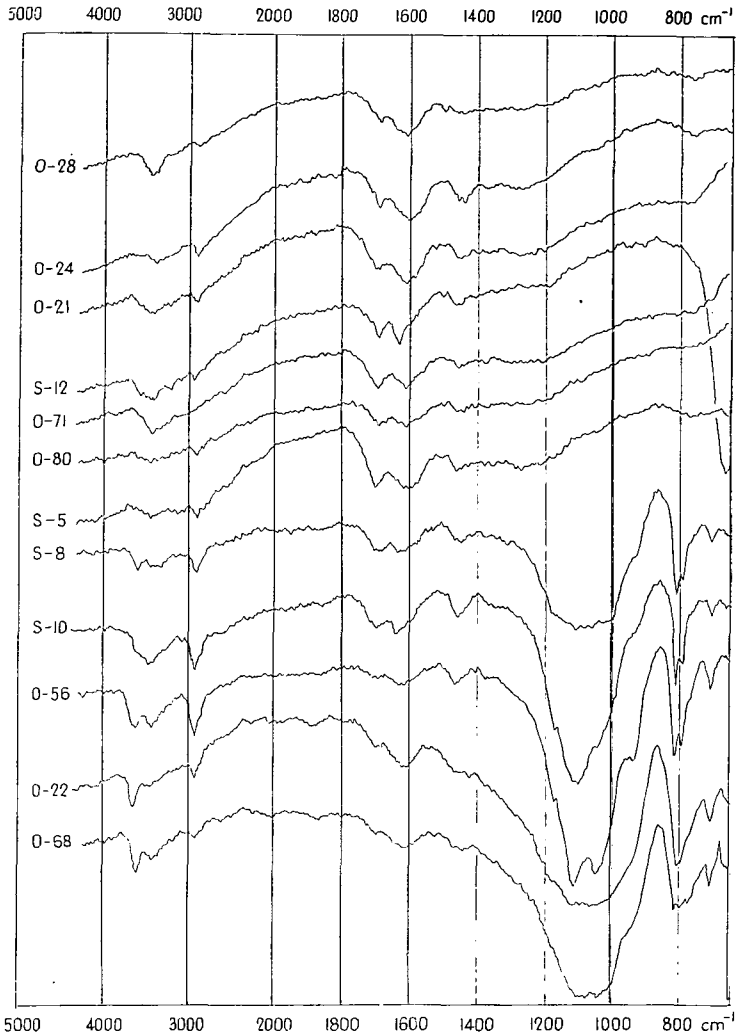

Fig. 3. Infrared spectra of organic substances belonging to Group II

may be originated by alcoholic OH-groups and substituted aromatic rings. In the spectrum of the xilite samples investigated the lack of absorption at 1.700 cm^{-1} is characteristic whereas at this wave number a definite absorption may be established in the spectrum of the Estonian kukersite kerogen. The same is clearly seen in the spectrum of lignite as well as in that of the brown coal samples, though with lower intensity. The infrared spectrum of the lignite, xilite and brown coal samples shows an intensive absorption at about 1.600 cm^{-1}.

Comparing the infrared spectra of the samples investigated and grouping those samples showing similarity in their main features, three groups may be distinguished.

In the spectra of samples of Group I the absorption band in the range 3.450—3.640 cm^{-1} attributed to OH-group appears with variable intensity, weak or no absorption may be established at 2.920—2.960 cm^{-1}, definite absorption may be observed at 1.625—1.642 cm^{-1} in the spectrum of several samples and a weak absorption at 1.440—1.460 cm^{-1} with about the same intensity as the band at 2.920 cm^{-1}. The lack of absorption at 1.700 cm^{-1} is characteristic to Group I as it was characteristically lacking also in the spectra of xilite samples and did not appear or merely with very weak intensity in the spectra of lignite and brown coal samples whereas was very definite in the spectra of Estonian kukersite kerogen.

The infrared spectra of the samples belonging to Group II shows an absorption in the range 3.450—3.680 cm^{-1}, however, with weaker intensity than the spectra of samples of Group I. On the contrary, the intensity of the absorption in the range 2.920—2.960 cm^{-1} is greater in most of the samples of Group II as compared to the intensity of the former band than in the case of Group I. Especially characteristic of Group II

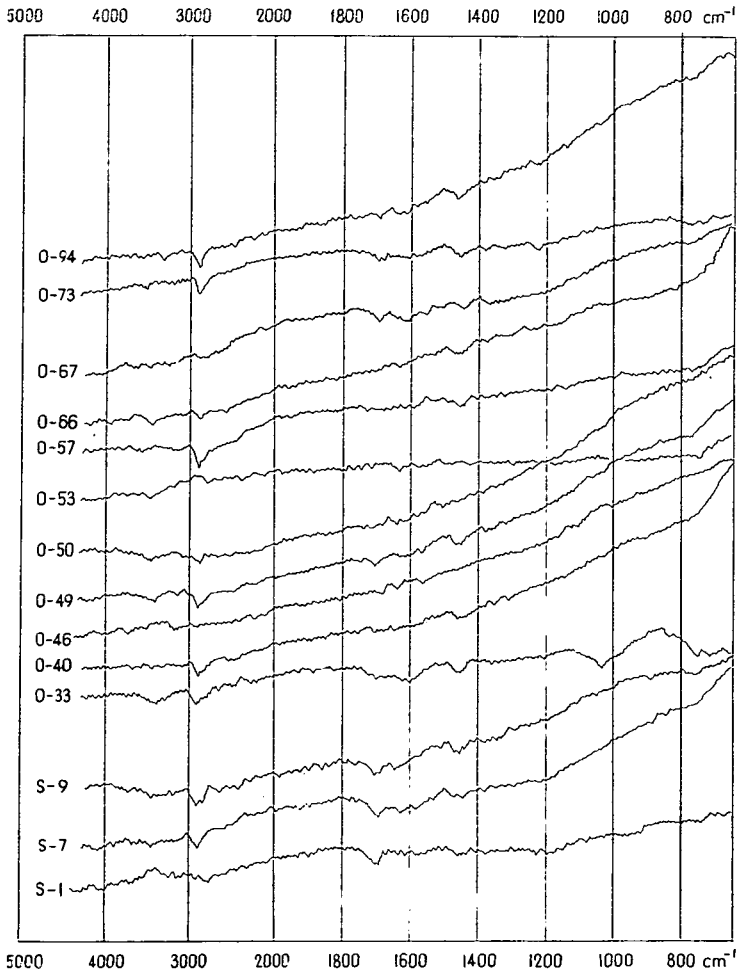

Fig. 4. Infrared specta of organin substances of group III

of less volatile compounds and the "fixed" carbon, respectively. According to the derivatograms the combustion of the organic material cannot be taken as complete till 600—700 °C since the TGA curves show a further if small loss of weight at higher temperatures, too.

In identifying the organic substance beside the DTA curves especially the consideration of the peculiarities of the DTGA and TGA curves may be helpful. Disregarding the very first endothermic effect at about 100 °C, the more pronounced the DTGA maximum between 200—300 °C and the corresponding TGA step showing to a significant loss of weight, the greater is the proportion of high volatile compounds, whereas, by decreasing amount of high volatile components the second DTGA maximum above 350 °C shifts toward higher temperatures and will be more intensive and, correspondingly also the TGA step of a more pronounced loss of weight shifts toward higher temperature ranges.

D. R. WILLIAMSON [1964] summing up several data concerning the thermal decomposition of Estonian oil shale kerogen, stated that the softening of the kerogen and the lost of the high volatile compounds begins at about 320—340 °C, whereas the decomposition of the less volatile components requires about 450 °C. In his paper, referring to the results of several authors, it is mentioned that the kerogen does not transform into soluble material below 325 °C and that the rate of the

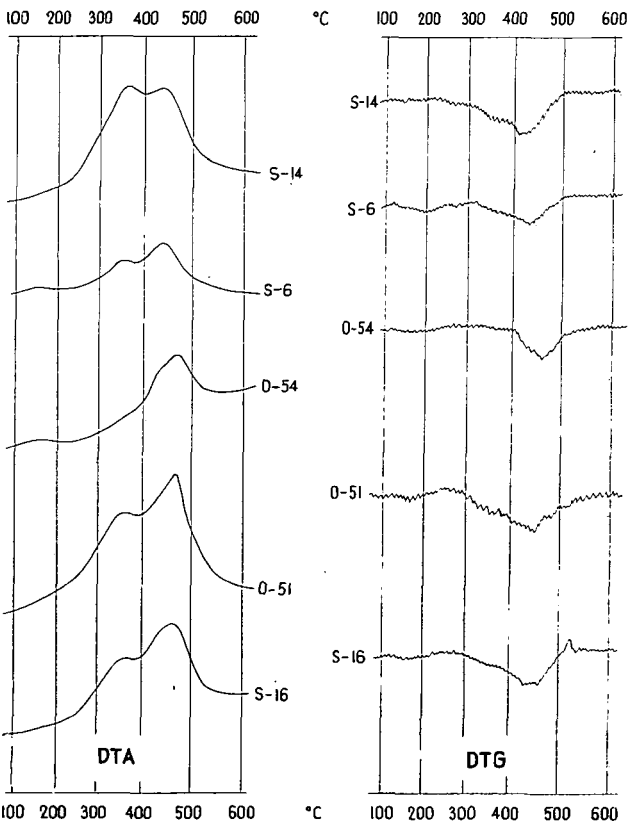

Fig. 6. Exothermic effects on the DTA and DTGA curves of samples of Group I

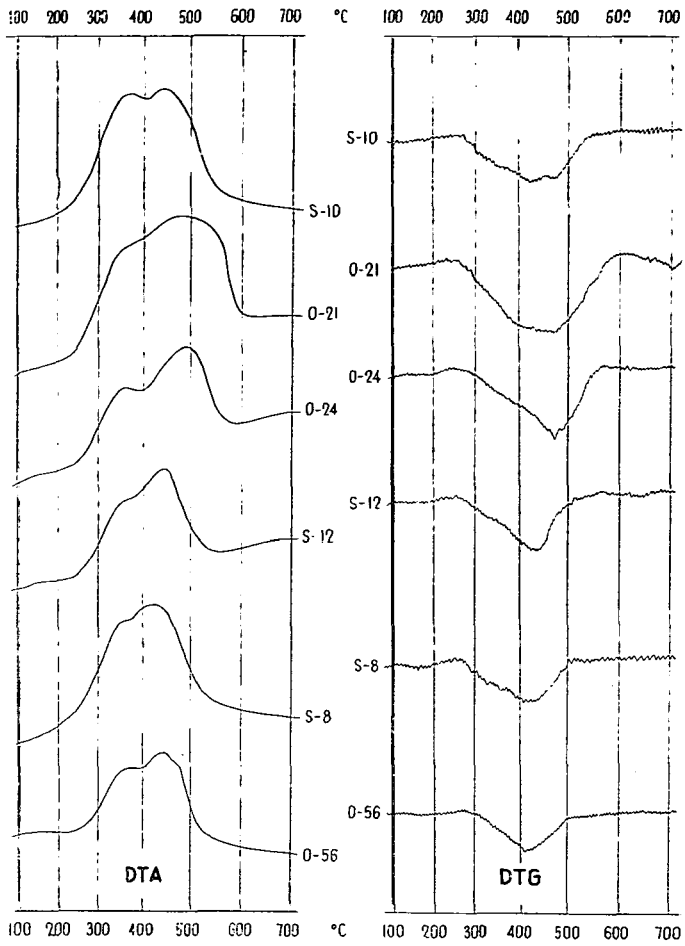

Fig. 7. Exothermic effects on the DTA and DTGA curves of samples of Group II

decomposition of the kerogen is nearly the same in 350—437 °C and 437—525 °C ranges and finally, an expressed change may be established in the rate of decomposition at 437 °C. Naturally, deviations from the values mentioned both toward the lower and the higher temperatures are possibly depending on the character of the kerogen sample.

The steps mentioned can also be recognized on the derivatogram of the kukersite kerogen used for comparison (in the figure showing only the DTA and DTGA effects in connection with the decomposition of the organic material) with more or less temperature deviations. On the TGA curve a very pronounced step appeared in the range 235—360 °C which equals to about 17 per cent loss of weight, the next two TGA steps at 360—460 ° and 460—580 °C are of the same intensity and the two corresponding DTGA maxima have also nearly the same character. The former step means 37 per cent and the second 39 per cent loss of weight. It seems that the evaluation of the character of the TGA and DTGA curves i. e. that of the

FORSMAN, J. P., J. M. HUNT [1958]: Insoluble organic matter (kerogen) in sedimentary rocks. — Geochim. Cosmochim. Acta *15*, 170—182.
GRIMSHAW, R. W., A. L. ROBERTS [1957]: Carbonaceous materials. — In: The differential thermal investigation of clays. Chapter XVI, 404—417. Mineralogical Society, London.
KINNEY, C. R. and D. SCHWARTZ [1957]: Partial air oxidation of Chattanooga uraniferous black shale. — Ind. Eng. Chem., *49*, 1125—30.
ROBINSON, W. E. [1969]: Kerogen of the Green River formation. — In: G. Eglinton et al.: Organic Geochemistry. Chapter 26, 619—637. Springer Verlag Berlin, Heidelberg, New York.
WILLIAMSON, D. R. [1964]: Retorting and other beneficiation of oil shales. — Colorado School of Mines Mineral Industries Bulletin 7, No 6, 1—13.

Manuscript received, June, 1972

PROF. DR. GYULA GRASSELLY,
MRS. DR. MARGIT AGÓCS
and MISS KATALIN NAGY
Institute of Mineralogy, Geochemistry and Petrography Attila József University,
Táncsics M. u. 2., Szeged, Hungary

Acta Mineralogica-Petrographica, Szeged, XX/2, 255—264, 1972

INVESTIGATIONS ON OXIDATION-REDUCTION RELATIONS OF CONSOLIDATED SEDIMENTS BY ZOBELL'S METHOD

M. HETÉNYI and M. VÁRHELYI

INTRODUCTION

Elucidation of the oxidation state of sedimentary rocks may help in studying the processes of sedimentation in characterizing and in further refining the classification of sedimentary rocks.

The exact determination of the state of oxidation conceals several difficulties both in the practical measurement and in its interpretation.

KRUMBEIN and GARRELS [1952] classified the sedimentary rocks on the basis of theoretically calculated Eh-pH diagrams, designing the regions in which the given phase is stable or precipitates from the solution.

It is usual to characterize the state of oxidation of rocks by the ratio of the ferrous and ferric content, the so-called grade of oxidation. So BURRI used the formula $\frac{2[Fe_2O_3]}{2[Fe_2O_3]+[FeO]}$ for determining the grade of oxidation, while according to SZÁDECZKY-KARDOSS the *"iron-oxidation-value"* or oxidation grade (O_{Fe}) is given by the formula $\frac{2\,Fe_2O_3}{FeO}$.

The disadvantage of systems based on such considerations originates from the fact that the oxidation state of the rock as a whole is expressed by the oxidation-reduction relations of a single component.

Several authors tried to characterize the oxidation state by treating a suspension of the rock with oxidizing agents and measuring the change in potential of the suspension. As examples, the following may be mentioned:

STURGIS [1936] followed the progress of the oxidation process by measuring the change of the dichromate-content of samples taken in regular time intervals from the supernatant of the suspension.

BOD and BÁRDOSSY [1962] studied the changes in potential as a function of time in suspensions containing potassium dichromate acidified with sulphuric acid.

ZOBELL [1946] used the oxidation-reduction capacity for characterizing non-consolidated sediments rich in organic material. His aim was to find an oxidizing agent which does not destroy the organic material, neither reacts with the components of the rock, affecting only the reversible oxidation-reduction system. Giving ferric chloride solution in small portions to the aqueous suspension, the potential was measured after reaching the equilibrium. The addition of ferric chloride was continued until no change in potential could be observed. The reducing property of the sediments was characterized by the course of the potential curve.

It could be concluded from earlier investigations of one of the authors [GRASSELLY and HETÉNYI, 1970] that ZOBELL's method, with suitable modifications, could be used for characterizing the oxidation state of consolidated sediments, too. It was, however, necessary to find first a method for interpreting the potential curve and the factors determining its course.

Our aim was to characterize the oxidation state of different sedimentary rocks with potential curves obtained by potentiometric titration and by values calculated from the curves.

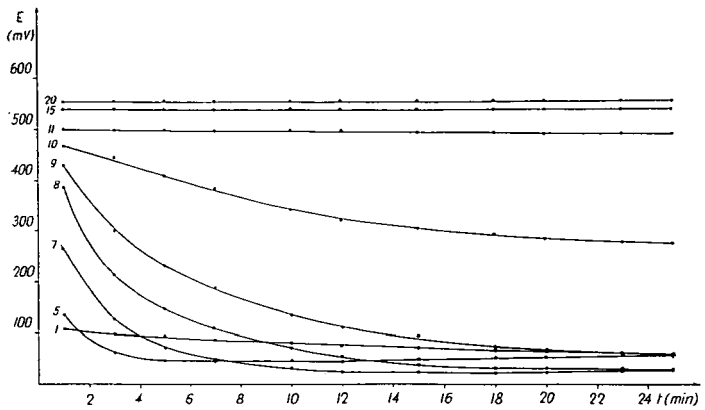

Fig. 1. The change of potential *vs.* time on addition of 1 to 20 ml 0.5 *M* $FeCl_3$

A necessary condition of the titration is a great change in free energy. If the difference between the normal potentials of the component participating in the reaction and of the titrating agent exceeds $4 \cdot 2.3 \cdot \frac{RT}{nF}$, then the change in potential is great enough in all kinds of electron transitions to permit the evaluation of the change in free energy. In the case of minor potential differences the titration curves can only be well evaluated by using a redox-system of greater difference in charge as oxidizing agent.

As the setting up of the equilibrium in the oxidation processes takes a certain time, for being able to determine the time necessary for attaining the equilibrium it proved necessary to measure the changes in redox potential as a function of time for the whole potential curve. Though most of the reversible oxidation-reduction processes are instantaneous ion-reactions, there may often occur secondary processes which also lead to equilibrium, but not instantaneously. Further, some time is necessary for the electrode to get into equilibrium with the solution and in different phases of the titration reactions of different velocity may occur.

Fig. 1 shows titration curves measured with different waiting periods. It can be seen from the curves that in different sections of the curves different time is necessary for reaching equilibrium. The equilibrium will be reached in 15—20 minutes in most cases. It is, however, necessary to remark that in model-experiments, especially if organic material is given to the system, or the samples contain originally organic material, much longer time is necessary to reach the equilibrium.

The measurement of the potential curve was carried out with the method described in the previous paper mentioned above. 5 g of the sample ground to 0,06 mm particle size were suspended in 100 ml dist. water and stirred with a magnetic stirrer. A Pt-electrode, a gas-inlet-tube for the nitrogen gas and an agar-agar bridge connecting the cell with a saturated calomel reference electrode were introduced through the cover.

The pH of the suspension was read at the beginning and after the end of the measurement. The oxidizing agent was added in portions of 0.5 ml, in certain potential ranges of 1.0 ml, the next portions being added after a relative equilibrium was reached.

The measured and calculated values used for characterizing the samples are the following:

Potential at saturation: E_{sat}

The quantity of oxidizing agent consumed up to the "point of inflexion": X

Slope of the curve: m

Reducing capacity: $\beta = \frac{\Delta c}{\Delta E}$

The reducing capacity indicates the change in redox-potential which can be reached by introducing a given external energy (oxidizing or reducing agent), i.e. the final state of energy of the system. Only few methods for characterizing the reducing capacity are found in literature.

MICHAELIS [1929] calculated by differentiating NERNST's equation for a system consisting of merely one redox-pair.

$$\beta = \frac{dx}{dE} = \frac{nF}{RT} x \frac{B-x}{B}$$

where B is the total concentration of the reduced and oxidized forms, and x is the concentration of the oxidized form.

This formula is difficult to use in practice, because systems consisting of a single pair of redox partners are rarely found.

According to NIGHTINGALE the reducing capacity of the system is given by the quantity of the external oxidizing or reducing agent which changes the redox-potential of the system by one unit. This definition can be well used in practice in presence of several redox systems, independently of the knowledge of all occuring reactions.

The calculations carried out according to NIGHTINGALE's method were based on the experimental data of our potential curves. Thus difference quotients calculated for the total titration curves were used for characterizing the samples.

INTERPRETATION OF THE POTENTIAL CURVES

The course of the potential curve, i.e. the potential values measured, are determined by the rate of reduction of the $FeCl_3$ added to the suspension examined, and therefore by the concentration ratio Fe(II):Fe(III) found, which is decisive for determining the potential. As can be seen from *Fig. 2,* most of the potential curves begin with an almost linear section, in which the potential shows only slight fluctuations close to the initial value of Eh. As in the first section of the potential curve no significant changes in potential occur, despite the adding of $FeCl_3$ solution, processes decreasing the Fe(III) ion concentration may be supposed. All processes or factors decreasing the concentration of the Fe(III) added tend to decrease the po-

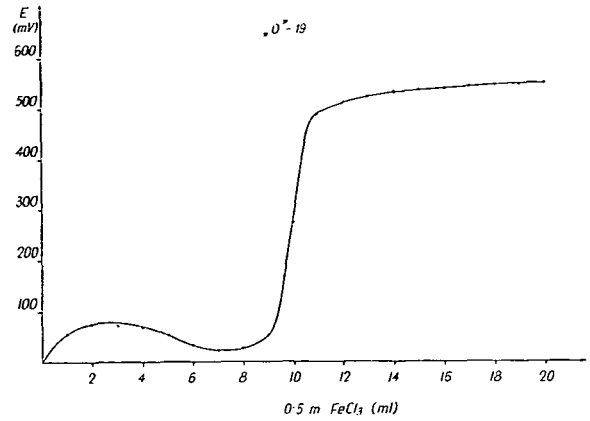

Fig. 2. Potential curve of sample "*O*—19"

tential. The decrease in Fe(III) concentration may also be due to the oxidation of some components of the suspension by the Fe(III) added. The change in the Fe(II): Fe(III) ratio may also be caused by Fe(II) ions dissolved from the rock, as well as by precipitation of the Fe(III) by hydrolysis, or by complex formation (e.g. in the presence of humic materials).

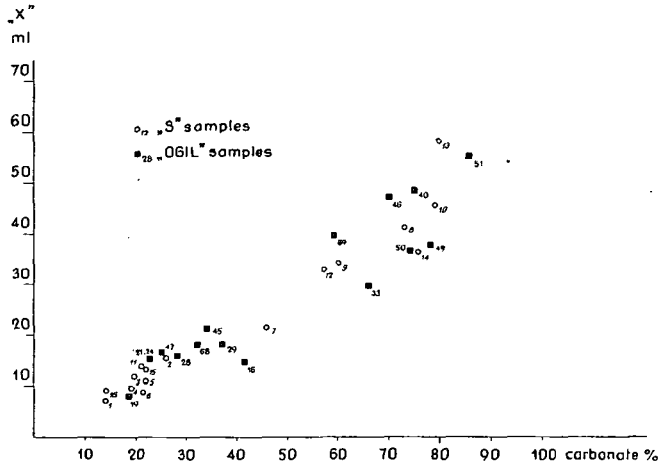

Fig. 3. Dependence of the value of *X* on the carbonate content of the samples

After these processes, as sudden increase in potential is observed in the solution, due to the increase in Fe(III) concentration. This is represented by section II of the potential curve.

In section III of the curve the potential becomes constant again corresponding to the Fe(II):Fe(III) ratio established.

It was attempted to find components and reactions playing a role in the different sections of the potential curve.

Concerning section I, among the possibilities mentioned the influence of carbonates was studied in detail. The value of X (used for characterizing this section) changes linearly with the calcium-magnesium-carbonate content of the samples. To corroborate this relationship, model-experiments were performed. 1 to 5 %

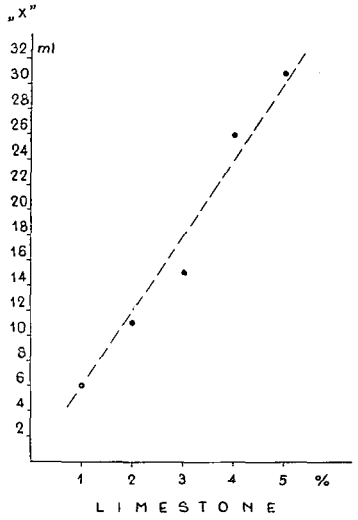

Fig. 4. Changes in X with increasing limestone content

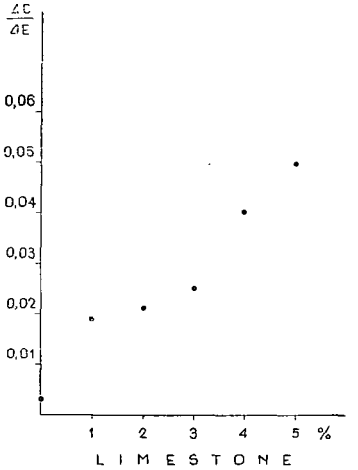

Fig. 5. Dependence of the redox capacity on the limestone content

limestone was added to a sample free of carbonate and the potential titration was carried out. Plotting the values of X as a function of the limestone content a linear relation was obtained *(Fig. 4, 5)*. Hence, it may be concluded that section I of the potential curve i.e. the quantity of oxidizing agent consumed is determined by the carbonate content. Higher carbonate content may conceal the effect of less active components or those present in lower concentration; so the effect of the carbonate content will dominate in the characterization of the total curve, i.e. of the redox capacity, though it does not play any role in the redox process itself.

Section II of the curve, i.e. the rise in potential may be characterized by the slope of this section which is the steeper the higher the velocity of the reaction causing the rise. These parameters depend on the quality and oxidation state of the materials taking part in the reaction. To verify this supposition, the following experiments were performed: To a sample practically free of carbonate, 1 to 10 % of a petroleum distillation fraction (300—350 °C) was given, the titrations performed, and the slopes of the respective potential curves determined. *Fig. 6* shows the slopes as

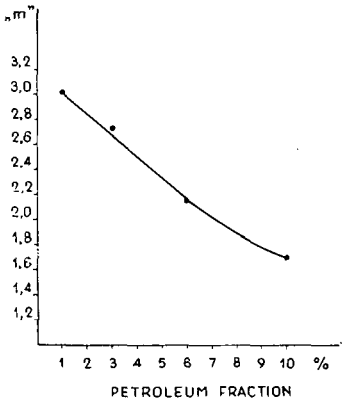

Fig. 6. Dependence of the slope of the potential curve on the quantity of petroleum distillation fraction added

a function of the petroleum concentration. Then, adding lignite, car-bonaceous material and kerogen to the same sample, the potential curves were measured again and the slope of the curves was determined. Significant differences between the effect of kerogen and of carbonaceous material were observed *(Fig. 7)*; these may be due to the fact that the kerogen becomes more oxidized during the extraction. The influence of the carbonaceous material on the steepness of the potential curve is most important, its slope being greater by one order of magnitude compared with other materials.

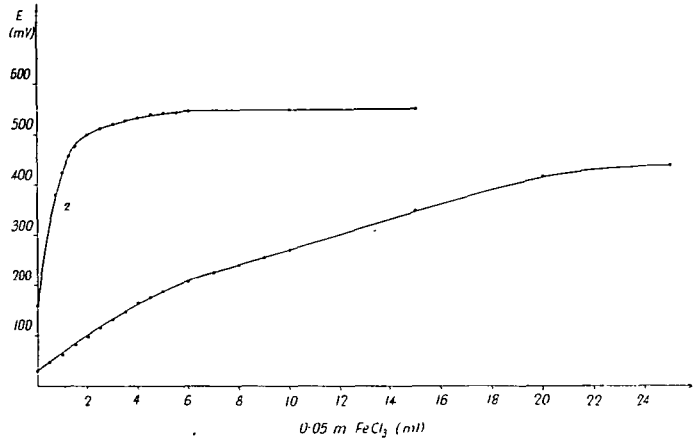

Fig. 7. Potential curves of coaly material *(1)* and of kerogen *(2)*

CALCULATIONS FOR CHARACTERIZING REDOX SYSTEMS

The fundamental electrochemical relationships cannot be applied in our calculations, since they hold only for reversible systems; hence, first of all, the reversible or irreversible character of the processes determining the potential is to be ascertained; further in most cases more than a single redox pair is to be taken into account. The reversibility is very important from experimental point of view because the redox capacity of irreversible systems is very low, and so, in measuring the redox potential instability may occur on the Pt-electrode.

According to EMSCHWILLER [1945] the reversibility or irreversibility of redox pairs is determined by the activation process of the system. The activation is composed of thermal and adsorptive activation. Thermal activation changes with concentration, while adsorptive activation is constant. If thermal activation is dominating in both the [ox] and [red] forms of a redox system, the system will be reversible, whereas it is irreversible if the activation is thermal in one form and adsorptive in the other. As activation = thermal activation + adsorptive activation, and one term of the expression being constant, in the extreme case of thermal activation = 0, reversible systems will formally show irreversible behaviour. In reversible systems:

$$E^0_{ox} > E^0_{redox} > E^0_{red} \cdot$$

In irreversible systems either E^0_{ox} or E^0_{red} can be reached and so

$$\text{either } E^0_{redox} > E^0_{ox}$$
$$\text{or } E^0_{redox} < E^0_{red} \cdot$$

Investigations on natural systems become more complicated by the fact that interactions between the different materials simultaneously present may occur. Simplification was attempted by basing the calculations on the most dominant system, while the others were neglected.

As the titration curve was used for characterizing the system and this curve was measured as a function of the quantity of the titrating agent, it was supposed that the potentials measured in the different sections were determined in the first line by the oxidizing agent used.

The suppositions concerning the quantitative decrease of the $FeCl_3$ added to the system were mentioned above; thus, among the possible equations given by POURBAIX for the Fe—H_2O system, the following were chosen for characterizing different sections of the titration curves.

In section I and II, supposing that hydrolysis is the factor determining the potential:

$$FeOH^{++} - Fe^{++} - H_2O + H^+ + e = 0 \qquad (1)$$
$$E = 0.877 - 0.0591 \text{ pH}$$

$$Fe(OH)_3 - Fe(OH)_2 - H_2O + H^+ + e = 0 \qquad (2)$$
$$E = 0.179 - 0.0591 \text{ pH}$$

For both sections, the calculated potential is the resultant of the values obtained from equation *1* and *2*.

In section III:

$$Fe^{+++} - Fe^{++} + e = 0 \qquad (3)$$
$$E = 0.746 + 0.0591 \log \frac{[Fe^{+++}]}{[Fe^{++}]}$$

Adding 2, 3, 4% limestone respectively or 2% limestone and 3% siderite to a rock originally free of carbonate, the potential curves were measured, interrupting the titration in each of the three sections, and the Fe(II) and Fe(III) content of the solution was determined where necessary for the calculation, the pH of the solution being measured during the whole run of the titration. The potential was calculated from the measurements. *Table 1* shows the difference of the potentials measured and calculated, expressed in mV.

In section III the difference between the measured and calculated values is not significant, especially taking into account the error of measurement of +50 mV given by ZOBELL; it should be remarked, however, that according to our experience, the error did not exceed about ±10 mV. In this section it is really reaction 3 by

TABLE 1

Carbonate added to the rock	Difference between measured and calculated values of Eh in mV		
	Section I	Section II	Section III
2% limestone	70	98	1
3% limestone	37	5	7
4% limestone	27	60	17
2% limestone + +3% siderite	16	81	5

which the potential is determined and the not too significant deviations observed are due to errors of measurement.

In sections I, II the occuring processes are too complicated to be exactly described on the basis of the measurements performed up to now. It seems probable that several processes ought to be taken into account. It is especially difficult to interpret the section II which represents a transitory state. The Fe(III) consuming process occured during section I; in section III the Fe(II); Fe(III) ratio characteristic for the given system has been already developed. While section I and III are more or less parallel to the abscissa, section II shows a steep rise. In this phase of the titration, important changes in potential are caused by addition of very small amounts of $FeCl_3$.

Taking into account also the above sources of error, the calculations presented in *Table 1* support the suppositions based on our measurements and verified by some model-experiments, namely that hydrolysis is the potential determining process in the first section of the titration.

Our measurements for studying some sedimentary rocks with the method described above led to the result that the differentiation between the types of the rock using $FeCl_3$ as oxidizing agent can be performed on the basis of the saturation potential. The starting potential of the suspension cannot be used for classification of samples, namely, it depends not so much on the oxidation state of the components, as rather on their solubility in water *(Fig. 8)*.

The saturation potential *(Table 2)* is suitable for differentiation of the groups, being 745 mV for manganese dioxide, 600 mV for bauxite, and 570 mV for quartzite;

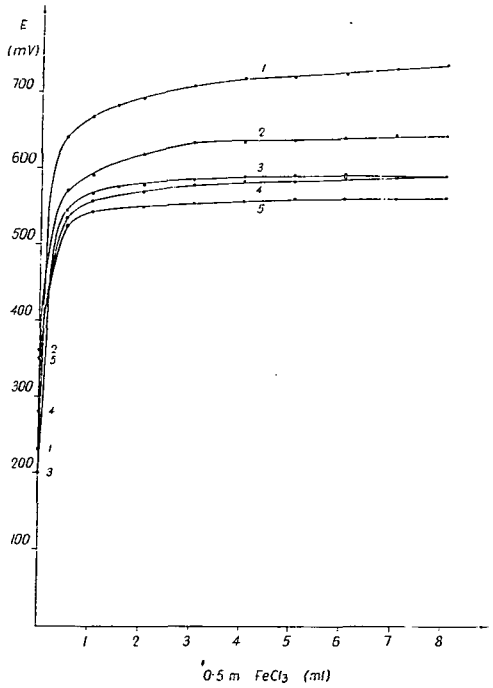

Fig. 8. Potential curves of sedimentary rocks of different type
1. Manganese oxide ore. *2.* Bauxite. *3.* Limey marl. *4.* Gypsum. *5.* Quartzite

it cannot be used, however, for finer differentiation within the groups. We tried also to use other oxidizing agents, such as potassium permanganate, ceric sulphate. These proved less suitable for separating the different groups on the basis of the saturation potential, however, the saturation potentials of different samples within the same group generally presented greater differences than in the case of titration with $FeCl_3$.

TABLE 2

Type of the rock	Sample	E_{sat} 0.5 N $FeCl_3$	E_{sat} 0.01 N $Ce(SO_4)_2$	E_{sat} 0.01 N $KMnO_4$
Resistite	Permian Sandstone	625 mV	1150 mV	1060 mV
	Sandstone of Hárshegy	600	1140	1085
Siliceous rock	Chert	580	1125	1122
	Firestone	566	1150	1125
	Quartzite	568	1120	1110
Argillite	Fire clay	650	1160	1123
	Laterite	664	1175	1085
	Bauxite	660	1140	1095
Oxidite	Manganese oxide ore	745	1145	1040
Carbonate rock	Marl	595	1150	1090
	Limey marl	592	1150	1070
	Limestone	600	1170	1040
Reducite	Siderite	505	1190	998
Evaporite	Halite	667	970	1000
	Anhydrite	633	1150	1062
	Gypsum	602	1165	1135

It is to be expected that the oxidation state of sedimentary rocks determined by potentiometric titration may be useful in their classification. The results reached up to now are, however, only of preliminary character, designing the way to be followed.

It is to be supposed that further improvement of the method will permit to distinguish more sharply the different types of sedimentary rocks.

SUMMARY

ZOBELL characterized the oxidation-reduction state of non-consolidated sediments rich in organic material by potentiometric titration using diluted $FeCl_3$ solution as oxidizing agent. This method was applied for consolidated sediments, too.

The time necessary for establishing the relative equilibrium in oxidizing processes shows differences, depending on the type of the samples; 15—20 minutes, as a minimum, are necessary.

On the potential curve, generally three sections can be distinguished. Section I (the quantity of oxidizing agent consumed) is determined by the carbonate content of the samples, the hydrolysis being the potential determining process.

A steep rise of the potential is characteristic for section II, the slope of the curve depending on quality and quantity of the organic material. By adding organic (kerogen and/or coaly) material to the system the potential rise can be decreased by an order of magnitude compared not only with different types of sedimentary rocks but also with samples containing petroleum distillation fraction as addition. The slope of the potential curves of samples containing kerogen was similar to that of rocks containing no (or very small quantities) of organic material. It can be supposed that the kerogen becomes more oxidized during the extraction.

Section III represents the equilibrium potential reached after the redox reaction.

The characterization of the systems by calculation is more difficult due to the complexity of the systems as well as to possible and uncontrolable secondary processes.

ACKNOWLEDGEMENT

The authors are indebted to PROF. DR. GY. GRASSELLY, Director of Institute, for helpful discussions and valuable advices.

REFERENCES

BOD, M., BÁRDOSSY, G. [1959]: A new method for the determination of the redox potential of sedimentary rocks. (In Hungarian) Geofizikai Közlemények *VIII*, 1—2, 53—65.

EMSCHWILLER, G. [1945]: Compt. Rend., *221*. p. 138—140.

GARRELS, R. M., CHRIST, C. L. [1965]: Solutions, Minerals and Equilibria. Harper and Row. New York.

GRASSELLY, Gy., HETÉNYI, M. [1970]: Some Problems in Determining the Oxidation State of Sedimentary Rocks, Acta Miner. Petr., *XIX*. p, 129—141.

MICHAELIS, L. [1929]: Oxidations-Reductions-Potentiale. Springer Verlag Berlin.

NIGHTINGALE, E. R. [1958]: Anal. Chem., *30*. p. 627.

POURBAIX, M. J. N. [1966]: Thermodynamics of dilute aqueous solutions. London.

STUR, J., MAREK, N. [1965]: Study of redox potential of multicomponent inorganic systems (In Hungarian). Szeged.

ZOBELL, C. E. [1946]: Studies on redox potential of marine sediments. Bull. Amer. Ass. of Petroleum Geologists *30*, 4, 477—513.

Manuscript received. June 20, 1972

MISS DR. MAGDOLNA HETÉNYI,
MISS MAGDOLNA VÁRHELYI
Institute of Mineralogy, Geochemistry and Petrography
Attila József University at Szeged
Táncsics M. u. 2.
Szeged, Hungary

Acta Mineralogica-Petrographica, Szeged, XX/2, 265—270, 1972.

MANGANESE DEPOSITS OF KOREA*

SOO JIN KIM

ABSTRACT. Deposits of many types are known in Korea, apparently none of notable size. They are found in the southeastern and central parts of South Korea and occur in Precambrian, Paleozoic, Mesozoic and Cenozoic rocks. Hydrothermal fissure filling deposits, hydrothermal replacement deposits, sedimentary deposits, and supergene epigenetic deposits are found. The hydrothermal deposits are associated with base-metal ores and also with gold-silver ores, which increase in tenor with depth as the manganese, usually in the form of rodochrosite, diminishes in tenor. Minor manganese oxide deposits associated with spilitization of andesite occur. One sedimentary bed of manganiferous rock intercalated into Precambrian dolostone ranges from 0.5 to 0.1 m in thickness over an outcrop length of 9 km; unfortunately the rock has been metamorphosed and contains a high percentage of silicates of no economic value as well as manganese carbonate.

INTRODUCTION

The manganese deposits of Korea (South Korea) are generally distributed in the southeastern and central parts of Korean peninsula. They occur in the pre-Cambrian, Paleozoic, Mesozoic, and Cenozoic rocks *(Fig. 1)*.

The manganese deposits of Korea can be classified genetically into:

1. Hydrothermal fissure filling deposits,
2. Hydrothermal replacement deposits,
3. Sedimentary deposits, and
4. Superficial deposits.

HYDROTHERMAL FISSURE FILLING DEPOSITS

There are two distinct types of hydrothermal fissure filling deposits. They are vein deposits and breccia-filling deposits.

Veins of the manganese ores are generally found in the Paleozoic dolostone and limestone, pre-Cambrian schists, Mesozoic andesite, granite, and sedimentary rocks, and Tertiary rhyolite. Manganese ore veins nearly always cut the general structures of the country rocks. The contact between the ore veins and their country rocks are generally sharp. The manganese ore veins are grouped as follows:

1. Veins of the manganese oxides only,
2. Veins of rhodochrosite with gold-silver ores,
3. Veins of rhodochrosite with base-metals, and
4. Veins of rhodonite only.

* Lecture delivered at the technical session of the Commission on Manganese (IAGOD) during the XXIV IGC, 25 August, 1972, Montreal, Canada.

FIG.1. DISTRIBUTION MAP OF MANGANESE DEPOSITS OF SOUTH KOREA

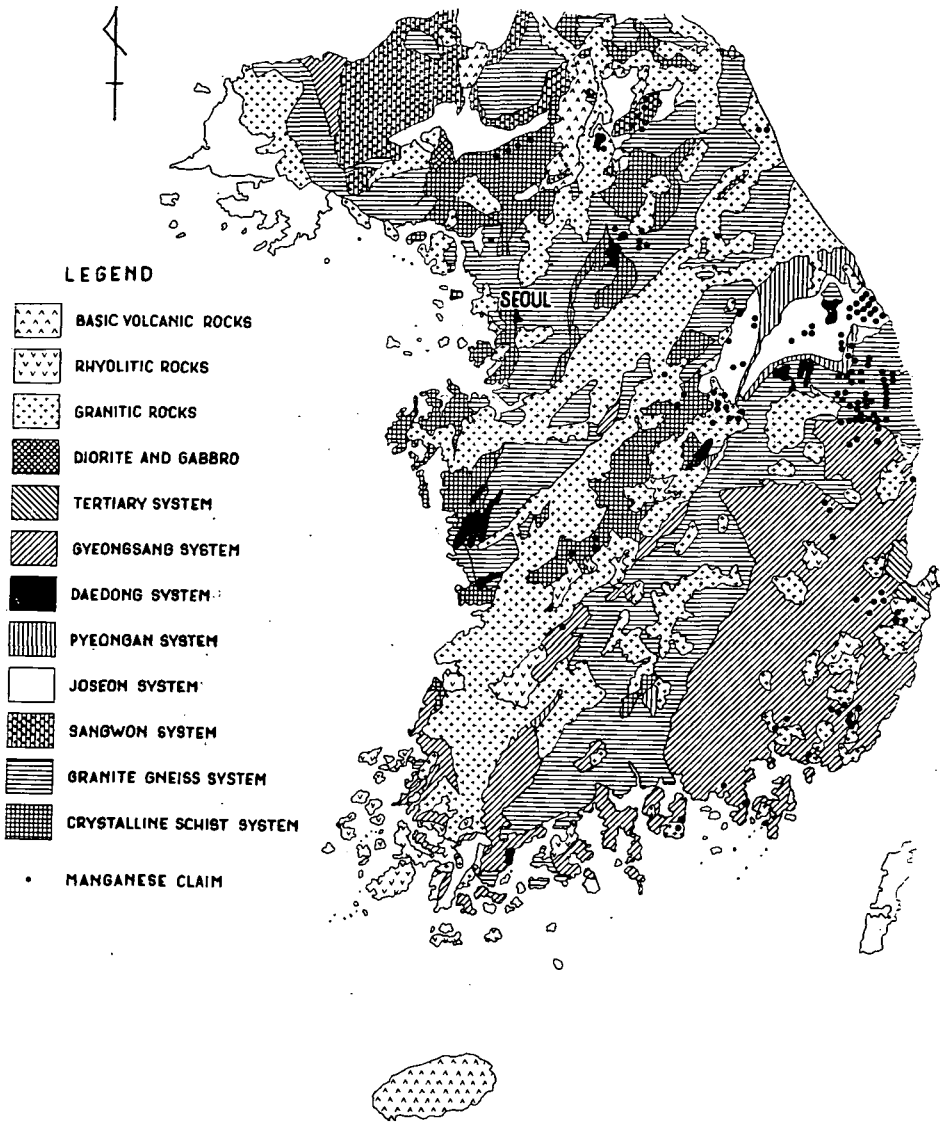

The manganese oxide veins of hydrothermal origin are generally found in the Mesozoic sedimentary rocks and Tertiary rhyolitic rocks. They are closely connected with the subvolcanic rocks in their genesis. Small-scale manganese oxide ores are also found in andesite. They are believed to have originated from spilitization of andesite.

The manganese carbonate veins were formed in close relation to granodiorite

or rhyolitic rock in their genesis. The manganese carbonate veins genetically connected with granodiorite generally accompany the gold-silver or base-metal ores. The manganese carbonate veins genetically connected with rhyolitic rocks frequently accompany the iron ores. The manganese carbonate veins in Dongnam Mine are associated with the magnetite ores of earlier replacement phase. They accompany the hematite ores in one and the same veins in places *(Fig. 2)*.

FIG. 2. GEOLOGIC MAP OF DONGNAM MINE, KOREA

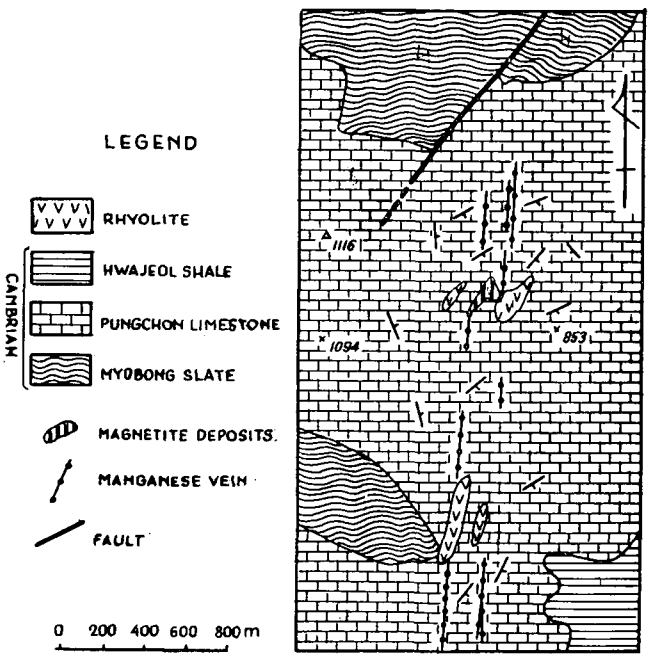

The manganese carbonate ores near the surface change gradually into gold-silver veins, or base-metal veins or replacement ore bodies with increasing depth. The outstanding example is observed in Yeonhwa Mine, where the large lead-zinc-copper deposits of vein and replacement characters were found below the rhodochrosite veins. Breccia-filling deposits are found in the Tertiary subvolcanic rhyolitic rocks *(Fig. 3)*. The rhyolitic rocks are throughly crushed along the contact with the country rocks. The highly porous interstices of the brecciated rhyolitic rocks are filled with the manganese oxide ores. The manganese oxides are also found in the fissures in rhyolite in the same area. It is uncertain whether the rhyolitic rocks were erupted in a submarine environment. Rhodonite veins in altered andesite are believed to have formed from the manganese and silica originating from spilitization of andesite.

HYDROTHERMAL REPLACEMENT DEPOSITS

The manganese deposits of replacement type are not abundant but they are very important as the main source of the manganese ores in Korea. The typical deposits of this type are Janggun manganese deposits in which the manganese

FIG.3. GEOLOGIC MAP OF YEONGIL MANGANESE DEPOSITS, KOREA

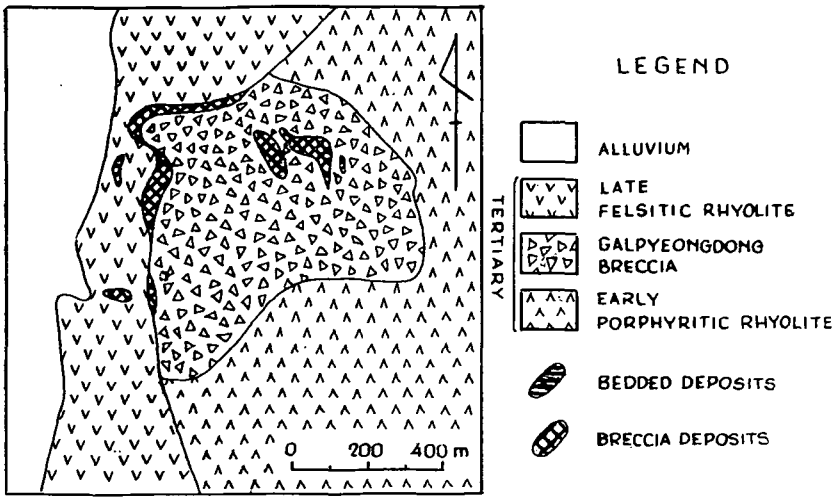

carbonate ores were formed by replacement of dolostone and limestone *(Fig. 4)*. Dolostone is developed only around the manganese carbonate ore bodies. It is believed that the manganiferous solutions arose along faults and replaced the dolostone along the fissures and along the beds. The extent of replacement by rhodochrosite along the beds is not great. The manganese carbonate ores decrease gradually with depth and conversely the base-metal ores increase in their amount. Although small masses of andesite are found near the ore deposits, they have no connection with the formation of the manganese deposits. It is believed that andesite intruded

FIG. 4. GEOLOGIC MAP OF JANGGUN MINE, KOREA

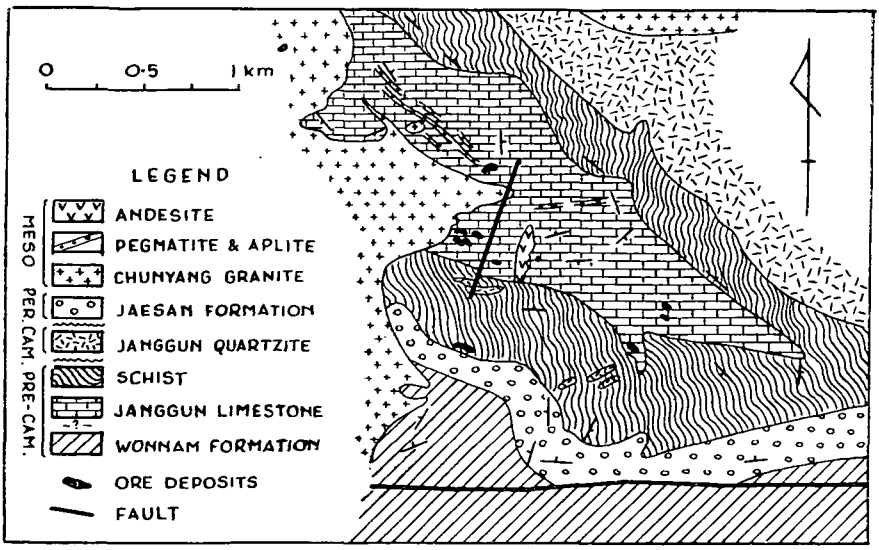

later than the manganese mineralization. The fact that the manganese ores are also found in the Permian schists in this area indicates that the manganese mineralization probably took place in the Mesozoic Period.

SEDIMENTARY DEPOSITS

Sedimentary manganese deposits in Korea are found in the pre-Cambrian and Paleozoic formations. The most important pre-Cambrian manganese formations are metamorphosed. They are mainly found in the central part of Korea. They occur in the dolostone and limestone or calcareous formations of the pre-Cambrian. The manganese formations in Gimhwa district are embedded in the thick dolostone having a strike of N40—70° E, and dip of 50—60° NW *(Fig. 5)*. The manganese formation ranges from 10 to 50 cm in thickness, and extends about 9 Km on the same horizon. The average grade of the ores is 20—30 % Mn. The ores are composed of rhodonite, rhodochrosite, manganoan dolomite and mangangarnet.

FIG. 5. GEOLOGIC MAP OF GIMHWA AREA, KOREA

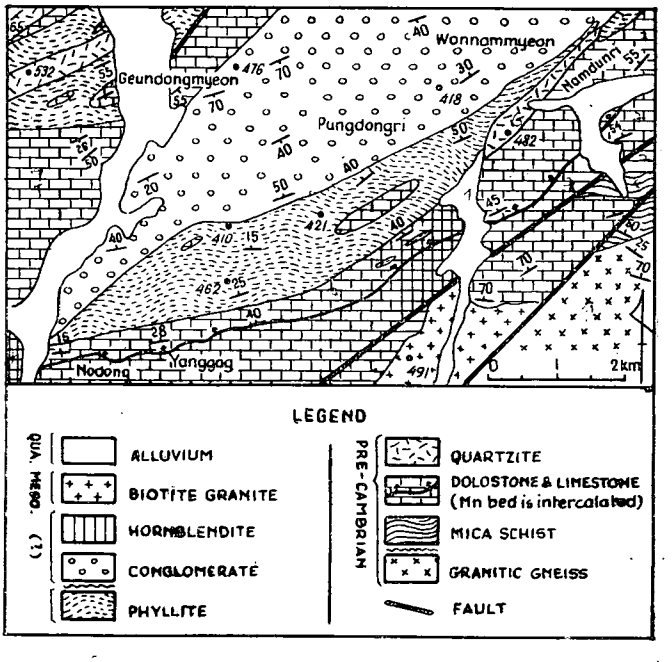

The manganese formations in Gapyeong district occur in mica schists along the schistosity. The ores are composed of rhodonite and manganiferous pyroxene.

Only thin lenses of the manganese otides are embedded in the Paleozoic shale in Samcheog district. It is very interesting that the small-scaled recent manganese conglomerate formation is found on the terrace near the Tertiary manganese deposits.

SUPERFICIAL DEPOSITS

In the past, most of the manganese oxide ores in Korea were produced from the superficial oxidation deposits. Nearly all the manganese carbonate and silicate deposits primary in nature are deeply oxidized near the surface. Typical superficial manganese deposits are Janggun, Yeonhwa and Dongnam mines. Original manganese carbonates are oxidized to various manganese oxide minerals such as manganite, birnessite, pyrolusite, nsutite, cryptomelane, and psilomelane. The manganese oxide ores are found as residual concentration deposits or as the cavity-filling deposits formed from the descending manganese colloids.

AGES AND TYPES OF MINERALIZATION

Manganese mineralization in the pre-Cambrian is characterized by sedimentary deposits associated with dolostone and limestone. In the Paleozoic, manganese was deposited so little as to be non-economic. In the Mesozoic, the manganese oxide and carbonate veins or replacement deposits were formed as the result of igneous activity such as intrusion of granodiorite, and the manganese oxide and silicate deposits were formed from spillitization of the andesitic rocks. In the Tertiary, the manganese oxide and carbonate veins and breccia deposits were formed in close connection with rhyolitic subvolcanic activity. In the Recent, the small-scale manganese conglomerate formations were deposited in a fluvial basin.

REFERENCES

KIM, G. W. and KIM, Y. Y. [1962]: Report on the limonite and manganese deposits at Susan. Geol. Surv. Bull. *5*, p. 43—73.

KIM, O. J. [1970]: Report on the Kyeongju manganese deposits. J. Korea. Mining Geol., *3*, p. 123—133.

KIM, S. J. [1970]: Mineralogy and genesis of the manganese ores from Janggun Mine, Korea. J. Geol. Soc. Korea *6*, p. 135—184.

KIM, S. J. [1970]: Manganese minerals from Janggun Mine, Korea. Proceedings of IMA-IAGOD, IAGOD Volume, p. 460.

KIM, S. J. [1971]: Mineralogical and genetic studies on the manganese deposits at Yeongil. J. Geol. Soc. Korea *7*, p. 122.

KIM, S. J. [1970]: Report on the manganese deposits at Dongnam Mine. (not published).

LEE, D. S. [1967]: Geological study of Janggun manganese mine J. Geol. Soc. Korea *3*, p. 51—59.

WHANG, I. J. [1968]: Report on the investigation of Samhan Janggun Mine. J. Korea Mining Geol., *1*, p. 9—30.

Manuscript received, July 10, 1972

PROF. DR. SOO JIN KIM
Department of Geology
Seoul National University, Seoul, Korea
Present address: Mineralogisch-Petrographisches Institut der Universität Heidelberg
69 Heidelberg, Federal Republic Germany

Acta Mineralogica-Petrographica, Szeged, XX/2, 271—286, 1972.

MINERALOGICAL STUDY OF THE NON-CLAY FRACTION IN THE BAUXITE AND THE ASSOCIATED ROCKS OF AZAD KASHMIR

K. A. MALLICK and M. VALIULLAH

ABSTRACT

Bauxite and the associated rocks from seven different localities of Muzaffarabad and Kotli areas of Azad Kashmir have been investigated for their non-clay mineral correspondence.

Rocks in contact with the bauxite are the fire clay at the base and Eocene shale at the top. The fire clay overlies the Muzaffarabad Formation of Permo-Carboniferous age.

The bauxite and the fire clay correspond closely with each other in their mineralogical composition. No relationship could be found between the top of Muzaffarabad Formation and the bottom of the fire clay.

The study reveals similar provenance and cycle of deposition for the fire clay and the bauxite with some breaks and changes when the pisolites of the bauxite were being formed.

INTRODUCTION

This paper deals with the mineralogical study of the bauxite deposits and the associated rocks in Azad Kashmir. Attempt has been made to reconstruct the depositional and post-depositional environments of the bauxite. This study also seeks to ascertion the degree of correspondence between the composition of bauxite and that of the associated rocks.

Besides the study of the physical properties, field relationships and structural continuity of the bauxite deposits and the associated rocks, a qualitative study of non-clay minerals was made to determine the mineralogical correspondence. Effort has also been made to trace the possible provenance of the fire clay and the bauxite.

GENERAL GEOLOGY

Reference to the geology of this region is found in the reconnaissance geological reports since 1879, but no attention was paid to the mineralogical study of the bauxite deposits and the associated rocks. Similarly as yet no information is available on the genesis of the bauxite or any other deposits of the area.

The bauxite and the associated rocks described in this paper are from Batmong and Khilla of Muzaffarabad area and Sawer Gunimalni, Khander, Kamroti, Nikial, and Salhun of Kotli Tehsil in Azad Kashmir territory *(Fig. 1* and *2)*. The rocks of this area comprise of Muzaffarabad Formation, Bauxite and Fire clays, Chhalpani Formation, Murree Group, Siwaliks and Alluviums of Permo-Carboniferous, Post Permian, Eocene, Middle Miocene, Pleistocene to Pliocene and Recent to Sub-Recent ages respectively.

Muzaffarabad Formation consists of limestone, dolomite and precipitation breccia. The limestone is thinly bedded, light gray to mottled gray and white in color, fine grained, hard and partly dolomitic. Joint and fractures are common.

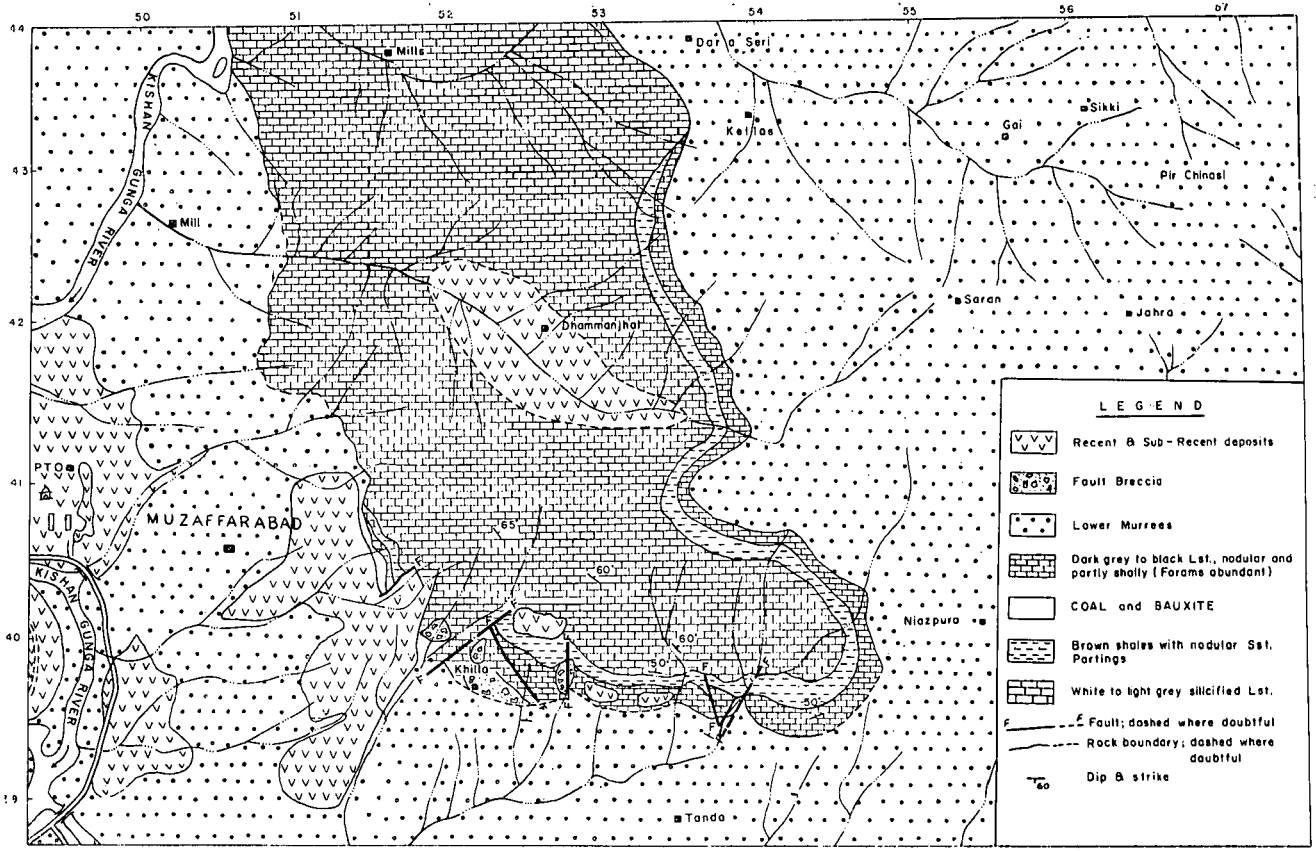

FIG. I GEOLOGY AND MINERAL RESOURCES OF MUZAFFARABAD AREA AZAD KASHMIR

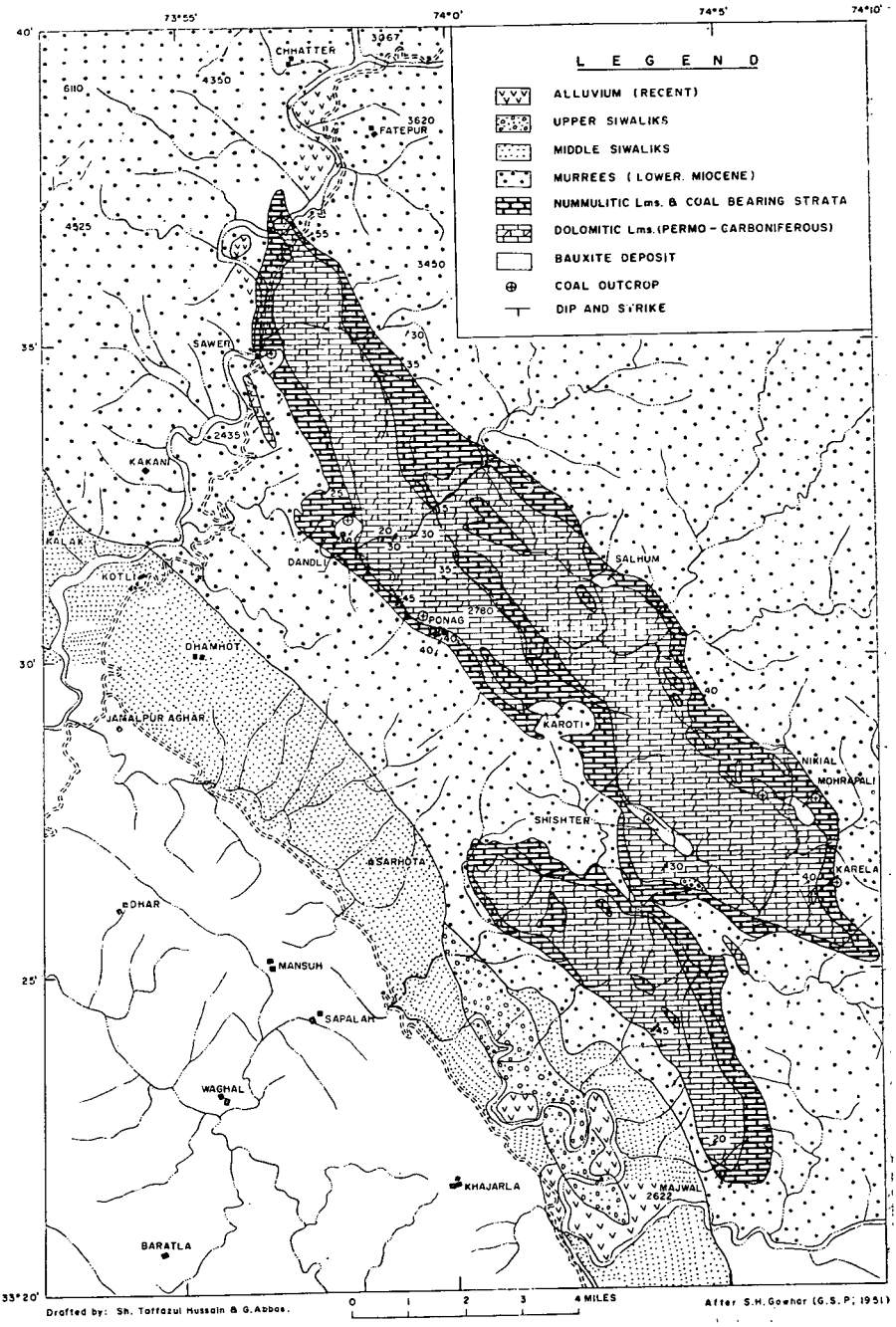

FIG. 2 GEOLOGY & MINERAL RESOURCES OF KOTLI TEHSIL, MIRPUR DISRICT, AZAD KASHMIR.

Above the limestone is the thinly bedded dark gray to black, compact and brittle dolomite.

Precipitation breccia stands out in relief on the top of the dolomite and contains disseminated lath like grains of quartz.

The fire clay and the bauxite overlie the Muzaffarabad Formation of Permo-Carboniferous age. The bauxite is light to dark gray, gray, yellow, brown and dirty white in color and occurs in small pockets and lenses in association with the basal bed of gray and dark gray fire clay. The top of the bauxite bed is pisolitic and grades into non-pisolitic variety at the bottom. Average thickness of the pisolitic bauxite is 2.5 feet and that of the underlying fire clay is 5—10 ft.

At some places the pisolitic bauxite has been completely eroded and only the poorly pisolitic part at the bottom is exposed.

The Chhalpani Formation of Eocene age overlies the bauxite and is a continuous belt of rocks of varying thickness in all the areas of Muzaffarabad and Kotli Tehsil. It is composed of dark carbonaceous light gray to olive and yellowish color calcareous shales; light gray medium grained sandstone; and dark gray to almost black nummulitic limestone. The dark carbonaceous shale above the pisolitic bauxite contains the coal.

METHOD AND MATERIAL

Two localities from Muzaffarabad area and five localities from Kotli Tehsil area as mentioned earlier were selected for sampling of the bauxite and the associated underlying and overlying rocks of Permo-Carboniferous and Eocene ages respectively.

The samples were collected by digging pits of different depths in the bauxite and the associated beds of the localities under study. The samples collected represent the rocks and the bauxite right from the top of Muzaffarabad Formation to the Eocene shales interbedded with limestone, overlying the pisolitic bauxite. Besides, the samples were also collected at various horizons of a bed. Physical differences in color, texture, structure and the thickness of a particular bed were important considerations during the collection of the samples. To facilitate the study of the degree of correspondence between the beds, special consideration was given to the samples collected from the contact zones of the beds.

Few samples have also been collected from the dolomite bed to determine the degree of correspondence, if any, between the dolomite and the overlying precipitation breccia of the same age.

MICROSCOPIC STUDY OF NON CLAY MINERALS IN THE BAUXITE AND THE ASSOCIATED ROCKS

The texture of the bauxite limits the microscopic examination of the minerals present in most of the ores. The feldspars, the amphiboles and pyroxenes are not present in fresh state, but they can be seen in their altered conditions. The feldspars occur as kaolinized and sericitized grains. The amphiboles and pyroxenes show alteration to biotite, epidote and small specks of iron oxide.

Banded algal structures are quite pronounced and conspicuous in the fire clay and the non-pisolitic portions of the bauxites.

The thin sections of the samples of the bauxite and the associated rocks from seven different localities of Muzaffarabad and Kotli Tehsil of Azad Kashmir were

examined to study the local variations in the shape, mineralogy, and stability of the mineral grains in the bauxite and the associated beds. Special attention was paid to the study of similar and dissimilar minerals in the bauxite bed in relation to the underlying Muzaffarabad Dolomite and the precipitation breccia. The overlying Eocene Formation which consists of interbedded shale and limestone was also examined megascopically and microscopically to determine the degree of correspondence of the bauxite with them. Special emphasis was given to the study of the samples collected from the contact of the two consecutive beds to facilitate the study of mineralogical transition or intermixing, if they were laid down in the same cycle of deposition with some degree of fluctuations in the depositional basin.

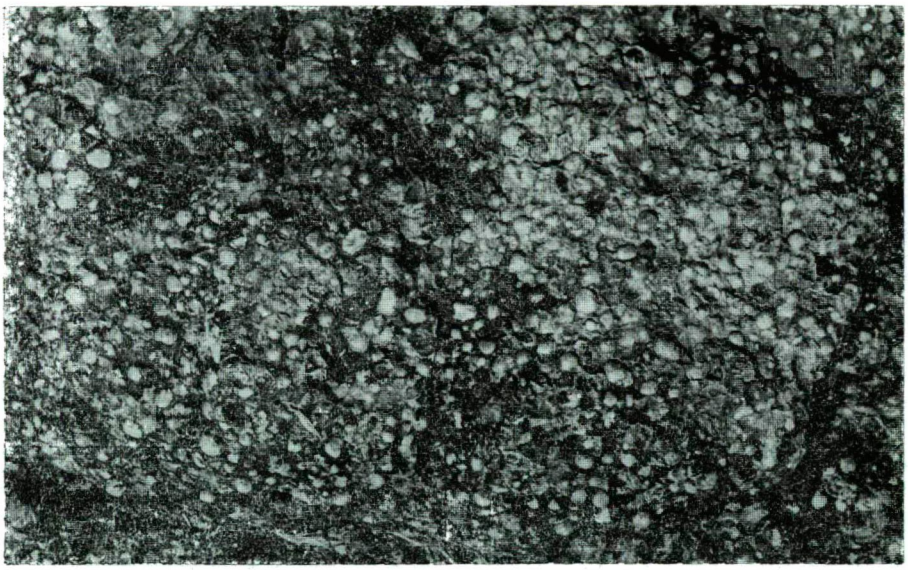

Fig. 3. Photograph showing the texture of the pisolitic bauxite in Salhun locality of Kotli Tehsil

The identification of non-clay minerals in the underlying Muzaffarabad Formation and the Eocene Formation which overlies the bauxite bed was not so difficult as the study of the minerals in the samples of the fire clay and the bauxites of all the selected localities under present investigation. The difficulty in identification of non-clay minerals in the fire clay and the bauxite bed was due to their higher degree of decomposition. The decomposition took place during the deposition of the fire clay and the bauxitization process. Diagenetic minerals such as kaolinite, biotite, epidote and iron oxide specks are quite pronounced and occur in association with the parent minerals like feldspar and amphiboles respectively and can easily be studied in thin sections of the fire clay and the bauxites *(Figs. 7* to *9)*.

In megascopic study the Muzaffarabad Dolomite appears as light gray to dull white. The texture is fine to medium grained. The aggregate of fine grains gives an appearance of sugary texture and can easily be seen without the aid of a magnifying lens. The structure is compact and the rock appears brittle when hammered. The thin sections of the dolomite show clustering of grains which is usually more pronounced in the coarser grains of the rocks. However, the clustering of finer

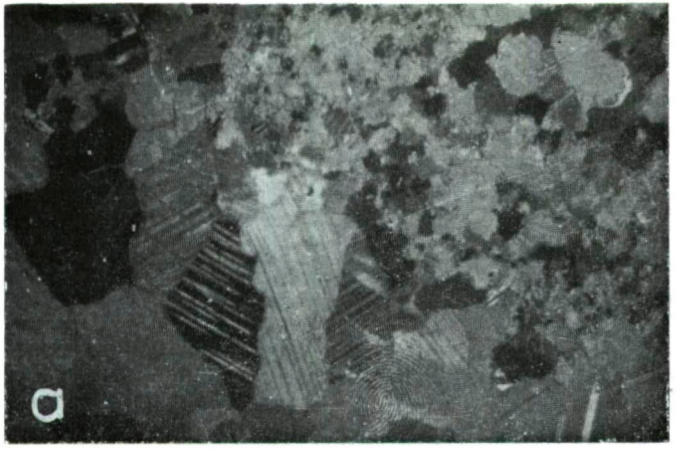

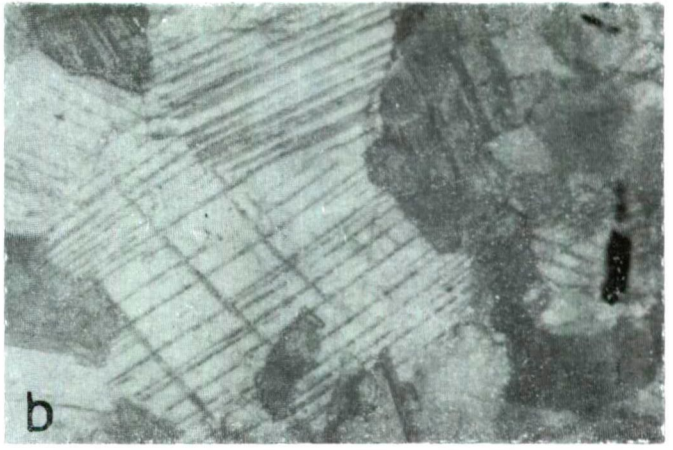

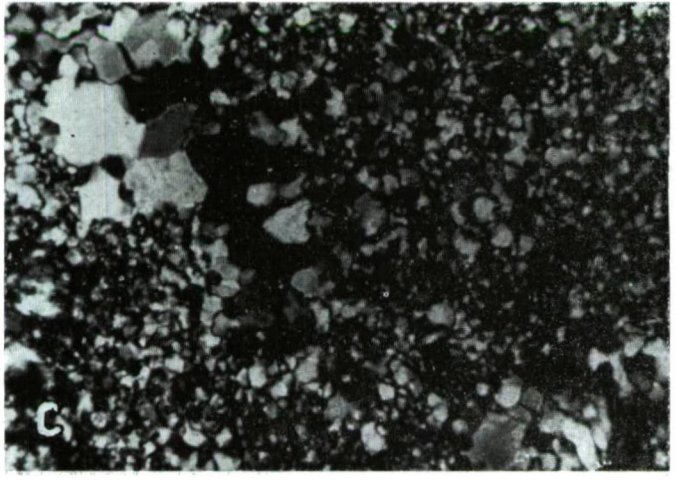

Fig. 4. a) Fine to coarse grained aggregate of anhedral crystals of dolomite from Khander, Kotli area with twinning lamellae in larger crystals only. x50.4, crossed polarizers. *b)* Anhedral crystals of dolomite with twinning lamellae and rhombohedral cleavage from Khandar, Kotli area. 50.4x, crossed polarizers. *c)* An aggregate of fine to coarse anhedral crystals of quartz in precipitation breccia from Khilla, Muzaffarabad area. x50.4, crossed polarizers

grains is also observed *(Fig. 4a)*. The grains of the dolomite appear as an aggregate of medium to coarse grains and exhibit granular texture. The cementing material between the grains is scanty and the grains lie in random orientations. Conspicuous partings and cleavage directions *(Fig. 4b)* are present. In some of the grains rhombic cleavages are quite pronounced. It appears that the dolomite is a product of interaction between the limestone and the sea water ladden with magnesium ions. Some grains of black opaque specks probably of iron oxide are also present.

The precipitation breccia forms the top of the Muzaffarabad Formation in nearly all the areas of Muzaffarabad and Kotli Tehsil of Azad Kashmir. The thickness of the precipitation breccia varies from one locality to another but no variation in mineralogy, texture and structure has been noted.

Megascopically the precipitation breccia is light gray to white. The main body of the sample shows fine grained texture but laths of chert up to two centimeters in size embedded in fine grained aggregates of the same material are common. With the aid of a magnifying lens the grains appear angular to subangular in their shape and are lithified very coherently and so the rock appears compact in its structure. In thin sections the grains of quartz appear to dominate the rock body. The cementing material between the grains is very scanty and the texture is quartzitic *(Fig. 4c)*. Few grains of orthoclase and albite showing kaolinization and sericitization effects were also found.

At Khander lateritic patches lie between the precipitation breccia and the fire clay. The laterite is reddish brown to dark brown in color and exhibits coarse to medium grained texture. No minerals could be identified in the hand specimens due to coatings of iron oxide on the grains.

The thin sections of the samples of laterite show the dominance of orthoclase and albite grains embedded in ferruginous matrix. Some grains of plagioclase and quartz were also found but they are not very common. Usually the grains of feldspars are angular to subangular in their shapes. Most of the grains are kaolinized and sericitized along the margins and cracks but the degree of alteration in feldspar grains of the lateritic patches is much less as compared to the same mineral in the fire clay and the bauxite bed *(Figs. 6, 7)*. Some of the larger grains of feldspars present in thin section of laterite samples *(Fig. 5a, d)* are showing kaolinization effect very conspicuously due to diagenesis.

The color of the fire clay ranges from black to brown and various light and dark shades between these two colors. The texture is fine grained and the structure is compact. The thickness of the bed varies from 3 to 6 feet. Few pisolites were also found in the fire clay. Due to fine grained texture and argillaceous nature of the rock the identification of minerals in the hand specimen is not possible.

The study of the thin sections of the rocks shows the presence of the grains of quartz, kaolinized and sericitized albite and orthoclase embedded in blackish brown argillaceous matrix. Few grains of ferro-magnesian minerals of pyroxene and amphibole groups were also found in altered conditions. The alteration product of these minerals is biotite, epidote and some clay minerals which appear dirty white and cloudy in thin sections. *(Fig. 6d.)* Flakes of biotite, few grains of apatite, anatase and epidote were also seen under the microscope. Exact identification of the mafic minerals is not possible due to intense decomposition of the mineral grains. However, their outline, the development of cracks and the black specks of iron oxide in the body of the grains are quite pronounced. Calcite and muscovite are common. Small specks of iron oxides with random distribution are of common occurrence in the main body of the rock. In all the samples of fire clays from the

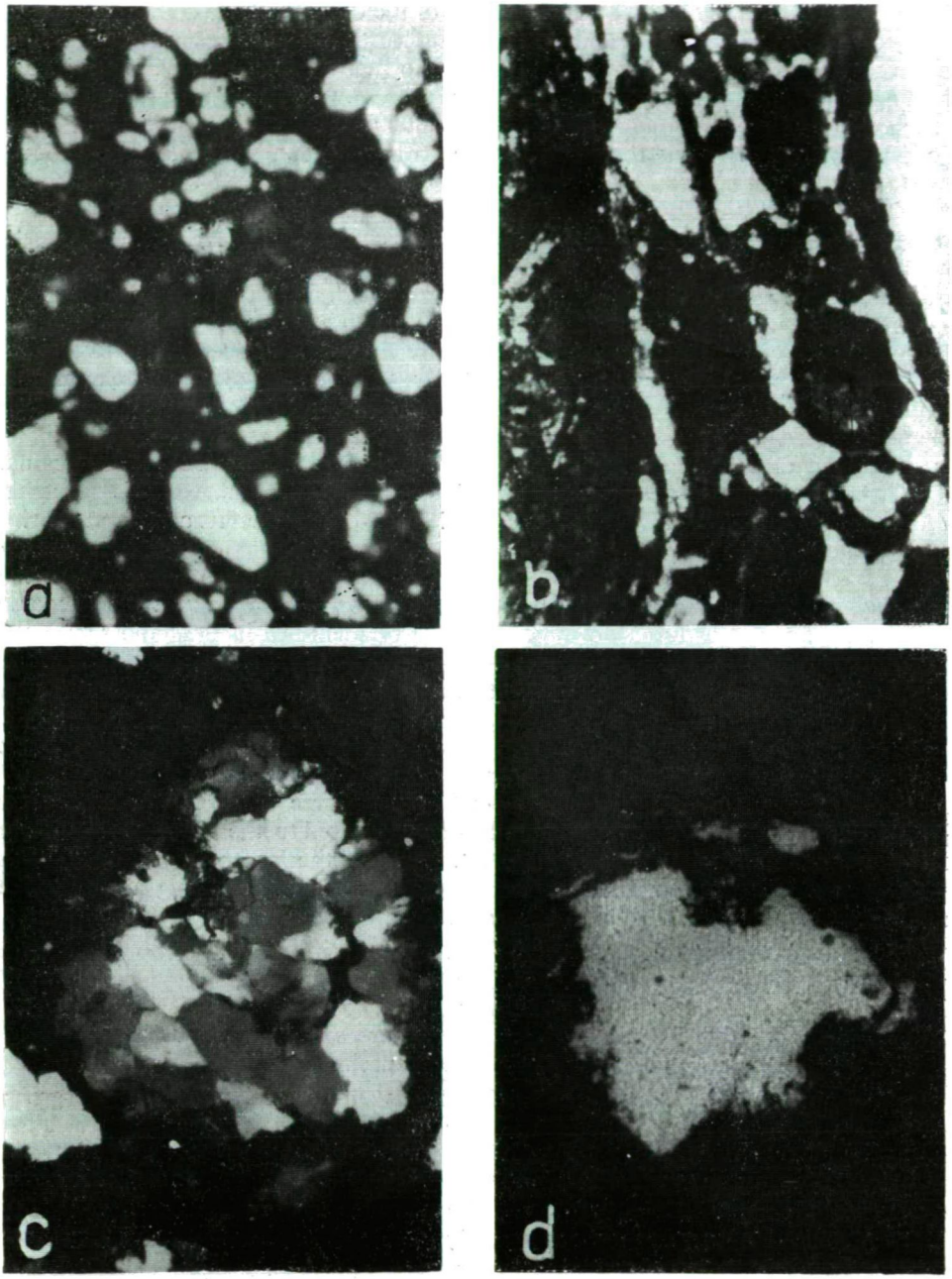

Fig. 5. a) Anhedral kaolinized grains of feldspar embedded in lateritic matrix from Khander, Kotli area. x50,4, polarized light. *b)* Less altered angular to subangular grains of feldspar embedded in lateritic matrix from Khander, Kotli area. x50.4, polarized light. *c)* An aggregate of feldspars and quartz grains surrounded by lateritic matrix from Khander, Kotli area. x50.4, crossed polarizers. *d)* A grain of feldspar surrounded by lateritic matrix from Khander, Kotli area, is kaolinized and angular in shape, x50,4, polarized light.

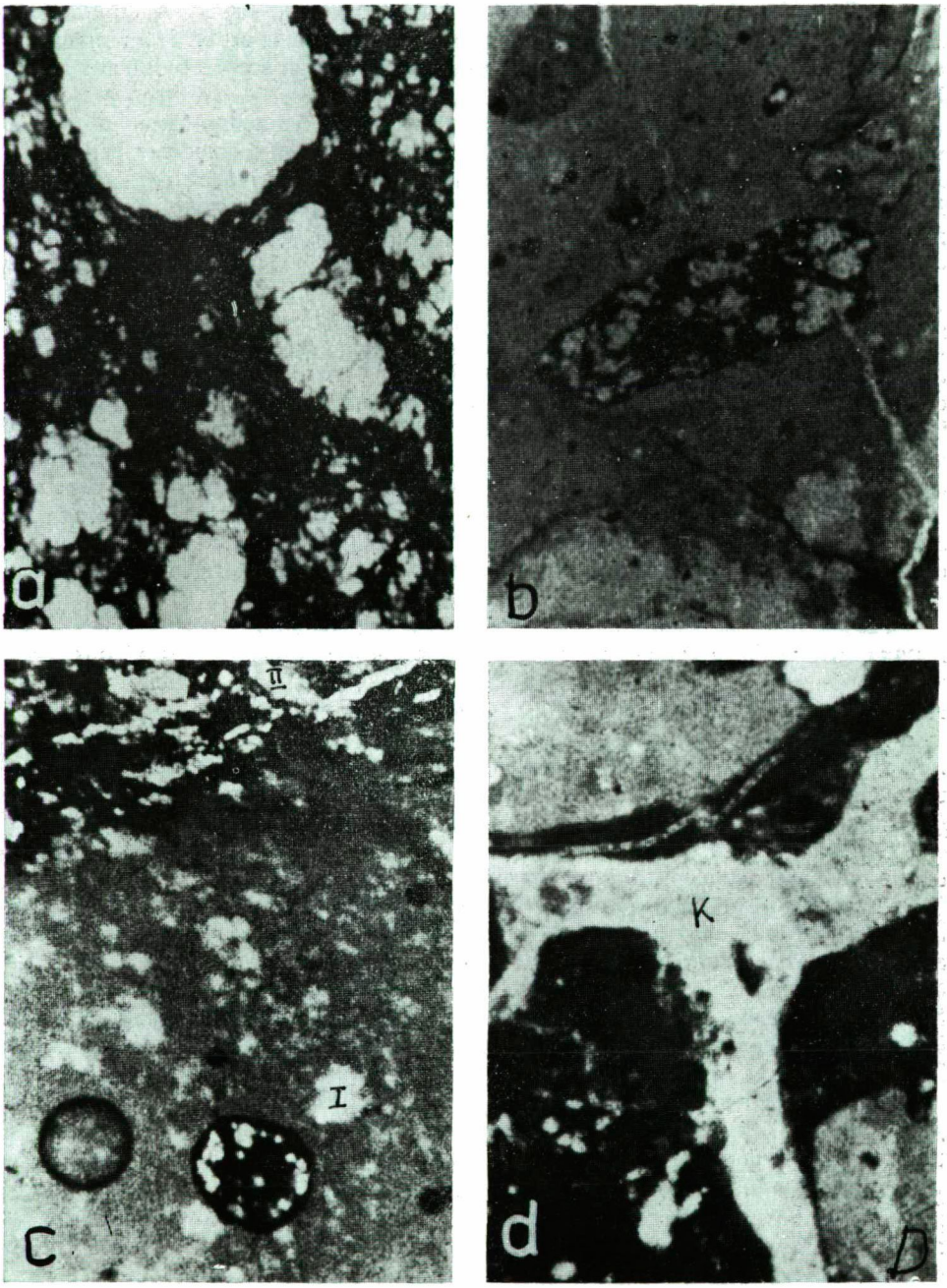

Fig. 6. a) Kaolinized feldspars in the fire clay from Salhun, Kotli area. x50.4, polarized light. *b)* Altered amphibole grain in the fire clay, from Khander, Kotli area. x50.4, polarized light. *c)* Pisolite and decomposed feldspar grains embedded in the fire clay from Nikial, Kotli area. 50.4x, polarized light. *d)* Decomposed feldspar grains and clays (k) filling the cracks in the fire clay from Khilla, Muzaffarabad area. x50.4, polarized light.

various localities of Muzaffarabad and Kotli Tehsil, banded structure is quite common and well pronounced *(Fig. 7a, b)*. The banded structure is probably an indication of the transportation of algal material along with the argillaceous sediments in the basin of deposition. It is also possible that the algal material had been present in the basin of deposition and so when the transported sediments came in contact with the algal materials, both were deposited together and formed the bed of the fire clay. The banded structure in the fire clay resembles much the structure usually found in the algal limestone and so it is possible that the conditions during the deposition of the fire clay were the same as required for the deposition of the algal limestone.

Megascopically the color of the bauxite samples ranges from black to light gray and various light and dark shades between the two colors. The pisolites in the bauxites range from 5 mm to 3 cm in diameter. The pisolites are more abundant at the top of the bed than at the bottom which is in contact with the top of the fire clay. The aggregate of smaller pisolites is not very tightly cemented and they can be seperated if pressed with the thumb. This property of friability is not common in case of those samples which contain larger pisolites but they are more firmly cemented and compact. The size of the pisolites and their color differ from one locality to another. Usually the pisolites in the bauxite samples of Batmong and Khilla localities of Muzaffarabad area are 2—8 mm in diameter and are less compact than the pisolites of the bauxite samples of various localities of Kotli area which range from 2 mm to more than 5 cm in diameter.

The thin sections of the bauxite samples show the presence of argillaceous and ferruginous matrix in which grains of orthoclase, albite, quartz, flakes of muscovite and biotite, are embedded. Few grains of anatase, apatite and calcite were also found. Specks of iron oxides were also seen under the microscope.

The grains of albite and orthoclase are angular to subangular in shape. These mineral grains are kaolinized and sericitized though their outlines are quite prominent. Generally in thin sections of the pisolites the mineral grains show their outlines quite conspicuously, but in some cases the grains are so intensely decomposed that the study of the shape is difficult *(Fig. 9)*. The internal structure of the pisoitesl commonly shows concentric character in all the localities under present investigation. In some of the pisolites few laths of feldspars appear as trapped grains in carbonaceous and argillaceous matrix. In others the rim is lined by altered grains of feldspars, and the internal material is carbonaceous to argillaceous with few grains of decomposed feldspar. In such pisolites the pisolitic structure is not well developed. Some of them exhibit random setting of non-clay mineral grains specially feldspars in them. It appears from the study of the internal structure of the pisolites that the local disturbances in the environment of bauxitization and pisolite formation were active and caused irregularities in the internal structure and setting of the mineral grains in them. Probably the disturbance in the supply of organic matter and the sediments were more intense at the time of bauxitization.

In non-pisolitic bauxite samples also some grains of feldspar and other minerals mentioned above are present, exhibiting the same degree of decomposition of the mineral grains as in the pisolites. In some cases the altered feldspars appear to dominate over the matrix *(Fig. 8b)*.

The matrix of the Eocene shale is argillo-ferruginous and appears as gray to grayish white in color. The mineral grains studied in the thin sections of the shale samples are angular to sub-angular orthoclase, albite, quartz, muscovite, biotite and specks of iron oxide in order of their abundance. The grains of orthoclase and

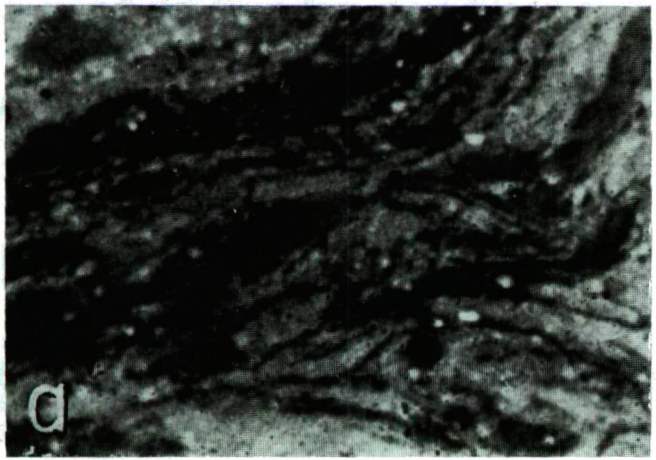

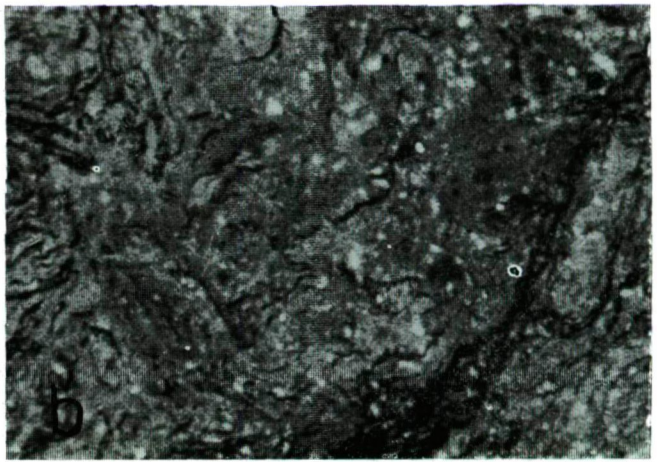

Fig. 7. a) Banded algal structure with fine grains of kaolinized feldspars in the fire clay from Khander, Kotli area. x50.4, polarized light. *b)* Closely banded algal structures with white spots of kaolinized feldspars in the fire clay from Khander, Kotli area. x50.4, polarized light. *c)* Decomposed feldspars grains are embedded in the fire clay of Khander, Kotli area. x50.4, polarized light.

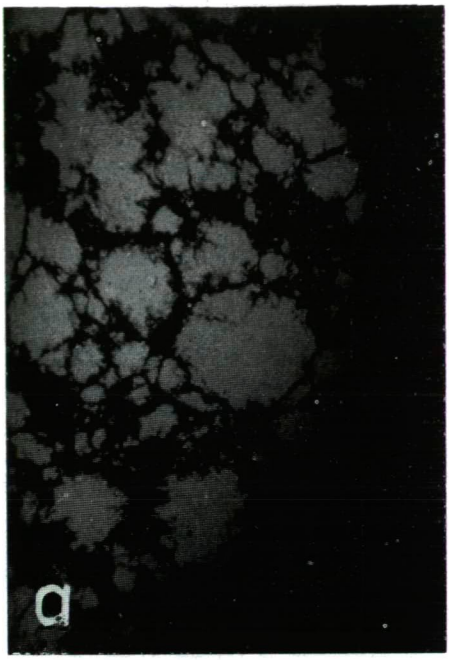
a

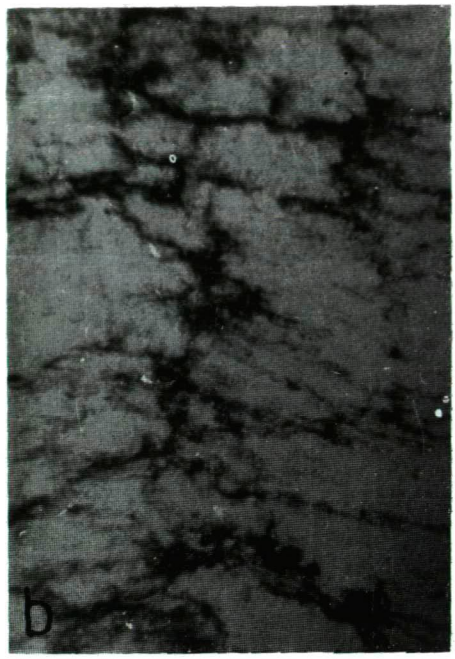
b

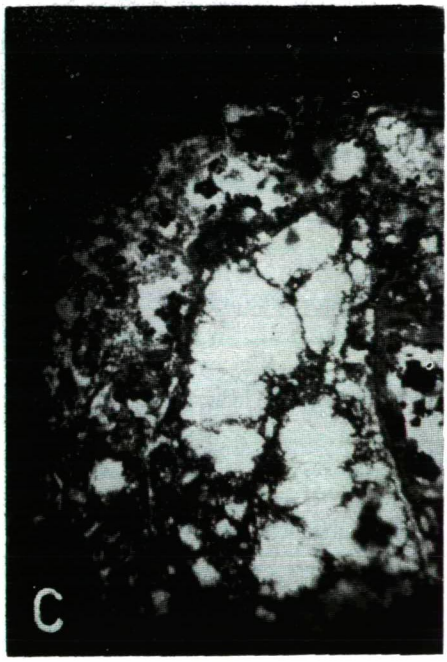
c

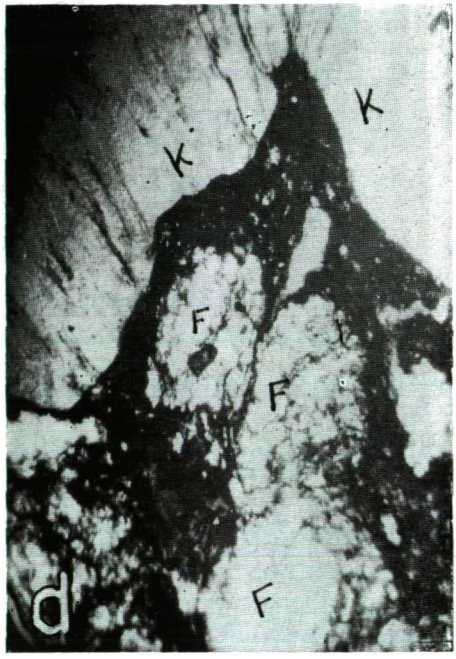
K
K
F
F
F
d

albite are kaolinized and sericitized but the decomposition of the grains is not as intense as in the samples of the bauxite and the fire clay. Kaolinization and sericitization are more conspicuous along the margins, cleavages and cracks, than on the main surface of the grains. Micrites and calcite grains are quite conspicuous and common.

DISCUSSION

The textural and mineralogical study of the samples in thin sections indicate dolomitization of the limestone which forms the base of Muzaffarabad Formation. It seems that prior to the deposition of precipitation breccia dolomitization of Muzaffarabad limestone was completed in the shallow marine environment which usually has a higher concentration of magnesium than the deep water of the sea [FAIRBRIDGE, 1963]. The dolomite because of its higher effective porosity as compared to the limestone allowed the siliceous solution to percolate through to the limestone at the base and fill the cavities present in it. Precipitation breccia veins and cavity fillings are also found in the dolomite, but they are not as common as in the limestone.

If it is supposed that deposition of the precipitation breccia was simultaneous with the dolomitization, then it becomes difficult to explain the presence of precipitation breccia in the cavities of Muzaffarabad Limestone.

The precipitation breccia is referred to either as silicified limestone [MASTER, 1957]; or lime breccia [G. M. C., 1965] or chert breccia [MR. S. H. FAROOQI, Pakistan Indust. Develop. Corp., personal communication, 1970]. The present study which is based on megascopic and microscopic identification of minerals in thin sections indicates that this bed is the result of siliceous precipitate. This conclusion is also supported by the differential thermal analysis data and the chemical analyses of the samples which show 95 % SiO_2 contents [MALLICK and VALIULLAH, 1971]. The similarity of the texture to the breccia is because of recrystallization and diagenesis. The precipitation from solution is also proved by its presence as cavity fillings in the Muzaffarabad Limestone as mentioned above. It therefore, appears appropriate to name this rock as precipitation breccia.

The presence of altered angular to subangular grains of feldspars, ferromagnesian minerals probably of amphibole group, the quartz grains in the argillaceous matrix of the fire clay and the pisolitic bauxite reveal their transported nature and a common source. The presence of lateritic patches containing comparatively fresher grains of minerals than in the fire clay and the pisolitic bauxite, and its position between them further indicate immature state of the material which formed the two beds.

The negative correspondence of the fire clay and the pisolitic bauxite with the associated underlying Muzaffarabad Formation and the overlying Eocene Formation is clearly indicated by the microscopic examination of the minerals in thin sections.

Fig. 8. a) Non-pisolitic bauxite from Nikial, Kotli area, with abundant fresh feldspar grains. 50.4x, polarized light. *b)* Non-pisolitic bauxite from Nikial, Kotli area, showing kaolinized feldspar grains in argillaceous matrix. 50.4x, polarized light. *c)* A part of the poorly developed pisolite from Batmong, Muzaffarabad area showing fine to coarse grains of feldspar trapped in it. x50.4, polarized light. *d)* Non-pisolitic bauxite from Khilla, Muzaffarabad area, showing kaolinized feldspar grains and some completely kaolinized feldspar (K). trapped in argillaceous matrix. x50.4, polarized light.

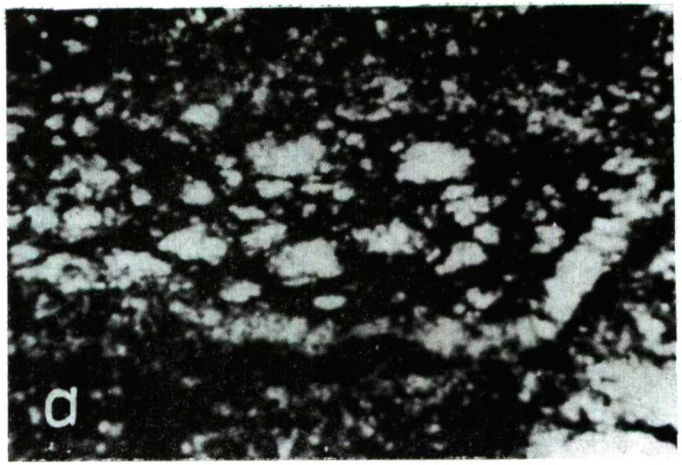

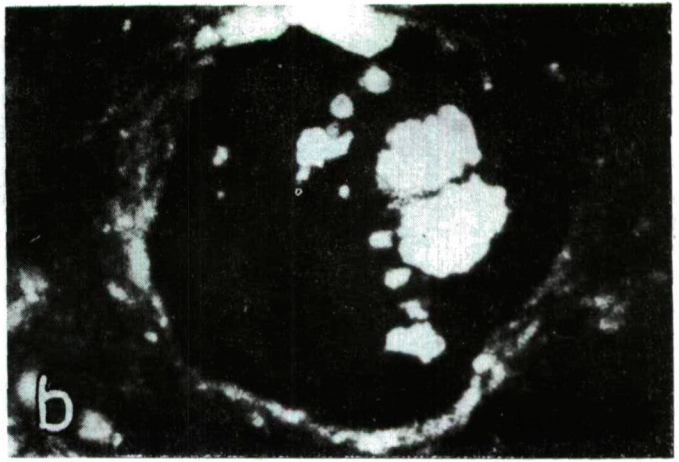

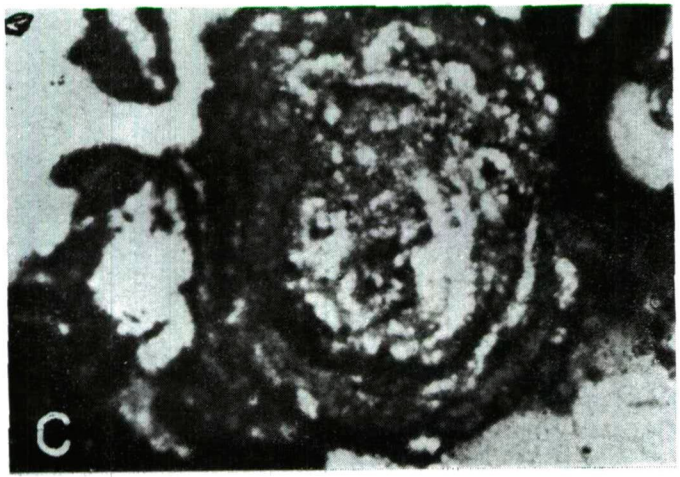

Fig. 9. a) Pisolitic bauxite from Batmong, Muzaffarabad area, showing concentric structure and enclosed decomposed feldspar grains. x80, polarized light. *b)* Pisolitic bauxite from Kamroti, Kotli area showing only the rim and few trapped decomposed feldspar grains. x50.4, polarized light. *c)* Pisolitic bauxite from Nikial, Kotli area, showing poor development of concentric structure and the mineral grains in it x50.4, polarized light.

The provenance of the fire clay and the pisolitic bauxite was most probably in the north and north east of Muzaffarabad trough which is occupied by the gneisses, schists, slates and the early Tertiary intrusions of granite, syenite, granodiorite and diorite.

The positive correspondence between the fire clay and the pisolitic bauxite, on the basis of their mineral assemblage is probably due to their common provenance. The cycle of deposition also appears to be the same with some fluctuations in sedimentation and shallowing of the depositional basin when the pisolitic bauxite was in the process of formation.

While studying the bauxites from Jammu province ASHOK [1967] concluded that the provenance of the bauxites is in Pir Panjal trap which is situated further north from the localities of the bauxite deposits. But the present study reveals that the source rocks of Azad Kashmir bauxites are the alkaline igneous and metamorphic rocks as mentioned above and is discussed below:

GEE [1957] is of the opinion that the basin structure of West Pakistan was emerging from the north and was submerging in the south during Mesozoic and Tertiary times. This statement further supports the possibilities of the source rocks for the fire clay and the bauxite deposits to be in the north.

The algal structure as seen in the thin sections of the fire clay and the bauxites *(Fig. 7)* is an indication of vegetation at the time of deposition of the two beds which would have been a cause of higher percentage of silica in the deposits.

The dominance of feldspar grains in the fire clay and the bauxite samples as compared to silica is probably because of the dominance of alkaline rocks in the provenance.

LOUGHNAN and BAYLISS [1961] described a large deposit of bauxite near Weipa, Queensland, Australia which formed from quartzose rocks containing less than 4% alumina.

The fire clay and the bauxites of Muzaffarabad and Kotli Tehsil do not show any degree of positive correspondence with the immediate underlying precipitation breccia of Muzaffarabad Formation with respect to the clay and non-clay minerals which are identifiable in the bauxite and the fire clay. Therefore, it is unlikely, at least in the area of the present study that the origin of the fire clay and the pisolitic bauxite is from the precipitation breccia of Muzaffarabad Formation, as suggested by Loughnan and Bayliss for the origin of Weipa bauxite of Queensland from quartzose rocks.

The desilicification of the overlying Eocene beds responsible for the origin of the precipitation breccia (previously called as silicified limestone) as suggested by MASTER [1958], does not seem very reasonable in the light of the present observations and their interpretations as discussed above. However, with the help of the available informations on clay formations and its age relationships and because silica precipitates in acidic environment, it is concluded that acidic oxidizing environments were present at the time of deposition of the precipitation breccia, the fire clay and the bauxites. The sutured texture present in the precipitation breccia may be attributed to the recrystallization and diagenesis of the siliceous precipitate.

CONCLUSIONS

1. The chert breccia should more appropriately be termed as precipitation breccia.
2. The precipitation breccia is a chemical precipitate with no change in the mineral composition from one locality to another and is not related to the bed below it.

3. Texture of the precipitation breccia is the result of diagenetic processes and recrystallization.
4. Dolomitization of Muzaffarabad Limestone took place prior to the deposition of the precipitation breccia on its top.
5. The fire-clay and the overlying pisolitic bauxite show mineralogical similarities.
6. The mineralogical similarities and undulatory contact between the top of the fire clay and the bottom of the bauxites which grades upward into highly pisolitic bauxite indicate same cycle of their deposition. Most probably shallower and agitating water environment was prevailing when the pisolitic bauxite was being deposited.
7. The bauxite and the fire clay are detrital in origin and have common parentage in alkaline igneous and metamorphic rocks exposed in the north and northeast of Muzaffarabad Trough.
8. The bauxite is immature with respect to alteration of its non-clay minerals.

ACKNOWLEDGEMENTS

The writers express their gratitude to M/S Pak Chrome Mines for the financial help to carry out the field work during 1967-68 and to DR. S. A. BILGRAMI, Director of the same organization for his critical review of the manuscript.

The transport and accommodation facilities provided by W. P. I. D. C. during the field work and collection of samples is also gratefully acknowledged. The cooperation of MESSRS. S. H. FAROOQI, NASIM AHMED KHAN, NIZAMUDDIN and ABDUL KARIM of the North Regional Office of the same organization is also acknowledged with thanks.

REFERENCES

ASHOK SINGH, CAILLERE, S. [1967]: Bauxites from Jammu Province. — C. R. Acad. Sc. Paris, Sec D *264* (18), 2177—2180).

FAIRBRIDGE, R. W. [1964]: The importance of limestone and its Ca/Mg content to Palaeo-climatology. — Problems in Palaeoclimatology, NATO Proceedings. Edited by NAIRN A. E. M., Interscience Publishers' N. Y., 431—478.

GEE, E. R. [1957]: Notes on Mesozoic Tertiary stratigraphy of the Punjab (NWFP) Sulaiman region. — Geol. Surv. Pak., (Unpublished report).

GEOL. Mining Consultants [1965]: Minerals Appraisal Survey Report, Quetta. — 51—69.

GOWHER, S. H. [1953]: Report on the occurrence of coal near Muzaffarabad in Azad Kashmir. — Geol. Surv. Pak., (Unpublished report).

HERON, A. M. [1950]: Directory of Economic Minerals. — Geol. Surv. Ind., Rec. *1*, 69.

IKRAMUDDIN, S. [1954]: Report on the Mineral Resources of Azad Kashmir. — Geol. Surv. Pak., (Unpublished manuscript).

LOUGHNAN, F. E., BAYLISS, P. [1961]: The mineralogy of the bauxite deposits near Weipa, Queensland. — Am. Min., *46*, 209—217.

MALLICK, K. A. [1967]: Weathering of rocks and mobility of elements in soil profiles of Mont. St. Hilaire, Quebec, Canada. — M. Sc. Thesis, McGill University, (Unpublished).

MALLICK, K. A., VALIULLAH, M. [1958]: Clay minerals in the Bauxite and in Associated Rocks of Azad Kashmir. — Clay Minerals, London, (Accepted for publication).

MASTER, J. M. [1958]: Notes on bauxite deposits of Muzaffarabad. — Geol. Surv. Pak., (Unpublished report).

Manuscript received, July 20, 1972

DR. K. A. MALLICK
DR. M. VALIULLAH
Department of Geology,
University of Karachi
University Road, Karachi-32, India

Acta Mineralogica-Petrographica, Szeged, XX/2, 287—309, 1972.

ROLE OF METASOMATISM IN THE LODE'S ENVIRONS OF GYÖNGYÖSOROSZI (MÁTRA MOUNTAINS)

J. MEZŐSI

SUMMARY

The mineralogical-petrological investigation of the associated rocks of dead galleries connecting the veins was performed; the lodes lie in the mine of Gyöngyösoroszi in four levels (i. e. in heights of +250, +300, +350 and +400 metres above sea level). In the mine's gangways Lower Tortonian andesite and andesite tuff can be found. The andesite consists partly of orthoandesite (in the level +400 metres) and partly of hypomagmatic products of different texture with slight pyritization. Silicification, as well as clay mineralization in the faulted zones are common phenomena.

On the basis of derivatographic investigations in the clay-mineralized associated rock the following clay minerals, resp. their assemblage could be determined among the secondarily formed minerals of the four levels: illite-type, montmorillonite-illite, montmorillonite-kaolinite, montmorillonite-jarosite, kaolinite with calcite, kaolinite with jarosite and calcite. In addition to the clay minerals in most of the cases gypsum occurred in considerable quantity.

On the basis of the X-ray diffractometric investigations the following can be stated. Independently of the K_2O-content of the sample formation of sanidine and adularia, i. e. the replacement of plagioclases by potassium feldspars did not followed, the higher potassium content is connected to sericite-illite and not to the potash-feldspars. As a result of silicification quartz occurs in considerable quantity in the fresh rock, too. Out of the clay minerals illite-sericite, montmorillonite and kaolinite could be demonstrated, the definite zonal arrangement could not be observed. The description of jarosite from this mine has not been referred yet.

As a result of the investigation of the alkali content of different levels it is obvious that where the rock is fresh and no fault zone exists, in the neighbourhood of the lodes the high values concerning the K_2O were found between 10 and 25 metres. In the sites, however, where fault zone can be found the rock type is changing, the decomposition and clay mineralization are characteristic, the indication character of K_2O is lost. According to the investigations performed up to now there is a relation between the K_2O and sulphide-S and the optimal value of it may be given between the weight per cent of 2.5 and 4.5 of K_2O and this may indicate the exploitable ores.

INTRODUCTION

The geological structure and map of the mine and environs of Gyöngyösoroszi were demonstrated by NOSZKY sen. [1927] and later by G. PANTÓ [1950] concerning the closer area. According to his opinion in the environs of the outcrops there are mainly andesites, and three types of them can be distinguished: andesite with inclusions, older decomposed andesite agglomerate with interbedded lava bodies, and younger andesite agglomerate. He observed the different rock alterations only in the proximity of the mine and connected them to the ore formation. These alterations may be greenstone formation, blistered transformation, silicification and "kaolinitization".

The Miocene volcanic formations were divided into lower, middle and upper series by SZÁDECZKY-KARDOSS, E. *et al.* [1958]. The ore-bearing veins belong to the Lower Tortonian series and in their surroundings strong chloritic, silicic and clay mineral alterations can be observed.

VIDACS, A. [1961] distinguished two great volcanic phases. The first phase is that mentioned also by PANTÓ and which is the andesite series of inclusion. The presence of this sequence was proved by the bores of Gyöngyösoroszi No. 2. [1964] and of Mátraszentimre No. 2. [1966]. The product of the other phase is a relati vely fresh dark-grey pyroxene-andesite (cover-andesite).

The ore-bearing lodes lie in the Lower Tortonian series. The associated rocks became in several places clay mineralized, silicified and chloritized, the regular propilite, however, has not developed in the levels discovered up to now.

Regarding the lodes numerous data were published by NOSZKY sen. [1927] and ROZLOZSNIK, P. [1942], the introduction of the vein system known at that time was performed by VIDACS [1957, 1961, 1966]. Concerning the paragenesis further data were published by PAPP, F. [1933], SZTRÓKAY, K. [1938, 1939, 1952, 1962], KOCH, S. [1953, 1958, 1970], NEMECZ, E. [1953], KASZANIIZKY, F. [1958, 1961] and RÓZSA, É. [1961].

The movements generating the lodes took place in different times. At the formation of the oldest fault system veins of breccia-character had developed which were penetrated several times by productive lodes. The second tectonic phase produced the ore-bearing lodes being of NNW-SSE, resp. NNE-SSW and WNW-ESE strike direction. Among these lodes considerable difference of age cannot be determined. The third and fourth tectonic phase did not generate exploitable lodes, the last phase is characterized by amethyst.

Recently two groups of lodes are under mining in different levels and the investigations relate to their environs. The first is the Károly-lode, the second one the Aranybányaérc.

ASSOCIATED ROCKS OF THE ORE-BEARING LODES

In the area of the mine the investigations performed up to now concerned only the substance, structure and paragenesis of the lodes disregarding the associated rocks, their alterations and secondarily minerals. SZÁDECZKY-KARDOSS, E. *et al.* [1958] stated only the fact that the lodes lie in the middle andesite sequence and in this variegated rock series several types can be distinguished: chloro-andesite, propilite, hydroandesite, silicoandesite, carboandesite, blistered andesite, andesite with pseudoagglomerate. These varieties could originate hypomagmatically, by metamagmatic transformation or by a later endo- and exometamagmatic transformation of low temperature.

Since 1970 a series of investigations have started aiming the determination of the role of associated rocks. Such dead galleries were chosen which are connected to each other by two lodes and the distance between them is great enough for observing the alterations of the associated rocks. For this purpose the *Károly, Aranybányabérc* and *Péter-Pál* lodes were chosen. These are nearly parallel and of similar strike and are exposed on several levels. The position of the dead galleries as compared to the lodes mentioned above, the places of sampling as well as the number of the samples are shown in *Fig. 1*. The sketch exactly demonstrates that the Károly lode is nearly of vertical position while the Aranybányabérc lode together with the Péter-Pál lode is of eastern dip. In the +400 m (lower) and +300 m levels sampling was performed by every ten metres while in the levels of +250 and +350 metres it was done by every ten metres near the lodes and every 20 metres farther from them. Consequently, about 170 samples were collected and the petrological, mineralogical investigation and alkali-content determination of them were performed.

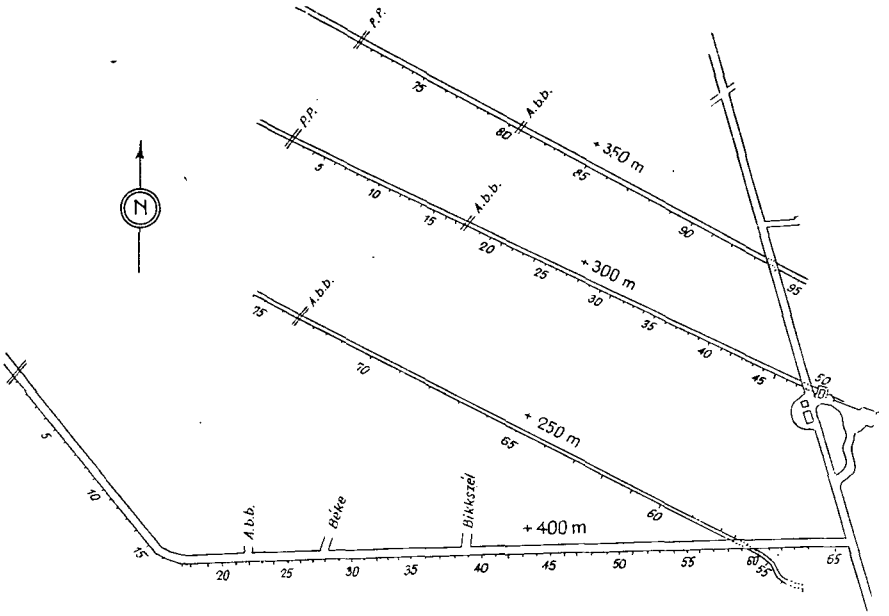

Fig. 1. Places of sampling in the dead galleries

The level of +250 metres

In the gallery of about 420 metres length the petrological formation of the rocks seems to be uniform. The compact rock of lighter-darker grey colour is mostly silicified, feldspar and chloritized pyroxene are characteristic. The slight pyrite impregnation seems to be common. More intensive clay mineralization occurs about 70 metres west of the Károly lode and in both sides of the Aranybányabérc lode.

On the basis of microscopic investigation only clay mineralization and silicic replacement indicates some variousness in the basic rocks. The original microlites can be rarely recognized, they are usually replaced by sericite and quartz of 0.01 to 0.02 mm measure, consequently only conclusions may be drawn to the original texture. Microscopic quartz veins frequently traverse the rock and the replacement of the basic substance is frequently observable.

The feldspar phenocrysts are well separated from the basic substance, their size may reach 2 millimetres and they are for the most part of columnar habit. Zonality cannot be observed, twin-formation is indistinct due to the chloritic and sericitic replacement. They are frequently dissected net-like by sericite *(Fig. 2)*. When in the rock's cave there are calcite crystals, the phenocrysts are also calcitized. The pyroxenes reaching 2 mm size are totally chloritized and always contain pyrite *(Fig. 3)*, their calcitization is less frequent.

Level of +300 metres

At the end of the gallery of Károly lode, i.e. in NW direction as well as in its environs the rock is compact, very hard and is of greenish-grey colour and of porphyric texture. The feldspars reaching the size of 3 millimetres are of whity-grey fatty colour, and often show idiomorphous cross section. Femic minerals cannot

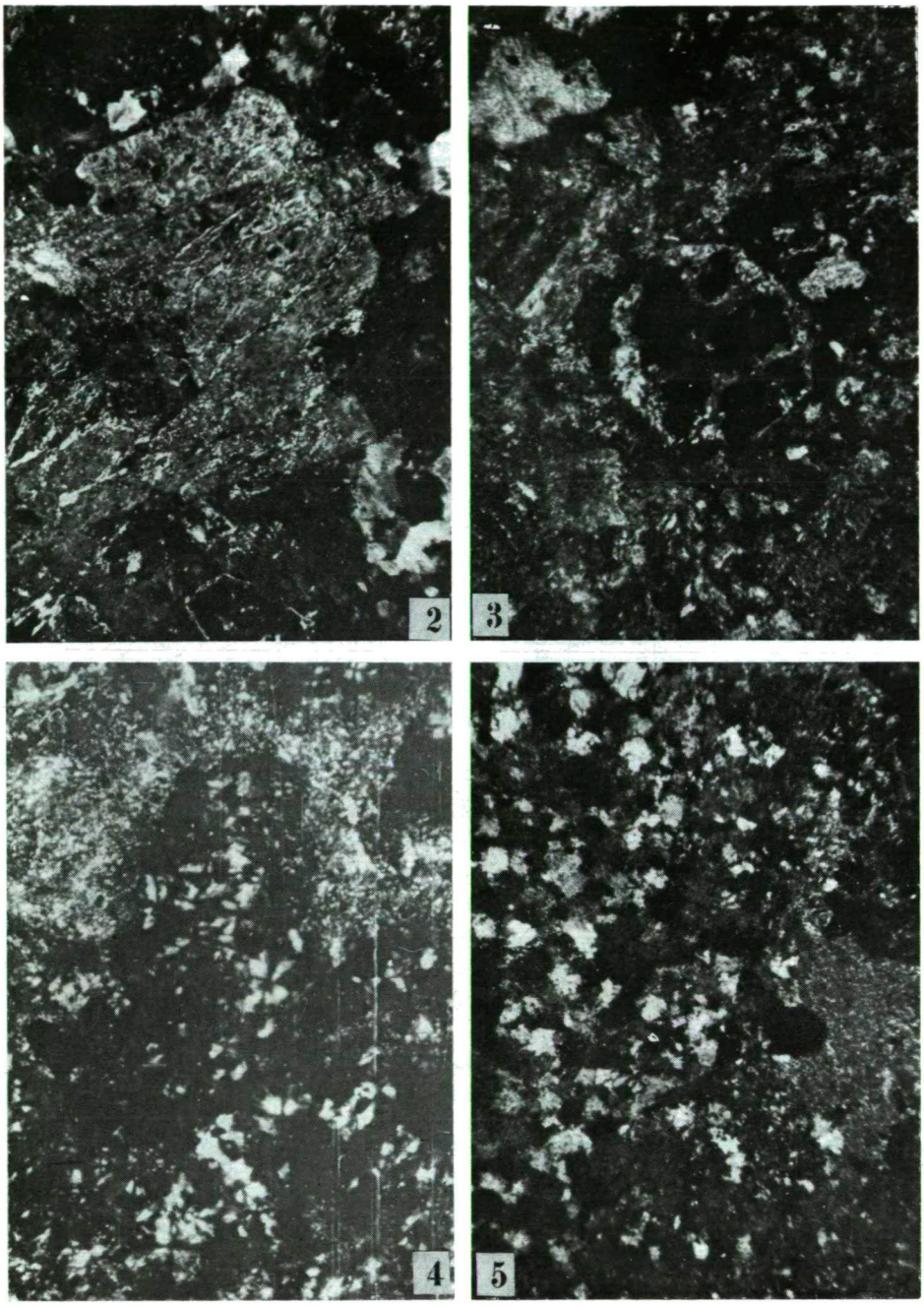

Fig. 2. Sericitized feldspar. +N X 80.
Fig. 3. Idiomorphic chloritized pyroxene cross section with pyrite. +N X 80.
Fig. 4. Chalcedonic replacement in the basic substance. +N X 80.
Fig. 5. Silicic, sericitic basic substance. +N X 80.

be observed microscopically. The rock is uniformly impregnated by pyrite, along the rips sometimes chloritic discoloration can be seen.

This type might be originally of pilotaxitic structure. The quantity of basic substance changes between 55 and 70 per cent, the phenocrysts are generally well separated. When no strong clay mineralization took place the thin pyrite veins can also be observed. Clay mineralization and silification may be of different degree, consequently the texture shows variegated picture. Silification is locally indicated by chalcedonous parts *(Fig. 4)* or by quartz-spots with sericitic parts *(Fig. 5)*.

Amongst the phenocrysts the feldspars prevail their quantity fluctuates between 20 and 25 per cent, except the fine-grained rocks (west of the Károly lode by 200 to 220 metres) where their quantity falls below 10 per cent. When the rock is of darker grey colour the feldspars are usually of zonal structure and the twin-formation is characteristic, these feldspars belong to the labradorite series *(Fig. 6)*. In these case only slight sericitization can be observed, sometimes calcitization occurs along the cleavage lines. The decomposed structure is more frequent and the sericitic pseudomorphism after the feldspars is also common due to the clay mineralization *(Fig. 7)*.

The femic minerals are represented by the rhombohedral and monoclinic pyroxenes. Be the feldspar any kind of form chlorite replaces the rhombohedral pyroxenes in every cases *(Fig. 8)* and the monoclinic ones are replaced by chlorite or calcite *(Fig. 9)*. It is frequent that in the chloritized pyroxene the quantity of pyrite is higher and its grain size if greater than in the rock itself, moreover, sometimes the substance of the rock does not contain pyrite and at the same time it is significant in pseudomorphs after pyroxenes. This pyrite is therefore of hypovolcanic character, it is simultaneous with chloritization and is older than that impregnating the rock.

In the dead gallery this rock type occurs within a distance of about 370 metres. Significant difference is shown only in the measure of decomposition and clay mineralization developed along the lithoclases. In this case the descendent solutions should also taken into consideration regarding the clay mineralization. The internal part of the single blocks are fresh and this is surrounded by a clay mineralized zone, and these often form pseudoagglomerate. The decomposing effect of the descendent solutions and the crumbling of pyrite are proved by the gypsum needles and crystal groups occurring in the yellowish-grey, yellowish-white clayey detritus.

In the fresh parts the pyrite veins are usually absent, they replaced by calcite veins of several centimetres size. Silification, sericitization and clay mineralization occur usually together which can be explained partly by the release of silicic acid in case of clay mineralization, partly the silicic acid content of the postmagmatic solutions resulting in the pyritization.

West of the Károly lode by about 50 metres there is a tuf intercalation which is locally of lapilli formation. In its western part grey-coloured breccia-like rock occurs in which angular white and grey nearly homogeneous detritus of about centimetre size was cemented. The white part are clay mineralized fragments, in general. The slight ore migration occurs rather in the cementing material. This breccia-like part indicates a fault line but its direction is indistinct due to the considerable clay mineralization. From the breccia-like part the rock is absolutely fades, it is a tuff powder with a few lapilli. In the smaller cavities of the rock sometimes idiomorphicu quartz of 2 to 3 mm occurs. The grain size of the tufaceous rock consisting mainly of quartz is about 0.05 mm. The cementing material is strongly sericitized. Its general textural sketch is shown in *Fig. 10*.

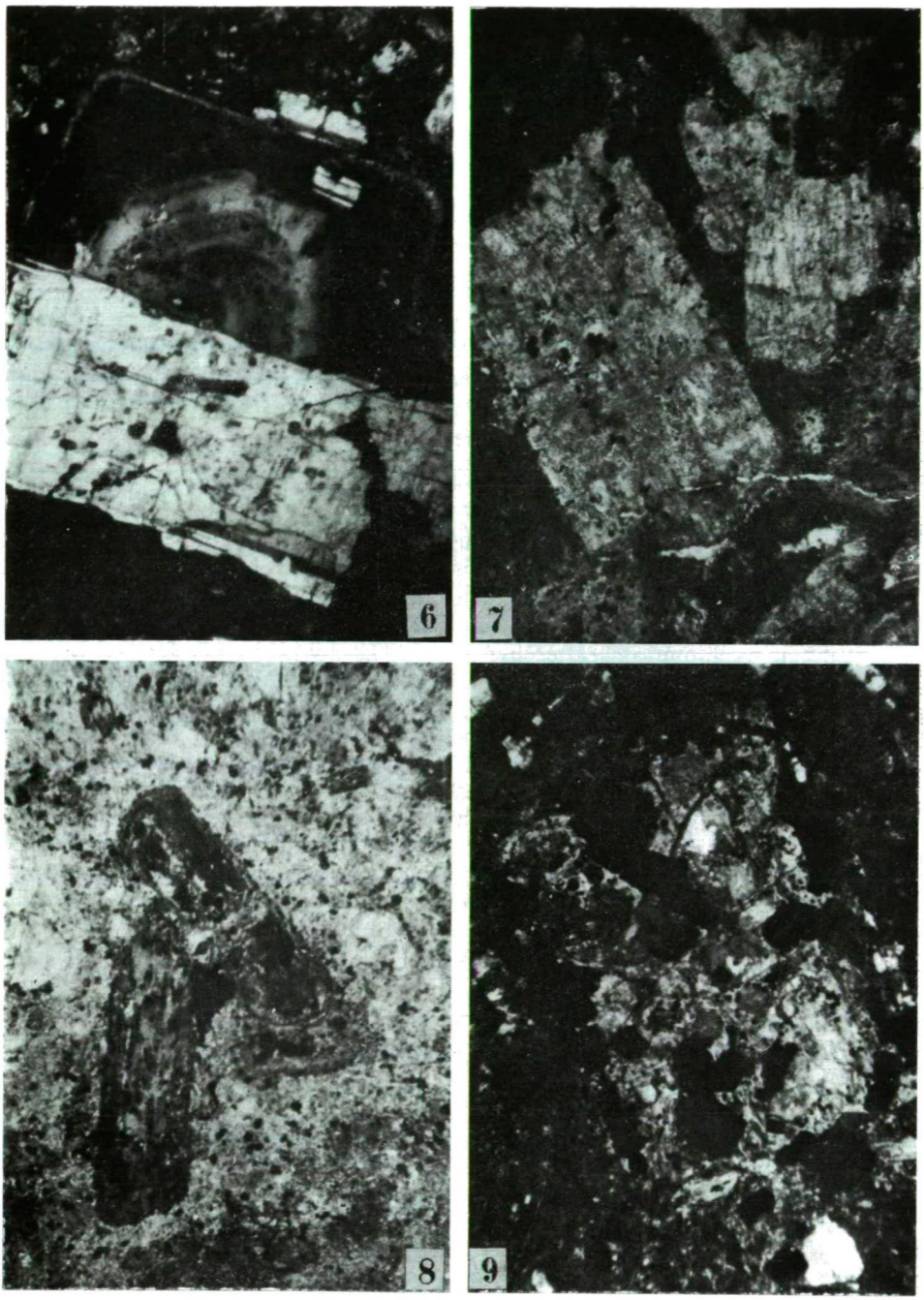

Fig. 6. Zonal feldspar. +N X 80.
Fig. 7. Sericite pseudomorph after feldspar. +N X 80.
Fig. 8. Chloritized pyroxene. // N. X 80.
Fig. 9. Calcitized augite with pyrite. +N X 80.

East of the andesite tuff greenish, compact andesite occurs up to the Károly lode. Feldspars of 2 to 3 mm and chloritic pyroxene of similar size represent the phenocrysts. The rock is impregnated by pyritic veins of a size less than one millimetre. In the cleavage faces the clay mineralization is of more significant role, beside the Károly lode the rock is faded.

Under microscope the original structure of the basic substance is unrecognizable due to partly the silification, partly the more considerable clay mineralization. The feldspars are usually replaced by secondarily formed sericite. Out of the femic constituents the rhombohedral pyroxenes were only chloritized and contain for the most part pyrite, the penetration twins are frequent. In case of monoclinic pyroxenes in addition to chloritization the calcitization can also be observed.

Level of +350 metres

It exposes the associated rock in a length of 415 metres northwest of the Károly lode. Southeast of the Péter-Pál lode light grey, locally whity grey rock strongly dissected by lithoclases can be found in a distance of about 50 metres. Along the cleavage faces the precipitation of pyrite is more intensive. In several places calcite veins of 1 to 3 cm size occur accompanied by pyrite bands. The decomposition, i.e. clay mineralization is more intensive along the lithoclases, locally yellowish-white, greyish-white pseudotuff developed. In the relatively fresh rock only the presence of feldspar phenocrysts may be supposed.

Southeastwards greenish-grey compact andesite occurs with calcite and chalcedony veins reaching 5 cm thickness. Out of the phenocrysts the fresh feldspars of 3 to 4 mm and chloritic pyroxene of 2 to 3 mm size are recognizable. The rock is impregnated by small quantity of pyrite. In smaller caves quartz crystals of centimetre size occur.

Southeast of the Péter-Pál lode between 100 and 160 metres the rock becomes pale but remains compact, the feldspar crystals are replaced by white clay mineralized spots, the basic substance is strongly silicified. The calcite veins are white-coloured and of coarse crystals. More intensive clay mineralization can be observed only besides the Aranybányabérc lode. This is superseded by greenish-grey compact andesite in which fresh tabular feldspars of 2 to 4 mm, and less chloritized columnar pyroxene of 2 to 3 mm occur. Along the fissures of the rock a more intensive clay mineralization took place followed first of all by the descendent solutions. Near the Károly lode there is a fine-grained, strongly silicified andesite, in this rock the clay mineralization is of less importance. In this type calcitic, pyritic and chalcedonic bands also occur.

The picture under the microscope exactly characterizes the transformation and alteration of the rocks which is represented by the varied appearance of the basic substance and by the state of the phenocrysts. The originally pilotaxitic texture remained only in the dark-coloured andesite, in case of more considerable silicification *(Fig. 11)* and sericitization *(Fig. 12)* the traces of the original texture appeared, as well. The local precipitation of calcite is limited more or less to the zones of calcite veins (associated rocks of the Péter-Pál and Aranybányabérc lodes). The large-scale replacement may generate pseudotuffic rocks.

Out of the phenocrysts the feldspars are always in greater quantity being of 1 mm size in the fine-grained rock and of 3 to 4 mm in general. When the measure of alteration is smaller, the zonal structure and twinning is fairly recognizable, in case of more intensive sericitization the crystal is reticulately dissected *(Fig. 13)* and when silification is of considerable size only the contours of the feldspars remain,

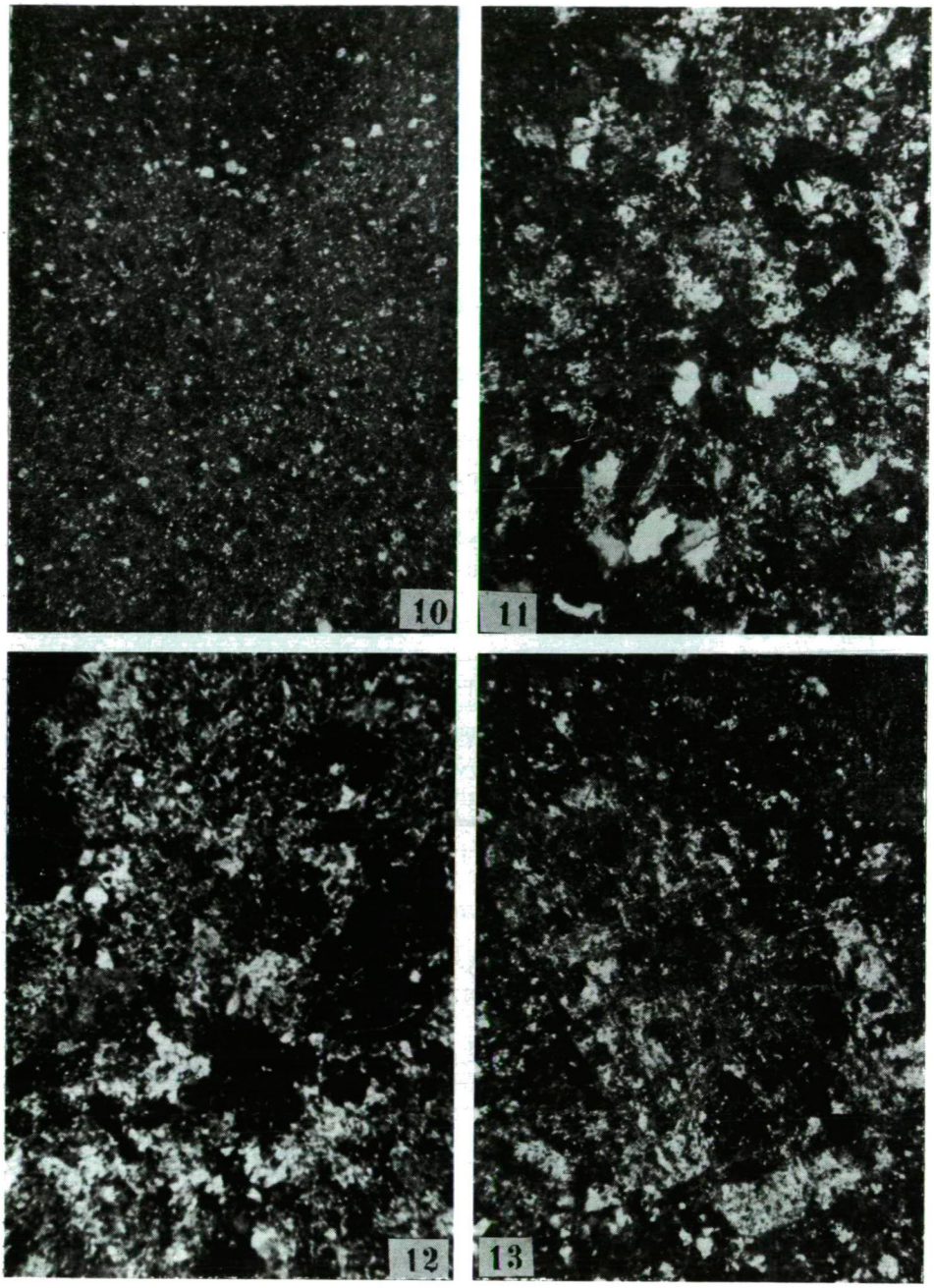

Fig. 10. Texture of andesite tuff. +N X 80.
Fig. 11. Silicified basic substance. +N X 80.
Fig. 12. Sericitic, silicic basic substance. +N X 80.
Fig. 13. Sericitized feldspar. +N X 80.

in general. The calcitic replacement of the feldspars is characteristic only in the carbonaceous zone.

Both the rhombohedral and the monoclinic pyroxenes can be traced, they may be max. 3 mm in size, their quantity falls behind 10 per cent. The rhombohedral pyroxenes are always pseudomorphs consisting of chlorite and usually are of reticulated dissection *(Fig. 14)*, in the netting the secondarily developed chlorite occurs. In addition to the chloritization the monoclinic pyroxenes often show calcitic replacement *(Fig. 15)*, in these cases the feldspars also endure smaller calcitic alterations.

In the neighbourhood of the Károly lode the biotite occurred only in one sample *(Fig. 16)* showing intense pleochroism and which is possibly the subsurface continuation of the superficial lava stream observed by PANTÓ, G. [1950].

Level of +400 metres (adit)

West of the adit between 550 and 670 metres there is a compact rock of darker greenish colour dissected by lithoclases. It contains phenocrysts of 1 to 3 mm size and is slightly pyritized. In several cases the relatively fresh parts are mottled by detritus of clay fraction and of limonitic colour, this part being of several centimetres.

Under microscope only the less silicified rocks show the originally pilotaxitic substance. The rock is sometimes traversed by quartz veins and in these cases the idiomorphic quartz is frequent *(Fig. 17)*. In the caves carbonates are of less importance. Out of the phenocrysts the feldspars belonging to the labradorite group may be of 2 to 2.5 mm in size, they are tabular, the smaller crystals are columnar habit. Zonality and the polysynthetic twinning are recognizable. Slight sericitization occurs rather along the cleavage lines. The pyroxene is always transformed. In these cases chloritization is negligible, serpentinization plays the predominant role (bastite; *Fig. 18*). In the relatively fresh rock only the hypersthene was transformed, the augite is nearly fresh and does not show alterations.

Eastwards this rock type is replaced by compact fine-grained rock of dirty-grey colour and along the fissures a thin decompositeod layer developed. On this detritus thin needles of gypsum and gypsum groups occur. Phenocrysts are unrecognizable still in the fresh parts of the rock. Under microscope it shows features according to which the rock might be a part of a thin lava stream which solidified originally also as a fine-grained rock. The major part of the basic substance is replaced by silica and sericite and in this substance the contours of sometimes idiomorphicu feldspars of just o.2 mm size can be observed. The femic constituents are represented by pyroxenes transformed intoc hlorite of 0.1 mm size.

In the gallery in a distance of about 110 metres eastwards dark-grey colored, locally greenish shaded compact rock occurs. It is abundant in phenocrysts. At the Aranybányabérc lode the rock is fresh and shows no alterations, the pyrite occurs sometimes in nodes.

Under microscope the prevailing basic substance (54.3 per cent) is of pilotaxitic texture and slightly impregnated by pyrite. The plagioclases belonging to the labradorite series (32 per cent) may be of 2.5 mm size. The greater ones are usually tabular, the smaller ones are of columnar habit. The zonality and twinning are frequent in both cases. All the transitions from the microlite to the phenocrysts can be observed. Out of the pyroxenes the augite is frequent (10.1 per cent). It is usually fresh, sometimes twinning is recognizable. The columnar crystals of hyper-

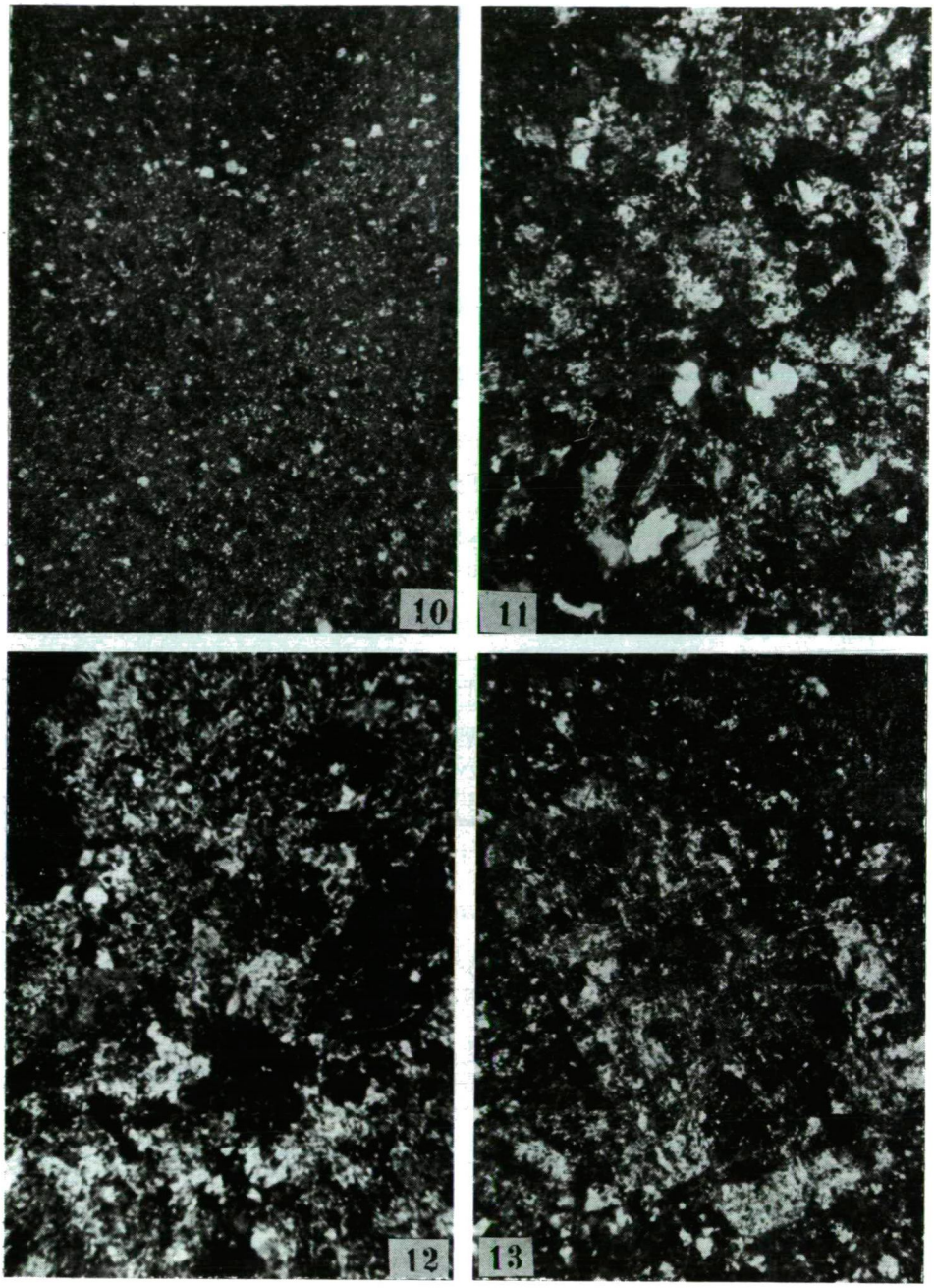

Fig. 10. Texture of andesite tuff. +N X 80.
Fig. 11. Silicified basic substance. +N X 80.
Fig. 12. Sericitic, silicic basic substance. +N X 80.
Fig. 13. Sericitized feldspar. +N X 80.

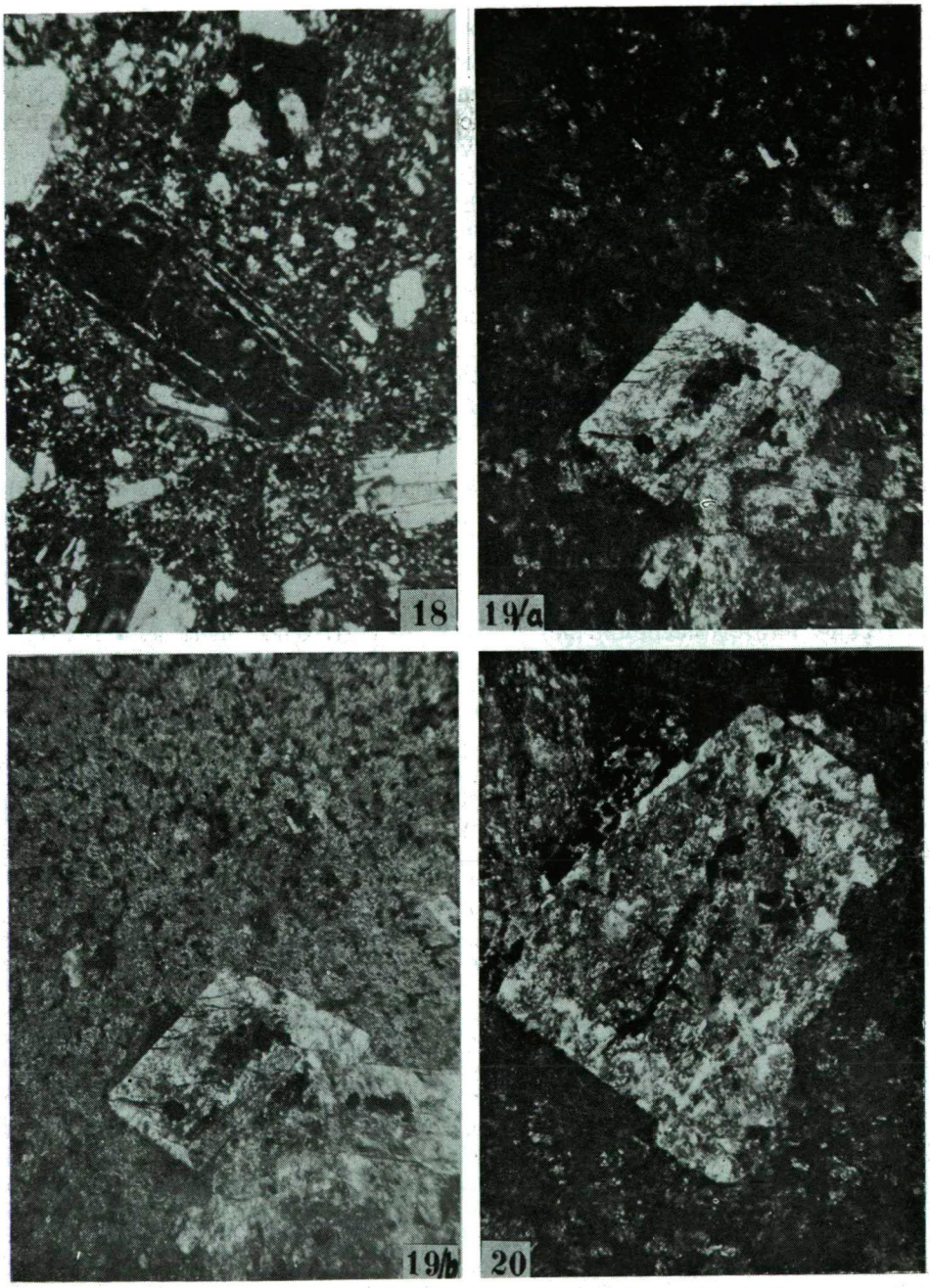

Fig. 18. Zonal feldspar and serpentinized hypersthene. +N X 80.
Fig. 19. Sericitized feldspar in silicic-sericitic basic substance. *a)* +N X 80. *b)* //N X80.
Fig. 20. Sericitic "zonal" feldspar. +N X 80.

sthene (3.6 per cent) transformed totally into seladonite. In certain samples the quantity of the phenocrysts may increase and sometimes chloritic parts occur.

West of the Károly lode within a distance of about 400 metres uniform greenish-grey coloured, compact rock occurs. The variety is given only by the fact that decomposition along the lithoclases, thin veins and fissures is in a more progressed state. In these cases the rock is traversed by yellowish-grey veins the material of which is clay mineralized detritus coloured by limonite containing often gypsum, moreover locally gypsous clay occurs. The fresh part of the rock is of splintery fraction and it is locally silicified. In the western side of the Károly lode where a smaller fault zone developed the clay mineralization is characteristic. In the relatively fresh rock only the feldspar phenocrysts may be supposed.

Under microscope the substance is sericitic, and silicic but often mottled. This derives from the fact that the orientation of the microlithes and silicic parts is nearly the same, further the pyrite grains, resp. the secondary minerals developed from them are of reticular occurrence which can be excellently seen under parallelled nicols *(Figs. 19a* and *19b)*. The sericitization of feldspars is common, the greater tabular crystals may be of 2.5 mm size, frequently only a smaller part of them remain intact but the zonal structure can be traced in these cases as well *(Fig. 20)*. The calcitic replacement is negligible. The pyroxenes grown up to 1 millimetres were fully serpentinized but are of less importance. They frequently contain pyrite inclusions. Chloritization is subordinate.

Taking into consideration the results of the petrological investigations it can be stated that several lava streams should be taken into account in this mine, moreover tuff intercalation also occurs. The position of the single rock types are demonstrated in a profile of N—S direction *(Fig. 21)*. In the level of +250 metres the solidified rock of a relatively uniform lava stream is of hypomagmatic character, the variousness is indicated only by the measure of alteration. Above this level (+300 metres) the andesite tuff may be a thinner intercalation, it rapidly wedges and it is absent in the over- resp. underlying strata. Above this layer a relatively thicker hypomagmatic mass occurs with varied clay mineralization and this shows transition towards the higher levels in a thin zone into microandesite with minimal phenocrysts. The overlying andesite is of ortho-character with fresh zonal feldspars and augites, the sericitization is subordinate. As contrasted to the chloritic character of the lower levels this feature is absent or subordinate.

DERIVATOGRAPHIC AND *X*-RAY DIFFRACTOMETRIC INVESTIGATION OF THE CLAY MINERALIZED ROCKS

The clay mineralization of the associated rocks is a common phenomenon due to the metasomatic effect of the hydrothermal solutions. NEMECZ, E. [1967] mentioned numerous factors in case of formation of the clay minerals which have different role in clay mineralization. Since in the investigated area the temperature and pressure seem to be equalized, as well as the alteration observed in the associated rocks relates to the relative standard value of the pH, the most important factors of clay mineralization the mineralogical composition and texture of the associated rocks as well as the concentration of the hydrothermal solutions may be regarded. It has also to be taken into consideration thət in these depths the vadose descendent solutions play also an important role and in this case certain salt concentration should also taken into account since the mining of Gyöngyös-

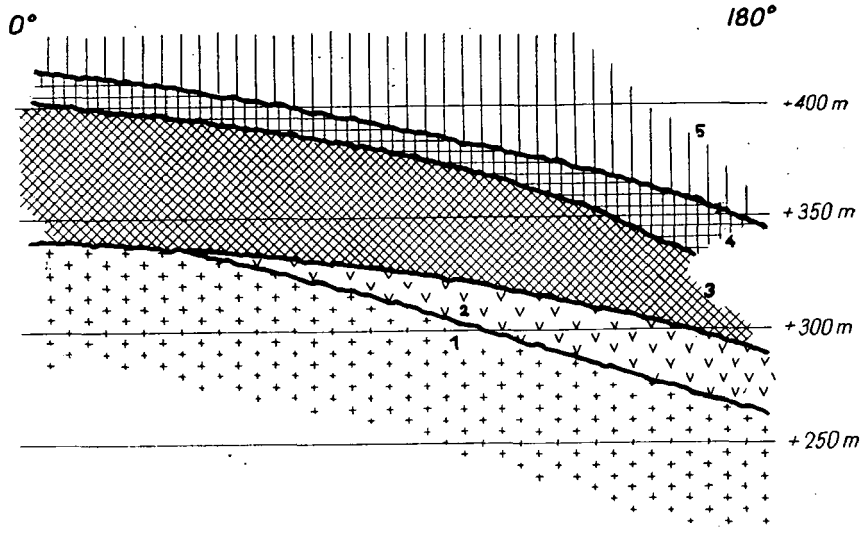

Fig. 21. Position of the lava streams in the galleries of the mine.

oroszi still belongs to the zone of active water exchange determined by CHOUKHROW [1965].

Taking into account these facts numerous derivatograms were performed from the clay mineralized rocks of the four levels. Definite types can only be separated only in a few cases. In most cases certain clay mineral occurs in addition to the prevailing clay mineral. Gypsum occurred nearly in every cases. This fact relates

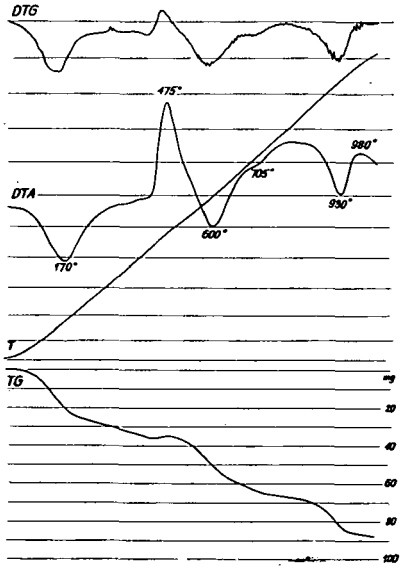

Fig. 22. Derivatogram of the clay mineralized illite-type rock.

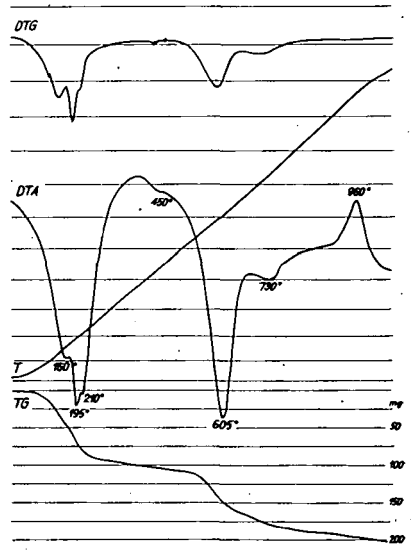

Fig. 23. Derivatogram of the clay mineralized montmorillonite-illite type rock.

to the phenomenon that clay mineralization is the result of not a single genetic process but in the course of formation the effects of both the ascendent and the descendent solutions played an important role.

On the basis of the derivatograms the following types were distinguished: illite-type *(Fig. 22)*, montmorillonite-illite-type *(Fig. 23)*, kaolinite-montmorillonite-type *(Fig. 24)*, kaolinitic type with calcite *(Fig. 25)*, kaolinitic type with jarosite and calcite *(Fig. 26)* and montmorillonitic type with jarosite *(Fig. 27)*.

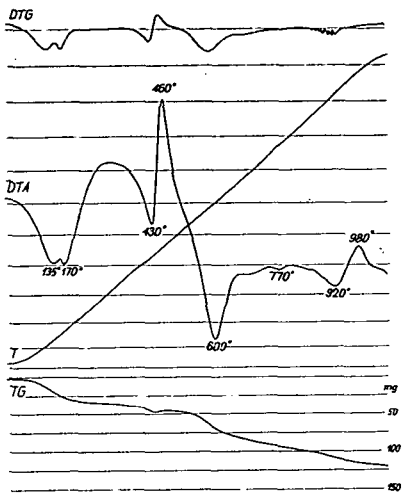

Fig. 24. Derivatogram of the clay mineralized kaolinite-montmorillonite type rock

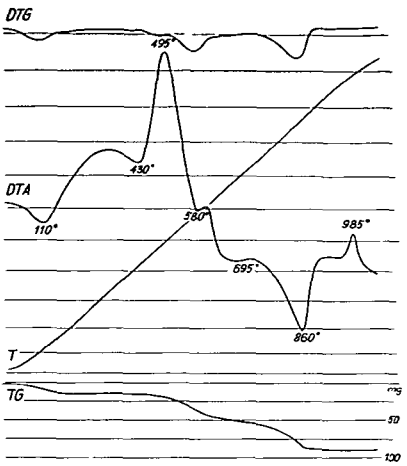

Fig. 25. Derivatogram of the clay mineralized kaolinite type rock with calcite.

The identification of *jarosite* is a new result since it has been unknown in the area of mining till now. According to KULP and ADLER [1950] in case of the members of the alunite-jarosite series there are two significant endothermal peaks. At the first one all the structural waters are released connected to the decomposition of the lattice, in the second endothermal reaction the SO_4 radicle connected to the aluminium or ferric-iron is released. Since the connection to the ferric-iron is weaker than to the aluminium, thus the temperature of the endothermal reactions will be lower than in case of alunite. In our case the endothermal reaction occurring at 440 °C is considerable and the connected loss of weight is 2.5 per cent measured in the TG curve, while at 790 °C the loss of weight is 3.6 per cent. Taking into consideration the values of the chemical analysis this corresponds to about 20 to 25 per cent jarosite.

Out of the decomposed and clay mineralized rocks of the different levels 40 samples were investigated by diffractograms. In general, the following can be stated.

Independently of the K_2O content of the sample no sanidine and adularia formation, i.e. the replacement of plagioclases by potash feldspars could be determined, this, however, has been expected on the basis of the microscopic investigations. The higher K_2O content is therefore connected not to the potash feldspars but to the clay minerals or to jarosite. Either the fresh or the decomposed rocks were investigated quartz occurred with highest intensity. This shows the considerable

silification of the rocks and the more important role of silicic acid of secondary appearance in case of claymineralization of the rocks. Nearly all the surfaces being decomposed or clay mineralized the gypsum interwoven with the detritus has appeared. The clear crystals of frequently 2 to 3 mm size as well as the crystal groups formed on the effect of the descendent solutions in the oxidation zone; these are youngest and are forming recently, too.

The most frequent mineral of the clay minerals is the illite (sericite). In this case first of all the $d \sim 10.0$ value could be taken into account, since the other lines of high intensity coincide or nearly coincide with the lines of other minerals. The case of montmorillonite was similar to this. In this case only the $d \sim 14{,}0$ values could taken into account where the values $d \sim 7.0$ were absent together with the $d \sim 3.54$ values, so the chlorite could be excluded. The montmorillonite frequently occurred together with jarosite which indicates the same formation conditions. In addition to illite the kaolinite plays less important role. Only in the neighbourhood of the Aranybányabérc lode occurred usually post-originated clay mineral or it appeared accompanying other secondary minerals. Here the fire-clay type (kaolinite-*d*) occurred.

Chlorite occurred only in the samples which showed clay mineralization of less measure. Though the chlorite remains stable in the oxidation zone due to its

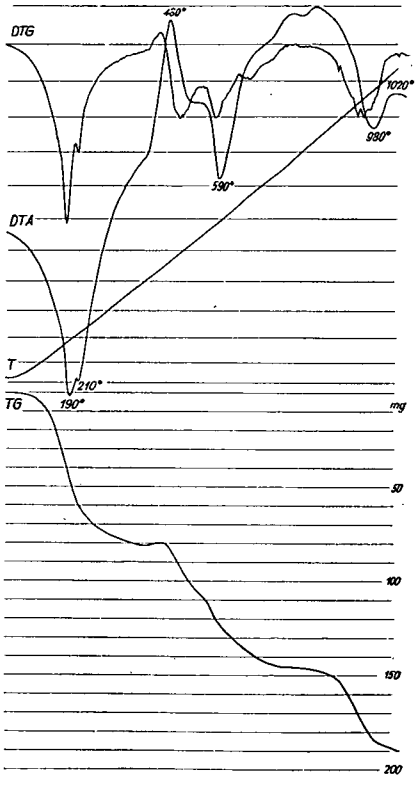

Fig. 26. Derivatogram of the kaolinite-type with jarosite and calcite.

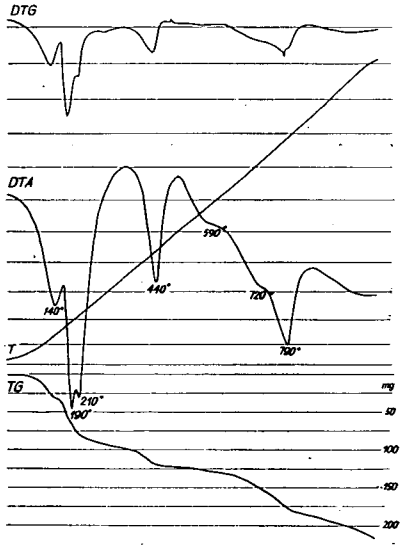

Fig. 27.
Montmorillonite-type with jarosite

high water content, it was absolutely absent in these clay mineralized zones and this is in correspondence with the former investigations.

Out of the secondarily developed minerals the determination of jarosite was done first in this area which could be identified in the diffractograms. The $d \sim 5.9$; 5.7; 5.09; 3.10; 3.07; 1.93 values unambiguously determined the mineral all the more so the d-values of the secondary minerals of this assemblage did not disturb these peaks. The place of occurrence is connected not always to the closeness of lodes, but it formed in the oxidation zone where the descending waters were of more considerable effect. It occurs usually together with certain kind of clay minerals, sometimes it is accompanied by gypsum. The regularity observed by MARTIN VIVALDI, J. *et al* [1971] in the gold mines of Rodilquilar could not be demonstrated in this area.

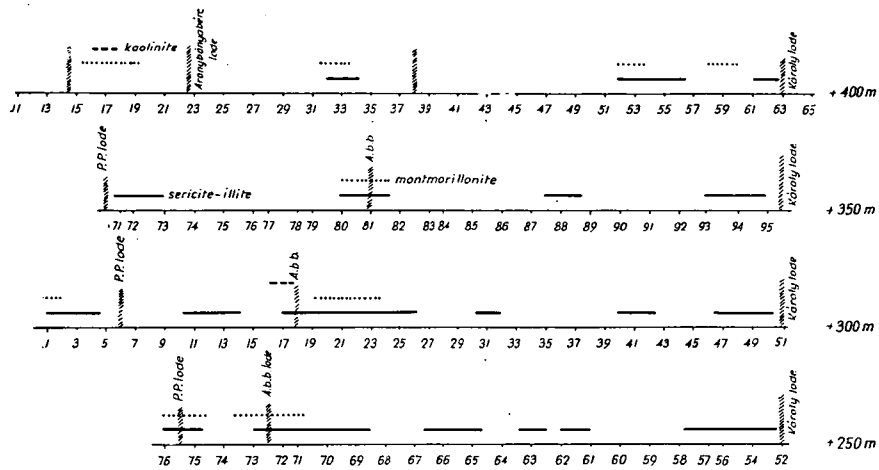

Fig. 28. Zonal arrangement of clay minerals

According to several observations in the course of hydrothermal metasomatism some zonal structure develops in the formation of the clay minerals, to a certain extent. In Hungarian relations this phenomenon has been investigated in details by NEMECZ, E. [1967] and SZÉKY-FUX, V. [1970]. NEMECZ related to the clay mineralized zone of the Mátraszentimre lode, as well.

On these bases the clay minerals occuring in the single levels' samples were demonstrated in a sketch profile *(Fig. 28)*. On this basis the general occurrence of illite can be unambiguously stated. Along the lodes, in general excellently crystallized illite structures were developed. Due to the replacement of plagioclases the Si/Al ratio is also displaced and, since the major part of Al_2O_3 will be bound the solution becomes richer in silicic acid. But a definite kaolinitic or montmorillonitic zone could not be separated. Near the Károly lode of greater importance only in the +400 metres level developed a montmorillonitic zone, the kaolinite was absent near the lode. In case of the Aranybányabérc lode of less significance there is an overlap among illite, montmorillonite and kaolinite. The overlap may be explained partly by the possibility of the transformation of these clay minerals into one another (illite-kaolinite, illite-montmorillonite), partly by the secondary development on the effect of descendent solutions. The statement of NEMECZ [1967] regarding the

conditions of the Tokaj Mountains is probably valid for the area of the Gyöngyösoroszi mine, i.e. considerable ore formation cannot develop together with kaolinite, because the high potash-content of the ascending solutions results in such a high pH-value, which is favourable for ore formation but hinders the formation of kaolinite. Consequently, the occurrence of kaolinite and montmorillonite cannot be assigned to the zonal arrangement but it was originated by other genetic processes, i.e. in this case the descending solutions provide the possibility of the formation of these clay minerals.

ALKALI CONTENT OF THE ASSOCIATED ROCKS IN THE DEAD GALLERIES OF THE FOUR LEVELS

In the mine's area the environs of the lodes show alkali contents and alkali ratios being dissimilar to those common in the orthoandesites. Some literature data relate to the fact that in the environs of lodes there is a potash anomaly and connection can be supposed between the ore formation and potash metasomatism.

In the environs of Boiskovo (Yugoslavia) where lead and zinc are mined KNĚZEVIČ, V. and DJORDEVIČ, P. [1968] observed that near the ore body the potash-content shows positive anomaly and reaches the maximum about between 25 and 30 metres. In the porphyric-keratophyric rock sanidine or orthoclase of sanidine character developed as a result of metasomatism. In this area the potash content, being high only in the environs of the ore bodies, can be regarded positive indicator.

SZÉKY-FUX, V. [1970] searched the connection of K_2O between the associated rock and ore formation in the area of Telkibánya (Hungary).

Investigating the mineral paragenesis of the gold mine of Rodalquilar (Spain) MARTIN VIVALDI, J. *et al.* [1971] found also potash anomaly along the lodes. On the basis of the mineralogical composition three zones were distinguished. The first one extended from the vein up to 30 to 35 metres, the second zone was found up to 60 metres while the third zone represented the original rock. The quantity of illite (sericite) increased only in the close neighbourhood of the vein, that of the kaolinite gradually increased from the second zone towards the lode and reached about 20 per cent along the vein. From the innermost zone the vermiculite and chlorite could not be determined, but the quantity of the alunite-jarosite series gradually increased towards the vein.

Since in the close neighbourhood of Gyöngyösoroszi considerable potassium enrichment can be observed together with sanidine formation in the area of Mátraszentistván, and similar phenomena occurred in the western neighbourhood of the mine it would be practicable to make investigations on the basis of which the fact could be stated that higher potassium content occurs near to the lodes and when this followed some kind of regularities could be demonstrated in case of increase or decrease of concentration in the dead galleries between the two lodes. The further question is that when there is a potassium enrichment the form of appearance will be sanidinization, adularia formation of sericitization. It is probable, too, that whether is there any regularity or connection between the change of potassium content and ore formation. The samples investigated were the same used in the mineralogical-petrological investigations, and place of sampling is shown in *Fig. 1.* The results are as follows.

The change of alkali content of the lowermost level (+250 m) is shown in *Fig. 29.* There is considerable difference in the potassium content from that of about 4 per cent of the hypomagmatically developed andesite, near the lodes the

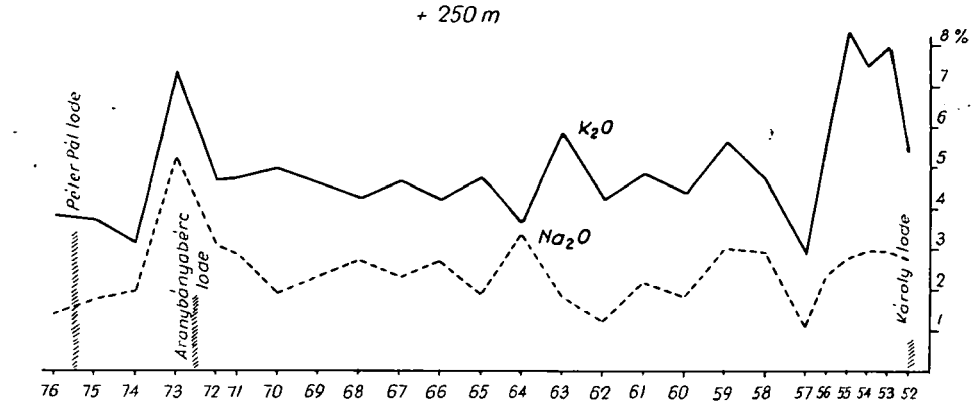

Fig. 29. Change of alkali content of the level +250 m.

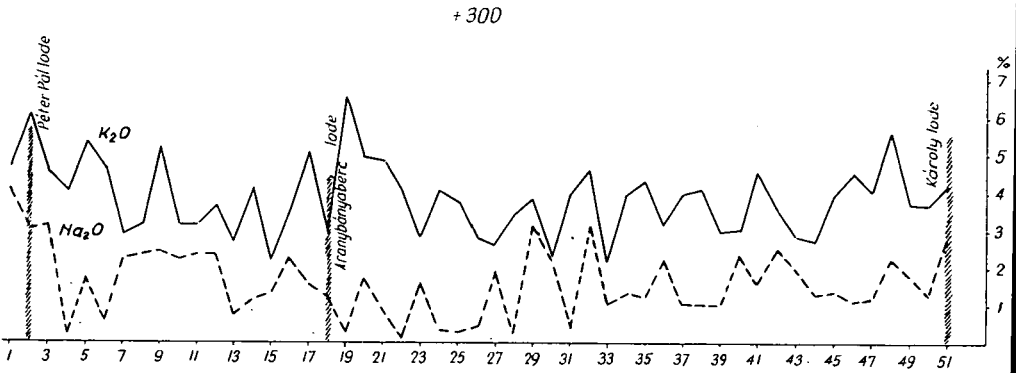

Fig. 30. Change of alkali content of the level +300 m.

K_2O content surpasses 8 per cent. Since the potash feldspar is absent in the mineralogical components, the considerably increased potash content is connected for the most part to illite and sericite. The level consists of uniform rock, decomposition is of less importance so the metasomatic effect of the hydrothermal solutions is demonstrated most pregnantly in these lodes. The change of Na_2O though with smaller values was nearly parallel with that of the K_2O.

In the level of +300 metres *(Fig. 30)* the petrological formations are more variegated, several lava streams and tuff levels can be distinguished and locally brecciated zone of lithoclases developed. This results in first of all that along the lodes the K_2O content is less characteristic but it surpasses 6 per cent. The quantitative change of the Na_2O content is similar to that of the underlying level, higher values occur in the fault zone.

In the level of +350 metres *(Fig. 31)* the petrological picture is changed. The andesite tuff is absent, clay mineralization is of less significance, silification is, however, increased and locally thin calcite veins also occur, i.e. the fluctuation of the K_2O content is less. The higher K_2O value is connected to the illite and sericite. The higher value between the Károly and Aranybányabérc lodes indicates a more

intensive clay mineralization. In this level the quantity of Na_2O sometimes surpasses that of the K_2O. In these cases the rock has been more fresh and clay mineralization was of less importance.

In the level of +400 metres *(Fig. 32)* where the silicified rock is orthoandesite the values of K_2O and Na_2O are nearly the same. In the Aranybányabérc lode, however, the K_2O value is high, i.e. the metasomatic effect of the hydrothermal solutions has prevailed. Between the Béke and Károly lodes in a distance of about 400 metres a rock originating from a relatively uniform hypomagma is exposed in the different stages of decomposition (effect of the descendent solutions) and metasomatic replacement and this results in the whimsical change of the values.

On the basis of the alkali content investigations it has become obvious that in case of fresh, faultless rocks free from clay mineralization and oxidized parts and where the rock type shows negligible changes, the values of K_2O are extremely high near the lodes (10 to 25 m), this anomaly, therefore, indicates the closeness of the lodes, in any other cases it has no indication character.

CONNECTION BETWEEN ORE FORMATION AND THE IGNEOUS ROCK

The igneous rock receiving the ores, the regional extension of the ore formation as well as the connection between the igneous rocks within the Carpathian Tertiary volcanic formations were formerly investigated.

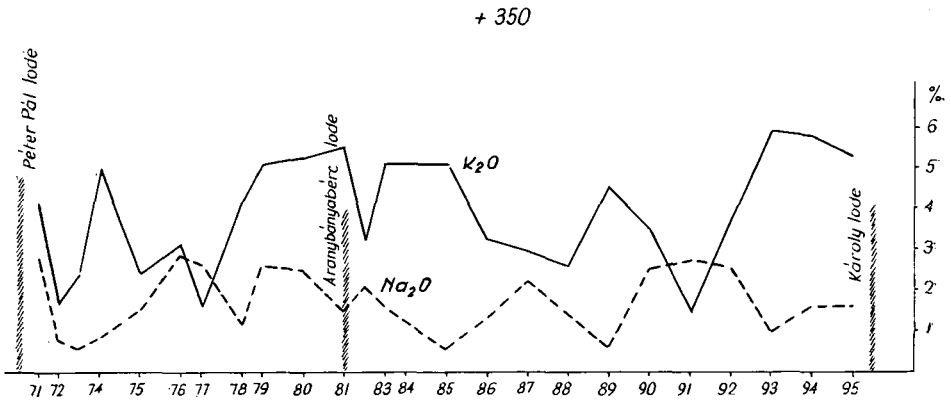

Fig. 31. Change of alkali content of the level +350 m.

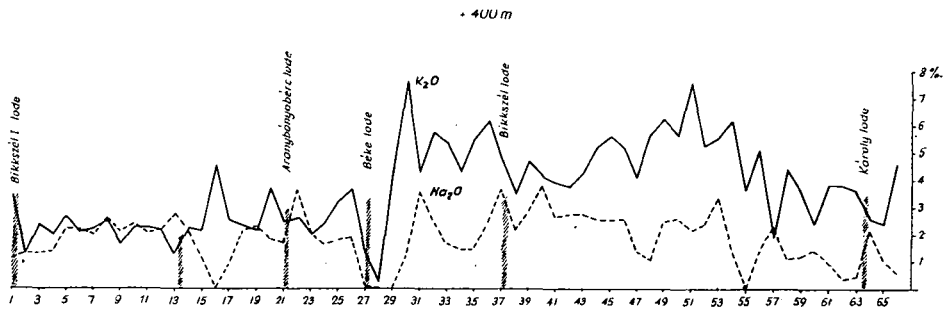

Fig. 32. Change of alkali content of the level +400 m.

SZÁDECZKY-KARDOSS, E. [1941] related to the fact that connection can be established between the ore distribution and crystallization degree of the igneous rock. According to the ratio of volume percentages of the rock-glass and crystalline substance the volcanites can be assigned to seven groups on the basis of the crystallization degree. On this basis the volcanites of the Mátra Mountains belong to the fifth group. The crystallization degree, of course, is only one of the numerous factors, therefore it cannot determine the necessary appearance of ore formation alone.

VENDEL, M. [1947, 1951] investigated the connections between the Cretaceous and Tertiary volcanic cycles. According to him there is a connection between the silicic acid content (SiO_2) and the intensity of ore formation. This is more obvious when demonstrating the intensity of ore formation in function of the NIGGLI's *si* or the weight percentual SiO_2 values.

According to PETRASCHEK, W. [1964] in the Carpatho-Balkanian ore province the lodes are connected to the Alpine metamorphism in space, time and substance. The common features of the Alpine-Mediterranean ore province are the uniform age as well as the Alpine magmatism within the whole mountain range, but the bed-forms are different.

PANTÓ, G. and MORVAI, G. [1967] in their metallogenetic grouping connect the ore formation of the Mátra Mountains to the Late Alpine phase, similarly to the ore formation of the Börzsöny Mountains and Telkibánya.

KOCH, S. and PANTÓ, G. [1970] introduce the characteristic parageneses and ore formations connected to the single Alpine tectonophases, among others the area of Gyöngyösoroszi, too.

According to SZÉKY-FUX, V. [1970] the most significant factor of the favourable appearance of the ore formation is the petrogenetic development of the rock. In her investigations at Telkibánya she searched the connection between the change of K_2O content and the intensity of ore formation.

GRASSELLY, GY. [1969]* raised the question that when the connection between the potash-metasomatism and the intensity of ore formation should be investigated the intensity of ore formation seems to be more suitable to indicate with the sulphide-S content, and in this way the connection mentioned above could be expressed by two parameters being measured by the same exactness.

For this purpose the samples which were investigated for alkalies have been investigated for their sulphide-S and sulphate content, too. Results together with the K_2O values are shows in *Fig. 33.* Between the potash-oxide and sulphide-S there is such a connection according to which the curves follow each other. In cases when the sulphur content shows higher values the pyrite formation on the cleavage faces and lithoclases is more intensive. From the similar character of the obtained values the conclusion can be drawn that in the associated rocks the migration of the potassium and sulphur containing solutions may have been the result of simultaneous of nearly simultaneous processes. The high potash-ion content ensured the migration of sulphides in solution and their precipitation under the suitable conditions. The sulphate content derives from the gypsum originated on the effect of the descendent solutions. These values are extremely high in case of fault zones and more intensive decomposition.

When demonstrating the weight per cent of the sulphide-S content in the weight per cent of the K_2O content *(Fig. 34)* and leaving the pyritic parts out of con-

* Personal communication.

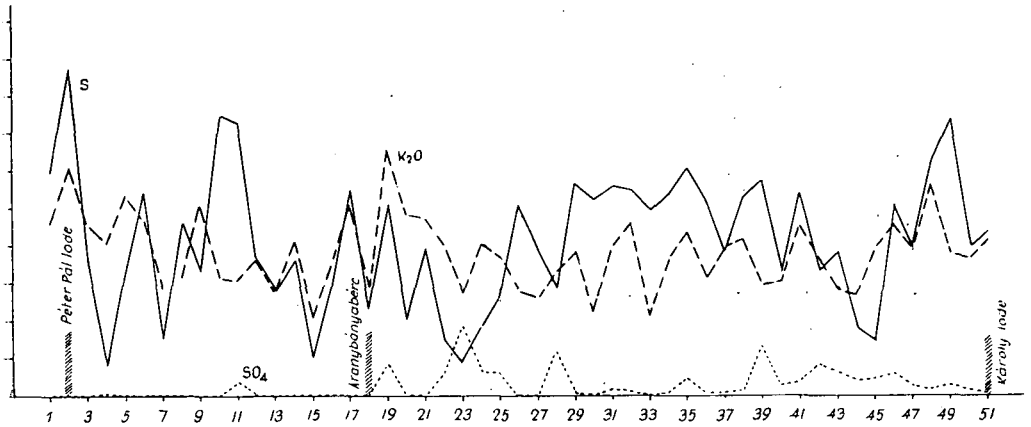

Fig. 33. Connection between sulphide-S, sulphate and K_2O

sideration, an optimal K_2O content can be determined necessary for ore formation which may be between 2.5 and 4.5 per cent. Recently this data concern only the single gallery of a single mine thus it cannot be of conclusive strength but the possibilities will be investigated in other occurrences, as well.

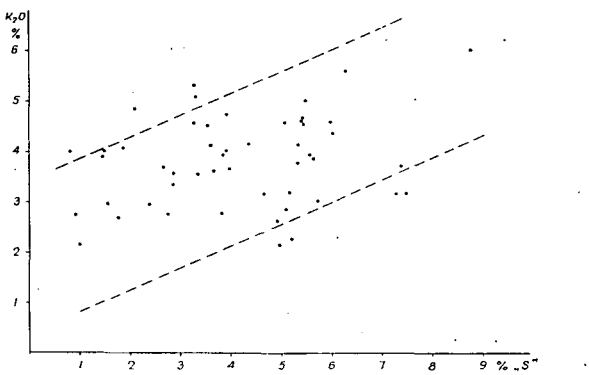

Fig. 34. Change of the ratio of K_2O and sulphide-S.

REFERENCES

KASZANITZKY, F. [1959]: A gyöngyösoroszi ércanyag származásáról és horizontális övességéről. MTA Geokém. Konf. Munk. 2.

KASZANITZKY, F. [1961]: Pyrrhotin Gyöngyösorosziból. Föld. Közl. *91*, p. 452.

KISS, J. [1964]: Allitos és sziallitos ásványok és szerepük a Középső Mátra ércesedésében. Földt. Közl. *94*, p. 422.

KNEŽEVIČ, V., DJORDEVIČ, P. [1968]: Alkali-K-Metasomatose als Indikator für die Anwesenheit einer Blei-Zink Mineralisation in Crna Gora. XXIII. Intern. Geol. Congress. Vol. *7*, p. 385.

KOCH, S., MEZŐSI, J., GRASSELLY, GY. [1949]: A gyöngyösoroszi Zgyerka altáró kőzetei és ásványai. Acta Miner. Petr. *III*, p. 1.

KOCH, S. [1954]: Minerals from Gyöngyösoroszi. Acta Miner. Petr. *VII*, p. 1.

KOCH, S. [1961]: The tertiary volcanic mineralization in Hungary. Acta Geol. Acad. Sci. Hung. *VIII*, p. 187.

KOCH, S. [1966]: Magyarország ásványai. Akad. Kiadó Budapest.
KOCH, S. [1958]: The associated occurrence of thee ZnS modifications in Gyöngyösoroszi. Acta Miner. Petr. *XI*, p. 11.
KOCH, S., PANTÓ, G. [1970]: Alpidisch-postmagmatische Mineralisationen Ungarns, ihre genetischen und paragenetischen Merkmale. Acta Geol. Acad. Sci. Hung. *14*, p. 161.
KORSHINSKIJ, D. S [1965]: Abriss der metasomatischen Prozesse. Akad. Verlag Berlin.
KULP, J. L., ADLER, H. H. [1950]: Thermal study of jarosite. Amer. Journ. Sci. *248*, p. 475.
MARTIN VIVALDI, J. L., SIERRA, J., LEAL, G. [1971]: Some aspects of the mineralization and wall-rock alteration in the Rodalquilar gold-field, S. E. Spain. IMA-IAGOD Meetings '70, Joint Symp. Vol. 2. p. 145.
NAGY, B., BORBÁCSI, A. [1966]: A mátraszentimrei ércesedés genetikai vizsgálata. MÁFI Évi Jel. *1964*. évről, p. 403.
NAGY, B. [1971]: A Mátra-hegységi képződmények áttekintő geokémiai vizsgálata. Földt. Közl. *101*, p. 62.
NEMECZ, E. [1953]: Halloysit Gyöngyösorosziból. Földt. Közl. *93*, p. 398.
NEMECZ, E. [1967]: Az agyagásványok képződési folyamatai, különös tekintettel a hazai előfordulásokra. Akad. dokt. ért. Kézirat.
NOSZKY, J. [1927]: A Mátra hegység geomorfológiai viszonyai. A debreceni Tisza István Tud. Társ. Honism. Biz. Kiadv. *3*.
PANTÓ, G. [1952]: A gyöngyösoroszi magmadifferenciáció és ércképződés. M. Tud. Akadémia Műszaki Tud. Oszt. Közl. *5*, p. 129.
PANTÓ, G. [1953]: Bányaföldtani felvétel Gyöngyösoroszin. MÁFI Évi Jel. az 1950. évről. p. 155.
PANTÓ, G. [1961]: Beszámoló a vulkáni hegységek időszerű kérdéseiről tartott vitaülésről. MÁFI Évi Jel. 1957—58. évekről. p. 525.
PANTÓ, G.—MORVAI, G. [1967]: Magyarország metallogenetikai térképe. MÁFI Évi Jel. 1965. évről. p. 481.
PAPP, F. [1953]: Ércvizsgálatok hazai ércelőfordulásokon. Földt. Közl. *83*, p. 8.
PETRASCHEK, W. E. [1964]: Die alpin-mediterrane Metallogenese. Geol. Rundschau *53*, p. 76.
RÓZSA, É. [1961]: The occurrence of striped calcites containing manganese in Gyöngyösoroszi. Acta Miner. Petr. *XIV*, p. 59.
ROZSLOZSNIK, P. [1942]: Adatok Gyöngyösoroszi környéki érctelérek ismeretéhez. MÁFI Évi Jel. 1936—38. évekről. p. 731.
SZÁDECZKY-KARDOSS, E. [1941]: Erzverteilung und Kristalinität der Magmagesteine im innerkarpatischen Vulkanbogen Mitt. d. Berg- und Hüttenmänn. Abt. Univ. Sopron *13*, p. 273.
SZÁDECZKY-KARDOSS, E. [1958]:. A vulkáni hegységek kutatásának néhány alapkérdéséről. Földt. Közl. *88*, p. 171.
SZÁDECZKY-KARDOSS, E. [1959]: A magmás kőzetek új rendszerének elvi alapjai. MTA Műszaki Tud. Oszt. Közl. *23*, p. 385.
SZÁDECZKY-KARDOSS, E. *et al.* [1959]: A Mátra hegység harmadkori vulkánjai. MTA Geokém. Konf. Munk. II. p. 29.
SZÁDECZKY-KARDOSS, E. [1966]: On the migration of volatiles and the changes at igneous contacts. Acta Geol. Acad. Sci. Hung. *10*, p. 263.
SZÁDECZKY-KARDOSS, E. *et al.* [1967]: Die Neovulkanite Ungarns. Acta Geol. Acad. Sci. Hung. *11*, p. 17.
SZÉKELY, Á. [1964]: A Mátra-hegységi ércesedést kísérő agyagásványokról. MÁFI Évi Jel. 1962. évről. p. 331.
SZÉKY-FUX, V. [1970]: Telkibánya ércesedése és kárpáti kapcsolatai. Akad. Kiadó, Budapest.
SZTRÓKAY, K. [1938]: Néhány ásvány Gyöngyösorosziból. Földt. Közl. *68*, p. 30.
SZTRÓKAY, K. [1939]: A gyöngyösoroszi ércelőfordulás mikroszkópi vizsgálata. Math. term. tud. Ért. *63*, p. 904.
SZTRÓKAY, K. [1952]: Cölesztin Gyöngyösoroszi ércteléreiből. Földt. Közl. *82*, p. 304.
SZTRÓKAY, K. [1962]: Inezit Gyöngyösoroszi ércteléreiből. Földt. Közl. *92*, p. 452.
TSCHUCHROW, F. W. [1965]: Über den möglichen Einfluss vadoser Wässer auf die Mineralisation einiger hydrothermaler Lagerstätten. Zeitschr. f. angew. Geol. *11*, p. 474.
VENDEL, M. [1947]: Studien aus dem jungen karpatischen Metallprovinz. József Nádor Műsz. és Gazd. Tud. Egyetem Bánya és Kohómérnöki Kar Oszt. Közl. *16*, p. 194.
VENDEL, M. [1951]: Összefüggések a magmák és az ércesedések között. MTA Műszaki Oszt. Közl. *1*, p. 138.
VIDACS, A. [1961]: Gyöngyösoroszi ércbánya hidrotermális telérei. MÁFI Évi Jel. 1957—58. évekről. p. 25.

VIDACS, A. [1957]: Structure and mineral association of the veins of the mine of Gyöngyösoroszi. Acta Miner. Petr. *10*, p. 77.
VIDACS, A. [1961]: A mátraszentimrei érckutató ferde fúrás. MÁFI Évi Jel. 1957—58. évekről. p. 77.

Manuscript received, May 10, 1972.

DR. J. MEZŐSI
Institute of Mineralogy, Geochemistry and Petrography, József Attila University, Szeged

Acta Mineralogica-Petrographica, Szeged, XX/2, 311—312, 1972.

MANGANESE DEPOSITS OF AROOSTOOK COUNTY, MAINE

L. PAVLIDES

RESUME OF 1971 RESEARCH ON MANGANIFEROUS DEPOSITS IN AROOSTOOK CO. MAINE, USA

Low-grade, lenticular, sedimentary ferruginous manganese deposits occur in 3 districts in northeastern Maine. They are enclosed in slate, siltstone, and graywacke of Silurian and Early Devonian (rare) age and are believed to have formed as impure chemical precipitates whose deposition was controlled by Eh-pH fluctuations [PAVLIDES, 1962]. The manganese occurs chiefly in carbonate (carbonate facies) and braunite, carbonate, bementite, and spessartite (local) in the hematitic (oxide facies) deposits.

Recently completed quadrangle mapping by LOUIS PAVLIDES in the southern manganese district of Aroostook County indicates that all the deposits except one (Lower Devonian) occur in the Silurian Smyrna Mills Formation of Llandovery to Early Ludlow age. The deposits locally contain magnetite believed to reflect the regional chlorite grade of metamorphism they have undergone. They occur on the limbs of an anticlinal orocline, the south flank of which strikes into the contact metamorphic aureole of several granitic plutons. The contact aureole is characterized by positive magnetic anomalies, the largest of which are caused by the contact metamorphosed ferruginous manganese deposits that have been recrystallized to manganiferous ironstones. Such ironstones consist of black fine-grained thinly layered quartz-free rocks composed chiefly of magnetite, manganiferous cummingtonite-grunerite amphibole and manganiferous garnet in various proportions and combinations within the different thin compositional layers and laminae of the rocks. Other associated metamorphic minerals that are locally present include biotite, fayalite, pyroxmangite, and possibly perovskite(?) and spinel(?). This mineral assemblage resembles that of the eulysites (except for the absence of pyroxene) described by TILLEY [1936]. The fraction of the manganese in the metamorphic minerals of the Aroostook "eulysitic" meta-ironstones awaits electron probe analysis.

REFERENCES

PAVLIDES, LOUIS [1962]: Geology and manganese deposits of the Maple and Hovey Mountains area, Aroostook County, Maine: U. S. Geol. Survey Prof. Paper *362*, 116 p.

TILLEY, C. E. [1936]: Eulysites and related rock types from Loch Duich, Ross-shire: Mineralog. Mag., v. *24*, p. 331—342.

Manuscript received, May 15, 1972.

LOUIS PAVLIDES
U. S. Geological Survey Bldg.,
Agric. Res. Center, Beltsville, Md.,
U. S. A.

Acta Mineralogica-Petrographica, Szeged, XX/2, 313—323, 1972.

GENETIC TYPES OF SEDIMENTARY MANGANESE FORMATIONS

V. P. RAKHMANOV and V. K. TCHAIKOVSKY

ABSTRACT

Sedimentary and volcanogenic-sedimentary manganese ore formation for the determination of main manganese formations characterized by specific features (lithologic, volcanogenic, facies, tectonic) is discussed. Manganese formations are divided into three main types: platform, transitional (subplatform and subgeosynclinal) and geosynclinal corresponding to large tectonic elements of the earth crust. According to lithologic features every type is subdivided into subgroups of manganese formations — terrigenous, carbonate and volcanogenic the quantitative correlation of which is different.

Taking into consideration difficulties of ascertainment of the true nature of manganiferous solutions main attention was paid to paragenetic connections and rock assemblages accompanying manganese ore-formation during the study of sedimentary manganese ores and metallogeny in different tectonic parts of the earth crust. A genetic classification of sedimentary manganese formations is suggested. Its scheme is: types of manganese formations—subgroups — manganese formations — deposits.

At present there are many works dealing with the geochemistry of manganese, regularities of manganese deposit distribution and conditions of their formation in different details and from various positions. In this regard VERNADSKIY's [1934], FERSMAN's [1939] and BETEKHTIN's [1946] works are generally known.

Much less work is related to the study of sedimentary and volcanogenic-sedimentary manganese ore formation for clearing up chief manganese formations characterized by specific features (lithological, volcanogenic, facies, structural-tectonic). Works by SHATSKIY [1954], STRAKHOV [1960, 1968], RUKHIN [1953], VARENTSOV [1961] have made a valuable contribution to clearing up the nature of latter.

This problem is also considered in the works of ZAKHAROV [1958], DZOTSENIDZE [1965], SAPOZHNIKOV [1967, 1970], SUSLOV [1966], SOKOLOVA [1968], ROY [1966, 1969] and others. Nevertheless there is no general point of view on particular parts of this problem. Therefore in this article we shall endeavour to be guided by more widespread ideas.

As it is known, the majority of the world manganese ore resources, in particular in the USSR, belongs to sedimentary-marine deposits subdivided into true sedimentary and volcanogenic-sedimentary according to the source of ore-bearing solutions [RAKHMANOV, 1970]. When choosing the main types of sedimentary manganese ore formations it is necessary to take into account that in some cases factors of exogenetic metallogeny and exogenetic rock and ore formation are considered while in others — hypogene, in particular volcanogenic factors.

Methods which we should use during a study of deposits and drawing up prognostic metallogenic maps for manganese ores are defined by the fact that economic

manganese deposits belong to sedimentary or sedimentary-volcanogenic formations. In the first place such methods are lithological-facies and formational. At the conferences in LOPI (Laboratory of Sedimentary Mineral Deposits, USSR) in 1968-1969 concerning drawing up prognostic and prognostic-metallogenic maps for manganese ores in perspective regions of Ural, Kazakhstan, Siberia and the Far East the necessity of using these methods for prognosis of manganese deposits was widely discussed. A recently published work by TCHAIKOVSKY, RAKHMANOV and KHODAK [1972] on basic principles of drawing up prognostic and prognostic-metallogenic maps for manganese ores is mainly devoted to a methodical problem.

The correlation of different genetic types is shown in the suggested classification *(Table 1)*. As stated above manganese deposits of the sedimentary type are the main commercial and the most widespread.

The task of this work is to carry out the analysis of true sedimentary and volcanogenic-sedimentary types of deposits on the basis of the formational method.

We do not deal with manganese deposits of the magmatogenic type as they are not connected with certain formations and are of no practical interest to the USSR and other countries.

It should be noted that volcanogenic-sedimentary ore deposits are sometimes associated with small manganese-bearing veins, derivates of hydrothermal or metamorphic solutions.

Now we shall review some classificational schemes of manganese formations and also choose names for sedimentary complexes with manganese ores.

According to SHATSKIY's well known determination, the formation is a natural complex of rocks in which separate parts, i.e. beds, layers are paragenetically associated with each other both in age and spatial respect. In accordance with this determination the manganese formation is considered to be a paragenetic association of rocks in which beds (bodies) of manganese ore or similar accumulations are a constant unit of the section. The origin of manganese formations in time and space

TABLE 1

Genetic classification of manganese deposits

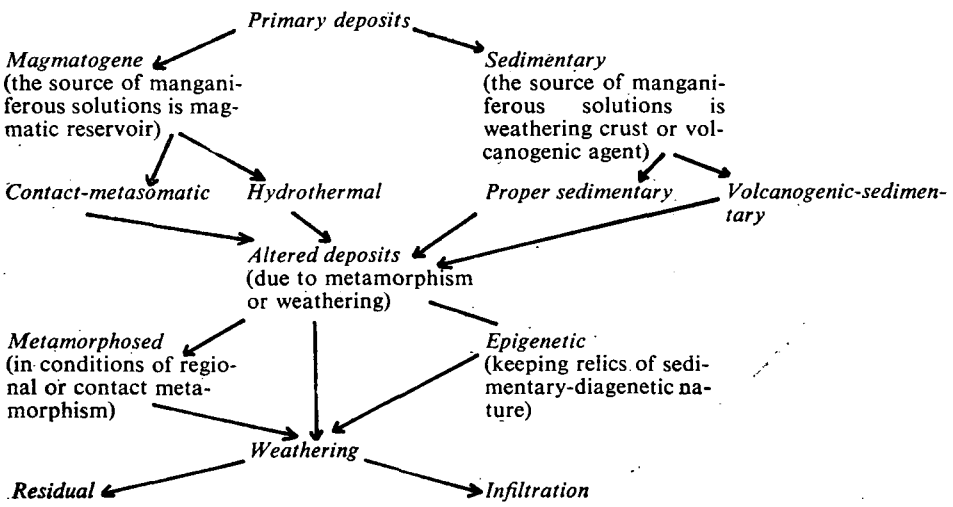

nearly corresponds to that of tectonic set up because they (i.e. formations) are usually separated by more or less large interruptions indicating tectonic reconstruction. Formations and tectonic set up are complete products with definite stages of the beginning and the end of a cycle.

Namely the study of paragenetic associations or formational analysis of rocks formed at different times, in any tectonic and paleogeographical environments and containing manganese ores and manganese-bearing rocks in any part of beds and layers is considered to be the basis of classificational prognostic-metallogenic schemes.

Classifying the main units-formations or subdividing every of them into smaller units one can build up one or another classificational scheme which can be used for revealing and analyzing the relationship between certain types of sedimentary rocks and associated sedimentary and volcanogenic-sedimentary manganese deposits and tectonic set up.

The most useful classification is a scheme where manganese formations are divided into three broad types: platform, transitional (subplatform and subgeosynclinal) and geosynclinal corresponding to larger tectonic elements of the earth crust. According to lithological features every type is divided into subgroups of manganese formations — terrigenous, carbonate and volcanogenic quantitative relations in which are given in the genetic classification of sedimentary manganese formations *(Table 2)*.

As seen in the table distribution of different subgroups of manganese formations in every given tectonic type is nonequivalent. From platforms to transitional and further geosynclinal regions there are appreciable decrease of terrigenous and sharp increase of volcanogenic and partially carbonate constituents in the subgroups of formations.

The majority of world resources of manganese ores (more than 60 %) is concentrated in deposits of terrigenous formation subgroups, especially in the quartz-sand-clay formation of platform and transitional types. Unique deposits of this subdivision have been reported from USSR — Nikopol, Bol'she-Tokmaksk and Chiatura, related to deposits of Nikopol or orthoquartzite-glauconite-clay manganese formation by VARENTSOV [1962]. These deposits have been related to the glauconite formation by SHATSKIY [1954].

We are not sure whether glauconite is a constant member of this formation and therefore we should prefer to name it a quartz-sand and clay formation, as it was adopted by the Atlas of lithologic-paleogeograpical maps of the Russian platform and its geosynclinal framing [1961].

In geological respect deposits related to the quartz-sand-clay manganese platform formation have much in common: the relation of ore concentrations to terrigenous sand-aleurite-clay, often siliceous chemogenous sediments, slope bed of manganese ore layers, their identical facies profiles. The profile changes uniformly from the shore line to the depth of the basin and is characterized by gradual change of oxide ores by carbonate ores through the intermediate zone in which mixed oxide-carbonate varieties are developed.

Common characteristics of the present formation deposits are also acknowledged by similar textular-structural ore appearance. As a rule, they were mainly formed in humid condition (Nikopol, Bol'she-Tokmaksk deposits). However, there are more or less considerable deviations connected with the fact that humid condition is changing into arid during the formation of manganese ores. For example

TABLE 2

Genetic classification of sedimentary manganese formations

Types of manganese formations	Subgroups of manganese formations and their quantitative relations (%)	Manganese formations	Deposits
Platform	Terrigenous — 75	Quartz-sand-clay	Nikopol. Bol'she-Tokmaksk — Pg_3 (Ukraina) Timna — S (Israil)
	Carbonate — 15	Dolotmite-terrigenous Limestone-dolomite	Nargeshum — P-T (Morocco) Imini-Tazdrem — Cr_2 (Morocco)
	Volcanogenic — 10	Volcanic-terrigenous Volcanic-carbonate Siliceous-iron	Pick Artillery, Lake Mid — N_2 (USA) Golconda — Q (USA) Urukum — S (?) (Mato Grosso, Brazil)
Transitional regions (subplatform and subgeosynclinal)	Terrigenous — 50	Quartz-sand-clay	Chiatura — Pg_3 (Georgia); Nizhneudinsk group — Pt_3 (Prisayanje)
	Carbonate — 20	Quartz-sand-clay „Gondite"	Madhya Pradesh — A (India) Nsuta — Pt_1 (Ghana)
	Volcanogenic — 30	Siliceous-limestone	Karadzhal — D_3 (Central Kazakhstan) Ulu-Telayk — P P_1 (West Ural)
		Limestone-dolomite Volcanic-terrigenous	Tetritskaroik group — Pg_1 (Georgia)
Geosynclinal (eugeosynclinal and miogeosynclinal)	Terrigenous — 10	Quartz-sand-clay	Iliktinsk — Pt_3 (Pribaikalie)
	Carbonate — 30	Limestone Dolomite-limestone Siliceous-limestone	Sagan-Zaba — A (Pribaikalia) Usinsk — Cm_1 (West Siberia) Takhta—Karacha — S (Middle Asia)
	Volcanogenic — 60	Spilite-keratophyre-siliceous	Primagnitogorsk group — D_{1-3} (South Ural); ores of the Dharwar system — A (st. Mysore, India)
		Porphyre-siliceous Siliceous-iron	Durnovsk — Cm_2 (Salair) Minas Gerais — Pt_2 (Brazil) Postmasburg — Pt_1 (RSA)

at Timna (Israel) manganese deposit copper concentrations are known to have been formed synchronously with manganese deposition [BENTOR, 1956].

Taking into account tectonic pecularities of the quartz-sand-clay manganese formation of the Chiatura deposit in the Georgian block — a hard mid massive in a geosynclinal zone, we relate it to the manganese transitional formation type although according to lithological facies, ore-mineralogical and geochemical characteristics, it is similar to that of the Nikopol deposit.

Quartz-sand-clay manganese formations of the transitional type are also typical of earlier epochs of manganese ore accumulation. So the quartz-sand-clay manganese formation is clearly distinguished among Upper Proterozoic (Riphean cycle) rock complex in Prisajnie connected with depositions of Karagass and Oselochnaya groups (the Nizhneudinsk group of manganese deposits). There is an opinion that it has been formed in subplatform conditions after the completion of Sayan tectogenesis [DYBROV, 1964]. Rocks of Karagass and Oselochnaya groups are subdivided into some series. Usually manganese mineralization is related to series in the base of which horizons of clastic and detrital depositions are developed (conglomerates, gravelites, sandstones, aleurites).

At the Iliktinsk deposit in Pribaikalia manganese ore concentrations are also related to the quartz-sand-clay manganese formation of the Goloustinsk series of Upper Proterozoic Baikal complex which had been formed in the marginal zone of the geosynclinal basin (miogeosyncline).

We suggest the gondite formation to belong to the quartz-sand-clay manganese formation.

It contains all characteristic rocks of the quartz-sand-clay formation in which gondite appearance is due to metamorphism. Primary composition of gondites was likely psammitic-pelitic with interlayers of manganese hydroxides. The present gondite formation of Central India contains rock layers composed mainly of quartz, spessartite and interbedded layers and interlayers of braunite ores, quartzites, schists. In addition to the above gondites contain hausmannite, rhodonite, manganese amphiboles, rhodochrosite.

The absence of volcanogenic products in these rocks suggests the origin of gondite manganese formation to have taken place in the outer tectonic zone of the geosynclinal region or in marginal relatively mobile belts of the platform.

Thus the name "gondite formation" in accordance with our understanding of this term can be adopted as "manganese metamorphic" in addition to "quartz-sand-clay formation".

The word "gondite" does not define the nature of the formation in its general use but only indicates a specific feature of the formation. The manganese quartz-sand-clay gondite formation is also characterized by discordant ore bedding on the base, composed mainly of gneisses, metamorphic schists [STRACZEK, SUBRAMANYAM *et al.*, 1956].

Further a part of ore beds related by VARENTSOV and others to the gondite formation with widespread volcanites which are typical of the Dharwar system (Mysore) is included into the subgroup of the volcanogenic formation. Therefore they are given the name "spilite — keratophyre — siliceous" *(Table 2)*.

Manganese content of the rocks of the manganese carbonate formation subgroup has economic significance. The following manganese formations are distinguished in this subgroup according to tectonic position, structure, composition and lithological-geochemical features of host rocks: *1)* limestone-dolomite and dolomite-terrigenous of the platform basement (deposits Imini-Tazdrem — Cr_2;

Nargeshum — P—T, Morocco); *2)* siliceous-limestone and dolomite-limestone of transitional regions (Karadzhal — D_3, Kazakhstan; Ulu-Telayk — P_1, West Priuralia); *3)* limestone, dolomite-limestone, siliceous-limestone of geosynclinal zones (Sagan-Zaba — A, Pribaikalia; Usinsk — Cm_1, Kuznetsk Alatau; Takhta-Karacha — S, Zeravshan ridge). Carbonate formations were formed in different tectonic conditions as proved by their distribution in the limits of platform, transitional and geosynclinal zones with or without manifestations of volcanism. Climate conditions during the evolution of manganese carbonate formations were different.

Manganese carbonate formations are mainly represented by shallow sea terrigenous-carbonate depositions transforming from inshore shallow water to the depth into relatively thick limestone, clayey-limestone and dolomite beds with clark and superclark up to ore concentrations of manganese when siliceous and other volcanogenic sediments occur among carbonate depositions.

Platform carbonate formations of the Morocco type (the Nargeshum deposit) are characterized by noticeable content of terrigenous red beds in the floor and roof of the formation. Oxide manganese ore beds (Imini-Tazdrem deposits, Morocco) are related to beds of Upper Cretaceous dolomites with interlayers of gypsum and anhydrites.

The well-known Ulu-Telyaksk deposit of carbonate manganese ores, in the USSR situated in the joint zone of the Russian platform and the Ural geosyncline and associated with the limestone-dolomite formation of transitional regions is also characterized by wide development of anhydrite beds of this formation. At the same time limestone, limestone-dolomite and siliceous-limestone, formations of geosynclinal zones have no distinct signs of arid conditions of their origin (Sagan-Zaba, Takhta-Karacha deposits, USSR). The dolomite-limestone formation of the Usinsk type is characterized by the relation of carbonate manganese ores to black bituminous limestones, pyritiferous carbonate and siliceous shales [RAKHMANOV, 1966].

Carbonate manganese formations located in platforms and transitional regions often contain layers of rich oxide ores (braunite-hausmannite, polianite, psilomelane ores and others) in which the manganese content is 40—45 % and more. Sometimes they also have higher content of barium, lead, zinc, copper [BOULANDON, JOURAVSKY, 1952].

In geosynclinal and transitional zones carbonate manganese formations contain mainly carbonate ores (rhodochrosite, manganocalcite, rhodochrosite-manganocalcite ores and others) with the tendency to superclark accumulation of iron, nickel, cobalt and other siderophile elements in certain facial conditions [PUSHKINA, 1960; VARENTSOV, 1962*b*; KHODAK, RAKHMANOV, 1966].

The content of base metals, the association with red beds and other signs confirm accumulation of carbonate manganese formations to have taken place in arid conditions; their characteristic features naturally become weak with transition from inshore-sea to deep-sea environment.

Volcanogenic manganese formations are more widely distributed in geosynclinal regions, they are less found in transitional-subplatform zones and as a rule, they seldom occur in platforms.

Recently a number of workers [KHERASKOV, 1951; SHATSKIY, 1954; VARENTSOV, 1962*a et al.*] have distinguished manganese volcanogenic-sedimentary formations subdivided due to their composition into the greenstone formation group associated with spilite-keratophyre effusive activity and the porphyry formation group with predominant development of granite-rhyolite volcanism.

The former are rather related to primary, the latter — to final phases of development of geosynclinal folded regions.

According to SHATSKIY, manganese ores of the given type are located within the formation and are not connected with interruption.

In spilite-keratophyre siliceous manganese formations poor silicate and sometimes carbonate manganese ores with small content of relatively rich oxide ores are more distributed; the oxide ores are considerably developed in the porphyry manganese formation.

Spilite-keratophyre-siliceous manganese formations are chiefly placed in eugeosyncline zones, and porphyry formations — in miogeosynclinal zones. Greenstone formations are characterized by higher content of silica; Cu, Ni, Co, V, Cr are present in superclark concentration; Pb, Ag, Au, As are rare.

A large group of the South Ural deposits and ore manifestations is connected with spilite-keratophyre volcanism. They are situated in Devonian jasper-siliceous rocks of the Magnitogorsk synclinore in the east slope of South Ural.

Porphyry-siliceous formations are characterized by wide distribution of manganese oxide Ores — pyrolusite or braunite-hausmannite, at times associated with iron ores. They have often rather high concentrations of barium, lead, zinc and other elements. The Durnovsk deposit situated in Salair may be an example of volcanogenic-sedimentary manganese deposits of the porphyry type.

Ore enclosing rocks in the Durnovsk deposit are represented by Lower and Middle Cambrian quartz porphyry, quartzite, tuff and tuffite.

Ore bodies interbedded with quartz porphyry, tuff, quartz-sericitic schist and quartzite form a manganese ore bed of 45—60 m thickness [SUSLOV, 1967].

The siliceous-iron formation is included into the group of volcanogenic manganese formations. Manganese is known to be widely distributed as associated element in jaspilite formations which are the largest Precambrian iron beds in the world (Minas Gerais — Pt_2, Brazil; Postmasburg — P_1, RSA). Manganese ore beds are mainly typical of marginal parts of proper siliceous-iron (jaspilite) formations where iron beds with manganese clark content are transformed into limestone-dolomite rocks with higher concentrations of this element. According to tectonic conditions of formation and specific features of ore mineralization manganese siliceous-iron formations are subdivided into eugeosynclinal, miosynclinal and platform types [VARENTSOV, 1962*b*].

It should be noted that important Precambrian manganese siliceous-iron formations practically are unknown in the USSR. However, some manganese ore manifestations are genetically connected with Precambrian siliceous-iron formations (Proterozoic manganese-iron quartzites of Sosnowy Baitz series and Andotsk series in Prisaynia, manganese ore concentrations in siliceous-iron bed of Malyi Khingan).

Probably in Brazil the iron-manganese Urukum deposit (S?) is related to the siliceous-iron formation of the platform type (State Mato Grosso). Here gentle bedding of ore enclosing rocks, absence of volcanogenic products in the section and signs of metamorphic transformation are characteristic for the whole complex of terrigenous siliceous-iron (hematite) depositions (Jagadigo group, about 700 m thickness) including concordant beds of manganese (cryptomelane) ores and situated in raised or lowered blocks of the Precambrian granitic basement. Some authors suppose precipitation of manganese to have taken place in the form of hydroxide in these deposits [BARBOSA, 1956].

An example of manganese volcanogenic formations of the transitional region is the formation of the Artvin-Somkhitsk block in Tetritskaroisk district (Georgia,

USSR). Beds of oxide manganese ores in the form of layers of small thickness occur in the transitional zone from the lower "flish" horizon to overlapped volcanogenic rocks of andesite-dacite composition. There are also ore-bearing tuff, tuff breccia, tuffaceous sandstone and fine conglomerate.

The volcanogenic formation subgroup of the platform type is represented by volcanogenic-terrigenous and volcanogenic-carbonate manganese formations. They are illustrated by Neogen manganese ore manifestations of Peak Artillery and Lake Mid regions in Colorado-Rio and a small Pleistocene manganese deposit in Golkonda, Central Nevada.

Some workers and especially SOKOLOVA [1968] have shown that manganese ores in Peak Artillery and the Lake Mid regions are of continental volcanogenic-sedimentary origin connected with water environment. Manganese ores were associated with terrigenous rocks (from conglomerate to sandstone and clay) and also andesite-basalt and fine-grained tuff. They contain higher lead (up to 5%) and copper (up to 0.3%). The oxide (psilomelane) ores of the Golkonda deposit are embedded in the base of calcareous tuffs.

Their specific feature is high content of wolfram (up to 6.19% WO_3, average 0.5%). Manganese solutions were brought into basins at the relatively late period of volcanism. Their formation is connected with hydrothermal solutions which in Pleistocene rose from depths along faults and joints of the Mesozoic basement [SOKOLOVA, 1968; KERR, 1940].

Manganese formations in these subgroups can be divided in their turn according to the degree of metamorphism of host rocks into metamorphosed and slight metamorphosed — epigenetic. So there is a quartz-sand-clay formation characterized by absence of metamorphism in the group of transitional regions. The important example of this subdivision is the widely known Oligocene manganiferous bed of the Chiatura deposit with manganese oxide, oxide-carbonate and carbonate ores.

Another quartz-sand-clay manganese formation so called "gondite", is also included into this subgroup; its rocks had undergone intensive metamorphism and lost primary sedimentary-diagenetic appearance. Numerous manganese deposits relating to Archeozoic and Proterozoic metamorphosed rocks of ancient platforms (Indian, African, Brazilian, Australian platforms) belong to this formation, too. The most typical regions of the gondite formation are the Central province of India (Madhya Pradesh), West Africa (groups "Birrim" in Ghana and "Ancongo" in Mali) and others. The gondite formation is characterized by specific rocks from phyllite, quartz-sericite, biotite and muscovite schists to quartzite and feldspar-quartz gneiss in which there are concordant beds of braunite ores and gondite rocks. Gondites are represented by specific paragenetic assemblage: quartz, spessartite, rhodonite, bustamite, manganese amphiboles and pyroxenes, braunite, hausmannite, biotite, muscovite, plagioclases.

Further it is necessary to review the subdivision of manganese superimposed formations or formations of weathering crust as they are sometimes called. Indeed there are many manganese formations with different manganese content where physical and chemical alteration may result in the formation of new manganiferous concentrations in supergene and other conditions. In the supergene zone manganese ore beds can be formed simultaneously in some different adjoining formations or their subgroups (terrigenous, carbonate, volcanogenic). In some cases the endogenous factor is important for secondary enrichment of manganese ores too. Therefore the formations with such ore beds should be named as primary formations adding words "with superimposed manganese protore".

The determination of the source of manganiferous solutions is of great importance for a correct relating of sedimentary manganese formations to any type or subgroup. So in conclusion we shall concern the source of manganiferous solutions.

The review of numerous works concerning this problem shows that the opinions of authors on the source of ore solutions vary at times. Every worker tries to confirm his point of view, moreover their concepts on the source of manganiferous solutions for the same object differing.

The first example: DZOTSENIDZE [1965], KHAMKADZE [1971] and others give data for the important Chiatura manganese deposit (USSR) showing that post-volcanic hydrothermal solutions of Upper Eocene volcanism but not weathering crust of eroded land were the source of manganese in the Oligocene sea of Georgia. At the same time concepts of BETEKHTIN [1946], STRAKHOV [1964] and other geologists on the Chiatura deposit as proponents of the opinion about the source of manganese from weathering crust of the Dzirulsk granitoid massive and Bajocian porphyrite series are generally known.

The other example: SOKOLOVA [1969], MIRTOV, TSYKIN *et al.* [1964] concerning the well-known Lower Cambrian Usinsk deposit of carbonate manganese ores in Kuznetsk Alatau suggest the formation of this deposit to have taken place in close connection with volcanic activity; synchronous volcanic exhalation was the source of ore solutions.

VARENTSOV [1962] and other authors, however, regard the Usinsk deposit to be "typical exogenous formation which was not controlled by volcanic processes ... Ore material was brought due to deep chemical alteration of land".

The problem of the manganese source is complex and debatable. Natural data and experiments suggest manganese in suspension and solution to have been lost by supergene waters from contemporary weathering crust. Some data suppose manganese to have been brought into sedimentary basins due to volcanic activity. And the longer (in the scale of geological time) manganese combinations which are in equilibrium with surrounding water environment of seas and oceans are kept in solution the more complicated is the genetic restoration of primary nature of manganese. Hence there are contradictory opinions concerning even such unique (in respect of manganese concentration) and well studied Oligocene deposits of the Black Sea basin as Nikopol, Bol'she Tokmaksk, Chiatura.

Important data are given by SKOPINTSEV and POPOVA [1963] who estimated total manganese in the water of the Black Sea to be about 100 million tons. It is not exception as SAPOZHNIKOV [1967] assumes that manganiferous ore sediments may be formed in inshore parts of the basin at favourable conditions (tectonic reconstruction causing stable rising currents etc.).

It is extremely difficult to ascertain the true nature of manganiferous solutions even by analogy with recent manganese ore formation. Taking into account the above, much attention was paid to paragenetic connections and rock assemblages accompanying manganese protore while studying sedimentary manganese ore formation and metallogeny in different tectonic parts of the earth crust. On this basis our genetic classification of sedimentary manganese ores has been built up.

Detailed geological study and ascertainment of the genesis of manganese deposits are very important as it allows to find out causes of paragenetic connections between manganese formations and inclosed deposits. On the basis of revealed regularities it is possible scientifically to set up prognosis and search for economic manganese ores. Clearing up paragenetic relations should be considered as necessary stage helping to learn their genetic connections.

REFERENCES

Atlas of lithologic-paleogeographical maps of the Russian platform and its geosynclinal framing. Moscow, Izd. AN SSSR, 1961.

BARBOSA, O.: Manganese at Urucum, state of Mato Grosso, Brasil. In: XX Congresso geologico international. Symposium del manganeso *3*, Mexico, 1956.

BENTOR, I. K.: The manganese occurrences at Timna (Southern Israel), a Lagoonal deposit. In: XX Congresso geologico international. Symposium sobre yacimientos de manganeso *4*, Asia y Oceania. Mexico, 1956.

BETEKHTIN, A. G.: Commercial manganese ores of USSR. Moscow, Izd. An SSSR, 1946.

BOULANDON, J., JOURAVSKY, G.: Manganese. Geologie des gites mineraux marocains. XIX. Congres geologique international. Monographies regionales. 3-e ser., Maroc, N 1, Rabat, 1952.

TCHAIKOVSKIY, V. K., RAKHMANOV, V. P., KHODAK, YU. A.: Principles of drawing up prognostic-metallogenic maps of manganese formations. Moscow, Izd. Nedra, 1972.

DIBROV, V. E.: Geology of central West Sayan. Moscow, Izd. Nedra, 1964.

DZOTSENIDZE, G. S.: Influence of volcanics on formation of sediments. Moscow, Izd. Nedra, 1965.

FERSMAN, A. E.: Manganese. In: "Geokhimiya", *4*, Moscow, Gosnauktekhizdat, 1939.

KERR, P. E.: Tungsten-bearing manganese deposits at Golconda, Nevada. Geol. Soc. Amer. Bull, *51*, 1940.

KHAMKHADZE, N. L.: Lithology of Oligocene manganese-bearing depositions of the north Georgian block. Tbilisi, Izd. Metsniereba, 1971.

KHERASKOV, N. P.: Geology and genesis of Eastern Bashkirian manganese deposits. In: "Voprosy litologii i stratigraphii SSSR. Pamyati akademika A. D. Arkhangel'skogo. Moscow, Izd. AN SSSR, 1951.

KHODAK, YU. A., RAKHMANOV, V. P.: Geochemistry of ore bed of the Usinsk deposit and underlying rocks. In: "Mestorozhdeniya margantsa Kuznetskogo Alatau". Moscow, Izd. Nauka, 1966.

MIRTOV, YU. V., TSYKIN, R. A., VALYUZHENICH, Z. L., ALEXANDROV, K. I.: Manganese and phosphorite Lower Cambrian and Upper Precambrian (Sinian) formations of West Siberia, Trudy *V* Vsesoyuzny litolog. Soveshchaniya. Tom. *II*, SO, AN SSSR, Novosibirsk, 1964.

PUSHKINA, Z. V.: On geochemistry of the Usinsk manganese deposit. Moscow, Dokl. AN SSSR, t. *135*, N 1, 1960.

RAKHMANOV, V. P.: Types of ores and host rocks of the Usinsk deposit. Moscow, Izd. Nauka, 1966.

RAKHMANOV, V. P.: On regularities of localization of manganese deposits and geological prognostic factors. In: "Voprosy rudnichnoy geologii. VIOGEM. Ch. 1. Belgorod, 1970.

ROY, S.: Syngenetic manganese formation of India, Jadavpur University, Calcutta, 1966.

ROY, S.: Classification of manganese deposits. Acta Mineralogica-Petrografica Szeged *19*, 67—83, 1969.

RUKHIN, L. B.: Elements of lithology. Moscow, Gostoptekhizdat, 1953.

SAPOZHNIKOV, D. G.: Some geological conditions of formation of manganese deposits. In: "Marganzevye mestorozhdeniya SSSR. Moscow, Izd. Nauka, 1967.

SAPOZHNIKOV, D. G.: Types of manganese deposits of USSR. In: "Sostoyanie i zadachi sovetskoi litologii". Moscow, Izd. Nauka, 1970.

SHATSKIY, N. S.: On manganese formations and metallogeny of manganese. Izv. AN SSSR, ser. geol., N 4, 1954.

SKOPINTSEV, B. A., POPOVA, T. P.: On manganese accumulation in waters of hydrogen sulphide-bearing bassins in the light of the Black Sea. Trudy GIN AN SSSR, vyp. 97, 1963.

SOKOLOVA, E. A.: Some regularities of localization of concentrations in manganese volcanogenetic-sedimentary formations. In: "Marganzevye mestorozhdeniya SSSR". Moscow, Izd. Nauka, 1967.

SOKOLOVA, E. A.: Regularities of formation of volcanogenic-sedimentary manganese ores. In: "Osadkoobrazovanie i poleznye iskopaemye vulkanicheskikh oblastei proshlogo", Moscow, Izd. Nauka, t. II, 1968.

STRACZEK, J., SUBRAMANYAM, M. R. *et al.*: Manganese ore deposits of Madhya Pradesh. In. XX Congreso geologico international. Symposium sobre yacimientos de manganeso *4*, Asia y Oceania. Mexico, 1956.

STRAKHOV, N. M.: Main types of litogenesis. Vol. 1—2. Moscow, Izd. AN SSSR, 1960.

STRAKHOV, N. M., SHTERENBERG, L. E.: On genetic type of the Chiatura deposit. Litol. i. polezn. iskop., N 1, 1964.

STRAKHOV, N. M., SHTERENBERG, L. E., KALINENKO, V. V., TIKHOMIROVA, E. S.: Geochemistry of sedimentary manganese process. Trudy GIN AN SSSR, vyp. 185. Moscow. Izd. Nauka, 1968.

Acta Mineralogica-Petrographica, Szeged, XX/2, 325—336, 1972.

METAMORPHISM OF SEDIMENTARY MANGANESE DEPOSITS

SUPRIYA ROY

ABSTRACT: Metamorphosed sedimentary deposits of manganese occur extensively in India, Brazil, U. S. A., Australia, New Zealand, U. S. S. R., West and South West Africa, Madagascar and Japan. Different mineral-assemblages have been recorded from these deposits which may be classified into oxide, carbonate, silicate and silicate-carbonate formations. The oxide formations are represented by lower oxides (braunite, bixbyite, hollandite, hausmannite, jacobsite, vredenburgite etc.), the carbonate formations by rhodochrosite, kutnahorite, manganoan calcite etc., the silicate formations by spessartite, rhodonite, manganiferous amphiboles and pyroxenes, manganophyllite, piedmontite etc. and the silicate-carbonate formations by rhodochrosite, rhodonite, tephroite, spessartite etc. Petrographic and phase-equilibia data indicate that the original bulk composition in the sediments, the reactions during metamorphism (contact and regional and the variations and effect of O_2, CO_2, etc. with rise of temperature, control the mineralogy of the metamorphosed manganese formations. The general trend of formation and transformation of mineral phases in oxide, carbonate, silicate and silicate-carbonate formations during regional and contact metamorphism has, thus, been established.

Sedimentary manganese formations, later modified by regional or contact metamorphism, have been reported from different parts of the world. The most important among such deposits occur in India, Brazil, U.S.A., U.S.S.R., Ghana, South and South West Africa, Madagascar, Australia, New Zealand, Great Britain, Japan etc. An attempt will be made to summarize the pertinent data on these metamorphosed sedimentary formations so as to establish the role of original bulk composition of the sediments, transformation and reaction of phases at elevated temperature and varying oxygen and carbon dioxide fugacities in determining the mineral assemblages in these deposits.

DEPOSITS OF SEDIMENTARY AND DIAGENETIC MANGANESE FORMATIONS

Unmetamorphosed volcanogenic-sedimentary manganese deposits have been described from Taratana, Pompo and Sabanill deposits (Cuba), Kokko, Pirika and Kinjo mine areas (Hokkaido, Japan), Coquimbo deposits (Chile), Artillery Peak (Arizona, U.S.A.), Lucifer area (Baja California, Mexico), Glib en Nam (Morocco) etc. Sedimentary deposits of non-volcanogenic source have been described from Chiatura, Nikopol, Babinsk, Usinsk, Ulu-Telyaksk (U.S.S.R.), Timna Dome (Israel), Urkut (Hungary), Imini-Tasdrent (Morocco), Western Mato Grosso (Brazil) and eastern Bolivia. The details of most of these deposits have been summarized by HEWETT and FLEISCHER [1960], HEWETT [1966] and ROY [1968, 1970]. The mineralogy of these unmetamorphosed sedimentary deposits, volcanogenic or non-volcanogenic, is very similar and is characterized by the presence of higher oxides or hydroxides (cryptomelane, psilomelane, pyrolusite, todorokite,

birnessite, manganite, vernadite etc.) or by carbonates (rhodochrosite, manganoan calcite) often with varying silica content. Only in very rare cases, braunite has been reported from volcanogenic sedimentary deposits (Glib en Nam, Morocco and Coquimbo, Chile) [HEWETT, 1966]. At Tiaratine L'Ayat, Morocco, hausmannite and jacobsite have been reported, which are however, clastic materials derived from older deposits [POUIT, 1964]. The deposition of manganese as higher oxide, hydroxide, or carbonate is controlled by the Eh and pH of the medium [BRICKER, 1965]. The manganese sulfide, alabandite, has not been reported from any sedimentary ore-body excepting from the recent depositions in the Black Sea [SOREM and GUNN, 1967] as it is precipitated only in very reducing condition.

In western Mato Grosso, Brazil and eastern Bolivia, unmetamorphosed oxide-facies iron formation is interstratified with primary manganese oxide in a non-volcanogenic environment [DORR, 1970]. Similar interstratification of manganese oxide beds with iron formation is found in the Kuruman District, South Africa.

Recent deposits of manganese nodules in deep sea and shallow waters, are consituted of 10 Å manganite and 7 Å manganite having the empirical formulas $3\,MnO_2.Mn(OH)_2.nH_2O$ and $4\,MnO_2.Mn(OH)_2.nH_2O$ respectively, birnessite (δ-MnO_2), todorokite and ranciéite [MANHEIM, 1965; PRICE, 1967; SOREM, 1967, 1967 etc.]. Very often these nodules have a high iron content and unless iron is diagenetically separated, ferro-manganese nodules are common.

The pyrolusite-psilomelane-manganite-rhodocrosite-manganocalcite assemblage of Chiatura and Nikopol are considered by BETEKHTIN [1937] to be gradational due to deposition from near-shore condition (oxidizing) to deeper zones (reducing) of the basin. STRAKHOV [1966], on the other hand, considered that the manganese carbonates have formed by diagenesis of oxidic sediments as indicated by the transition of higher oxides to carbonates with manganite (Mn^{3+}) as intermediate member. STRAKHOV [1966] mainly attributed the concentration of manganese in sedimentary ores of recent and ancient deposits to diagenesis and accordingly recognized different types: lacustrine sedimentary-diagentic, lacustrine-diagenetic, shallow-water diagenetic, shallow-water sedimentary-diagenetic and marine and sedimentary-diagenetic ores.

Diagenetic redistribution and reconstitution in deep-sea and shallow water manganese and ferro-manganese nodules have been reported by a number of workers including LYNN and BONATTI [1965], MANHEIM [1965], STRAKHOV [1966], BOSTRÖM [1967], PRICE [1967], SEVAST'YANOV [1968], CALVERT and PRICE [1970] and this is of considerable importance in the separation of iron and the formation of manganese carbonates. BOSTRÖM explained LYNN and BONATTI's find of diagenetic manganese carbonate by the following reaction:

$$xCaCO_3 + yMn^{2+} = (Ca_{x-y}Mn_y)CO_3 + yCa^{2+}.$$

Studies on behavior of manganese minerals in elevated temperature

Considerable work on the behavior of low temperature manganese minerals when subjected to elevated temperature, has been done in the laboratory. Consequently a fairly good idea about the formation and transformation of manganese minerals in rising temperature has been obtained. These data, mainly derived from phase equilibria studies and differential thermal analysis, may be effectively utilized in explaining the mineral assemblages of metamorphosed manganese formations and are summarized in Table 1.

TABLE - I

TRANSFORMATION OF MANGANESE MINERALS IN RISING TEMPERATURE

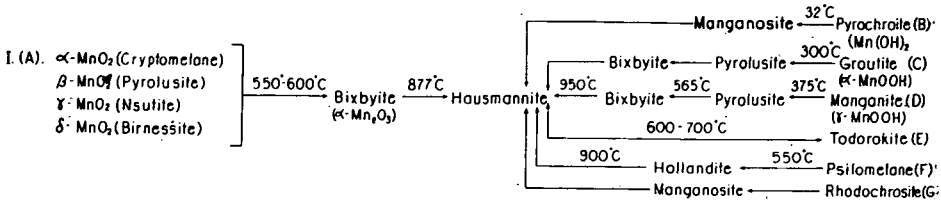

II. with SiO_2 (A) IA, IC, ID, IE + SiO_2 (oxides or hydroxides) ⟶ Braunite and/or Rhodonite (depending upon fo_2).

(i) $7MnO_2 + SiO_2 = 3Mn_2O_3.MnSiO_3 + O_2$

(ii) $2MnO_2 + 2SiO_2 = 2MnSiO_3 + O_2$

(B) IG + SiO_2 (Carbonates) Rhodonite, Tephroite Or Braunite

(i) $MnCO_3 + SiO_2 = MnSiO_3 + CO_2$

(ii) $2MnCO_3 + SiO_2 = Mn_2SiO_4 + 2CO_2$

(iii) $7MnCO_3 + SiO_2 + 3/2O_2 = 3Mn_2O_3.MnSiO_3$

III. with Iron Oxide Or Hydroxide: IA, IC, ID, IE + Iron Oxide Or Hydroxide (oxides or hydroxide) ⟶ Bixbyite (α-Mn_2O_3 with upto 60% Fe_2O_3) ⟶ Jacobsite and/or ($MnFe_2O_4$) Vredenburgite ($MnFe_2O_4$ with excess Mn_3O_4 in solid solution).

IV (A). Braunite ($3Mn_2O_3.MnSiO_3$) ⟶ Tephroite (Mn_2SiO_4) + Hausmannite (Mn_3O_4). (B). $3Mn_2O_3.MnSiO_3 = 7MnSiO_3 + 3/2\,O_2$. (Braunite) (Rhodonite)

V. Bementite $(Mn, Mg, Fe)_6Si_4(O,OH)_{18}$ ⟶ Braunite ⟶ Rhodonite

VI. $MnCO_3 + MnSiO_3 = Mn_2SiO_4 + CO_2$. (Rhodochrosite) (Rhodonite) (Tephroite)

VII. $6MnSiO_3 + O_2 = 2Mn_3O_4 + 6SiO_2$ (Rhodonite) (Hausmannite)

VIII. $2(Mn,Fe)SiO_3 + 3/2\,O_2 = MnFe_2O_4 + MnSiO_3 + SiO_2$ (Pyroxmangite) (Jacobsite) (Rhodonite)

XI. (A). $Mn_2SiO_4 + SiO_2 = 2MnSiO_3$ (Tephroite) (Rhodonite). (B). $6Mn_2SiO_4 + O_2 = 6MnSiO_3 + 2Mn_3O_4$ (Tephroite) (Rhodonite) (Hausmannite)

References to table 1

I. A. Ukai *et al*, 1956; Klingsberg & Roy, 1959: Okada, 1959 *a* & *b;* Faulring *et al*, 1960, Hahn & Muan, 1960. I. B. Klingsbery & Roy, 1959.

I. C. Lima-de-Faria & Lopes Vieira, 1965. I. D. Das Gupta, 1965. I. E. Okada, 1960.

I. F. Fleischer and Richmond, 1943; Wadsley, 1950; Fleischer, 1964.

I. G. Cuthbert and Rowland, 1947: Kulp *et al*, 1949.

II. A. *(i) & (ii)* Huebner, 1967. II. B. *(i) & (ii)* Yoshinaga, 1958.

II. B. *(iii)* Huebner, 1967.

III. Roy, 1970.

IV. A. Pavlovitch, 1931. IV. B. Huebner, 1967.

V. Ito, 1961.

VI. Yoshinaga, 1958.

VII. Huebner, 1967.

VIII. Roy, 1970.

IX. A. & B. Huebner, 1967.

(In Table 1 instead of XI read IX)

REGIONALLY METAMORPHOSED SEDIMENTARY MANGANESE FORMATIONS

The regionally metamorphosed sedimentary manganese formations may broadly be divided into three types according to their mineral assemblages.

(i) Deposits consisting of metamorphic oxide and silicate assemblages and devoid of carbonates

The geology and mineralogy of the regionally metamorphosed Precambrian sedimentary manganese formations of India in the Sauser, Aravalli, Champaner and Khondalite Groups were discussed at considerable length by FERMOR [1909], ROY [1966, 1970], ROY and MITRA [1964], ROY and PURKAIT [1968] and others. These non-volcanogenic sedimentary deposits, subjected to different grades of regional metamorphism from quartz-albite-muscovite-chlorite subfacies (greenschist facies) to granulite facies in different parts [ROY, 1970], are characterized by oxidic manganese ores, sharply interbanded with manganese silicate rocks (gondite). In the oxidic ore beds, braunite is the first metamorphic mineral to appear in the quartz-albite-muscovite-chlorite subfacies and the mineral is stable throughout the greenschitc, almandine-amphibolite and granulite facies. Bixbyite appears in the quartz-albite-epidote-biotite subfacies in association with hollandite, jacobsite (with high Fe_3O_4 content) and braunite and persists in the higher grades. Hausmannite, jacobsite (with high Mn_3O_4 content) and vredenburgite appear in the staurolite-almandine subfacies and continue to granulite facies in association with braunite. The texture of the ore exhibits a remarkable change with the degree of metamorphism [ROY, 1970]. In low-grade facies, fine grained and relict colloform textures are exhibited by manganese oxide minerals constituting the ore-bodies. Braunite and hollandite are stretched and elongated, showing preferential dimensional orientation parallel to the banding. A schistosity is thus imparted on the ores perpendicular to the direction of maximum compression. Braunite-bixbyite-hollandite ores of greenschist facies often show microfolding and translation twin is developed in hollandite. In high-grade metamorphism, the texture of the oxidic minerals in the ores is characteristically granoblastic. In these ores exsolution of hausmannite in the octahedral plaine of jacobsite and rhodonite are characteristic.

The manganese silicate rocks (gondite are essentially constituted of spessartite and quartz, very often with rhodonite (and/or pyroxmangite, bustamite) and sometimes manganiferous aegirine, aegirine-augite (blanfordite, brown manganiferous pyroxene), diopside, manganiferous magnesioriebeckite (juddite) and richterite-tremolite (winchite, tirodite), manganiferous micas and piedmontite. Rhodochrosite and tephroite are characteristically absent. The field and laboratory studies confirm that the oxidic ore-bands and the sharply interbanded manganese silicate rocks are separate entities. Both were laid down as carbonate-free syngenetic sediments in separate beds and were regionally metamorphosed.

Regionally metamorphosed manganese formations of Otjosondu, S.W. Africa [ROPER, 1956] occur in three stratigraphic zones in the Precambrian Damara System, associated with itabirite-schist and quartzite. Interbanded oxidic and manganese-silicate layers, metamorphosed to almandine- amphibolite facies, are represented by braunite-bixbyite-hollandite-jacobsite-hausmannite-vredenburgite assemblage and by spessartite-rhodonite-diopside-acmite-quartz assemblage, respectively. These manganese formations are, thus, similar to those in India, although the association of the former with metamorphosed bedded iron formation (itabirite schist) differentiates them from the latter.

The manganese formations of S. Ural [BETEKHTIN in ZVEREFF, 1953] of Paleozoic age, have been regionally metamorphosed and the oxidic and silicate formations contain braunite and spessartite-rhodonite-bustamite-piedmontite assemblages respectively.

The deposit at Tierre, W. Africa, regionally metamorphosed to the chlorite zone, exhibits only manganese silicate (spessartite-quartz) assemblage [SERVANT, 1956] and is devoid of metamorphic oxides. This deposit, therefore, represents only admixed manganiferous sediments with manganese oxide, clay, silica etc.

Manganese deposits of volcanogenic-sedimentary spilite-keratophyric type, later metamorphosed regionally, are found in Japan [WATANABE *et al*, 1970*a*]. At Shiromaru mine near Tokyo, such deposits metamorphosed in low-temperature high-pressure condition (as shown by the presence of cymrite), consist of braunite-rhodonite assemblage. At Muramatsu mine, Hagashaki Prefecture, similar manganese formations metamorphosed to amphibolite facies, exhibit a mineral assemblage: braunite-rhodonite-piedmontite-spessartite.

(ii) Deposits exhibiting manganese silicate-carbonate assemblage

The manganese silicate-carbonate formation of Precambrian Minas Series at Minas Gerais, Brazil, metamorphosed to quartz-albite-epidote-almandine subfacies, consist of rhodochrosite-manganoan calcite-rhodonite-pyroxmangite-tephroit-spessartite-kupfferite-bementite-neotocite-alabandite-graphite-quartz assemblage. The local manganese oxide concentrations are supergene higher oxides, but for the minor hausmannite formed by the dissociation of rhodochrosite during metamorphism [HOREN, 1953]. The widespread presence of graphite and alabandite ensures the original depositional condition of the sediments of negative Eh and pH around 7 in an euxinic environment and as such manganese oxides and hydroxides could not form [DORR *et al*, 1956]. PARK (pers. com.), however, considers that alabandite formed entirely due to later contact metamorphism. In fact, PARK *et al* [1951] and others concluded that this manganese-silicate-carbonate formation is a product of contact metamorphism of syngenetic sediments.

At Serra do Navio deposit, Brazil, impure manganese carbonate, with concentration of silica and alumina at places, were originally deposited in an environment of low redox potential in a basin of restricted circulation (NAGELL, 1962). These were later regionally metamorphosed to give rise to recrystallized rhodochrosite bodies with rhodonite, spessartite and picrotephroite. Metamorphic manganese oxides are absent.

Metamorphosed manganese formations of Sierra Nevada, U.S.A., have undergone a higher degree of metamorphism than that of the Coast Ranges of California [HEWETT *et al*, 1961]. Some of the more important deposits in Sierra Nevada exhibit the following mineral assemblages: rhodochrosite-tephroite-rhodonite-spessartite (Big Indian Deposit, Korn County: Precambrian); rhodochrosite-tephroite-rhodonite-spessartite and minor bementite and neotocite (Calaverous Formations: Late Paleozoic); hausmannite: tephroite-rhodonite-spessartite-alleghanyite-piedmontite-bementite-rhodochrosite (Smith Prospect, Amador Group: Jurassic).

The Buckeye deposits (late Jurassic to early Cretaceous) of California Coast Range has been metamorphosed to blueschist facies [HUEBNER, 1967], with the following mineral assemblages: oxide — hausmannite, braunite; silicate — carbonate — rhodochrosite, bementite, 7 & 12 silicates. Hausmannite and braunite are associated with rhodochrosite, as euhedral crystals. Braunite also exhibits fine to coarse laminations which might have been sedimentary in origin. According

to HUEBNER [1967], the Buckeye deposit originally formed by precipitation from thermal waters on ocean floor and was later regionally metamorphosed.

The Manganese Shale Group of the Harlock Dome, Merionethshire, Great Britain, has been metamorphosed to chlorite zone and exhibits an assemblage of rhodochrosite-spessartite-quartz [WOODLAND, 1939]. Tephroite is absent. The higher oxides present are all supergene.

Rhodochrosite-rhodonite-spessartite assemblage has been recorded in metasedimentary lenses and beds in basic lava and tuff regionally metamorphosed to chlorite zone in western Otago, New Zealand [HUTTON, 1957]. Metamorphic oxides of manganese as well as tephroite are absent.

At Kiuragi mine, Saga Prefecture, Japan [WATANABE *et al*, 1970*a*], manganese silicate-carbonate formations of volcanogenic Jasperoid Formation type have been metamorphosed regionally to amphibolite facies, with the following mineral assemblage: tephroite-rhodonite-spessartite-rhodochrosite-jacobsite (with exsolved galaxite).

Around Tamworth, New South Wales, Australia, sedimentary manganese deposits regionally metamorphosed to low grade [SEGNIT, 1962] occur enclosed in phyllites and siliceous rocks. The only metamorphic oxides present are hausmannite and jacobsite with a silicate-carbonate assemblage tephroite-knebelite-mangandolomite-spessartite. At Danglemah deposit, tephroite-mangandolomite, rhodonite-tephroite-spessartite-hausmannite and quartz-knebelite assemblages occur.

(iii) Deposits exhibiting both metamorphic oxides and silicate-carbonate assemblages

The regionally metamorphosed manganese deposits of S. Khingan [CHEBOTAREV, 1960] and the Karadzhal deposit, Central Kazakhstan [MAKSIMOV, 1960; KALININ, 1965; NOVOKHATSKY, 1970], U.S.S.R., constitute a distinct type as they contain both metamorphic low oxide and silicate-carbonate assemblages. The S. Khingan deposits exhibit braunite-hausmannite-hematite-magnetite and rhodochrosite-tephroite-rhodonite-bustamite assemblages. The Karadzhal deposit (volcanogenic-sedimentary; NOVOKHATSKY, 1970) exhibits assemblages of braunite-hausmannite-jacobsite and manganocalcite-rhodochrosite-rhodonite-tephroite. According to KALININ [1965], however, the Karadzhal deposits first underwent regional metamorphism of low grade when oxidic ore bands were converted to braunite and the carbonate manganese formations (with siliceous material) were recrystallized into rhodochrosite-manganocalcite-quartz-chalcedony. This was followed by contact metamorphism when braunite-hausmannite-jacobsite assemblage formed in the oxidic bands and the silicate-carbonate bands were reconstituted to manganocalcite-rhodochrosite-rhodonite-tephroite assemblage. Thus, in different parts of these deposits, a sedimentary facies change from manganese oxide to carbonate was present which were reconstituted on metamorphism. Another characteristic feature of these deposits is that the oxidic manganese ore bands are interlayered with iron formation similar to that at Otjosondu, S.W. Africa and western Mato Grosso (Brazil).

SEDIMENTARY MANGANESE FORMATIONS AFFECTED BY CONTACT METAMORPHISM

Sedimentary manganese formations later modified by contact metamorphism have been described principally from Japan [WATANABE, 1959, 1960; WATANABE, YUI and KATO, 1970*a*, 1970*b*], Sweden [KOARK, 1970] and India [ROY, 1966, 1970].

Bedded volcanogenic manganese and iron-manganese formations of Jasperoid type occur mainly in the Paleozoic Chichibu geosyncline in Japan. Deposits of Mesozoic (S. Shikoku) and Miocene age (Fossa Magna region and Hokkaido) are also found. Many of these deposits have later been modified by contact metamorphism, among which those at Kaso Mine (Tochigi Prefecture), Noda Tamagawa (Iwate Prefecture), and Kanoiri-Yokoneyama are important.

The manganese deposits of Kaso Mine were metamorphosed thermally to hornblende-hornfels facies as shown by the development of cordierite-biotite hornfels in the enclosing rocks [WATANABE *et al,* 1970*a*]. YOSHIMURA [1939] described as many as forty different minerals from this mine-area. Abundant occurence of tephroite, rhodonite, rhodochrosite, alabandite, jacobsite etc. has been reported. Later pyrometasomatism and boron metasomatism gave rise to huebnerite, jimboite, wiserite, pyrosmalite and manganpyrosmalite, caused by later granitic intrusions.

At Noda-Tamagawa mine, manganese orebodies of Paleozoic (Chichibu Complex) age occur as roof-pendant on the Tanchata granite (Cretaceous). According to WATANABE [1959] *et al* [1970*b*] the manganese formation here has suffered a higher grade of contact metamorphism (hornblende-hornfels to pyroxene-hornfels facies) than that in the Kaso Mine, as shown by the presence of sillimanite, andalusite and cordierite in pelitic hornfelses enclosing the orebody. The sharply banded manganese formations are characterized by different mineral assemblages. Rhodochrosite (major)-tephroite-galaxite-maganosite assemblage is most common and is often in contact with hausmannite-rich lenses. Manganese-bearing pyroxenes and amphiboles occur in hornfelses on the footwall side. Interbanded braunite-rich (braunite-hausmannite-tephroite-barite) and braunite-poor (rhodonite-quartz-alkali pyroxene-alkali amphibole) assemblages also occur in this part. Tephroite and rhodonite-rich assemblages (with rhodochrosite and spessartite) are considered to have formed as reaction skarns. Pyrochroite, in pyrochroite-manganosite-tephroite-galaxite-rhodochrosite-barite-alabandite assemblage, has formed by hydration (by residual magmatic water) of manganosite which again formed by thermal dissociation of rhodochrosite, hausmannite and possibly hydrous manganese silicates constituted the original sedimentary manganese deposits at Noda Tamagawa.

The manganese deposits of Kanoiri and Yokneyama mines, Ashio Mountainland, have been thermally metamorphosed to orthopyroxene-cordierite-biotite hornfels (pyroxene-hornfels facies) by later granitic bodies [WATANABE *et al,* 1970*a*]. Tephroite, rhodonite, bustamite and spessartite are principal minerals in the assemblage with minor pyroxmangite and Mn—Ca pyroxene. No rhodochrosite is left after contact metamorphism.

The manganese formations at Nyberget, Långban and Ultevis, Sweden, are of volcanogenic-sedimentary type associated with jaspilitic iron formation. All these deposits show polymetamorphic history and in the deposits at Nyberget and Långban, the latest progressive facies is equivalent to albite-epidote hornfels facies, whereas that of Ultevis is equivalent to albite-epidote hornfels facies [KOARK, 1970]. The mineral assemblages in these deposits are as follows:

Nyberget: (oxide) braunite, hematite, jacobsite; (silicate) spessartite, rhodonite, urbanite, richterite, manganophyllite, piedmontite, schefferite, and barite, calcite.

Långban: (oxide) braunite, hausmannite, manganosite; (silicate) rhodonite, schefferite, richterite, spessartite, tephroite, manganophyllite and numerous minerals with Pb, As, Sb, Be, Ba, Ti etc.

Ultevis: (oxide) braunite, hollandite, bixbyite, hematite: (silicate) spessartite, piedmontite, viridine, mica.

The Precambrian Champaner Group or rocks (including bedded manganese formations, pure and impure limestone, quartzite and pelitic rocks) in Gujarat, India, show a low grade regional metamorphism to quartz-albite-muscovite-chlorite subfacies. A small patch of these rocks, at Jothvad, has been invaded and enclosed by later porphyritic biotite-granite (Erimpura Granite) which has thermally metamorphosed the manganese formation and the country rocks to hornblende-hornfels facies grading into pyroxene-hornfels facies near the aureole. The thermally metamorphosed manganese oxide assemblage (braunite-hollandite-bixbyite-hausmannite) is sharply interbanded with manganese silicate rocks (spandite-rhodonite-bustamite-blanfordite-brown manganese pyroxene-winchite-tirodite-piedmontite-manganophyllite-alurgite). The manganese formation is characteristically devoid of rhodochrosite and tephroite indicating an original bulk composition free of manganese carbonates.

DISCUSSION

Manganese sediments, formed by chemical precipitation, may be constituted of higher oxides of manganese (with dominant Mn^{4+}), manganese hydroxides (manganite in particular) and manganese carbonate (rhodochrosite, manganocalcite etc.). Braunite is also rarely detected in unmetamorphosed volcanogenic sediments. Alabandite is practically absent in the sediments.

Primary deposition of manganese only as higher oxides and hydroxides (cryptomelane, todorokite, birnessite, 7Å and 10Å manganites etc.), generally in association with iron, has been demonstrated by recent nodular deposits in shallow water and deep sea as well as in the bog manganese ores of Sweden and Norway [LJUNGGREN, 1955]. These deposits also demonstrated that the formation of manganese carbonate and the separation of iron took place by diagenesis. STRAKHOV [1966] considered most of the ancient manganese carbonate deposits as sedimentary-diagenetic. Rhodochrosite may, however, be also directly precipitated as a primary mineral.

Metamorphism of manganese formation leads to reconstitution of minerals due to rising temperature, pressure and the effect of f_{O_2}, f_{CO_2}, etc. The initial chemical and mineralogical composition of the sediments largely controls the metamorphic mineral assemblages. In case of oxidic sediments, a progressive reduction is observed in rising temperature during metamorphism (I. A. to I. F. Table 1), giving rise to lower oxides such as bixbyite, hollandite and hausmannite. The hydroxides, groutite and manganite, are first dehydrated in rising temperature to pyrolusite and then reduced to hausmannite through bixbyite (I. C. & I. D.; Table 1).

Admixture of oxides and hydroxides of manganese and iron in the sediments convert, during metamorphism, to iron-rich bixbyite and jacobsite (and/or vredenburgite). With silica present in the sediment, the manganese oxides and hydroxides react with it during metamorphism giving rise to braunite or rhodonite depending upon the oxygen fugacity [HUEBNER, 1967]. Thus, a sediment, predominantly rich in manganese oxide and/or hydroxide, and admixed with limited iron and silica, will be reconstituted to braunite-bixbyite-hollandite-jacobsite-hausmannite-vredenburgite assemblage when subjected to high grade metamorphism (almandine-amphibolite or pyroxene-hornfels facies). The relative abundance of Mn, Fe, Si, Ba etc. in the sediments controls the presence or absence of the different phases to a great extent. In greenschist or albite-epidote hornfels facies, hausmannite, jacobsite (high-iron type) and vredenburgite are generally absent.

Where oxides and/or hydroxides of manganese are admixed with silica and argillaceous matter in high proportions, an assemblage of spessartite-rhodonite-quartz, often with manganiferous pyroxenes and amphiboles, is formed during metamorphism.* The resulting manganese silicate rocks are generally interbanded with oxidic bands (India; Otjosondu; Ultevis, Nyberget, Sweden) where metamorphic reactions where confined to the bands themselves, controlled by the original bulk composition. In some cases, mixed manganese oxide-silicate assemblages are also found (Shiromaru, Japan: Braunite-rhodonite; Muramatsu, Japan: Braunite-rhodonite; Nuramatsu, Japan: Braunite-rhodonite-piedmontite-spessartite). In these volcanogenic sedimentary (Jasperoid type) deposits of Japan, braunite formed as primary mineral in the sediment [WATANABE *et al,* 1970*a*], which perhaps was reduced to form rhodonite (IV. B., Table 1) and by reaction with admixed Ca, Al etc., gave rise to spessartite and piedmontite. Rhodonite may be oxidized to hausmannite and silica [HUEBNER, 1967] and pyroxmangite has been demonstrated [ROY, 1970] to have oxidized to rhodonite and jacobsite (VII & VII, Table 1) in manganese silicate rocks. Deposits of manganese silicate rocks without any association of metamorphic oxides (Tiere, W. Africa) may be explained by the relative paucity of manganese oxides in the original sediments.

Manganese carbonate sediments without admixture are recrystallized without change of mineral phases in low grade metamorphism. In high grade metamorphism, rhodochrosite dissociates to MnO (manganosite) and CO_2 and the manganosite is readily oxidized to hausmannite [CUTHBERT and ROWLAND, 1947; KULP *et al,* 1949]. When silica and argillaceous matter are associated with manganese carbonate sediment, an assemblage of rhodochrosite (and/or manganoan calcite) -rhodonite-pyroxmangite-tephroite-spessartite is formed during metamorphism (Minas Gerais, Brazil; Sierra Nevada, U. S. A.,; Kiuragi, Noda Tamagawa, Japan etc.). The formation of rhodonite and tephroite may be explained by the reactions shown in Table 1 (II. B. i & ii) and their formation is controled by Mn:Si ratio in the sediment. The formation of tephroite is further controlled by f_{O_2} and f_{CO_2} in rising temperature and, therefore, its formation cannot be predicted by the grade of metamorphism. Tephroite is also characteristic of silicate-carbonate assemblage only and cannot form in carbonate-free silicate rocks (India, Otjosondu, S. Ural etc.) even in high grade metamorphism as explained by ROY and PURKAIT [1968].

The metamorphosed carbonate-silicate rocks are characteristically poor in or devoid of metamorphic manganese oxides which is explained as due to absence of higher oxides in the sediments. However, hausmannite is sometimes reported from these assemblages (Minas Gerais, Smith Prospect, Buckeye, Tamworth, Noda Tamagawa etc.) which apparently formed by the dissociation of rhodochrosite. The presence of braunite at Buckeye and Noda Tamagawa may be explained either by recrystallization of sedimentary braunite in volcanogenic formation (WATANABE *et al,* 1970*b*] or by the reaction II. B. *(iii)* in Table 1 [HUEBNER, 1967] which is a rare phenomenon in natural deposits.

It may, therefore, be concluded that abundance of lower oxides in metamorphosed manganese assemblages with total absence of rhodochrosite and tephroite is an unequivocal evidence of an original carbonate-free oxidic sediment. On the other hand, the presenc eof tephroite and/or rhodochrosite, with absence or minor pre-

* Alternatively a bulk composition rich in low temperature manganese silicates (bemetite, neotocite etc.) might also give a similar assemblage on metamorphism. But this possibility demands that manganese oxides and manganese silicates were deposited as thin interbands with a sharp and alternate change of Eh and pH which is rather unlikely.

sence of lower oxides (as dissociation or reaction product of rhodochrosite), is indicative of an original carbonatic sediment. The question, however, remains whether these oxidic manganese sediments (which are also generally iron-rich) escaped diagenetic reconstitution before metamorphism and also whether the carbonatic manganese sediments (generally iron-poor) were all diagenetic products. Studies on recent manganese nodules show that iron separates out at the first stage of diagenesis followed by change of manganese oxide to manganese carbonate. But this process depends on the extent of burial, presence of organic matter, pressure of dissolved carbonate in pore waters etc. When some of these agencies fail to act, the diagenesis is not complete and if followed closely by contact or regional metamorphism, the primary sediments may be directly metamorphosed. All manganese carbonate in sedimentary manganese deposits, however, may not be diagenetic and direct precipitation of manganese as carbonate rhodochrosite, depending on Eh, pH and activity of dissolved CO_2 in the medium, is also probable [BRICKER, 1965].

REFERENCES

BETEKHTIN, A. G. [1937]: On the genessis of the Chiatura manganese deposit. In Trudy konferentsii po genezisu rud zheleza, margantsa i aluminiya. Moscow-Leningrad. IZD, An SSSR.

BOSTRÖM, K. [1967]: The problem of excess manganese in pelagic sediments. In Abelson, P. H. (ed.) Researches in Geochemistry, v. 2, p. 420—452.

BRICKER, O. [1965]: Some stability relations in the system Mn—O_2—H_2O at 25 ° and one atmosphere total pressure. Am. Mineral., *50*, p. 1296—1354.

CALVERT, S. E. & PRICE, N. B. [1970]: Composition of Mn nodules and Mn carbonates from Loch Fyne, Scotland. Contr. Min. Petr., *29*, p. 215—233.

CUTHBERT, F. L. & ROWLAND, R. A. [1947]: Differential thermal analysis of some carbonate minerals. Am. Mineral., *32*, p. 111.

CHEBOTAREV, M. V. [1960]: Geological structure of the S. Khingan manganese deposits and essential composition of its ores. Int. Geol. Rev., *2*, p. 851—866.

DAS GUPTA, D. R. [1965]: Oriented transformation of manganite during heat treatment. Min. Mag., *35*, p. 131—139.

DORR, J. V. N. II. [1970]: Iron formation and associated manganese in Brazil. In Int. Symp. „Geology and genesis of Precambrian Fe—Mn Formations"; Kiev. Preprint.

DORR, J. V. N. II., COELHO, I. S. and HOREN, A. [1956]: The manganese deposits of Minas Gerais, Brazil, 20th Int. Geol. Congr., Symp. Mang., *3*, p. 277—346.

FAULRING, G. M., ZWICKER, W. K. and FORGENG, W. D. [1960]: Thermal transformations and properties of cryptomelane, Am. Mineral., *45*, p. 946—959.

FERMOR, L. L. [1909]: The manganese ore deposits of India. Mem. Geol. Surv. Ind., *37*.

FLEISCHER, M. [1964]: Manganese oxide minerals VIII. Hollandite. In Bala-Mrishma, S. (ed.) Advancing Frontiers in Geology and Geophysics, Indian Geophysical Union, Hyderabad, India, p. 221—232.

FLEISCHER, M. & RICHMOND, W. E. [1943]: The manganese oxides: a preliminary report, Econ. Geol. *38*, p. 269—286.

HAHN, W. C. & MUAN, A. [1960]: Studies in the system Mn—O: The Mn_2O_3—Mn_3O_4 and Mn_2—O_4——MnO equilibrium. Am. J. Sci., *258*, p. 66—78.

HEWETT, D. F. [1966]: Stratified deposits of the oxides and carbonates of manganese. Econ. Geol., *61*, p. 431—461.

HEWETT, D. F., CHESTERMAN, C. W. & TREXEL, B. W. [1961]: Tephroite in California manganese deposits. Econ. Geol., *56*, p. 39—58.

HOREN, A. [1953]: The manganese mineralization at the Merid mine, Minas Gerais, Brazil, Ph D Thesis, Harvard University.

HUEBNER, J. S. [1967]: Stability relations of minerals in the system Mn—Si—C—O. Ph D Thesis, The Johns Hopkins University.

HUTTON, C. O. [1957]: Contributions to the mineralogy of New Zealand, Part IV. Trans. Roy. Sec., New Zealand, *84*, p. 791—803.

ITO, K. [1961]: Thermal transformation of bementite. Journ. Jap. Assoc. Min. Petr. Econ. Geol., *45*, p. 289—218.

KALININ, V. V. [1965]: Iron-Manganese ores of Karadzhal deposits. "Nauka" Publication, Moscow, p. 1—124.
KLINGSBERG, C. & ROY, R. [1959]: Stability and interconvertibility of phases in the system Mn—O——OH. Am. Mineral., *44*, p. 819—838.
KOARK, H. J. [1970]: Sedimentary manganese ores in the Precambrian of Sweden. In Int. Symp. "Geology and genesis of Precambrian Fe—Mn Formations: Kiev. Preprint.
KÜLP, J. L., WRIGHT, H. D. and HOLMES, R. J. [1949]: Thermal study of rhodochrosite. Am. Mineral., *34*, p. 195.
LIMA-DE-FARIA, J. C., LOYES-VIEIRA, A. [1964]: The transformation of groutite (α-MnOOH) into pyrolusite (MnO_2). Min. Mag., *33*, p. 1024—1039.
LJUNGGREN, P. [1955]: Differential thermal analysis and x-ray examination of Fe and Mn bog ores. Geol. Foren. Förhandl., *77*, p. 135—147.
LYNN, D. C. & BONATTI, E. [1965]: Mobility of manganese in diagenesis of deep sea sediments, Marine Geol., *3*, p. 457—475.
MAKSIMOV, A. A. [1960]: Types of manganese and iron-manganese deposits in Central Kazakhstan. Int. Geol. Rev., *2*, p. 508—520.
MANHEIM, F. T. [1965]: Manganese-iron accumulation in the shallow marine environment. Narragansett Marine Lab., Univ. Rhode Is., Occasional Publication, *3*, p. 217—276.
NAGELL, R. H. [1962]: Geology of the Serra de Navie manganese district, Brazil. Econ. Geol., *57*, p. 481—499.
NOVOKHATSKY, I. P. [1970]: Ferruginous-siliceous formations of Paleozoic age in Kazakhstan. In Int. Symp. "Geology and genesis of Fe—Mn Formations". Kiev. Preprint.
OKADA, K. [1959*a*]: Thermal study of some cryptomelanes: Journ. Jap. Assoc. Min. Petr. Econ. Geol., *44*, p. 23—33.
OKADA, K. [1959*b*]: Thermal study on some birnessites. Journ. Jap. Assoc. Min. Petr. Econ. Geol., v. *44*, p. 48—56.
OKADA, K. [1960]: Thermal study on some todorokites: Journ. Jap. Assoc. Min. Petr. Econ. Geol., *45*, 49—53.
PARK, C. F., DORR, J. V. N. II., GUILD, P. W. & BARBOSA, A. L. M. [1951]: Notes on manganese ores of Brazil. Econ. Geol. *46*, p. 1—22.
PAVLOVITCH, ST. [1931]: Transformation of braunite by heating. Compt. Rend., Acad. Sci. Paris, *192*, p. 1400—1402.
POUIT, G. [1964]: Les gites de manganèse Marocains encaisses dans les formations carbonates: Elements pour une synthese. Chron. Mines, p. 1—23.
PRICE, N. B. [1967]: Some geochemical observations on manganese-iron oxide nodules from different depth environments. Marine Geol., *5*, p. 531—538.
ROPER, H. [1956]: The manganese deposits at Otjosonda, South West Africa. Int. Geol. Congr. Symp. Mang., *2*, p. 115—122.
ROY, SUPRIYA [1966]: Syngenetic Manganese Formations of India, Jadavpur University, Calcutta, p. 1—219.
SEGNIT, E. R. [1962]: Manganese deposits in the neighbourhood of Tamworth, New South Wales, Proc. Aust. Inst. Min. Meta., *202*, p. 47—61.
SERVANT, J. [1956]: Les Gisements et indices de manganese de l'Afrique Occidentale Francaiso. 20th Int. Geol. Congr., Symp. Mang., *2*, p. 89—114.
SEVAST'YANOV, V. F. [1968]: Redistribution of chemical elements as a consequence of oxidation-deoxidation processes in sediments of the Mediterranian sea. Litho. & Min. Res., *4*, p. 438—443.
SOREM, R. K. [1967]: Manganese nodules: nature and significance of internal structure. Econ. Geol., *62*, p. 141—147.
SOREM, R. K. & GUNN, D. W. [1967]: Mineralogy of manganese deposits, Olympic Peninsula, Washington, Econ. Geol., *62*, p. 22—56.
STRAKHOV, N. M. [1966]: Types of manganese accumulation in present day basins: their significance in understanding manganese mineralization. Int. Geol. Rev., *8*, p. 1172—1196.
UKAI, Y., NISHIMURA & MAYEDA, T. [1956]: Mineralogical study on the manganese dioxide minerals. Mem. Coll. Sci., Univ. Kyoto, Ser. B., *23*, p. 203—322.
WATANABE, T. [1959]: The minerals of the Noda Tamagawa mine, Iwate Prefecture, Japan. Mineral. Journ., v. 2, p. 408—421.
WATANABE, T., KATO, A. & ITO, J. [1960]: The minerals of the Noda Tamagawa mine, Iwate Prefecture, Japan. II. Pyrochroite ore and its origin. Mineral. Journ., *3*, p. 30—41.
WATANABE, T., YUI, S. & KATO, A. [1970*a*]: Bedded manganese deposits in Japan. In Tatsumi, T. (ed.) Volcanism and Ore Genesis. Univ. Tokyo Press, p. 119—142.
WATANABE, T. YUI, S. & KATO, A. [1970*b*]: Metamorphosed bedded manganese deposits of the Noda Tamagawa mine, In Tatsumi, T. (ed.), Univ. Tokyo Press, p. 143—152.

WOODLAND, A. W. [1959]: The petrography and petrology of the lower Cambrian manganese ores of West Merionethshire. Quart. Journ. Geol. Soc. London, *95*, p. 1—35.
YOSHIMURA, T. [1939]: Studies on the minerals from the manganese deposit of the Kaso Mine, Japan. Journ. Fac. Sci. Hokkaido Univ., *4*, p. 313—452.
YOSHINAGA, M. [1958]: A thermodynamic study of equilibrium relations among some manganese minerals introduced during the epoch of thermal metamorphism. Min. Journ., *3*, p. 400—417.
ZVEREFF, R. [1953]: Les gisements manganesiferes de l'Oural Meridional (d'apres A. Betekhtin), Annales des Mines, 142c annee, VIII, p. 44—45.

Manuscript received, May 16, 1972.

PROFESSOR SUPRIYA ROY
Dept. of Geological Sciences
Jadavpur University
Calcutta-32, India

Acta Mineralogica-Petrographica, Szeged, XX/2, 337—362, 1972.

AN ANISIAN WETTERSTEIN LIMESTONE REEF IN NORTH HUNGARY

G. SCHOLZ

SUMMARY

In the vicinity of Aggtelek and Jósvafő in North Hungary there is a fossil reef formation with an extension of several km² belonging to the Anisian member of the Wetterstein sedimentary sequence. Surrounded by Dasycladacea-bearing sediments, the reef complex can be split up into three main facies: *1.* a central reef with colonial corals, hydrozoans and Calcispongia; *2.* a reef slope under heavy wave action with a paleobiocoenosis consisting of brachiopods, molluscs and echinoderms; *3.* a more quiet-water reef slope with echinoderms and molluscs. The growth of the 500- to 600-m-thick reef complex began in early Pelsonian time and stopped before the deposition of the Upper Illyrian-*Diplopora annulatissima* Horizon. In the Late Illyrian the entire reef was covered by dasycladaceous sediments. The paper is terminated by the descriptions of a new calcareous sponge (*Colospongia catenulata macrocatenulata* n. ssp.), a new hydrozoan (*Axopora aggtelekensis* n. sp.) and a new coral (*Protoheterastrea pseudocolumellaris* n. sp.).

INTRODUCTION

The area under consideration is situated between Aggtelek and Jósvafő villages on the southern margin of the southern limestone zone of the Gemerides *(Fig. 1)*. Constituted by shales, marls and limestone laminae, the Campilian beds are overlain by the Lower Anisian (Hydaspian) Horizon which is represented by Gutenstein limestones and dolomites. The Anisian age of the overlying Wetterstein limestone and dolomite sequence was proved by Z. SCHRÉTER [1935, p. 148] and K. BALOGH [1961, p. 370; 1964, p. 362 and Table 4] with brachiopods and Dasycladaceae belonging to the Decurtata Horizon. According to these authors, the Wetterstein facies still continues in the Ladinian Stage, a statement evidenced by finds of *Daonella lommeli* WISSMANN and *diplopora annulata* SCHAFHÄUTL from outside the area under consideration.

In the existing publications the "lagoonal" or "reef" facies with Dasycladaceae, calcareous sponges, corals, brachiopods and crinoids of the Wetterstein Formation are dealt with at large [K. BALOGH 1948, p. 920; 1950, p. 237] without their being discriminated on map. The present writer's investigations have been aimed at filling this gap and at specifying the environmental conditions by a more accurate description and delimitation of the particular facies.

I. THE FACIES OF THE WETTERSTEIN FORMATION

Overlying the Gutenstein Beds, the Middle to Upper Anisian Wetterstein sequence includes the following heteropical facies:

1. Dasycladaceous Limestones Surrounding the Reef

Taking the reverse of Walther's Faziesregel, the writer supposes the reef formation to be discussed later to have formed a body intertonguing with the dasycla-

daceous limestone facies which had originally surrounded it *(Fig. 1 and 3)*. Because of the overall tilting of the sequence, however, gradually younger members of the essentially synchronous facies are met with as one proceeds from the NE to the SW *(Fig. 2)*. Accordingly, older and younger beds of even the dasycladaceous limestones themselves can be observed on the surface.

(a) The dasycladaceous limestones of the deeper level are usually in immediate contact with the grey bituminous dolomites of the Gutenstein Formation. Along the Jósvafő road and the Csurkólápa, these dolomites grade literally into the dasycladaceous limestones.

At both localities it can be readily observed that the Gutenstein dolomites turn gradually white, thus grading into the Wetterstein dolomites, well-stratified, of saccharoidal texture. Above these follow red-mottled, dolomitic limestones overlain by 35 to 40 cm of red, compact, unfossiliferous limestone which is followed, on its turn, by light grey dasycladaceous limestones containing the following Pelsonian fossils *(Fig. 1)*:

DASYCLADALES:
Physoporella dissita (GÜMBEL) PIA (Localities 1, 4, and 33; *Plate II, Fig. 1*)
Physoporella pauciforata pauciforata (PIA) BYSTRICKÝ (Localities 2, 4, 33; *Plate II, Fig. 2*)
Diplopora hexaster PIA (Locality 2; *Plate II, Figs. 3—4*)
Oligoporella pilosa pilosa PIA (Localities 2, 4, 33; *Plate II, Fig. 5*)

FORAMINIFERA:
Ammobaculites radstadtensis KRISTAN-TOLLMANN (Locality 1 of the *Fig. 1*)
Meandrospira dinarica KOCH.-DEV. et PANTIĆ (Localities 1, 4, 33; *Plate I, Figs. 1, 3*)
Meandrospira insolita (HO) (Locality 1; *Plate I, Fig. 2*)
Endothyranella cf. *pentacamerata* SALAJ. (Locality 1; *Plate I, Fig. 6*)
Calcitornella sp. (in KOEHN-ZANINETTI) (Locality 1; *Plate I, Fig. 5*)

BRYOZOA (Locality 1)

BIVALVIA (Locality 1)

GASTROPODA (Locality 1)

The dasycladaceous limestones are locally *(Fig. 1)* interbedded with onkoidal limestone banks suggestive of local turbidities of varying intensity. The onkoids vary between a few mm and a couple of cm in diametre. Their concentric, interwoven blue-algal filaments have surrounded foraminiferal tests and rock and mollusc fragments. Their size and shape have been controlled, beside the shape and size of the object overgrown, by the duration of their growth. The onkoids of the deeper-seated onkoidal banks are small and unsorted (disordered), while the country rock is of somewhat coarser grain size *(Plate III, Fig. 2)*. The onkoids of the higher-seated banks are larger and display a bedded pattern. Those of each particular onkoidal band are of roughly the same size, though there are considerable differences in this respect between different bands *(Plate III, Fig. 1)*. The groundmass of the "bedded" onkoids is of relatively finer grain size than that of the "sterile" bands between the onkoidal bands.

The onkoidal limestone is undoubtedly the heteropical facies of the deeper-seated dasycladaceous limestone: a fact evidenced by the microfossils of Localities 5, 7 and 32 corresponding to those of the former. Let us quote the fossils:

FORAMINIFERA:
Meandrospira dinarica KOCH.-DEV. et PANTIĆ
Meandrospira insolita (HO).
Endothyranella cf. *pentacamerata* SALAJ
Calcitornella sp. (in KOEHN-ZANINETTI).

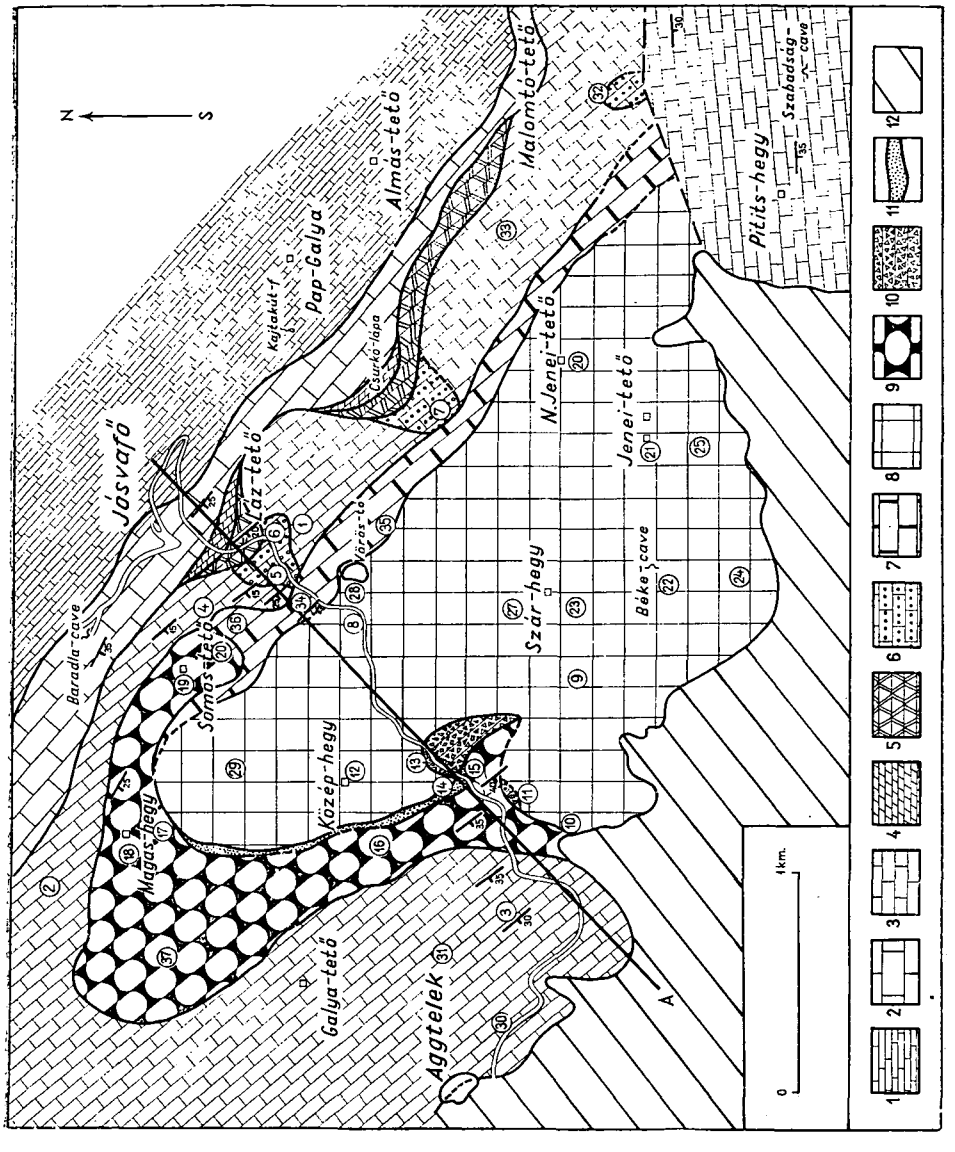

Fig. 1. Facies map of the Trias in the vicinity of Aggtelek
1. Campilian marl and limestone. *2.* Gutenstein limestone and dolomite. *3.* Dasycladaceous Wetterstein limestone. *4.* Wetterstein dolomites of saccharoidal texture. *5.* Calcareous dolomite, dolomitic limestone. *6.* Onkoidal Wetterstein limestone. *7.* Bioclastic Wetterstein limestone with echinoderms and molluscs. *8.* Unstratified limestone. *9.* Wetterstein limestone, thick-bedded, bioclastic with brachiopods and echinoderms. *10.* Red-cemented intraformational breccia. *11.* Wetterstein limestone with crinoid fragments. *12.* Pannonian gravel and sand. *13.* Profile line of Textfig. 2. *14.* Sampling points.

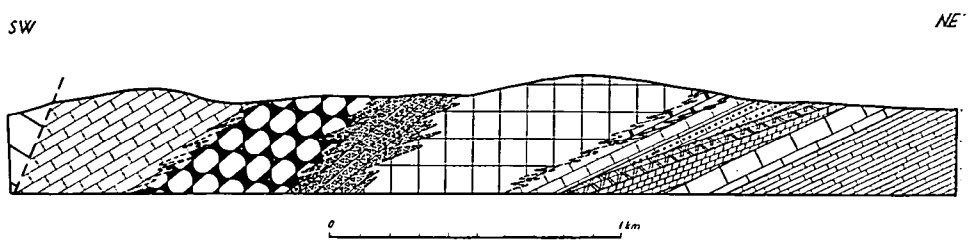

Fig. 2. Geological section of the investigated area. For explanations, see Fig. 1.

(b) Lying on the SW side of the reef complex, *the higher horizon of the dasycladaceous facies* (Localities 3, 30 and 31) has yielded the following fossils:

DASYCLADALES:
Physoporella dissita (GÜMBEL) PIA
Physoporella sp.

FORAMINIFERA:
Ammobaculites radstadtensis KRISTAN-TOLLMANN
Ammobaculites wirtzi KOEHN-ZANINETTI *(Plate I, Fig. 8)*
Trochammina almtalensis KOEHN-ZANINETTI *(Plate I, Fig. 7)*
Neoendothyra reicheli REITLINGER *(Plate I, Fig. 4)*
Earlandinita elongata SALAJ
Earlandinita oberhauseri SALAJ
Duostomina sp.

2. *Facies of the Reef Complex*

Within the reef body enclosed in the dasycladaceous limestones three main facies can be distinguished: *(a)* back-reef, *(b)* central reef, *(c)* fore-reef sediments *(Fig. 3)*. These are characterized by the following:

(a) Situated on the NE margin of the complex, the *back-reef* can be traced in 150 to 200 m width on the present-day surface. It consists of bioclastic limestones, rich crinoid and echinoid fragments, whose sorting is dependent on the turbidity of the environment of deposition. Nevertheless, the water cannot have been too agitated, as the skeletal elements, otherwise slightly rounded, are occasionally embedded without isolating from the other. Of the crinoids the ossicles of *Entrochus silesiacus* BEYRICH as well as *Encrinus* and *Dadocrinus* are recognizable (Localities 34, 35 and 36). Most of the echinoid spines are "piquants", while thin-spined forms, suggestive of a quiet-water environment occur just sporadically. Beside the above, a few fragments of larger *Naticopsis* have been observed to pattern the composition of the fauna.

The echinoderm-and-mollusc facies of the back-reef is replaced somewhere around the Somos-tető by brachiopodal limestones. Although undoubtedly older than the otherwise totally similar fore-reef facies, the brachiopodal limestones appear to be connected with this through the western and southwestern neighbourhood of the hill Magos-hegy. Therefore the description of the back-reef will be given together with that of the fore-reef.

(b) Striking NW-SE, the *central reef* exposed in a width greater than 1 km along the road is constituted by unstratified or thick-bedded limestones of somewhat darker shade. Characteristic fossils of these are calcareous sponges, colonial corals and hydrozoans which, however, do not belong to the most frequent because of having been reworked and diagenetically altered. The voids and cavities of the

original reef skeleton are filled up by fibrous calcite. Geopetal cavity-filling can be observed to be accompanied by re-sedimentation phenomena.

In part of the central reef, more massive, colonial corals (*Pinacophyllum* cf. *parallelum* FRECH, *"Thecosmilia,, subdichotoma* MÜNSTER and other representatives of *"Thecosmilia"*) are predominant (Localities 9, 10 and 11; *Plate IV, Fig. 2 and 3*). With their massive, straight polyparia, these seem to have acted as brakers protecting the more loosely packed colonies, composed of ramose and more gracious forms, of the biocoenosis of the innermost parts of the reef complex (Locality 8, *Plate IV, Fig. 1*). Although the systematic determination of these more gracious corals often happens to be impossible to carry out because of their recrystallized internal structure, it appears that among these too, again the representatives of *"Thecosmilia"* shared predominance with *Protoheterastraea pseudocolumellaris* n. sp. *(Plate V, Fig. 2; Plate VI, Fig. 15)*.

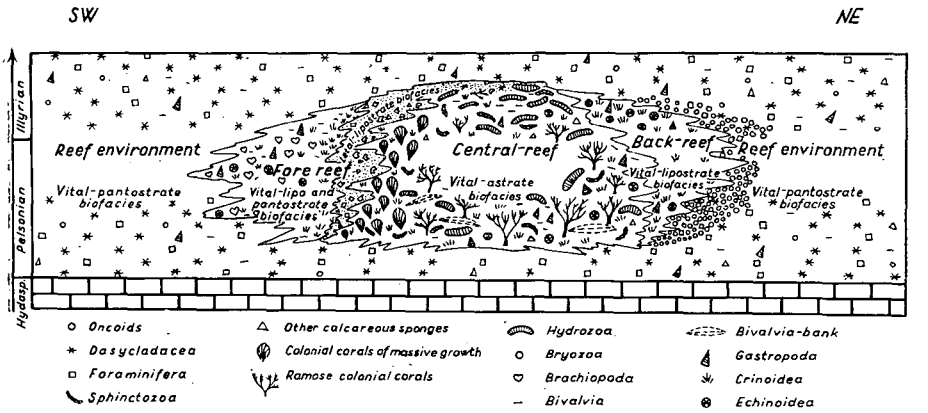

Fig. 3. Original distribution of the biofacies in the investigated area as sketched along the track of Fig. 2.

In the more protected parts of the central reef, beside the hydrozoans, e.g. *Axopora aggtelekensis* n. sp. *(Plate IV, Fig. 4; Plate V, Fig. 1—6)*, the calcareous sponges, e.g. *Colospongia catenulata* OTT *macrocatenulata* n. ssp. *(Plate VI, Fig. 1 and 14)*, *Dictyocoelia manon* MÜNSTER *(Plate VI, Fig. 14)*, *Leiospongia reticularis* MÜNSTER *(Plate VI, Fig. 13)*, *Poronidella* sp. *(Plate VI, Fig. 9)* show an overall distribution.

In the afore-mentioned reef portions (Locality 8) there are 10- to 20-cm-thick lenses constituted by lamellibranchs such as *Daonella moussoni* MERIAN *(Plate VI, Fig. 2, 3, 4)*, *Daonella böckhi* MOJSISOVICS *(Plate VI, Fig. 11)*, *Posidonia* cf. *wengensis* WISSMANN *(Plate VI, Fig. 8)*. Small-sized *Gastropoda* also occur: *Omphaloptychia* sp. *(Plate VI, Fig. 6)*, *Euomphalus* sp. *(Plate VI, Fig. 5)*, and *Worthenia* sp. The crinoids are also frequent: *Entrochus silesiacus* BEYRICH *(Plate VI, Fig. 12)*, *Encrinus* sp. *(Plate VI, Fig. 10)*, *Isocrinus* sp. and *Dadocrinus* sp.

In the northwestern, Középhegy, part of the central reef some manifestations of shallowing of the water cover of the reef can be observed. Nota bene, the resulting intensification of wave activities must have increased, as it looks, the rate of comminution and have led to a decrease of the coarse components. The organic remnants have become poorer; corals and crinoids can be encountered just sporadically;

however, the representatives of *Dasycladaceae* appear instead. The hydrozoans and sphinctozoans (e.g. *Axopora aggtelekensis* n. sp., Localities 12 and 29) have subsisted.

The central reef is traceable farther east of the road, across the hills Szárhegy and Nagy Jenei-tető up to the Ladinian limestone mass of the Pitits-hegy. In this area the exposures are less satisfactory though, yet all the above phenomena can be observed.

(c) Situated on the SW margin of the reef complex, the *fore-reef* consists of limestones similar, in both colour and detrital texture, to the limestones of the central reef. The only difference is the lack of autochtonous fossils of colony-building organisms. The intraformational limestone debris decreases in grain size with the distance away from the central reef, while the degree of sorting increases in the same direction. This fact testifies to the origin of the debris from the erosion of the central reef.

The oldest part of this facies, adjacent to the echinoderm-and-mollusc beds of the back-reef and immediately overlying the lower horizon of the dasycladaceous limestones, is the brachiopodal limestone belt extending over the crest of the hills Somos-tető and Magos-hegy and seemingly intertonguing along the dip with the central reef. The localities (Nos 17, 18, 19, 20 and 30) falling into this belt contain the following Recoaro-type fauna:

BRACHIOPODA:

Spiriferina avarica BITTNER (Localities 17, 18; *Plate VII, Fig. 10*)
Mentzelia mentzelii DUNKER (Localities 16, 17, 18, 37; *Plate VII, Fig. 4, 5*)
Coenothyris vulgaris SCHLOTHEIM (Localities 16, 17, 18, 37; *Plate VII, Fig. 2b*)
Decurtella decurtata GIRVAN (Localities 17, 18; *Plate VIII, Fig. 7*)
Boeckithyris angustaeformis (BÖCKH) (Localities 19, 20; *Plate VIII, Fig. 4b*)
Tetractinella trigonella (SCHLOTHEIM) (Localities 16, 19, 20, 37; *Plate VIII, Fig. 1a, 1c*)
"Rhynchonella attilina" BITTNER (Localities 19, 20; *Plate VIII, Fig. 5g*).

BIVALVIA:

"Ostrea" sp. (Locality 18; *Plate IX, Fig. 1*).

CRINOID ossicles (Localities 16, 19, 20, 37).

The fore-reef facies on the SW side of the central reef begins with an unsorted intraformational breccia consisting of the mixed detritus of light reef limestones and red crinoidal limestones with a grain size ranging up to the calcirudite fraction *(Plate VII, Fig. 1)*.

Adjacent to the external side of this formation suggestive of the prevalence of wave action is a narrow zone consisting almost totally of crinoid debris *(Fig. 1; Plate VII, Fig. 2)* which is followed, on its turn, by a wider zone rich in brachiopods. This is overlain farther SW by the already-mentioned higher dasycladaceous limestone horizon. The brachipodal limestone has yielded the following fauna:

BRACHIOPODA:

Mentzelia mentzeli DUNKER (Localities 15, 16; *Plate VII, Fig. 3*)
Koeveskallina koeveskalliensis (SUESS) BÖCKH (Locality 15; *Plate VII, Fig. 6*)
Spiriferina avarica BITTNER (Locality 15; *Plate VII, Fig. 7*)
Spiriferina ptychitiphila BITTNER (Locality 15; *Plate VII, Fig. 8*)
Spiriferina fragilis SCHLOTHEIM (Locality 15; *Plate VII, Fig. 9*)
Spiriferina manca BITTNER (Locality 15; *Plate VII, Fig. 11, 12, 13*)
Tetractinella trigonella (SCHLOTHEIM)(Localities 15, 16; *Plate VIII, Fig. 1b, 1d*)
Decurtella decurtata (GIRVAN) (Locality 15; *Plate VIII, Fig. 3a, 3b*)
Coenothyris vulgaris (SCHLOTHEIM) (Localities 15, 16; *Plate VIII, Fig. 2a*)
Boeckithyris angustaeformis (BÖCKH) (Locality 15; *Plate VIII, Fig. 4a, 4b, 4c, 4d, 4e*)
"Rhynchonella" attilina BITTNER (Locality 15; *Plate VIII, Fig. 5a-f, 9*)

Norella cf. *refractifrons* BITTNER (Locality 15; *Plate VIII, Fig. 6*)
"Rhynchonella" alteplecta BÖCKH (Locality 15; *Plate VIII, Fig. 8*)
Aulacothyris angusta (SCHLOTHEIM) (Locality 15; *Plate VIII, Fig. 10*).

BIVALVIA:
Pecten sp. div. (Locality 15; *Plate IX, Fig. 3, 4*)
Prospondylus sp. (Locality 15; *Plate IX, Fig. 2*)
Mytilus sp. (Locality 15; *Plate IX, Fig. 5*)
Pteria sp. (Locality 15; *Plate IX, Fig. 6*)
Daonella aff. *moussoni* MERIAN (Locality 15; *Plate IX. Fig. 10*)

GASTROPODA:
Stuorella sp. (Locality 15; *Plate IX, Fig. 7, 8*)
Temnotropis sp. (Locality 15; *Plate IX, Fig. 9*).

ECHINOIDEA:
Plate fragments of *Miocidaris* sp. (Locality 15; *Plate IX, Fig. 11*)
Echinus spines (Locality 15; *Plate X, Fig. 1—14*).

Near the reef margin the brachiopod shells occur separated into single valves and the crinoids are also frequent. As one proceeds farther away, one can observe the brachiopod valves to occur unseparated, the crinoids being replaced by echinoids. This suggests the hydrodynamic energy of the environment to have decreased. Unlike the sediments of the central reef, the interstices of the larger grains of the sediment occurring here are not filled by sparry calcite.

3. Age and Significance of the Reef Complex

As testified by the stratigraphic ranges of the fossils met with *(Fig. 4)*, the development of the reef totalling 500 to 600 m in thickness can be supposed to have

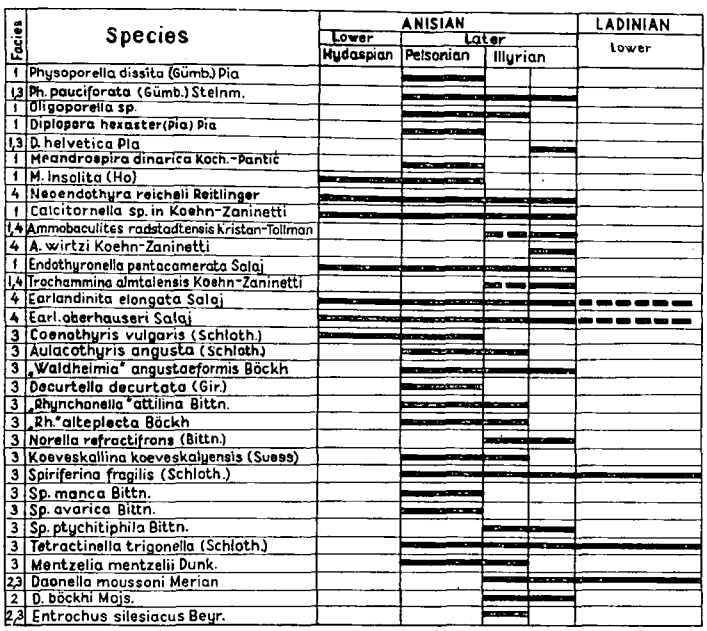

Fig. 4. Distribution within the facies and stratigraphic ranges of biochronologically evaluable species
FACIES: *1.* Dasycladaceous limestone surrounding the reef. *2.* Central reef. *3.* Formations of the reef margin. *4.* Dasycladaceous limestone overlying the reef formation.

begun in Early Pelsonian time and to have ended around the Middle Illyrian. In Late Illyrian time the entire area seems to have been covered by dasycladaceous-foraminiferal sediments preceding the *Diplopora annulatissima* Zone (see p. 340).

The Jósvafő-Aggtelek Reef Formation belongs to the open-water, offshore shelf reef facies whose recent counterparts can be met with in the Red Sea [W. SCHÄFER 1967, 1969]. At any rate, the Formation appears to be the oldest of all the Alpinotype Middle Triassic reef deposits described hitherto. According to M. SARTHEIN [1965], H. MILLER [1965] and others, the conclusions as to the occurrence in the Northern Alps of Anisian reef formations can rely merely on the presence of their debris available over a vast area, because no real reef complex has been preserved there.

II. PALEONTOLOGICAL PART

This chapter includes the descriptions of a few new fossil forms found by the author.

Sphinctozoa

Genus: Colospongia LAUBE, sensu OTT 1967

Colospongia catenulata OTT 1967 ssp. *macrocatenulata* nov. ssp.

Plate VI, *Fig. 1 and 14*

HOLOTYPUS: Plate VI, *Fig. 14.*

LOCUS TYPICUS: Locality 8, to the SW of Jósvafő *(Fig. 1).*

STRATUM TYPICUM: Wetterstein reef limestone of Pelsonian age.

DIAGNOSIS: The new subspecies corresponds to the type of the species, but the diametre of the chambers is greater than 6.8, considered to be a limiting value characteristic of the species.

DESCRIPTION: According to E. OTT [1967, p. 31], the genus *Colospongia* is poor in diagnostic features as compared to the other representatives of *Sphinctozoa.* Therefore the discrimination of its species would have to rely on the mode of growth and the size and shape of their chambers. None of the 300 chambers of *C. catenulata* measured by him did exceed 7 mm in diametre. In the Jósvafő material, however, several specimens were found which attain even 9 mm in chamber diametre, their other characteristics being the same as those of OTT's species. Therefore these forms can be regarded just as a larger subspecies of *C. catenulata.*

Hydrozoa

Ordo: Milleporina HICKSON 1901

Familia: Axoporidae BOSCHMA 1951

Genus: Axopora M. EDWARD et J. HAÎME 1850

Axopora aggtelekensis n. sp.

Plate IV, *Fig. 4*; Plate V. *Fig. 3—6*

HOLOTYPUS: Plate V, *Fig. 3, 4.*

LOCUS LYPICUS: Locality 8, SW of Jósvafő *(Fig. 1).*

STRATUM TYPICUM: Pelsonian Wetterstein reef limestone.

DIAGNOSIS: Massive, nodule-like colony with very thin, equal and closely spaced pores penetrating into the spongy coenenchyma. There are only gastropores in each of which a gracious, smooth-faced, spongy gastrostyle can be found.

DESCRIPTION: Flat, massive, nodule-like, of irregular outline, the colonies vary in size, sometimes attaining even 10 to 15 cm in thickness. The surface of the colony is dotted densely with tiny, subcircular gastropores. No dactylopores. The gastropores often attain a length of 10 to 12 mm. Their longitudinal sections are somewhat curved or slightly undulated. In the centre of each pore there is a long, thin gastrostyle. Each gastrostyle has a smooth surface, but the wall of it is of spongy structure. The distance between the boundaries of the gastrostyle and gastropore is 1.5 to 2 times the diametre of the gastrostyle. The colonies used to have a spongy, milleporoid coenenchyma which was destructed during diagenesis. Remnants of coenenchyma, if any, can sometimes be observed in the immediate vicinity of the pores only. The pores had no independent wall, therefore their outline is rather irregular in both transversal and longitudinal sections. No tabulae could be detected, but their absence may be a secondary phenomenon. The gastrostyles were preserved by the fine calcareous ooze that penetrated into them during burial. However, the spongy coenenchyma has been dissolved and replaced by fibrous calcite.

COMPARISON: Thus far only three genera of Eocene-Oligocene age, *Axopora* M. EDWARD et J. HAÎME, *Diamantopora* WEISFERMEL and *Axoporella* BOSCHMA, have been assigned to the *Axoporidae* family. The last two are represented each by the genotype only. The *Axopora* genus, however, includes 9 species.

The diagnostic features of both the species and the genera are rather differently interpreted. According to W. WEISFERMEL [1913], e.g. *Diamantopora* would be characterized by a comparatively thin, compact, shaft-shaped gastrostyle, Axopore, on its turn, by a spongy and considerably wider one. H. BOSCHMA [1951, p. 32], on the contrary, suggests that *Axopora* too had a solid gastrostyle whose thickness varied from species to species. This same author believes *Diamantopora* to be characterized by having more irregularly polygonal gastropore mouths. On the other hand, the pore openings of *Axopora* would be much more circular according to him. This, however, seems to be only the result of the preservation state, as WEISFERMEL put it very clearly [1913, p. 109], that the two specimens on which the genus *Diamantopora* was based were deficient, silicified and impregnated with iron hydroxide.

The genus *Axoporella* described by H. BOSCHMA [1954] was recovered from the Hungarian Eocene. The single species belonging here, *Axoporella kolosváryi,* differs from *Axopora* just by the fine spines ornamenting the surface of the gastrostyle, as the surface of the gastrostyle of both *Axopora* and *Diamantopora* is grooved.

However, there is much uncertainty about the discrimination of the *Axopora* species as well. According to P. M. DUNCAN [1866], the main reason for the difficulties faced in establishing specific features are due to the simplicity of structure. Although H. BOSCHMA [1951, p. 28] emphasizes the divergencies of the species within the genus in respect of the means of colony-building, the structure of coenenchyma, the size of pores and the shape of the gastrostyles, he points out at the same time the variability of what are considered to be specific features.

Nevertheless, with a view to its characteristics, the form under consideration is believed to belong certainly to the genus *Axopora*. Morphologically, it stands closest to *A. michelini* DUNCAN and *A. solanderi* (DEFRANCE). The small and rare tabulae and the longitudinal grooving of the gastrostyles are the only characteristics distinguishing *A. aggtelekensis* from *A. michelini*. Particularly striking is the ressemblance of our species to the variety of *Plate VII, Fig. 2* in P. M. DUNCAN [1866].

Accordingly, the ressemblance of *A. Aggtelekensis* to *A. solanderi* can be taken to be natural, for DOLLFUS [1906] and H. BOSCHMA [1951] consider this last-mentioned form to be identical with *A. michelini*.

By the way, the Aggtelek species is very similar to *Diamantopora lotzi* WEISFERMEL, both in habit and the thinness of the gastrostyles, as well. In addition, as shown by W. WEISFERMEL [1913, p. 110, Plate 14, Fig. 2], *D. lotzi* has only sporadical tabulae.

All in all, on account of the great difference in age as compared to the Lower Tertiary forms, *A. aggtelekensis* should be discriminated specifically.

Anthozoa

Ordo: Scleractinia BOURNE 1900

Subordo: Faviina VAUGHAN et WELLS 1943

Familia: Stilophyllidae VOLZ 1896

Genus: Protoheterastrea WELLS 1937 (pro Hexastraea VOLZ 1896, non SISMONDA 1871)

Protoheterastrea pseudocolumellaris n. sp.

HOLOTYPUS: Plate VI, *Fig. 15.*

LOCUS TYPICUS: Locality 8, SW pf Jósvafő *(Fig. 1).*

STRATUM TYPICUM: Pelsonian Wetterstein reef limestone.

DIAGNOSIS: A *Protoheterastrea* in which, unlike in the case of the two species known hitherto, the septa of the first cycle are intergrown in the centre of the calix giving birth to a pseudocolumella.

DESCRIPTION: Colony markedly ramose. The polyparia, after reaching the point of ramification, describe subparallel curves. 3 to 6 mm in diametre, they are circular or slightly elliptic in crosssection. The theka is thick, its external wall is covered by folds of varying width, there are no longitudinal ribs. Characteristically enough, 6 septa of the first cycle are strikingly well-developed and regular as compared to the subsequent ones. The septa of the second cycle are thinner and shorter; the third cycle is incomplete in most of the cases. Accordingly, the number of the septa is by one lower than in the case of the two St. Cassian species described by W. VOLZ [1896]. The upper edges of the septa are indented, their sides being horizontally grooved. VOLZ's Taschenknospung could also be observed: it is the curving of one of the septa of the first cycle combined with part of the mother calix that has produced the theka of the new individuum. The endotheka is constituted by well-developed tabulae extending from wall to wall.

COMPARISON: The new species differs from the Upper Ladinian *P. fritschi* (VOLZ) and *P. leonhardi* (VOLZ) by the fusion of the first six septa in the centre of the calix. Less frequently, the septa of the first cycle may happen not to be completely intergrown and only one of them extends up to or even beyond the middle of the calix. In the centre of the polyparium a columella-like product can be observed in both cases. As for the rest of the features, however, there is no difference between the three species.

REFERENCES

BALOGH, K. [1948]: Beiträge zur Geologie des südlichen Teiles des im weiteren Sinne genommenen Sziliceer Plateaus. — Annual report Hung. Geol. Inst. 1939—40. *2*, pp. 927—938.

BALOGH, K. [1950]: La stratigraphie du Trias dans le nord de la Hongrie. — Földt. Közlöny. *80*, pp. 231—237.

BALOGH, K. [1961]: Das Mesozoikum Nordungarns. — Annal. Inst. Geol. Publ. Hung., *49*, pp. 365—379.

BALOGH, K. [1964]: Die geologischen Bildungen des Bükk-Gebirges. — Annal. Inst. Geol. Publ. Hung., *48*, 2, pp. 557—719.
BITTNER, A. [1890]: Brachiopoden der alpinen Trias. — Abh. Geol. Reichsanst. Wien *14*, pp. 1—325.
BITTNER, A. [1902]: Brachiopoden und Lamellibranchiaten aus der Trias von Bosnien, Dalmatien und Venetien. — Jahrb. Geol. Reichsanst. Wien *52*, 3—4. pp. 495—642.
BITTNER, A. [1912]: Brachiopoden aus der Trias des Bakonyer Waldes. — Result. Wiss. Erforsch.: Balatonsees. — Palaeontol. d. Umgebung d. Balatonsees *2*, pp. 1—59.
BITTNER, A. [1912]: Lamellibranchiaten aus der Trias des Bakonyer Waldes. — Result. Wiss. Erforsch. Balatonsees. — Palaeontol. Umgebung Balatonsees *2*, pp. 1—106. Wien.
BOSCHMA, H. [1951]: Notes on Hydrocorallia. — Zool. Verh. Mus. Leiden *13*, pp. 1—49.
BOSCHMA, H. [1954]: Die Familie Axoporidae. — Verslag Kon. Ned. Akad. Wetensch. Amsterdam *63*, pp. 1—8.
BOSCHMA, H. [1956]: Milleporina and Stylasterina. — Treatise on Invertebrate Paleontology (ed.: R. C. Moore). F. Coelenterata. — Lawrance, Kansas.
BOSCHMA, H. [1963]: The generic name Axopora. — Proc. Kon. Ned. Akad. Wetensch. Amsterdam *66*, pp. [107—117.
BOSCHMA, H. [1963]: Notes on species of the genus Axopora. — Proc. Kon. Ned. Akad. Wetensch. Amsterdam *66*, pp. 118—129.
BYSTRICKÝ, J. [1955]: Beitrag zur Stratigrapie des Südslowakischen Karstes. — Geol. Práce, Zprávy *3*, pp. 52—57. Bratislava.
BYSTRICKÝ, J. [1957]: Beitrag zur Kenntnis der Diploporen der Gemeriden-Trias. — Geol. Šborník. Bratislava *8*, 2. pp. 239—241.
BYSTRICKÝ, J. [1964]: Stratigrafia a Dasycladaceae mezozoika Slovenského Krasu. — Bratislava, pp. 1—204.
CLOUD, P. N. [1952]: Facies relationships of organic reef. — Bull. Amer. Ass. Petrol. Geol., *36*, *2*, pp. 2115—2150.
DUNCAN, P. M. [1866]: A Monograph of the British Fossil Corals. — Palaeontogr. Soc. London. I.
FLÜGEL, E. [1958]: Die Hydrozoen der Trias. — Neues Jahrbuch. — Geol. Paläont. Abh. Abt. B. Stuttgart *109*, pp. 1—108.
FRECH, F. [1890—91]: Die Korallenfauna der Trias I. — Die Korallen der juvavischen Triasprovinz. — Palaeontographica. Stuttgart *37*, pp. 1—116.
FRECH, F., VOLZ, W. [1896—97]: Die Korallenfauna der Trias II. — Die Korallen der Schichten von St. Cassian in Südtirol. — Palaeontographica *43*, Stuttgart, pp. 1—124.
GAETANI, M. [1966]: Decurtella, nuovo genere triassico di Rhynchonellida. — Trias in Lombardia II. (Studi geologici e paleontologici XVI.) — Riv. Ital. Paleont., *72*, 2, pp. 343—356.
KERKMANN, K. [1966]: Über "Oolithe und Stromatolithe" und die Beteiligung von Algen und der Kalksteinbildung. — Wiss. Zeitschr. Hochsch. Architekt. Bauwesen. Weimar *13*, 3, pp. 293—302.
KERKMANN, K. [1966]: Zur Kenntnis der Riffbildungen in der Werraserie des thüringischen Zechsteins. — Mitt. Geol. Inst. Bergakad. Freiberg *181*, pp. 123—140.
KITTL, E. [1891—94]: Die Gastropoden der Schichten von St. Cassian in der südalpinen Trias. — Annalen Nat. hist. Hofmuseums Wien *6*, 2, pp. 166—262; *7*, 1, pp. 35—97; *9*, 2, pp. 143—277.
KITTL, E. [1912]: Materialien zu einer Monographie der Halobiidae und Monotidae der Trias. — Res. wiss. Erforschung Balatonsees. — Palaeontologie Umgb. Balatonsees *2*, 4, Wien, pp. 1—229.
KITTL, E. [1912]: Trias-Gastropoden des Bakonyer Waldes. Res. wiss. Erforsch. Balatonsees. — Palaeontol. Umgb. Balatonsees *2*, 5, Wien, pp. 1—54.
LOGAN, B. W., REZAK, R., GINSBURG, R. N. [1964]: Classification and environmental significance of algal Stromatolithes. — Journ. Geol., *72*, Chicago, pp. 68—83.
KRISTAN-TOLLMANN, E., TOLLMANN, A. [1967]: Crinoiden aus dem zentralalpinen Anis (Leithagebirge, Thörler Zug und Radstädter Tauern). — Wiss. Arbeit. Burgenland *36*, Eisenstadt, pp. 1—33.
MILLER, H. [1965]: Die Mitteltrias der Miemiger Berge mit Vergleichen zum westlichen Wettersteingebirge. — Verhandl. Geol. Bundesanst., Wien, pp. 187—212.
OTT, E. [1967]: Segmentierte Kalkschwämme (Sphinctozoa) aus der alpinen Mitteltrias und ihre Bedeutung als Riffbildner im Wettersteinkalk. — Abh. Bayer. Akad. Wiss. Math.-nat. w. Kl. München, N. F. *131*, pp. 5—96.
PIA, J. [1940]: Wirtelalgen (Dasycladaceen) aus den anisischen Kalken des Szilicei fennsik in Nordungarn. — Abh. min.-geol. Inst. Tisza-Univers., Debrecen, *18*, (Sonderdr. aus Tisia *4*) pp. 1—7.
PIA, J. [1942]: Übersicht über die fossilen Kalkalgen und die geologische Ergebnisse ihrer Untersuchung. — Mitt. Alpenländ. Geol. Verein. (Mitt. Geol. Ges. Wien) 33. pp. 11—34.

SARNTHEIN, M. [1965]: Sedimentologische Profilreihen aus den mitteltriadischen Karbonatgesteinen der Kalkalpen nördlich und südlich von Innsbruck. — Verhandl. Geol. Bundesanstalt Wien, *1—2*, pp. 119—162.
SCHÄFER, W. [1967]: Biofazies-Bereiche im subfossilen Korallenriff Sorso (Rotes Meer). — Senckenbergiana Lethea *48*, pp. 107—133.
SCHÄFER, W. [1969]: Sorso, Modell der Biofazies-Sequenzen im Korallenriff-Bereich des Schelfs. — Senckenbergiana Maritima (I) *50*, pp. 165—188.
SCHRÉTER, Z. [1935]: Die geologischen Verhältnisse der Umgebung von Aggtelek. — Relat. Annuae Inst. Geol. Publ. Hung. 1925—28. pp. 145—155.
SICKENBERG, O. [1932]: Eine rhätische Korallenriff aus der Osterhorngruppe. — Verh. Zool. Botan. Ges. Wien, *82*, pp. 35—40.
SIEBER, R. [1933]: Paläobiologische Untersuchungen an der Fauna der Rötewand Riffmasse in der nördlichen Osterhorngruppe. Anzeig. Österr. Akad. Wiss. Math.-nat. w. Kl. Wien, *19*, 1—3, pp. 238—240.
VINASSA DE REGNY, P. [1912]: Trias-Spongien aus dem Bakony. Res. wiss. Erforsch. Balatonsees. — Palaeont. Umgb. Balatonsees *1*, 2, Wien, pp. 1—22.
VINASSA DE REGNY, P. [1912]: Neue Schwämme, Tabulaten und Hydrozoen aus dem Bakony. — Res. wiss. Erforsch. Balatonsees. — Palaeont. Umgb. Balatonsees *1*, 3, pp. 1—17.
VINASSA DE REGNY, P. [1912]: Trias-Tabulaten, Bryozoen und Hydrozoen aus dem Bakony. — Res. wiss. Erforsch. Balatonsees. — Palaeont. Umgb. Balatonsees *1*, *4*, pp. 1—22.
VOGEL, K. [1963]: Riff, Bioherm, Biostrom. — Neues Jahrb. Geol. Pal. Monatsh., Stuttgart, *12*, pp. 680—688.
WEISFERMEL, W. [1913]: Tabulaten und Hydrozoen. — In: Böhm, J.—Weisfermel, W.: Über tertiäre Versteinerungen von den Bogenfelser Diamantfeldern. — Beitr. geol. Erforsch. Deutsch. Schutzgeb., Berlin, *5*, pp. 83—111.
ZANKL, H. [1969]: Der hohe Göll. Aufbau und Lebensbild eines Dachsteinkalk-Riffes in der Obertrias der Nördlichen Kalkalpen. — Abh. Senckenberg. Nat. f. Ges. *519*, pp. 1—96.

Manuscript received, June 10, 1972.

DR. GÁBOR SCHOLZ
Hungarian State Geological Institute
Népstadion út 14, Budapest XIV.
Hungary

PLATES I — XI

PLATE I

Fossils from the sediments of the reef environment

1. *Meandrospira dinarica* KOCH.-DEV. et PANTIĆ (× 100).
2. *Meandrospira insolita* (HO), *Endothyra* sp. (× 80).
3. *Meandrospira dinarica* KOCH.-DEV. et PANTIĆ (× 100).
4. *Neoendothyra reicheli* REITLINGER (× 70).
5. *Calcitornella* sp. (in KOEHN-ZANINETTI) (× 100).
6. *Endothyronella* cf. *pentacamerata* SALAJ (× 100).
7. *Trochammina almtalensis* KOEHN-ZANINETTI (× 100).
8. *Ammobaculites wirtzi* KOEHN-ZANINETTI (× 75).

The specimens *1, 2, 3, 5* and *6* derive from Locality 1, specimens *4, 7* and *8* from Locality 3 (see *Fig. 1*).

PLATE II

Fossils from the sediments of the reef environment.

1. *Physoporella dissita* (GÜMBEL) (× 13).
2. *Physoporella pauciforata* (GÜMBEL) (× 13).

3. *Diplopora hexaster* PIA (×12.5).
4. *Diplopora hexaster* (PIA) (×12.5).
5. *Oligoporella* sp. (×13).

Specimen *1* derives from Locality 1, the rest from Locality 2 *(Fig. 1)*.

PLATE III

The onkolite zone

1. Man-tall limestone block with "bedded" onkoids.
2. Small onkoids distributed in "non-bedded" pattern from the limestones of the basal horizon of the formation (×10).
3. Large, regular onkoid which has overgrown a *Meandrospira* (×10).
4. Onkoids (×10).

Specimens *1* and *3* derive from Locality 5, specimen *2* from Locality 6, specimen *4* from Locality 7 of *Fig. 1*.

PLATE IV

Fossils from the sediments of the central reef

1. Bush-like colony of gracious, ramose corals (×1.2).
2. Large massive colony of *"Thecosmilia"* sp. from the braker region of the reef complex. Natural size.
3. *Pinacophyllum* cf. *parallelum* FRECH from the braker region. 2/3 of the original size.
4. *Axopora aggtelekensis* n. sp. Thin section parallel to the surface of the colony (×15).

Specimens *1* and *4* derive from Locality 8, specimen *2* from Locality 9, specimen *3* from Locality 11 of *Fig. 1*.

PLATE V

Fossils from the sediments of the central reef

1. *Axopora aggtelekensis* n. sp. Surface of the colony (×1.3).
2. *Protoheterastraea pseudocolumellaris* n. sp. Natural size. Paratypoid.
3. *Axopora aggtelekensis* n. sp. Polished section. Holotype (×1.3).
4. Idem. Polished section parallel to the surface of the colony (×1.3).
5. *Axopora aggtelekensis* n. sp. Thin section perpendicular to the surface of the colony (×15).
6. One of the gastropores of specimen *5*, with a gastrostyle in the centre (×50).

All specimens derive from Locality 8 (above the Vörös-tó) of *Fig. 1*.

PLATE VI

Fossils from the sediments of the central reef

1. *Colospongia catenulata* OTT ssp. *macrocatenulata* nov. ssp. (×1.7).
2., 3., 4. *Daonella moussoni* MERIAN (×1.8).
5. cf. *Schizostoma* sp. (×2).
6. *Omphaloptychia* sp. (×3).
7. Skeletal elements of crinoids (×1.2).
8. *Posidonia* cf. *wengensis* WISSMANN (×2).
9. *Poronidella* sp. (×2).
10. Ossicles of *Encrinus*. Natural size.
11. *Daonella böckhi* MOJSISOVICS (×1.5).

12. Entrochus silesiacus BEYRICH (×1.2).
13. Corroded surface of reef limestone with specimens of *Leiospongia reticularis* MÜNSTER (×1.2).
14. Colospongia catenulata OTT ssp. *macrocatenulata* nov. ssp. and *Dictyocoelia manon* MÜNSTER (x1.8).
15. Protoheterastrea pseudocolumellaris n. sp. Holotype, longitudinal section. Natural size.

All specimens derive from the locality above the Vörös-tó (*Fig. 1,* Locality 8).

PLATE VII

Rocks and fossils from the fore-reef sediments

1. Intraformational breccia from Locality 13 of Fig. 1.
2. Massive crinoid remnants from Locality 14 of Fig. 1.
3. Mentzelia mentzelii DUNKER (1.1x). Locality 15.
4. Idem (×1.3). (Localities 17—18).
5. Idem (×1.3). (Localities 17—18).
6. Koeveskallina koeveskalyensis (SUESS) (×2). Locality 15.
7. Spiriferina avarica BITTNER (×2.1). Locality 15.
8. Spiriferina ptychitiphila BITTNER (×1.2). Locality 15.
9. Spiriferina fragilis (SCHLOTHEIM) (×2). Locality 15.
10. Spiriferina avarica BITTNER (×2.4). (Localities 17—18).
11., 12., 13. Spiriferina manca BITTNER (×2.2). Locality 15.

PLATE VIII

Fossils from the fore-reef sediments

1. a—d. Tetractinella trigonella (SCHLOTHEIM). Natural size.
2. a—b. Coenothyris vulgaris (SCHLOTHEIM) (×1.2).
3. a—b. Decurtella decurtata (GIR.) (×3). (Locality 15).
4. a—e. Boeckithyris angustaeformis BÖCKH (×1.3).
5. a—g. "Rhynchonella" attilina BITTNER (×1.6).
6. Norella cf. refractifrons BITTNER (×2.6).
7. Decurtella decurtata (GIR.) (×3). (Magashegy).
8. "Rhynchonella" alteplecta BÖCKH (×3).
9. "Rhynchonella" attilina BITTNER (×1.6) (Locality 15.).
10. Aulacothyris angusta (SCHLOTHEIM) (×2).

Specimens *1a, 4b* and *5g* derive from the Somostető (Loc. 19, 20), specimens *1c, 2b* and *8* from the Magas-hegy (Loc. 17, 18), the rest from the dolina near the Béke-cave (Locality 15).

PLATE IX

Fossils from the fore-reef sediments.

1. Ostrea sp. (×2). (Magashegy, Locality 18).
2. Prospondylus sp. (×2). (Locality 15).
3. Pecten sp. (×3). (Locality 15).
4. Pecten sp. (×4). (Locality 15).
5. Mytilus sp. (×1.6). (Locality 15).
6. Pteria sp. (×6). (Locality 15).
7., 8. Stuorella sp. (×6). (Locality 15).
9. Temnotropis sp. (×6). (Locality 15).
10. Daonella cf. *moussoni* MERIAN (×2). (Locality 15).
11. Miocidaris sp. Fragment of plate (×5). (Locality 15).

Specimen *1* derives from the Magas-hegy, the rest derive from the dolina near the Béke-cave.

PLATE X

Fossils from the fore-reef sediments

1. Echinoid spine, indented on both sides (×2.5).
2. and *3*. Idem (×2.7).
4. Flattened echinoid spine (×3).
5. Echinoid spine ("piquant") (×2).
6. Lanceolate echinoid spine (×2).
7. *Isocrinus* sp. Ossicles (×2.2).
8. Spine of an echinoid carrying acute spines on both sides (×1.2).
9. and *10*. *Miocidaris* sp. Fragment of plate (×5).
11. Echinoid spine of bullet shape (×2).
12. *Tetractinella trigonella* (SCHLOTH.) and ossicle of *Encrinus* sp. (×1.5).
13. Festooned echinoid spine (×3).
14. Ossicles of *Encrinus* sp. (×1.3).

All fossils derive from the doline near the Béke-cave (Locality 15 of the geological map of *Fig. 1*).

PLATE XI

Thin sections from the sediments of the reef complex

1. Cavernous reef limestone with fibrous, void-filling calcite. Central reef, Vörös-tó. (×10).
2. Thin section of a typical reef limestone similar to the former. Central reef, entrance to Béke-cave (×10).
3. Bioclastic, compact sediment of the fore-reef. Locality near the Béke-cave (×10).
4. Cross section of a brachiopod shell figuring as a sedimentary trap and of an echinoid spine in the limestone of the fore-reef. Locality near the Béke-cave (×10).

Sample *1* derives from Locality 8, sample *2* from Locality 21, samples *3* and *4* from Locality 15 of *Fig. 1*.

1

2

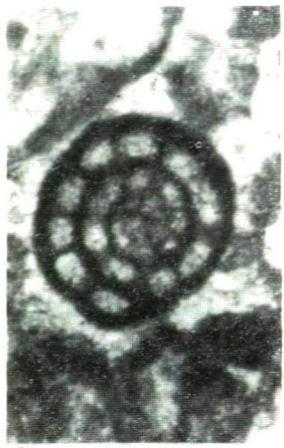

3

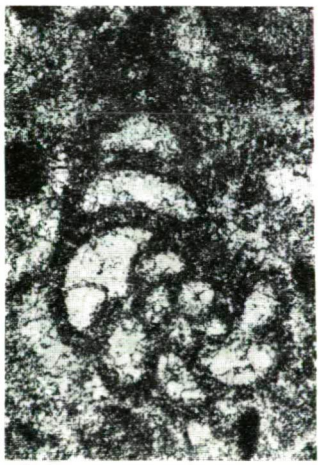

4

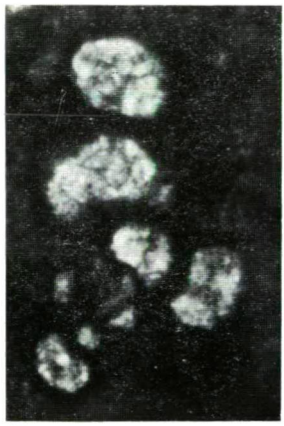

5

6

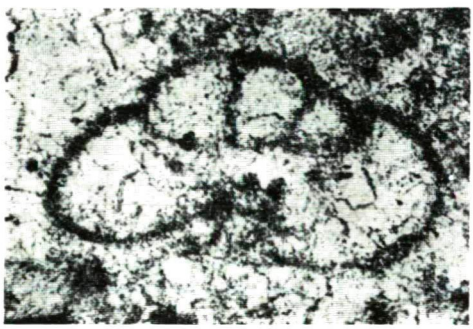

7

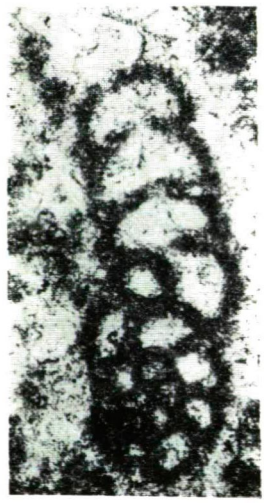

8

1

2

3

4

5

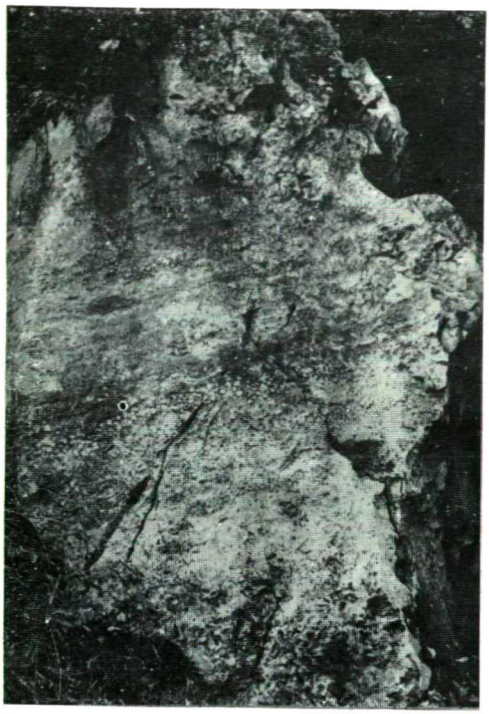

1

2

3

4

1

2

3

4

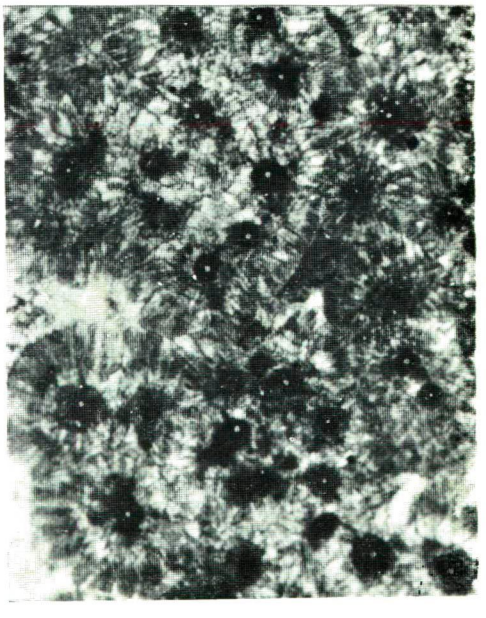

1

2

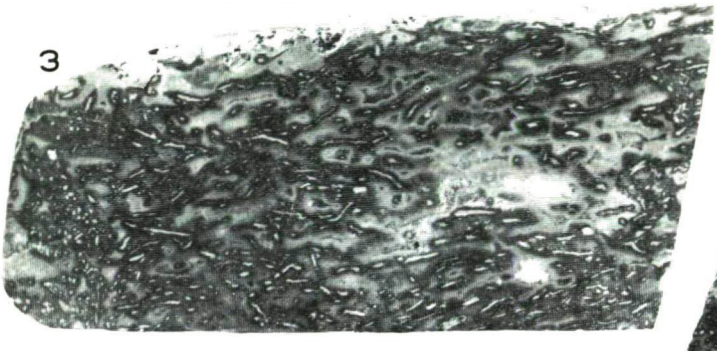

3

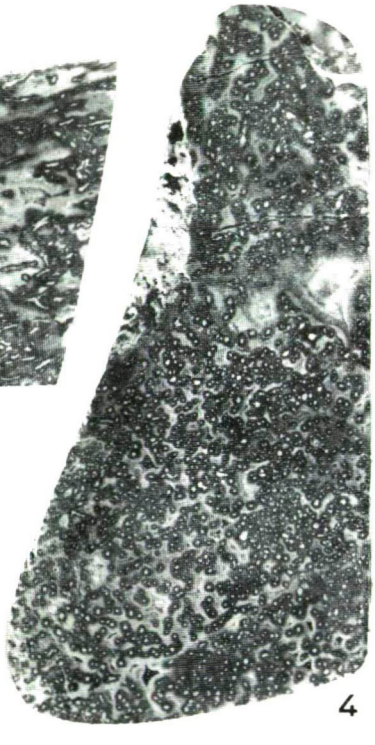

4

5

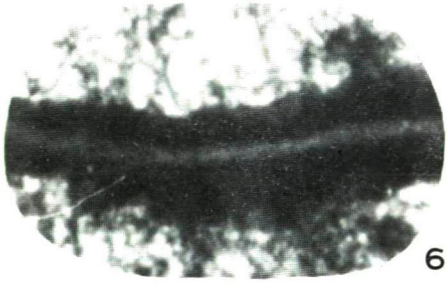

6

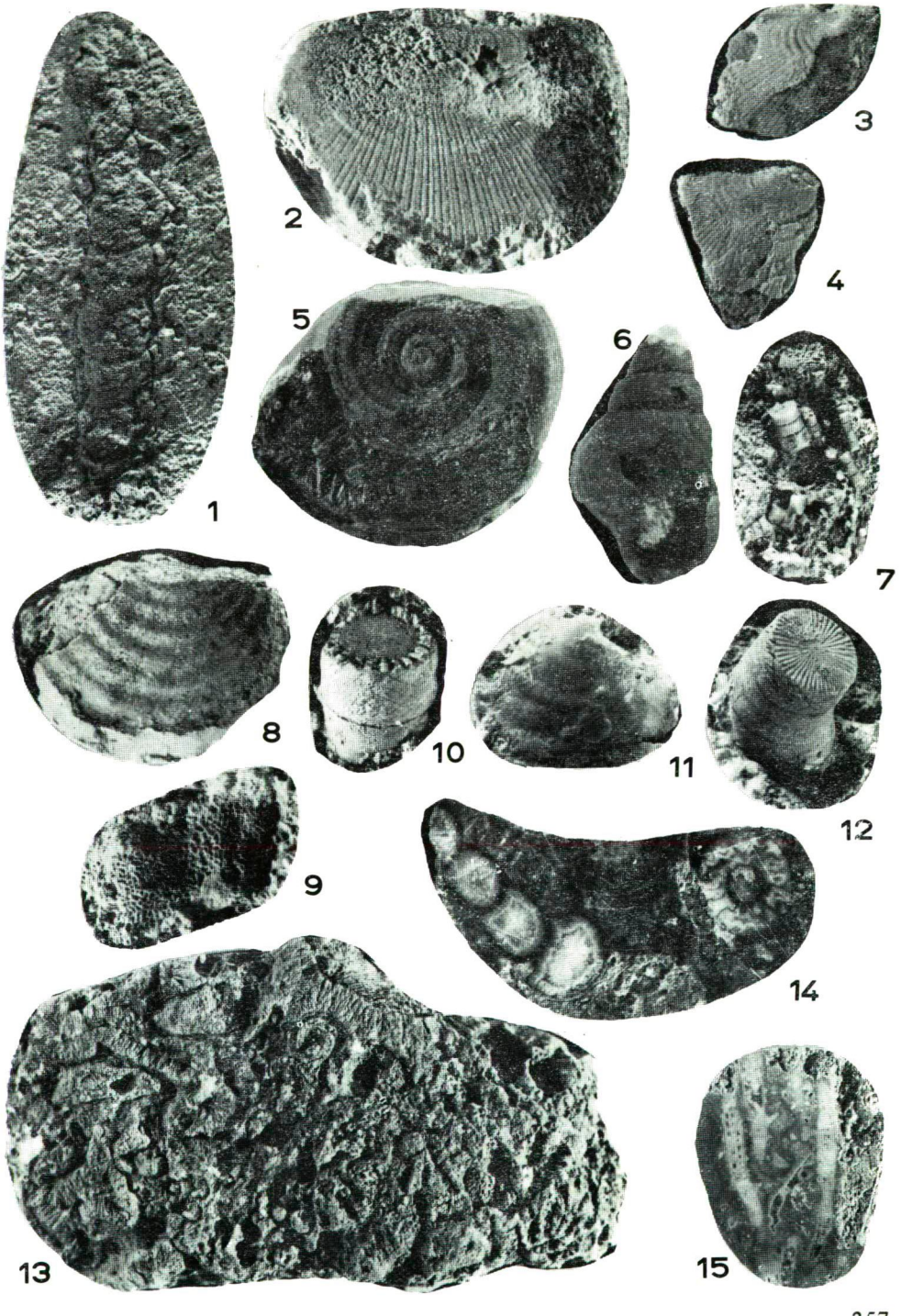
1
2
3
4
5
6
7
8
9
10
11
12
13
14
15

1

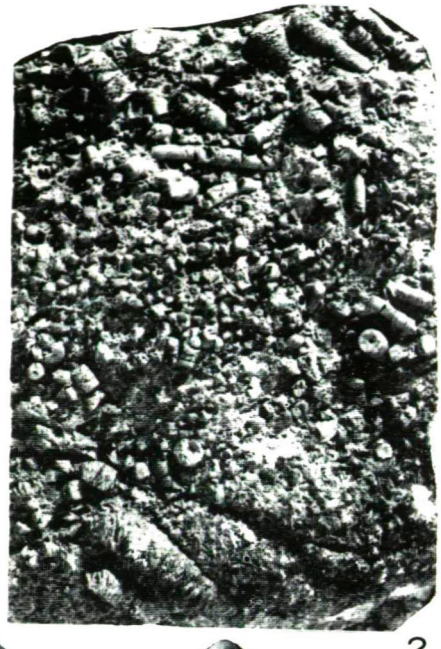

2

3

4

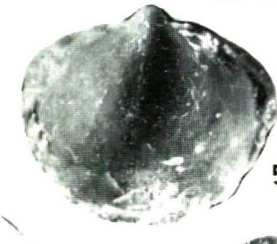

5

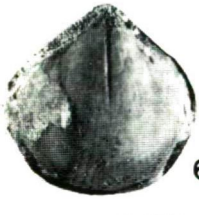

6

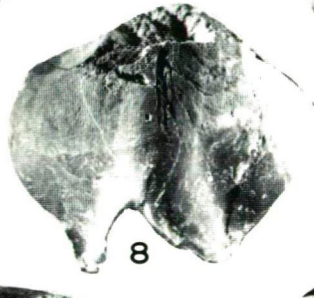

8

7

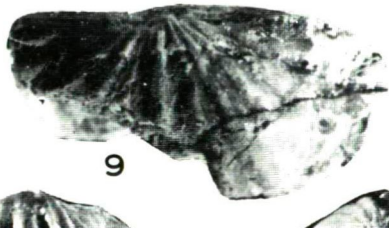

9

10

11

12

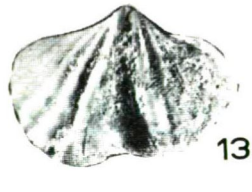

13

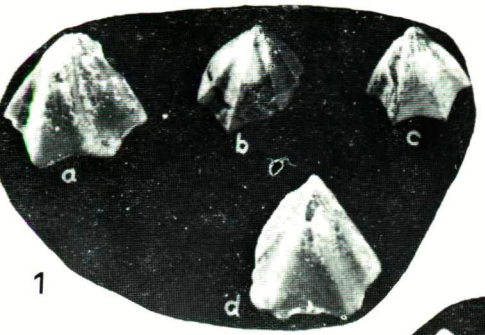

1

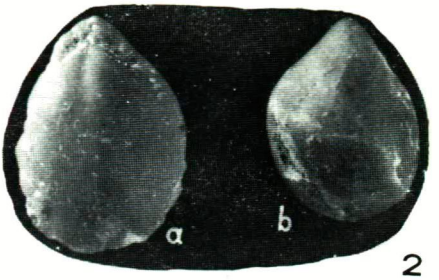

2

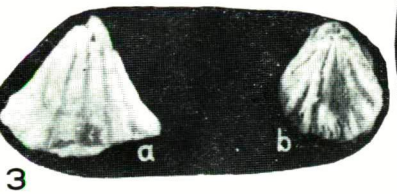

3

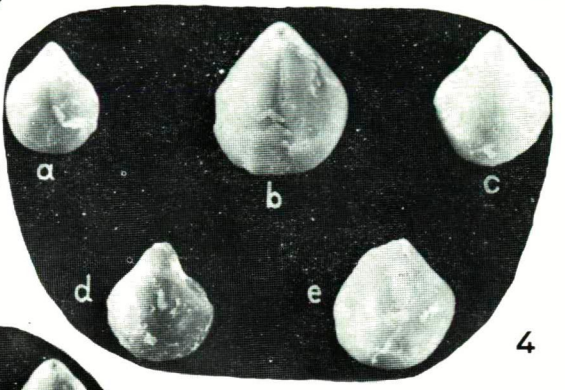

4

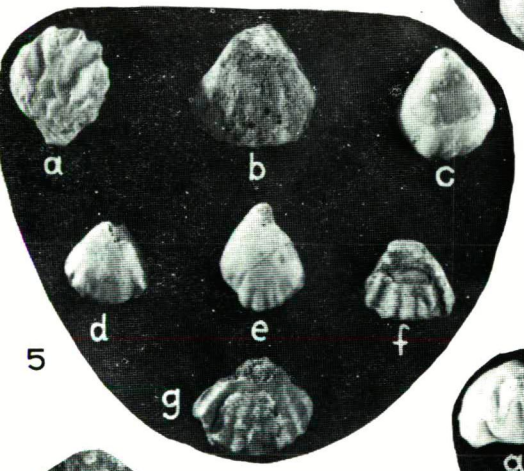

5

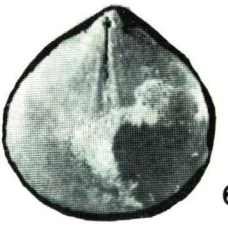

6

7

8

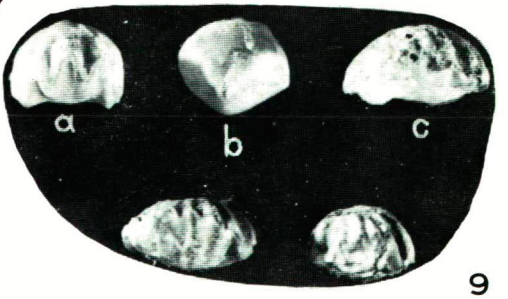

9

10


1
2
3
4
5
6
7
8
9
10
11
12
13
14

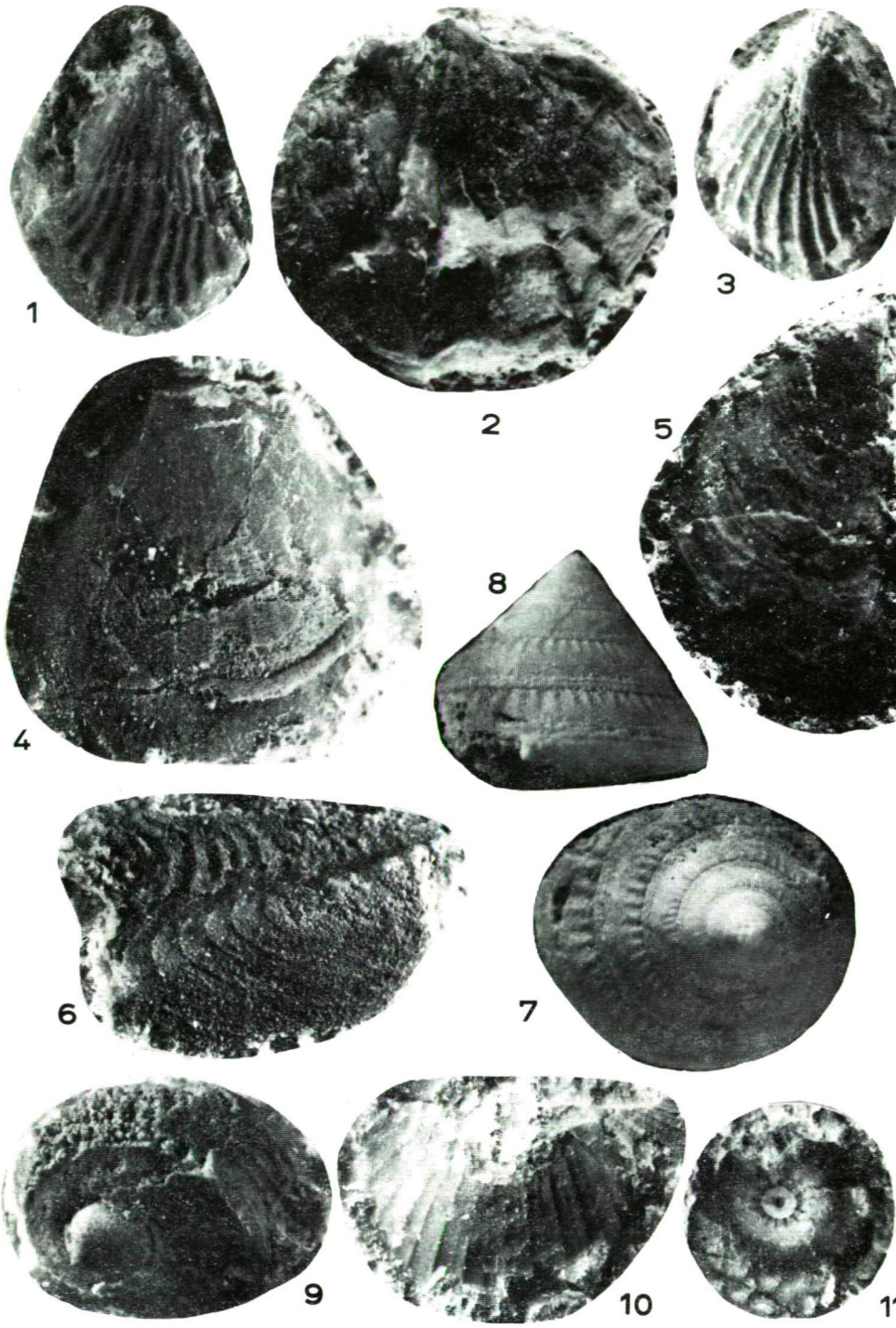
1
2
3
4
5
6
7
8
9
10
11

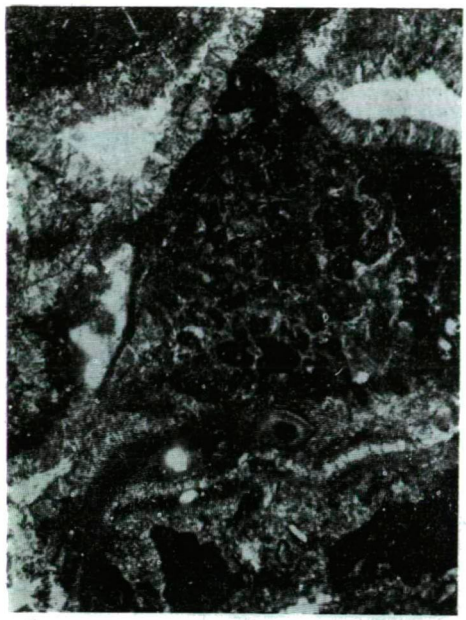

1

2

3

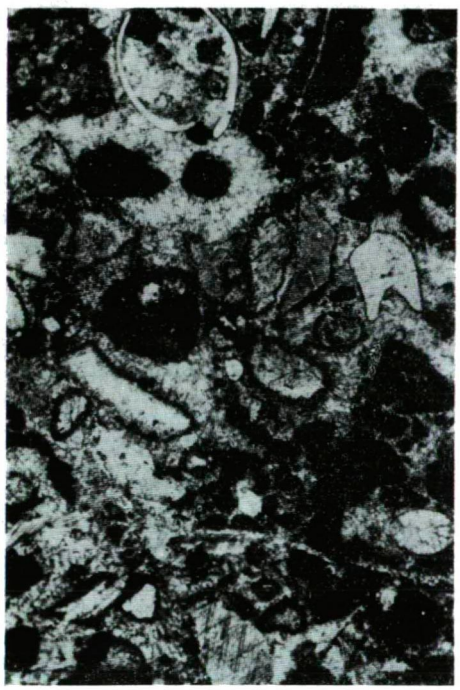

4

Acta Mineralogica-Petrographica, Szeged, XX/2, 363—381, 1972.

GEOCHEMICAL STUDIES ON THE FORMATION OF IRON-MANGANESE NODULES AND CRUSTS IN RECENT BASINS
I. ENINGI-LAMPI LAKE, CENTRAL KARELIA

IGOR M. VARENTSOV

ABSTRACT. The processes of formation of iron-manganese nodules and crusts have been studied on an example of the Eningi-Lampi lake, Central Karelia, where the relationships between the source of the ore, sedimentary materials and areas of their accumulation prove relatively simple and apparent. Nodules and crusts are composed mostly by birnessite, amorphous hydrous ferric oxides and hydro-goethite. They occur, as a rule, on the surface of relatively coarse-grained sediments, at the ground-water interface. Considerably in a lesser extent are found the nodules in the upper part (0—5 cm) of the red-brown flooded watery mud covering dark-green, black muds. The nucleus of nodules, or the basis of crusts of iron-manganese hydroxides are various, frequently altered, fragments of rocks, sometimes pieces of wood. Distribution of Mn and Fe in sediments and waters of the lake is considered. It is shown that $\frac{Mn}{Fe}$ ratio considerably decreases in waters, sediments and nodules of the lake with the moving off the source. The main role in the process of formation of iron-manganese nodules belongs to the selective chemosorption interaction (with autocatalytic oxidation) of component-bearing solutions with active surfaces.

INTRODUCTION

The less studied is a certain geological event, the more numerous are points of view on its genetic essence. This is true relative to the problem of formation of sedimentary iron and manganese ores.

The study of the ore formation processes in recent basins has some advantages over investigations of ore formation of the geological past. This concerns the possibility of carrying out direct observations, establishing the main geochemical characteristics controling the ore-forming processes, the relative evidence of interrelation between environmental elements of the basin. In this respect many lakes are characterized by the simplicity of relationships between the sources of ore components and areas of their accumulation, as compared to the mediterranean seas and larger basins.

The formation of iron-manganese ores in the lakes of Central Karelia is rather extensive. However, among many ore-bearing lakes of this region the Eningi-Lampi lake is characterized both by a pronounced manifestation of these processes, and rather simple relationships between the source of the ore, sedimentary material and areas of their accumulation. Such simple and evident relationships between the principal environmental elements of the basin, the possibility of carrying direct observations on the mode of occurrence, ores, sediments, measuring of pH, Eh in waters, muds, the collecting of the necessary ore samples, allow to regard the Eningi-Lampi lake as a certain model of ore-formation in similar basins. The consideration of the specific features of the iron-manganese ore-genesis in other basins, permits to use the materials that serve as a basis of this particular model, for establishing a general model of sedimentary Fe-Mn ore formation.

The principal task of this paper is an attempt to present some fundamental data that characterize geochemical peculiarities of the process of iron-manganese ores formation in the Eningi-Lampi lake, Central Karelia.

GENERAL CHARACTERISTICS

The Eningi-Lampi lake is a relatively narrow (1.0—1.7 km) basin extending over 7 km towards SSE-NNW. The maximum depth of the lake does not exceed 6 m. The Porusta river falling into the lake from the South-South-East is the main feeding artery, its waters being discharged into the Southern depression of the lake *(fig. 1—3)*. In the north-west part the waters of the Eningi-Lampi lake fall via a small channel into the Seletskoe lake, the latter in its turn, is connected with one of the greatest lakes of Karelia, i.e. Seg-Ozero-Lake *(fig. 1—2)*. The tributaries of the Eningi-Lampi lake drain the areas composed of Lower Proterozoic metavolcanites of the basic composition that also make up the bedrocks of the banks and numerous islands of the lake.

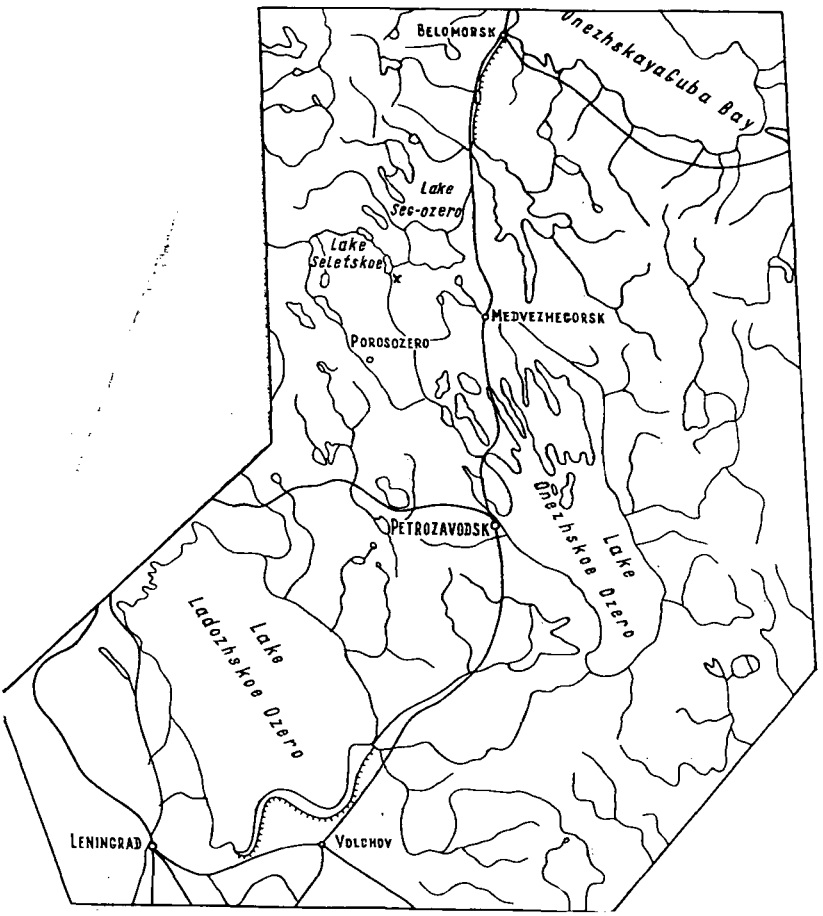

Fig. 1. Index map of the lakes of Central Karelia. x-Region of the Lake Eningi-Lampi.

Mineralization and ionic composition of waters, the Lake Eningi-Lampi (see fig. 2) TABLE 1

Analyst: M. I. STEPANETS

№	№ Station	Depth (m)	Date of sampling (1967)	Sample №	Measurement at the sampling		CONTENT p.p.m										CONTENT mg/equ								
					pH	Eh	Dry res.*)	Dry res.**)	Ca^{++}	Mg^{++}	Na^{+}	K^{+}	HCO_3^-	Cl^-	SO_4^-	ion sum.	Ca^{++}	Mg^{++}	Na^{+}	K^{+}	cat. sum	HCO_3^-	Cl^-	SO_4^-	anion sum.
1.	—	0,0	28/7	101	5,90	+490	56,00	36,00	3,60	3,28	0,73	0,40	21,96	0,74	2,88	33,59	0,18	0,27	0,03	0,01	0,49	0,36	0,02	0,06	0,44
2.	—	0,0	29/7	105	4,45	+440	68,00	44,00	5,40	2,19	1,09	0,72	29,28	0,74	0,96	40,38	0,27	0,18	0,05	0,02	0,52	0,48	0,02	0,02	0,52
3.	2a	0,0	31/7	122	7,25	+510	48,00	32,00	2,80	3,89	0,73	0,40	21,96	1,17	1,92	32,87	0,14	0,32	0,03	0,01	0,50	0,36	0,03	0,04	0,43
4.	2b	2,70	31/7	131	6,75	+510	48,00	32,00	3,60	2,19	0,86	0,41	21,96	1,10	0,96	31,07	0,18	0,18	0,04	0,01	0,41	0,36	0,03	0,02	0,41
5.	2g	1,50	1/8	139	7,10	+440	44,00	24,00	2,80	1,70	0,73	0,40	14,65	0,35	3,35	23,98	0,14	0,14	0,03	0,01	0,32	0,24	0,01	0,07	0,32
6.	2s	3,80	1/8	147	6,80	+405	60,00	28,00	1,80	2,80	0,73	0,40	19,76	0,21	1,44	27,14	0,09	0,23	0,03	0,01	0,36	0,32	0,01	0,03	0,36

1. The sample No. 101, Porusta-River, 1,5 km upstream the mouth of the river.

2. The sample No. 105. Truckling out of ground waters near the bank ledge of the lake's bay, to south-east from the cape Shuavan-Degi. The area of trickling out 10×5 m, the sand is stained by reddish-brown and black Fe—Mn hydroxides, on the water one can distinctly see the black films of Mn hydroxides. Near the area of trickling out the lake's water pH 6.000.

3. The sample No. 122, Porusta River, 20 m upstream the mouth.

4. The sample No. 131. The middle of the mouth part of the Porusta River, bottom water.

5. The sample No. 139. Estuary of Porusta-River, bottom water.

6. The sample No. 147. Centre of the Southern part of the lake, bottom water.

*) Dry residue, not ignited.

**) Dry residue, ignited.

A noteworthy feature of the cliffs, accumulations of rocks and boulders is the black crust of manganese, and to a lesser extent ferric hydroxides, that cover their surface above the water line. Such growths of Mn- and Fe- hydroxides on the surface of the rocks are frequently characterized by a lineation that seemed to correspond to the higher water levels; similar coatings of Mn and Fe hydroxides have been observed below the water-level.

GEOCHEMICAL CHARACTERISTICS OF THE LAKE WATER

The waters of the Eningi-Lampi lake are brown coloured due to the presence o dissolved humic substances and suspended organic material. Their mineralization varies from 23.98 to 40.38 mg/l; among anions predominant are HCO_3^{-1} (14.65—

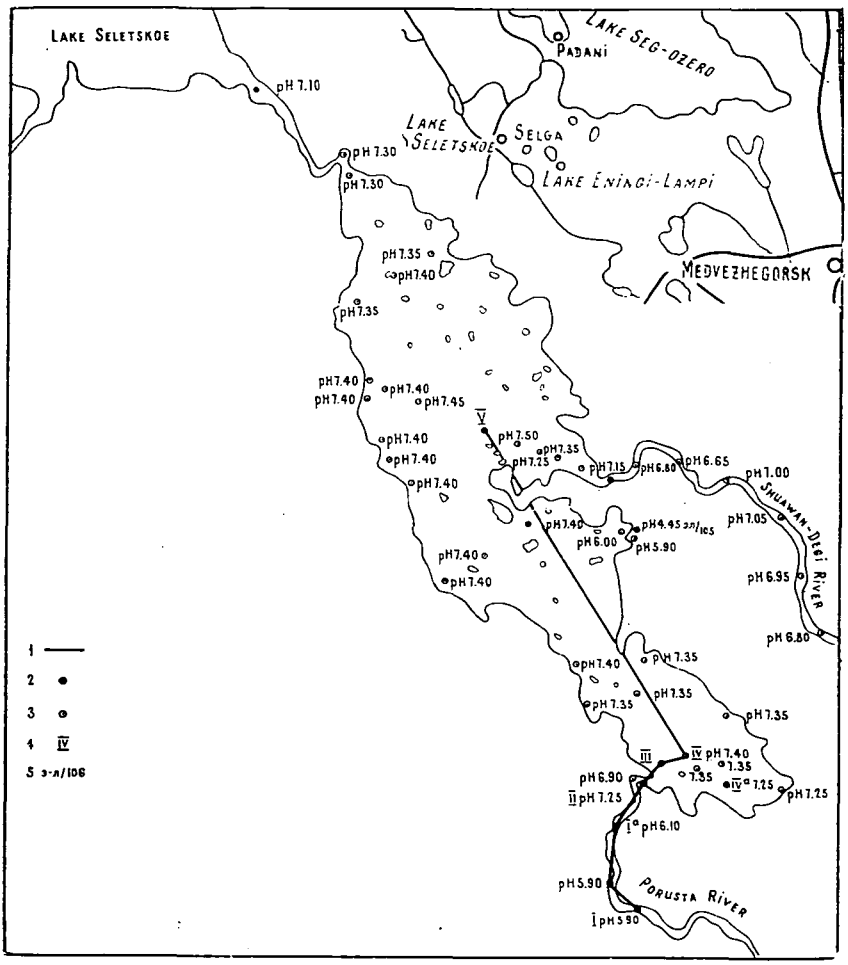

Fig. 2. The schematic map of stations where collected water-samples, measured pH, Eh, the Lake Eningi-Lampi. *1.* The line of geochemical section. *2.* The stations of water sampling, characterized by chemical analysis. *3.* The stations where pH, Eh were measured. *4.* Index on geochemical section and on the schematic map. *5.* Sample number. Note: the pH values shown on the schematic map for surface water.

29.28 ppm), among cations — Ca^{++} (1.80—3.60 ppm); Mg^{++} (1,70—3.89 ppm), the organic matter content reaching 32.86 ppm. In Table 1—2 *(fig. 2)* the pH, Eh values for the surface and bottom waters are given. Worth attention is the increasing of the pH values from the main tributary of the lake — the Porusta river (5.90). At the mouth of this river pH of the surface water increases up to 7.25, this value is typical to the surface waters of the southern depression, whereas in the northern depression pH increases up to 7.45 (see *fig.* 2).

Manganese and iron in the lake waters. The determination of the total Mn- and Fe contents was carried out by M. I. STEPANETS in the chemical laboratory of the Geological Institute of the USSR Academy of Sciences by colorimetric methods. The samples were fixed by adding 25% H_2SO_4 for obtaining pH less than 2. Before an analysis the samples had been treated with an acid for obtaining the reliable total contents. Just on the spot of sampling the study of relationships between a suspended and dissolved Mn and Fe forms was carried out. The analysis of the filtrate that passed through a membrane filter with pores size — 0,5μ, and that of the suspension on the filter show that 92% of Mn and 48% Fe of the total contents respectively were present in a dissolved form. Table 2 presents the total contents of Mn and Fe in the water of the lake according to the main profile *(fig. 2)*. The higher Mn and Fe contents were observed in the tributaries of the lake; they can be correlated, as a rule, to the lower pH values of the water. Thus, in the Porusta river there have been observed relatively high Mn and Fe contents that were considerably decreasing towards its mouth estuary (mg/l) for Mn: 871 → 110 → 68 → 48, for Fe: 420 → 400 → 300 → 200, the pH values increasing from 5.90 to 7.10. Differences in the rate of decreasing of Mn and Fe concentrations in this part of the Porusta river have been reflected in the $\frac{Mn}{Fe}$ values ($n \times 100$): 216.88 → 27.25 → 22.66 → 24.00. These data show that on the given part of the Porusta river a noticeable separation of Mn and Fe takes place, a considerable part of Mn is released from solution and not supplied into the lake.

The difference between the Mn and Fe contents in the surface water of the southern and northern parts of the lake is insignificant. In the centre of the northern basin the Mn and Fe contents (ppb) in the surface water are 35 and 200 respectively. Despite a small depth of the lake and possible wind mixing, the bottom waters still differ considerably in higher Mn and Fe concentrations, as well as in lower pH values, as compared to the surface waters (see Table 2).

SEDIMENTS

A relatively wide range of sediments is being accumulated in the Eningi-Lampi lake, from boulder-pebble to silt-clay sapropel-like muds. Each type is characterized by a certain localization, clear specific character of the chemical composition *(fig. 3.)*. In general, terrigenous components of the sediments of the lake are products of destruction, mostly of the Lower Proterozoic volcanogenic series of the basic composition that underwent a greenstone alteration. It means that the clastic sediments of the lake have a distinct greywacke composition: quartz, irregularly angular grains (up to 75%), feldspars, mostly plagioclases of the series albite-labradorite (up to 15%) fragments of siliceous rocks, hornfels (up to 20%), fragments of chloritic, epidotitic, biotite schists, amphibolites, gneisses and other rocks — up to 40%. The coarse-clastic varieties are, as a rule, considerably enriched in fragments of rocks, whereas fine-grained sediments — in mineral components: quartz, feldspars, dark-coloured minerals.

TABLE 2

*Content of iron and manganese in water of the Lake Eningi-Lampi, Central Karelia**)

№	Station №	Sample №	Index on the scheme**)	pH	Eh (mv)	Depth (m)	Content (ppm)		Mn/Fe ($n \cdot 10^2$)	Notes
							Mn	Fe		
1.	—	101[a]	I	5,90	+490	0,0	871	420	206,88	
2.	—	101	I[a]	5,90	+490	0,0	110	400	27,25	
3.	2[a]	122	II	7,25	+510	0,0	68	300	22,66	
4.	2[a]	124	II	6,75	+440	2,70	80	300	26,66	Bottom water
5.	2[g]	139	III	7,10	—	0,0	48	200	24,00	
6.	2[e]	142	IV	7,40	+540	0,0	39	150	26,00	
7.	2[e]	143	IV	7,20	+440	2,40	51	200	25,50	
8.	1[d]	111	V	7,45	+510	0,0	35	200	17,50	
9.	2[b]	131	—	6,76	+510	2,70	70	300	23,33	Middle of the mouth, Porusta River (bottom water)
10.	2[s]	147	—	6,80	+405	3,80	51	250	20,40	Centre of Southern part of the lake (bottom water)
11.	—	105	—	4,45	+440	—	95	7000	1,36	Trickling out of ground waters
12.	—	106	—	6,90	+582	0,0	99	900	11,00	Shuavan-Degi River, 200 m upstream the mouth

*) *Analyst:* M. I. STEPANETS, Geol. Inst. Ac. Sci. USSR, the samples were collected 29 July to August 1, 1967 Determinations of Mn, Fe were performed by colorimetric methods.

**) *See fig. 2.*

Boulder-pebbly, gravelly deposits, coarse- and middle-grained sands are accumulated predominantly in the channel of the Porusta river as a narrow (50—100 m) band that is framing the shores of the lake *(fig. 3)*. Their composition reflects mineralogy, petrography of the basic metavolcanites composing the drainage areas. If to exclude iron-manganese nodules and crusts developed in these areas, the amounts of the concerned components in coarse- and middle grained sands are as following (weight %, in brackets — mean): Fe: 1,91—11.49 (5.79); Mn: 0.03—1.41 (0.44); P: 0.004—0.22 (0.058); CO_2: nil — 0.08 (0.06); C_{org}: 0.64—2.16 (1.40).

Fine-grained sands — coarse-grained silts are an intermediate type of a sediment developed between the areas of more coarse-grained varieties and prevailing in the lake of silt-clayey, sapropel-like muds. They are stretching as a relatively narrow (20—100 m) band that separates these sediments *(fig. 3.)*. They are characterized by the following contents of the components concerned: Fe: 3.25—6.66 (4.95); Mn: 0.07—0.16 (0.11); P: 0.06—0.10 (0.08); CO_2: 0.08—0.36 (0.21); C_{org}: 5.50—6.24 (5.84).

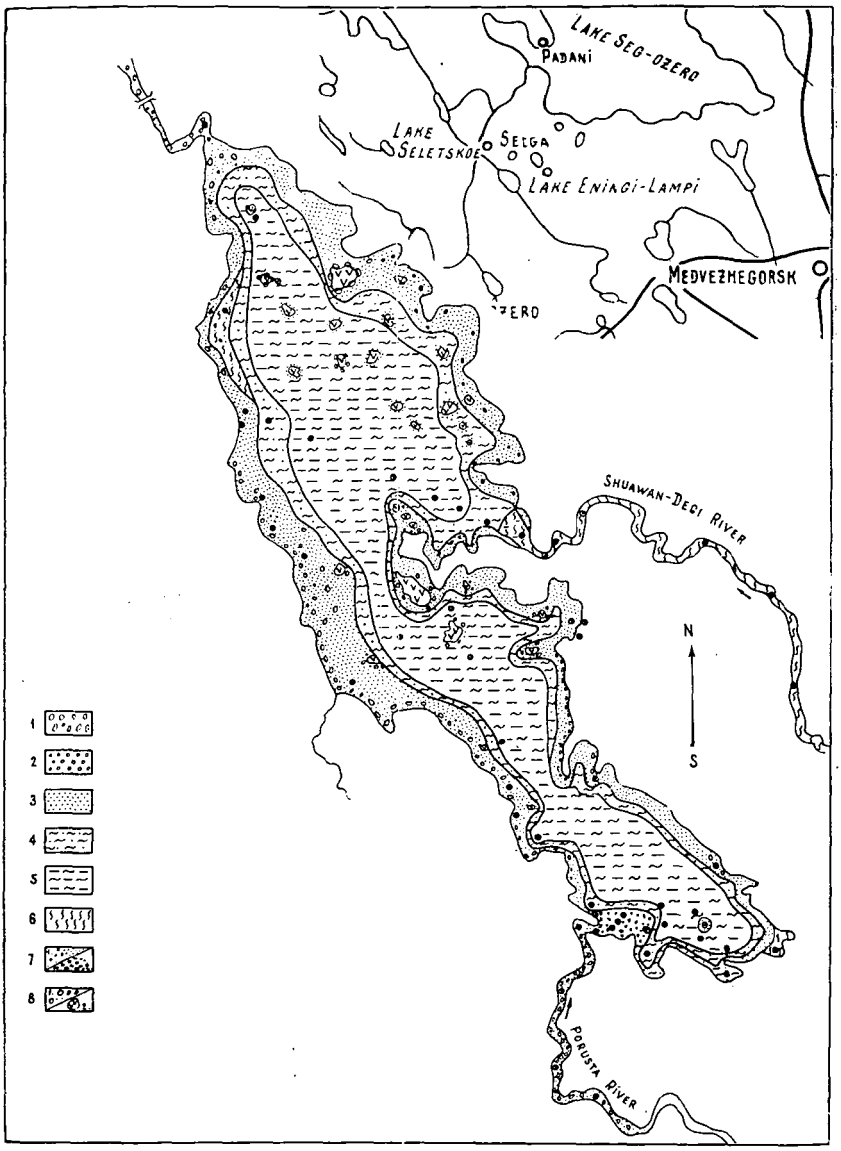

Fig. 3. Schematic map of sediments (Depth: 0,0—10 cm), the Lake Eningi-Lampi. Sediments: *1.* Boulders-pebbles, predominance of basic palaeovolcanites, quarzites, gneisses, granulites, altered arkoses. *2.* Gravel (see the composition above) greywackes. *3.* Greywacke sands coarse-medium-grained. *4.* Greywacke fine-grained sands coarse-grained silts. *5.* Fine-grained silty-clayey muds with considerable admixture of fine plant detritus, sapropel-like organic matter (the muds greenish-grey, dark, often with reddish-brown watery muds). *6.* Peat-like sediments, presented by plant detritus accumulations. *7.* 1) The nodules of Mn, Fe hydroxides. 2) Crust-like agregates of the nodules of Mn, Fe hydroxides. *8.* Coatings, crusts of Mn, Fe hydroxides 1) around sandy-pebbly fragments; 2) around blocks, boulders, outcrops of country rocks near the water level of the lake. Note: the circle with point — the stations where collected the samples of sediments, water, measured pH, Eh.

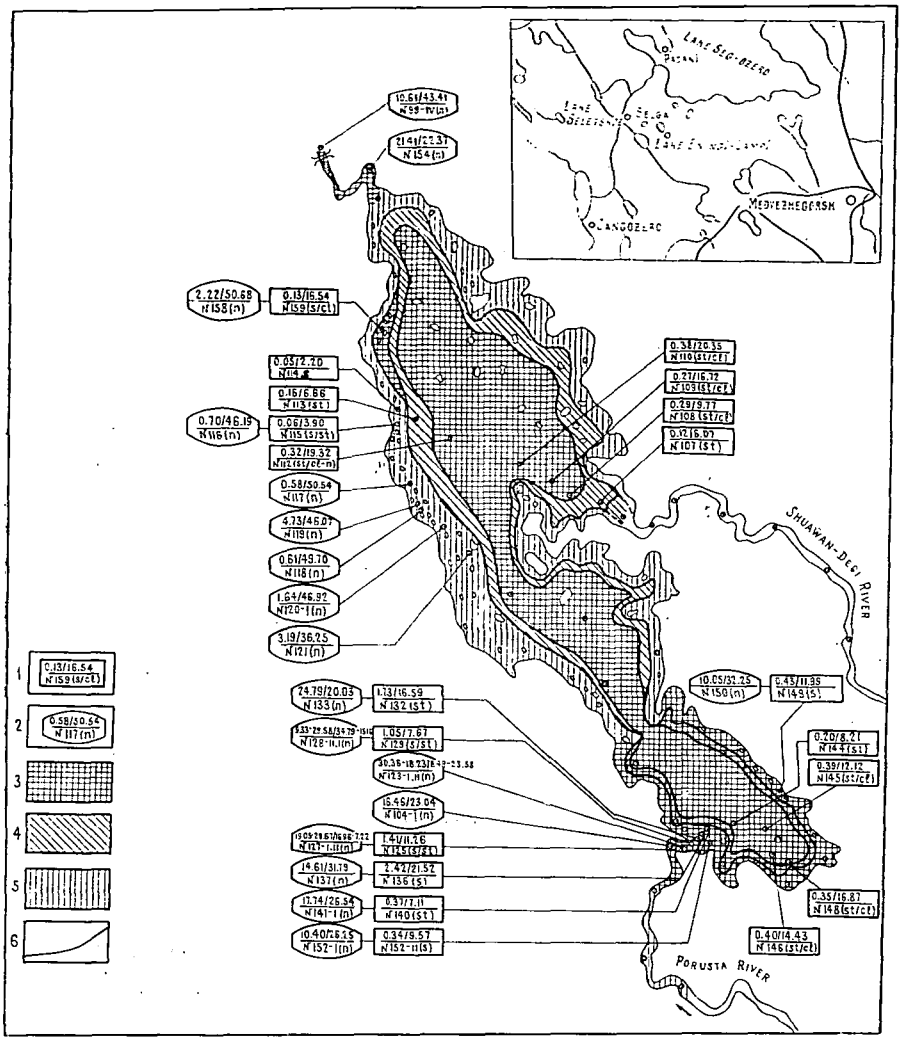

Fig. 4. Schematic map of Fe (wt.%) distribution in sediments (Depth 0,0—10,0 cm), Lake Eningi-Lampi. *1.* Stations where samples of sediments recovered. *2.* Stations where samples of nodules and crusts of Mn, Fe hydroxides recovered. Above the line, numerator — Mn content, denominator — Fe content (wt.%). Under the line — the number of sample, type of sediment: *S* — sand, *St* — silt; *s/cl* — silty clay, *n* — nodule crust of Mn, Fe hydroxides. *3.* Sediments of Fe content 10.00—20.00% (including ore accumulations). *4.* Sediments of Fe content 5.00—10.00%. *5.* Sediments of Fe content less 5.00%. *6.* Borders of sediment distribution with the given gradation of Fe content.

Silt-clayey muds are the preponderant sediments developed on a greater part of the lake. These are dark-green, greyish-green, seldom black muds enriched in a fine-dispersed sapropel-like organic matter. Above they are, as a rule, covered by reddish-brown watery mud (0.5—5 cm) in the composition of which there prevail suspended particles of ferric hydroxides; down the column, green-grey muds (about 25—50 cm) are replaced by black varieties. The total thickness of muds in the central part of

the lake is over 3 m. The clay components of these sediments are presented by extremely degraded minerals from the group of montmorillonite, chlorite, biotite-vermiculite and their mixed-layered intergrowths. In other words, the composition of clastic and clayey components of these muds indicate a certain composition of initial rocks the products of which were subjected to intense leaching and decomposition.

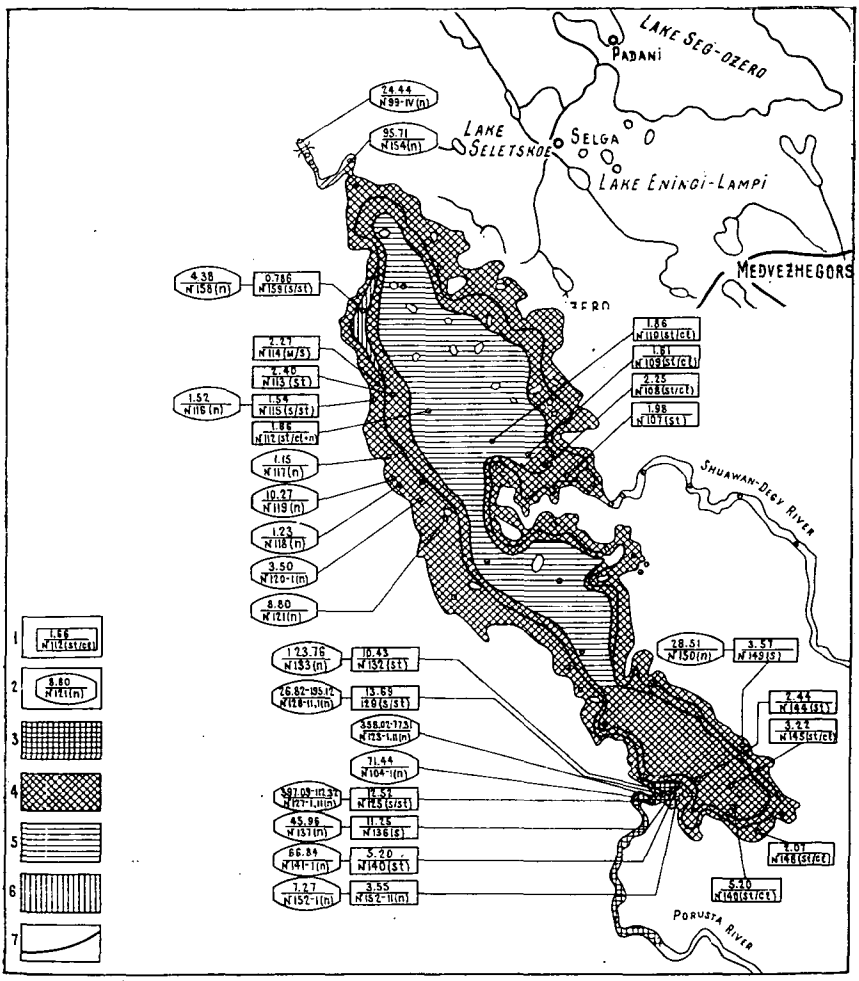

Fig. 5. Schematic map of ratio $\frac{Mn}{Fe}$ (n×100) distribution in sediments, Eningi-Lampi Lake. *1.* Stations where samples of sediments recovered. *2.* Stations where samples of nodules and crusts of Mn, Fe hydroxides recovered. The numerator — value of ratio $\frac{Mn}{Fe}$ (n×100); the denominator — number of sample, in brackets — sediment type: *S* — sand, *st* — silt, *s/cl* — silty clay, *n* — nodule, crust of Mn, Fe hydroxides. Gradational values of ration $\frac{Mn}{Fe}$ (n×100) in sediments. *3.* $\frac{Mn}{Fe}$ (n×100) over 10.000. *4.* $\frac{Mn}{Fe}$ (n×100):2.00—10.00. *5.* $\frac{Mn}{Fe}$ (n×100) 1.00—2.00. *6.* $\frac{Mn}{Fe}$ (n×100) lesser 1.00. *7.* Borders of sediment distribution with the given gradation of ratio $\frac{Mn}{Fe}$ (n×100).

In the Northern (North. dep.) and Southern depressions (South. dep) of the lake these muds considerably differ in their chemical composition (weight percentage, in brackets — the mean, *m:* mean for these sediments of the lake),

Fe: South dep. 12.12—16.87 (14.37); North dep. 6.07—20.35 (14.46); *m:* 14.45.

Mn: South dep. 0.35—0.40 (0.38); North dep. 0.12—0.38 (0.26); *m:* 0.31.

P: South dep. 0.10—0.31 (0.23); North dep. 0.18—0.32 (0.22); *m:* 0.22.

CO_2: South dep. nil-0.54 (0.33); North dep. 0.24—0.84 (0.54); *m:* 0.46.

C_{org}: South dep. 10.03—12.93 (11.98); North dep. 4.74—20.68 (12.41) *m:* 12.24.

$\frac{Mn}{Fe}$ $(n \times 10^2)$; *m:* South dep. 2.64; North. dep. 1.79.

The data cited show that variations of Mn and Fe contents in the lake sediments *(fig. 4,5)* are subjected to a relatively well-pronounced tendency: with the moving from the Porusta river, the main source of ore components, via the southern depression towards the northern one of the lake, Mn concentrations considerably decrease, whereas Fe concentrations, on the contrary, increase. This can be rather clearly seen in $\frac{Mn}{Fe}$ ratio $(n \times 10^2)$ for silt-clayey sapropel-like muds: southern (2.64) and northern (1.79) depressions *(fig. 5, 6, 7, 8)*.

In sandy-silt deposits and silt-clayey sapropel-like muds of the lake the amounts of trace elements $(n \times 10^{-4}\%)$ have been determined by a spectral method (I. YU. LUBCHENKO, A. I. GUSAREVA, GIN of the USSR Academy of Sciences): V 8—33; Cr 5—42; Ni 5—21; Co 5—31; Cu 5—10; Pb 2—12; Ge < 1—10; Mo 1.0—10.0; Ga 3—14 (Table 3). The relationships of some of these elements and the main components of a sediment are not always subjected to well-pronounced regularities. The following associations can be established concerning the character of the positive correlation of these elements: Fe — C_{org} — CO_2 — P ---------- Mn; V — Cr — C_{org}; Mn — Ni — Co — C_{org} ---------- Fe (the dashed line denoted a weak correlation). Such elements as Cu, Pb, Mo fall to form any pronounced association.

IRON-MANGANESE NODULES, CRUSTS

The Eningi-Lampi lake is characterized by a wide development of Fe—Mn accumulations presented by nodules, crust-shaped hydroxide formation of these metals. Despite comparatively small extensions of this basin there can be observed a clear diversity of nodular types, crusts differing in mode of occurrence, morphology, structure, composition and areal localization.

Mode of occurrence. Fe—Mn nodules and crusts are found, as a rule, in the areas of sedimentation of coarse-clastic deposits of gravelly—pebbly sands—coarse silts *(fig. 3,4)*. Almost always do they laying on the ground-water interface. Less frequently they can be observed in a thin (1—5 cm) watery layer of the reddish-brown mud covering greenish-grey, dark silty-clayey muds with rather high amount C_{org} (up to 13.00%) *(fig. 8.)*. In these muds, as well as in sapropel-like varieties almost no nodules were found. Only in the marginal parts of the zone of silt-clayey sapropel-like muds, in the uppermost 5—7 cm of a sediment were observed sporadic (roughly 0.1% from the volume of a sediment) microconcretions (1—3 mm) of iron hydroxides. These microconcretions are relics that were temporarily preserved when a sediment was passing to more reducing conditions, as such muds rich in organic matter were being accumulated.

TABLE 3

Fe, Mn, CO_2, C_{org}, V, Cr, Ni, Co, Cu, Pb, Ge, Mo, Ga
*content in the sediments, the Lake Eningi-Lampi**)

№	Sample №	CONTENT												
		(wt) %				p.p.m								
		Fe	Mn	CO_2	C_{org}	V	Cr	Ni	Co	Cu	Pb	Ge	Mo	Ga
1	107	6,07	0,12	0,24	8,69	30	42	21	31	5	6	2,0	1,1	12
2	108	9,77	0,22	0,34	20,68	24	34	11	12	5	2	<2,0	1,0	6
3	109	16,72	0,27	0,58	17,79	17	24	10	11	5	2	<1,0	1,0	3
4	110	20,35	0,38	0,84	4,74	32	25	10	20	5	3	<1,0	2,4	4
5	113	6,66	0,16	0,36	5,50	14	16	6	8	5	4	<1,0	1,2	4
6	114	2,20	0,05	nil	1,15	15	18	5	5	9	4	<1,0	1,0	5
7	126	4,00	0,40	0,26	5,86	33	42	14	12	10	4	<1,0	2,1	14
8	130	3,25	0,07	0,08	6,24	26	23	9	8	5	4	<1,0	1,8	11
9	146	14,43	0,40	0,54	12,93	31	41	16	26	5	3	<1,0	2,0	9
10	148	16,87	0,35	0,44	12,96	44	41	16	19	5	3	<1,0	2,5	8
11	149	11,99	0,43	nil	1,09	16	8	5	11	5	6	<1,0	5,8	11
12	159a	16,54	0,13	—	—	8	5	5	8	5	12	10,0	10,0	3

1. The mud dark green, brownish, sandy fine-grained with plant detritus. Sample No. 107, Shuavan-Degi River, 200 m, upstream from the mouth.

2. The mud dark green with thin (10 mm) cover of brown watery mud, silty-clayey, with considerable content of sapropel-like material. Sample No. 108. Open part of Shuavan-Degi River estuary.

3. The mud greenish-brown, silty-clayey with considerable content of sapropel-like material. Sample No. 109, see *fig. 4,5.*

4. The mud dark-green with brown-olive tint, sandy-clayey, covered by characteristic brown watery mud. Sample No. 110. Middle part of Northern depression of the lake; see *fig. 4,5.*

5. The mud greenish-brown, sandy with prominent content of sapropel-like material. Sample No. 113, see *fig. 4,5.*

6. The mud greenish-brown, sandy with small nodules of Mn, Fe hydroxides, oftenly growing around the clastic grains. Sample No. 114, see *fig. 4,5.*

7. The mud dark-olive, clayey with abundant plant remnants, Sample No. 126, Porusta River, 200 m upstream from the mouth, see *fig. 4,5.*

8. The mud dark green, sandy, silty with plant detritus. Sample No. 130, mouth of Porusta-River, the middle part, *see fig. 4,5.*

9. The mud dark green silty-clayey with prominent amounts of sapropel-like material. Sample No. 146, *see fig. 4,5.*

10. The mud dark, silty-clayey covered by characteristic thin (to 1 cm) layer of brown watery mud, and containing substantial amount of sapropel-like material. Sample No. 148, see *fig. 4,5.*

11. The sand greenish-gray, gravely with nodules of Fe—Mn hydroxides. Sample No. 149, see *fig. 4,5.*

12. The relatively dense peat-like mass, composed by grass vegetations, contains penny-like nodules of Fe, Mn hydroxides. Sample No. 159a, see *fig. 4,5.*

*) Determinations were done by using the spectral analysis, I. YUR. LUBCHENKO, A. I. GUSAREVA, Mn, Fe, CO_2, C_{org} were determined by R. M. MICHAILOVA, V. P. SIMONOVA; Geol. Inst. Ac. Sci. USSR.

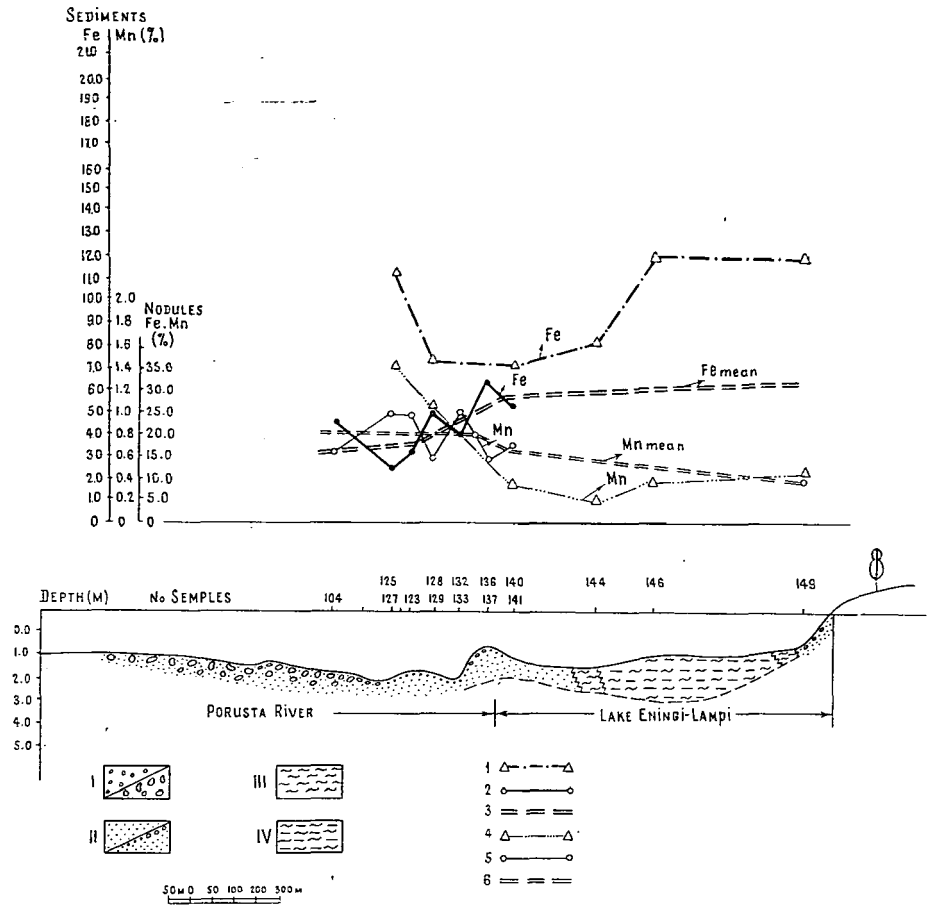

Fig. 6. Distribution of Fe, Mn concentrations in sediments, nodules and crusts from Porusta River across the Southern basin of the Lake Eningi-Lampi. I. a) Gravel-pebbly sediments with boulders, the fragments of volcanic metabasites predominated. b) The same as "a" but with coatings and crusts of Fe, Mn hydroxides. II. a) Coarse-medium-grained greywacke sands;, b) The same as "a" but with nodules and crusts of Fe, Mn hydroxides. III. Greywacke sands fine-grained — silts coarse-medium-grained. IV. Fine-grained silty, clayey sapropel-like muds, dark, greenish-gray. Content (wt.%): 1) Fe in sediments; 2) Fe in nodules, 3) Fe in nodules, mean values, 4) Mn in sediments, 5) Mn in nodules, 6) Mn in nodules, mean values.

Morphology. Nodules and crusts of Fe and Mn hydroxides can be regarded as different morphologically but uniform relative to their genetic essence of formation. They are presented by growths of Fe and Mn hydroxides on active surfaces. Detrital particles playing the role of a nucleus around which a gradual growth of Fe and Mn hydroxides is proceeding, may serve as such surfaces for the nodules.

Crusts and crust-shaped formations are coatings of Fe and Mn hydroxides on relatively large surfaces of boulder fragments, the rock walls etc.

The following morphological types of nodules and crusts can be distinguished in the basin concerned:

1. Irregular rounded nodules sized 1—3 to 70, average 15—30 mm. Frequently such nodules remind small book shots and beans.

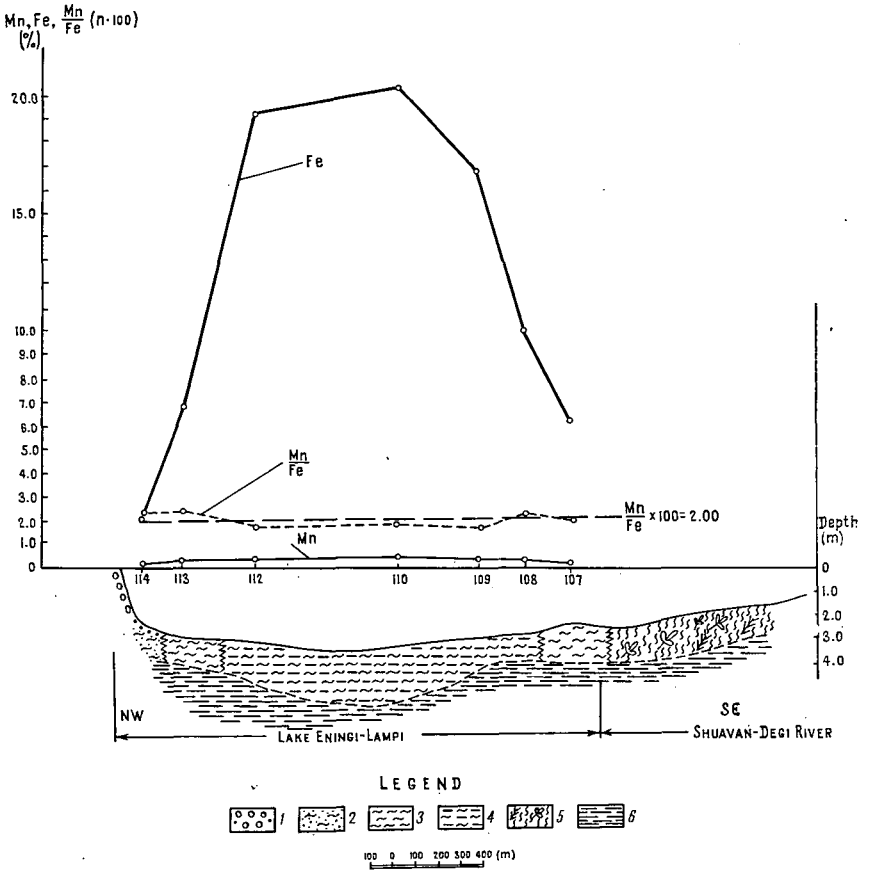

Fig. 7. Distribution of Fe, Mn (wt.%) and ratios $\frac{Mn}{Fe}$ (n×100) in sediments across the Northern basin of the Lake Eningi-Lampi from Shuavan-Degi River. *1.* Gravel-pebbly sediments with boulders, the fragments mainly of volkanic metabasites. *2.* Greywacke silty sands. *3.* Greywacke silts. *4.* Fine-grained silty-clayey sapropel-like muds. *5.* Sandy-silty peat-like accumulations, essentially enriched by plant detritus. *6.* Country rocks- glacial pale-gray clays.

2. Accretions of bean nodules forming aggregates and crusts up to 15—50 mm thick and sized 30—70 cm. Such accretions can be found in the areas of intense development of nodules (mouth-estuary of the Porusta river).

3. Penny-shaped and discoidal nodules that are elongated in the plane concentric overgrowths of clastic particles. Sizes: 3×25×25 up to 10×60×80 mm.

4. Overgrowths with Mn and Fe hydroxides in the shape of thin coatings, crusts on rock fragments, boulders, prominences of shore outcrops near the water line. Their thickness is from a quota (pigmentation of the surface-) to 30—50 mm.

Structure and composition. It has been said above that nodules and crusts are overgrowth of Fe and Mn hydroxides on the active surfaces. It follows from the field observations and microscopic study of thin sections that such coatings usually occur on an altered, corroded surface that plays the role of an activized basis. The

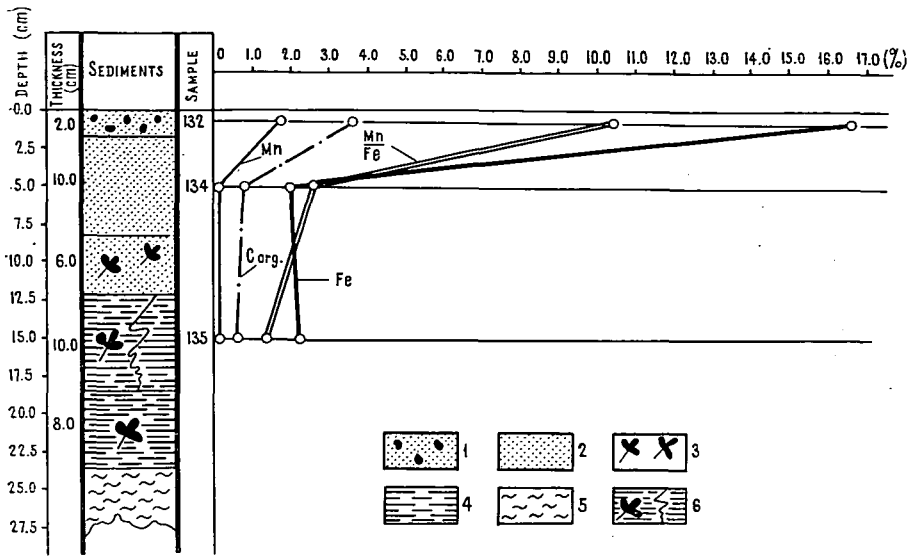

Fig. 8. Distribution of Mn, Fe, C_{org} (wt.%) and $\frac{Mn}{Fe}$ (n×100) in the column of sediments (cm) (station 2b, mouth part of estuary of Porusta-River). *1.* Sand greenish-olive coarse-grained with gravel particles covered by brown watery mud. Upper 2 cm of the sand are essentially enriched in nodules of Mn, Fe hydroxides. *2.* Sand greenish-olive coarse-grained with coalified detritus. *3.* Coalified plant detritus. *4.* Mud dark, almost black, sapropellike enriched by coalified plant detritus. *5.* Gray silt. *6.* Lateral substitution of black mud by greenish-gray varieties.

latter in the most cases is overgrown with the thinnest (0.01—0.5 mm) coating of Fe hydroxides. Then, this hydroxidic ferrugineous coating, depending on the composition of interacting solutions, pH, Eh values, can be overgrown with Mn or Fe hydroxides, or their complex mixture *(fig. 9)*.

In some cases (the mouth, estuary of the Porusta river) in thin sections of the nodules there can be observed patches and/or concentric layers of chlorite-like substance that is isotropic to a considerable degree, but clearly crystallized into aggregates of needle-shaped and tabular crystalls (up to 0.01 mm) on the contact of Fe and Mn hydroxides. Rather sporadic are patches of ferrugineous carbonates in hydrogoethitic parts of the nodules. These authigenic newly-formed minerals are considered as the later relative to hydroxidic phases of nodules.

Table 4 and 5 present the composition of the nodules and crusts concerned *(fig. 10)*. The study carried out enable to distinguish the following types:

1. Properly manganese that are predominantly composed of birnessite with an admixture of Fe hydroxides. The Mn content is up to 33%, that of Fe up to 8—10%;

Fig. 9a. 1. The quarzite pebble coated by Fe—Mn hydroxides, thickness to 1—3 mm. Similar pebbles, boulders, coated by Fe—Mn hydroxides occur on the bottom of the channel, connected the Lakes Eningi-Lampi and Seletskoe Ozero (see *figs. 4,5*), sample No. 99. *2.* Shot-like nodules of Mn, Fe hydroxides (see Table 4, *figs. 4,5*), sample No. 133. Mouth of Porusta-River. *3.* The pebble of altered basic volcanite coated by Fe, Mn hydroxides. Bottom view. The upper part of the pebble, rising above the water-sediment interface is covered by black Fe—Mn hydroxides, thickness to 25—40 mm. The lower part of the pebble is free of Fe—Mn hydroxide coatings. Sample No. 156, Northwestern part of the lake.

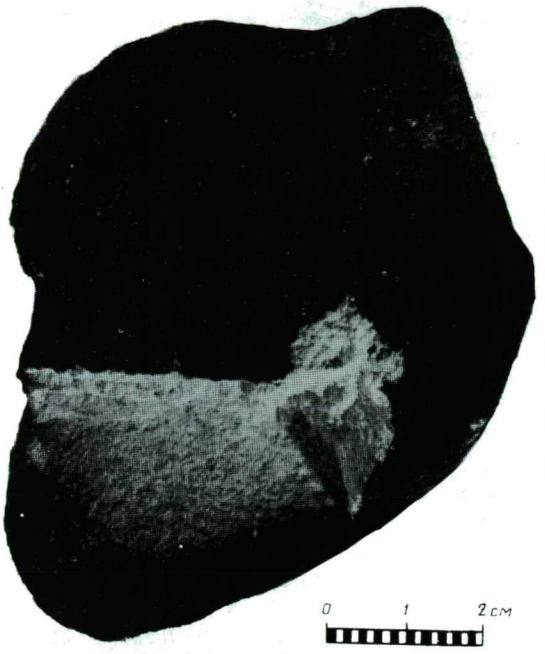

1

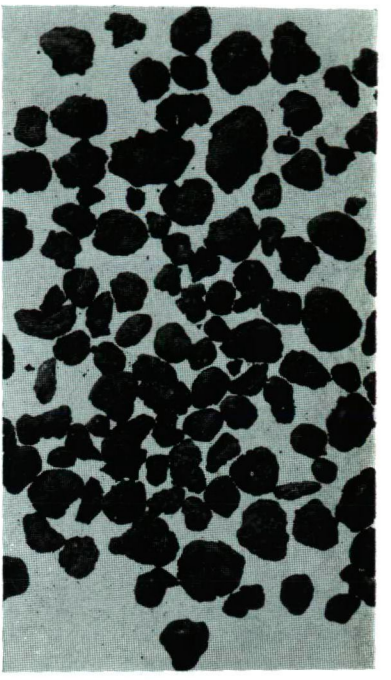

2

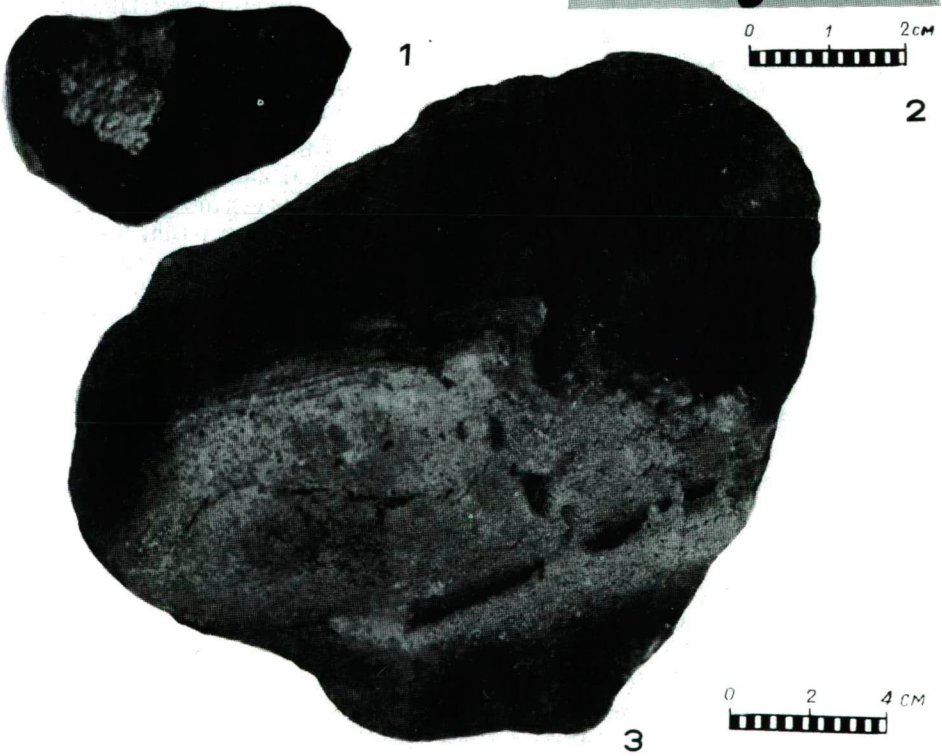

3

$\frac{Mn}{Fe}$ (n. 100)=330−413. The Mn hydroxides are associated with Co, n. 10^{-4}% (120−180), Zn (104−402); Ba 0(1.27—2.15%).

2. Properly ferrugineous presented by X-amorphous Fe hydroxides, hydrogoethite, goethite, lepidocrocite, Fe up to 51%, Mn−2%, $\frac{Mn}{Fe}$(n · 100)=3.92. Fe hydroxides are associated with (n · 10^{-4}%); Ni (5−40); Cu (3—13); C_{org} 0.85−1.80%, CO_2 1.44− 3.46%.

3. Nodules and crusts of an intermediate, Fe—Mn composition mostly widedeveloped. Worth attention is that the terrigenous components of ores are associated with V (nil−34) and Cr (nil−4), (n · 10^{-4}%) *(fig. 10,11)*.

Localization and lateral changes. Sufficient accumulations of Fe and Mn nodules and crusts in the Eningi-Lampi lake are formed in the areas where the rates of their formations considerably exceed those of terrigenous sedimentation. These phenomena are most clearly seen in the places of a rather intense water currents, and, on the contrary, can not be observed in the areas where, in accordance with hydrodynamic conditions, there takes place an increase of accumulation of fine-grained sediments enriched in organic matter. Thus, in the course of the Porusta river, in its estuary and delta an intense development of Fe and Mn nodules and crusts can be observed. The sediments associated with Fe and Mn formations are presented by gravelly and pebbly sands *(figs. 3, 5, 6, 7)*. The amount of Fe and Mn nodules in the estuary-delta of the river reaches 50—80% of the sediment mass. A wide development of crusts, and to a lesser extent nodules, has been observed in a shallow (up to 2.5 m) stream of a relatively rapid current connecting the Eningi-Lampi lake with the Seletskoe Ozero one. Bottom sediments in this case are also presented by pebbles, gravel and sand. Within the lake the Fe and Mn nodules develop among sandy coarse-silty sediments framing this basin along the periphery *(figs. 3, 4, 5)*.

Fe and Mn nodules of the lake are characterized by a regularly lateral changing of composition, from the source of ore components to the relatively far remoted areas of their accumulation. When following the lateral alteration of Mn and Fe amounts (see *figs. 7, 8, 9)* in nodules and crusts through its estuary and the Southern part, towards its North-Eastern shore and then the Northern basin, one may pay attention that the Mn-content in this direction decreases significantly, whereas that of Fe increases. Approximately the same pattern of distribution was observed before when reviewing the behaviour of these elements in the waters and sediments of the lake *(figs. 4, 5, 6, 7)*.

/ TION OF Fe AND Mn ORES IN THE ENINGI-LAMPI LAKE

Both all the above observations, and the data of experimental studies may serve as a basis for considerations on the formation processes of Fe and Mn ores. It should be emphasized that the nodules and crusts of Fe and Mn hydroxides are

---

Fig. 9b. Photomicrographs. *1.* The core of the nodule — the gravel fragment of quarzite, covered by Fe—Mn hydroxides, around which is developed the mixture of Fe—Mn hydroxides and patches of chlorite-like mineral. Sample No. 133-IV. Polarized light, x14 (see Table 4, *figs. 4,5,* 9a/2). *2.* The core of the nodule — the gravel fragment of quarzite, around which grown alternating concentric sayers of Fe, Mn hydroxides (black) and the mixture of Fe, Mn hydroxides with patches of chlorite-like mineral. Sample No. 133-V. Polarized light, x10 (see photo 1). *3.* Gravel fragment of arkose landstone, grown over by Fe, Mn hydroxides. Sample No. 104-II. Polarized light, x15, (see Table 5, *fig. 4,5*). *4.* Corrosive nature of contact of quartz and feldspathic grains, forming the core (fragmented part of photo 3) with the growing on Fe, Mn hydroxides. Plane light, x 100.

1

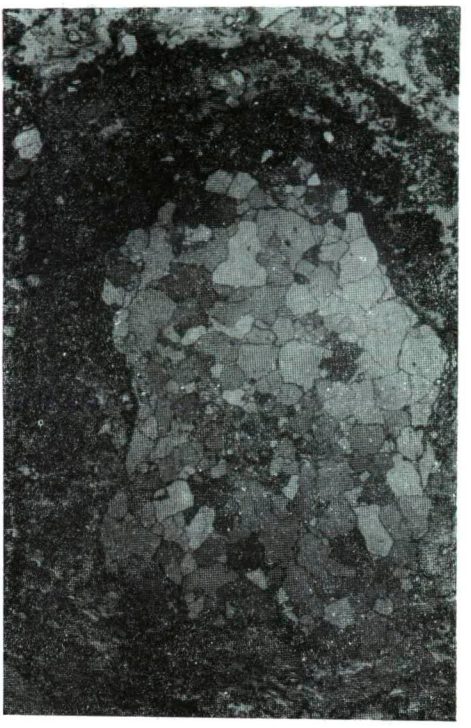

2

3

4

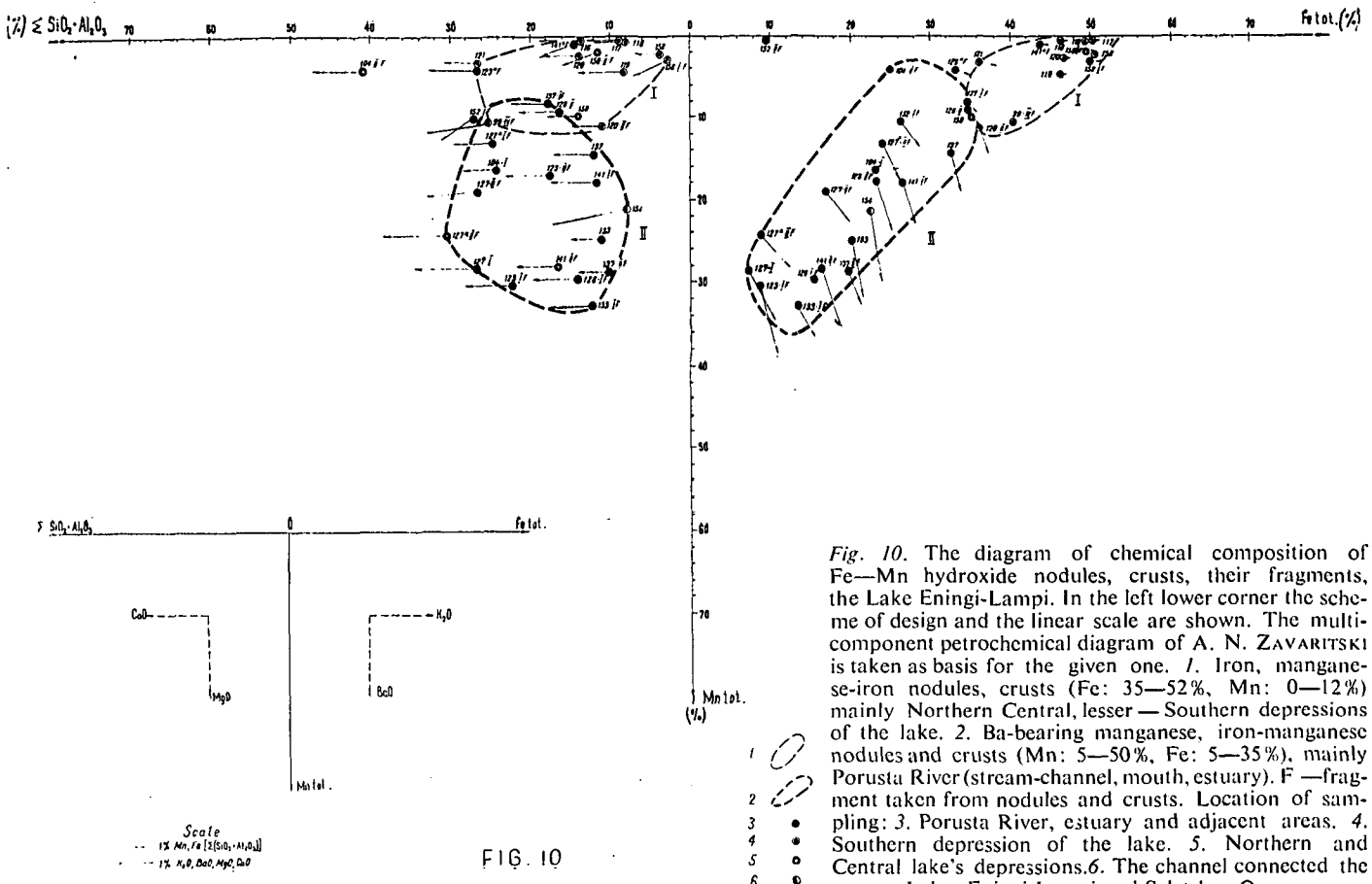

FIG. 10

Fig. 10. The diagram of chemical composition of Fe—Mn hydroxide nodules, crusts, their fragments, the Lake Eningi-Lampi. In the left lower corner the scheme of design and the linear scale are shown. The multicomponent petrochemical diagram of A. N. ZAVARITSKI is taken as basis for the given one. *1.* Iron, manganese-iron nodules, crusts (Fe: 35—52%, Mn: 0—12%) mainly Northern Central, lesser — Southern depressions of the lake. *2.* Ba-bearing manganese, iron-manganese nodules and crusts (Mn: 5—50%, Fe: 5—35%), mainly Porusta River (stream-channel, mouth, estuary). F —fragment taken from nodules and crusts. Location of sampling: *3.* Porusta River, estuary and adjacent areas. *4.* Southern depression of the lake. *5.* Northern and Central lake's depressions. *6.* The channel connected the Lakes Eningi-Lampi and Seletskoe Ozero.

V, Cr, Zn, Cu, Ni, Co, Pb *content and general composition of nodules, crusts and their fragments, the Lake Eningi-Lampi*[*)]

TABLE 4

№	Sample №	CONTENT (p.p.m) V	Cr	Zn	Cu	Ni	Co	Pb	(Wt %) SiO_2	TiO_2	Al_2O_3	Fe_2O_3	FeO	CaO	MgO	MnO	MnO_2	P_2O_5	Na_2O	K_2O	H_2O^+	H_2O^-	CO_2	C_{org}	BaO	Sum	Fe_{tot}	Mn_{tot}	$\frac{Mn}{Fe}(n \cdot 10^2)$
1	133	nil	3	127	3	8	60	8	8,19	0,75	3,25	28,64	nil	1,00	nil	7,20	30,40	TR	0,34	0,34	4,83	9,62	3,46	1,12	1,70	100,84	20,03	24,79	123,76
2	133—I	nil	nil	154	4	8	120	3	8,39	0,23	3,00	18,56	0,52	1,32	0,24	6,80	43,66	nil	0,42	0,52	4,76	8,49	2,46	0,54	0,90	100,81	13,38	32,86	245,59
3	137—I	II	4	104	5	10	120	4	16,71	1,08	1,23	48,84	0,93	1,21	nil	3,69	8,86	0,01	0,51	0,31	4,49	8,92	1,96	1,80	0,20	100,75	34,88	8,46	24,25
4	137—II	TR	4	131	2	7	180	3	8,21	0,73	2,04	28,05	nil	1,00	0,08	7,11	36,60	TR	0,34	0,40	5,52	7,97	1,44	0,62	0,95	100,76	19,62	28,64	145,97
5	141—I	nil	nil	146	3	5	130	3	10,46	1,08	1,24	37,23	0,64	1,42	nil	4,15	23,00	TR	0,47	0,36	5,00	9,58	3,00	1,66	1,27	100,36	26,54	17,74	66,84
6	141—II	9	nil	208	2	1	150	3	13,39	0,73	3,24	20,66	nil	1,32	nil	5,82	37,62	nil	0,77	0,59	4,34	8,05	1,78	0,60	1,70	100,61	16,06	28,28	176,09
7	150	nil	4	175	4	20	60	—	10,95	1,08	3,00	49,84	0,50	1,21	nil	3,01	12,22	0,005	0,51	0,36	6,08	8,23	1,82	1,39	0,39	100,58	35,25	10,05	28,51
8	154	34	4	402	13	41	60	5	7,48	0,24	0,44	31,98	nil	2,37	0,49	1,93	31,53	0,01	0,23	0,34	10,25	7,24	3,22	0,85	2,15	100,75	22,37	21,41	95,71

1. Bean-like nodules, the interior part is composed by black hydroxides of manganese (birnessite), the external crust — by X-ray amorphous iron hydroxides. Sample No. 133, see *fig. 10,11.*

2. The material composing the interior part of bean-like nodules; the main phase — birnessite, X-ray amorphous iron hydroxides. Sample No. 133-I, see *fig. 10,11.*

3. The brown hydroxides composing the external crust of the nodules. The main phase — goethite, minor one — birnessite, admixture of clastic quarz and feldspars. Sample No. 137-I, see *fig. 10,11.*

4. The black earthy substance of nodules, presented by birnessite and goethite. Sample No. 137-II, see *fig. 10,11.*

5. Small nodules (1—10 mm), their interior part composed mainly by birnessite, the external crust — by goethite. Sample No. 141-I, see *fig. 10,11.*

6. Black hydroxides composing the interior part of nodules, the main phase-birnessite, the minor one — X-ray amorphous iron hydroxides. Sample No. 141-II (see sample No. 141-I, *fig. 10,11*).

7. The small nodules, irregularly rounded (2—20 mm), crust-like coatings of pebbles; their bottom part composed by iron hydroxides, the interior part — by manganese hydroxides. In the sample predominate goethite, minor phase — birnessite. Sample No. 150, see *fig. 10,11.*

8. Manganese, iron hydroxides coating as thin crust pebbles, boulders, the surfaces of the country rocks near the water edge. The main phase — birnessite, the minor one — X-ray amorphous iron hydroxides. Sample No. 154, see *fig. 10,11.*

*) V, Cr, Cu, Ni, Co determined by colorimetric methods, Zn — by polarographic one with preliminary chromatographic separation. The total silicate analysis was done by E. V. SHURIGINA, M. G. SEMENOVA in the chemical laboratory, headed by E. S. SALMANSON; Geol. Inst. Acad. Sci. USSR

Chemical composition of iron-manganese nodules and crusts, the Lake Eningi-Lampi

TABLE 5

№	Sample №	Depth (m)	Depth downward from the sediment's surface (cm)	CONTENT (wt %)																	$\frac{Mn}{Fe}$ (n·10²)
				SiO_2	TiO_2	Al_2O_3	Fe_2O_3	FeO	CaO	MgO	MnO	MnO_2	P_2O_5	Na_2O	K_2O	H_2O^+	H_2O^-	CO_2	C_{org}	BaO	Sum	
1.	104—1	0—3	0	20,04	0,50	4,17	32,01	0,03	1,02	nil	1,22	24,56	TR	1,12	0,73	6,53	4,08	2,32	0,62	—	99,76	71,44
2.	104—2	0—3	0	35,62	0,87	5,36	30,12	0,74	1,53	nil	0,82	5,51	0,10	2,30	0,98	6,70	2,52	1,10	0,65	—	99,90	16,35
3.	116	1,80	0—3	11,83	0,20	1,99	63,14	2,61	1,36	nil	0,91	nil	0,19	0,41	0,22	9,72	3,64	0,70	2,65	—	99,75	1,52
4.	118	2,20	0—5	7,17	1,00	2,08	68,60	2,21	1,02	nil	0,79	nil	0,80	0,32	0,12	11,23	2,36	0,56	1,68	—	99,96	1,23
5.	119	1,90	0—3	7,04	0,50	1,26	64,00	1,68	1,47	nil	1,71	5,59	0,07	0,20	0,14	8,83	4,64	1,36	1,90	—	100,19	10,27
6.	121	2,00	0—3	22,06	0,12	4,38	51,39	0,42	1,14	nil	1,66	2,91	0,03	1,44	0,56	6,75	4,12	1,16	1,44	0,03	99,61	8,80
7.	123—I	2,70	0—3	18,69	0,15	3,62	12,13	nil	1,48	0,08	4,86	42,10	nil	0,84	0,62	5,86	5,11	1,72	0,96	2,07	100,29	358,02
8.	123—II.	2,70	0—3	17,03	0,16	0,57	33,16	0,50	1,37	0,08	5,24	22,43	0,01	0,68	0,48	5,54	5,52	4,04	1,57	1,38	99,76	77,31
9.	123[a]	2,70	0—3	24,67	0,16	1,92	46,58	0,64	1,54	0,08	3,87	1,60	0,19	1,09	0,47	6,62	4,96	2,56	2,38	0,15	99,48	12,12
10.	127—I	3,10	0—2	23,23	0,15	3,57	10,10	0,28	1,94	nil	4,35	40,04	nil	1,24	0,79	5,06	4,88	2,32	0,46	1,47	99,88	397,09
11.	127—II	3,10	0—2	25,24	0,15	1,45	23,93	0,28	1,54	0,12	3,76	25,55	nil	1,09	0,73	5,39	5,40	3,42	0,94	0,87	99,86	112,32
12.	133	2,20	0	2,64	0,25	1,06	72,00	0,41	0,78	0,05	1,56	1,60	0,04	0,15	0,09	11,17	4,51	1,10	2,20	S=0,11	99,72	4,38

1. The reddish-brown manganese-iron hydroxides growing around the clastic sandy-gravel grains. According to X-ray analysis, the main phase — goethite, the minor one — birnessite. Sample No. 104-I. *Analyst:* G. V. MOTUSOVA.

2. The substance composing the external parts of the nodules — presented by enlongated crystalline grains with metallic lustre. According to X-ray analysis — the main phase — goethite. Sample No. 104-II. *Analyst:* G. V. MOTUSOVA.

3. The reddish-brown iron hydroxides, composing small pennylike nodules. Sample No. 116. *Analyst:* G. V. MOTUSOVA.

4. The small (2—20, m. 3 mm) rounded, penny-like nodules, composed by intimate intergrowth of iron hydroxides with manganese hydroxides. Sample No. 118. *Analyst:* G. V. MOTUSOVA.

5. The crust-like growths around the clastic gravel grains, penny-like nodules composed by iron hydroxides with admixture of manganese hydroxides. Sample No. 119. *Analyst:* G. V. MOTUSOVA.

6. The small nodules (2—5 mm), their external part composed by reddish-brown iron hydroxides, the core — black manganese hydroxides. Sample No. 121. *Analyst:* M. I. STEPANETS.

7. The black earthy manganese hydroxides, presenting the general mass of the small (2—20 mm) nodules irregularly round-shaped. The main phase, according to X-ray analysis, — birnessite. Sample No. 123-I. *Analyst:* M. I. STEPANETS.

8. The crusts of reddish-brown iron hydroxides mixed with manganese hydroxides, composing the outer part of small (2—20 mm) irregularly round-shaped nodules, Sample No. 123-II. *Analyst:* M. I. STEPANETS.

9. The reddish-brown iron hydroxides with small admixture of manganese hydroxides; separated from the small (2—20 mm) irregularly round-shaped nodules. Sample No. 123a. *Analyst:* M. I. STEPANETS.

10. The black manganese hydroxides, separated from the small (m. 10—15 mm) nodules irregularly-rounded with granulose surface. The bottom part of the nodule composed by iron hydroxides. The main upper part of it, contacting considerably with bottom water consists of black, earthy manganese hydroxides. Sample No. 127-I. *Analyst:* M. I. STEPANETS.

11. The reddish-brown hydroxide of iron and manganese (see the sample No. 127—I). According to X-ray analysis, the main phases — birnessite and β-Fe_2O_3.

12. The relatively large bean-like nodules. Their inner part composed by birnessite, the outer one — by X-ray amorphous hydroxides of iron. Sample No. 133. *Analyst:* G. V. MOTUSOVA.

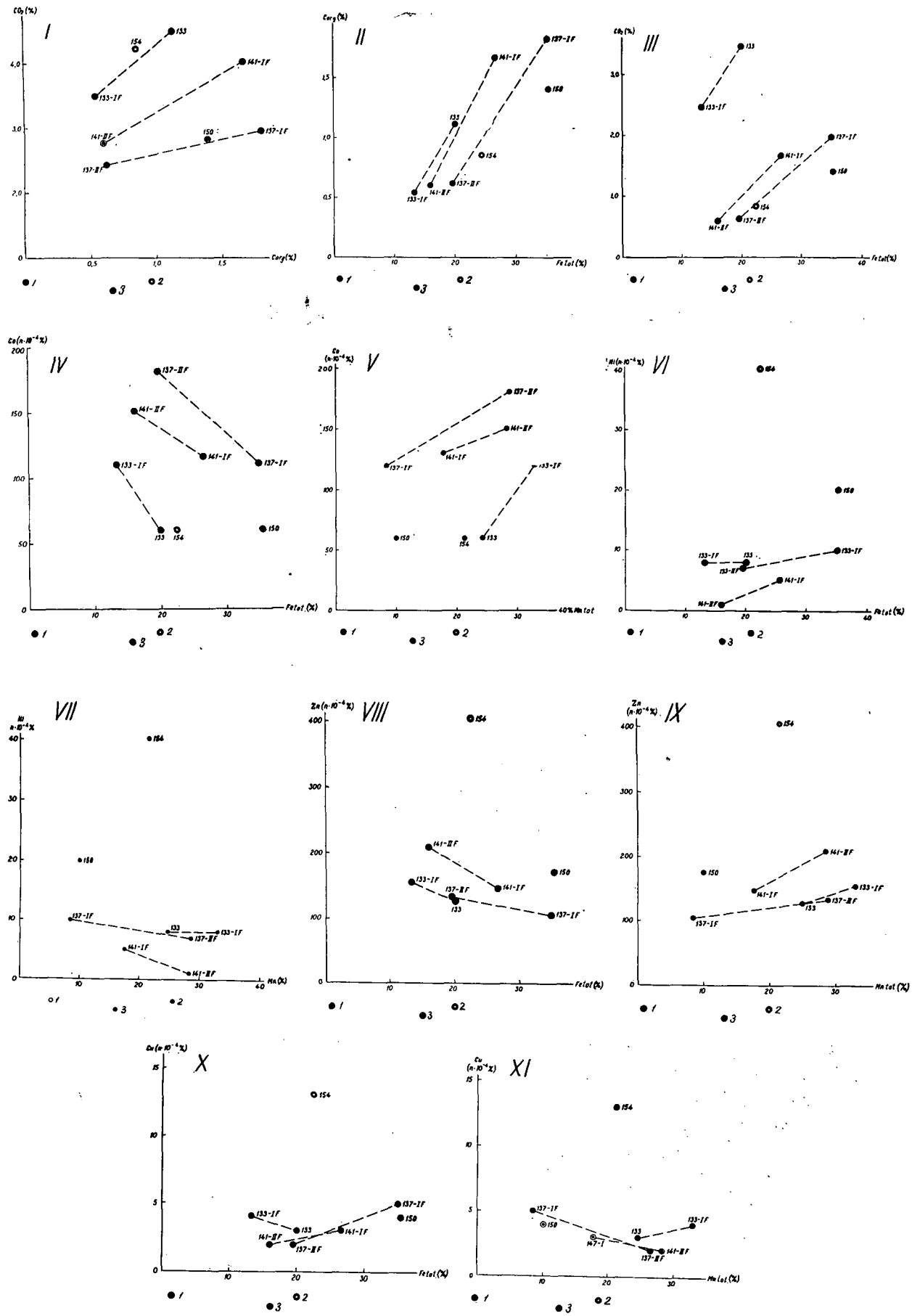

Fig. 11. The relationships between main components and the minor ones in fragments and the phases of Fe—Mn hydroxide nodules, crusts, the Lake Eningi-Lampi (see Table 4). I. The relationships C_{org} and CO_2. *1.* Porusta-River (the stream-channel, mouth, estuary); *2.* Northern and Central depressions of the lake. *3.* Southern depression of the lake. II. The relationships Fe_{tot} and C_{org}, for the legend see No. I. III. The relationships Fe_{tot} and CO_2. IV. The relationships Fe_{tot} and Co. V. The relationships Mn_{tot} and Co. VI. The relationships Fe_{tot} and Ni. VII. The relationships Mn_{tot} and Ni. VIII. The relationships Fe_{tot} and Zn. IX. The relationships Mn_{tot} and Zn. X. The relationships Fe_{tot} and Cu. XI. The relationships Mn_{tot} and Cu.

regarded as coatings and growths on active surfaces. They occur at the ground-water interface, and considerably less frequently — in the upper part (0—5 cm) of brown semi-liquid watery mud. In interacting waters the Mn (up to 98%) and Fe (up to 48%) are present in a dissolved form — mainly as organic complexes (humic, fulvo-acids, etc). As a result of such interaction, the formation of oxide Mn and Fe phases and associated metals takes place on the active surfaces. An analysis of observations, results of our experimental studies [VARENTSOV, 1970] and the data of some authors [MORGAN, STUMM, 1964; STUMM, STUMM—ZOLLINGER 1968; MICHARD 1969] allow to consider this process as very selective, chemosorption accumulation with autocatalytic oxidation. The reactional products formed in the course of this interaction promote the new acts and cycles of the process, causing its autocatalytic character. In other words, newly formed phases of Mn, Fe hydroxides promote the new acts of the process, playing the role of active sorbents. As a matter of fact, the process of such chemosorption autocatalytic accumulation of some transitional metals: Mn, Fe, Ni, Co can be lasted for geologically long time, when the interaction with the solutions of a wide concentration range ($10^{-2}-10^{6}$ ppb) of these constituents take place.

The similar mechanism of formations may be used for explanation of the observed compositional variations of the Mn, Fe hydroxide nodules and crusts. The manganese, presented almost in a soluble form, removed from solution not far from the source (Porusta river). The considerable amounts of iron, presenting in particulated form, were accumulated in the zone of fine-grained muds enriched by C_{org}. After the deposition, at the decay of Fe-bearing suspended material the Fe compounds moved by upward diffusion in bottom waters [SEMENOVITCH, 1960], and then transfered to the areas of nodules, crusts accumulation, where one can observe relatively higher values of pH, Eh.

ACKNOWLEGMENTS

Discussions with Professors P. P. TIMOFEEV, P. E. OFFMAN, K. K. ZELENOV, I. V. CHVOROVA, nd D. G. SAPOZHNIKOV have been helpful. The author is grateful to E. A. STRAVINSKAIA, V. P. TEPANOV for the assistance in field work. N. I. KARTOSHKINA helped in laboratory preparations, . V. SOKOLOVA made the X-ray analyses.

REFERENCES

ICHARD, GIL. [1969]: Dépôt de traces de manganèse par oxidation. „Comptes Rendus Acad. Sci.", Paris, t. *264*, (12 novemb. 1969), Ser. D, pp. 1811—1814.

MORGAN, J. J., STUMM, W. [1964]: The role of multivalent metal oxides in limnological transformations as examplified by iron and manganese. In: "Second Internat. Conf. on Water Pollution Res.," Sect. I, No 6, Nippon Toshi Center, Tokyo.

SEMENOVITCH, N. M. [1960]: Investigation of chemical exchange between the bottom and the water mass of the lake. In "Lakes of Central part of Karelian Isthmus", Transact. of Limnological Laborat., Academy Sci., USSR, v. *XI*, Publish. Acad. Sci. USSR, Moscow-Leningrad.

STUMM, W., and STUMM—ZOLLINGER, E. [1968]: Chemische Processe in Natürlichen Gewässern. "Chimia", Zürich, *22*, No 8, 325—337.

VARENTSOV, I. M. [1970]: The processes of formation of iron-manganese nodules in the Lakes of Central Karelia. In: "Concretions and Concretionary Analysis", Leningrad, pp. 104—106.

Manuscript received, May 20, 1972.

DR. IGOR M. VARENTSOV
Geological Institute of the Academy of Sciences of USSR
Pyzhevsky pereulok 7,
Moscow Zh-17, USSR

Acta Mineralogica-Petrographica, Szeged, XX/2, 383—391, 1972.

LETTERS OF THE COMMISSION ON MANGANESE (IAGOD)

REPORT ON THE TECHNICAL SESSIONS OF THE WORKING GROUP ON MANGANESE FORMATION, MONTREAL, CANADA

August 23 and 25, 1972.

JOHN VAN N. DORR II.
Vice-President

The Working Group for Manganese Formation (now the Commission on Manganese) held two sessions at which scientific papers were presented during the XXIV International Geological Congress at Montreal, Canada. In addition, after the business meeting on August 24, a 45 minute program on the exploration for, mining of, and extraction of metallic values from deepsea manganiferous nodules was presented by Messers. RAYMOND KAUFMAN and ROYAL HAGGERTY of Deepsea Venture, Inc. Attendance at the scientific sessions was over 50 persons at each session. The sessions were chaired by JOHN VAN N. DORR II, at the request of PROF. GYULA GRASSELLY, our President.

Twelve papers were scheduled but three authors were unable to attend the Congress and thus only 9 papers were presented.

On August 23, PROF. GRASSELLY of Attila József University, Szeged, Hungary presented the first paper, entitled *Thermal stability and oxidation of Mn_3O_4 in the presence of other manganese oxides.* The paper is printed elsewhere in this volume.

The second paper was presented by DRS. R. K. CORMICK, D. A. CRERAR, and H. L. BARNES of Pennsylvania State University USA, entitled *Geochemical controls on manganese distribution in amphibolite-grade metamorphic rocks,* and is printed elsewhere in this volume.

This paper was followed by a paper by PROF. RONALD K. SOREM of Washington State University, Pullman, Washington, USA, on *Mineral recognition and nomenclature in marine manganese nodules.* PROFESSOR SOREM's abstract follows:

> In the literature of the past twenty years or more there is much confusion concerning the primary oxide minerals in marine manganese nodules. Most mineral identifications have been based upon X-ray diffraction powder data and have unfortunately been hampered by poor sampling, poor patterns, and non-uniform nomenclature. Difficulties have also arisen because of the lack of agreement on the nature and distribution of amorphous oxide material in nodules. The net result has been general lack of effective communication between many persons who have serious and similar interests in the problems of the character and origin of manganese nodules. It would appear that an attempt to set this mineralogical house in order is long overdue.
>
> The following specific causes of confusion should be considered.
>
> 1. Most nodule samples used for X-ray diffraction have been impure mixtures.
> 2. Most X-ray samples have been altered by grinding.
> 3. Most nodule materials are poorly crystalline or amorphous and give diffuse X-ray patterns under even the best conditions.

4. Crystalline nodule materials have simple structures which permit ionic substitution, so *d*-spacings are somewhat variable for any one mineral.
5. Preferred orientation is common and affects X-ray patterns strongly.
6. The weak and diffuse X-ray patterns commonly obtained are difficult to compare with reference patterns published in tabular form.
7. Identification problems have led to erroneous nomenclature, where names for synthetic compounds (e.g., 10 Å -manganite) have been introduced for minerals (e.g. todorokite) already properly named.
8. Optical properties and textural relationships of minerals have been essentially ignored.

Four years of concentrated research on manganese nodules and the results of many years of mineralogical work on manganese ores prompt the following suggestions to improve the present situation.

1. Standard X-ray diffraction patterns of common supergene manganese minerals like birnessite, todorokite, rancieite, cryptomelane, and nsutite should be published and exchanged between research labs.
2. Standard X-ray samples should be chemically analyzed.
3. To avoid analysis of mixtures, all sampling for X-ray diffraction should be controlled by optical study of good quality polished sections.
4. All sampling of nodule materials for X-ray diffraction should be restricted to selective scratching or chipping of optically homogeneous areas. Grinding should be avoided to insure sharpest possible diffraction lines. Samples large enough for diffractometer slide mounts are rarely monomineralic and may show preferred orientation. The same problems occur in capillary tube samples. A thin fiber mount is best.
5. Electron probe analyses should be correlated wherewer possible with optical data and should represent X-ray microsamples.
6. Valid new minerals, if they are found, should be properly characterized by X-ray, chemical, and optical data, and given names approved by nomenclature organizations.

It seems likely that most nodule mineralogical research is undertaken to aid in solving the general problems of nodule origin and history of growth. It is therefore suggested that wherever possible the data gathered be presented in a manner which will clearly show the relationship of the samples studied to the entire nodule under investigation. This can be done conveniently by using a photomacrograph of an entire nodule cross-section, preferably obtained with vertical illumination similar to that of the ore microscope, as a map on which data can be plotted.

DR. ALLAN R. FOSTER, also of Washington State University, then gave a paper on the *Growth history of manganese nodules from the Baja California Seamount Province*, the abstract of which follows:

Study of 46 manganese nodules collected from 9 separate dredge hauls 370 km southwest of Baja California, Mexico, has provided new insight into the processes controlling nodule formation. Detailed studies of polished nodule cross-sections, using ore microscopy, XRD, and XRF macroprobe techniques reveal intricate internal structures and systematic chemical and mineralogical variations.

Nodule growth is attributed to discontinuous accretion of thin, opaque, crystalline or X-ray amorphous shells about a central core (commonly a nodule frag-

ment). Crystalline laminae composed of intimate intergrowths of cryptocrystalline todorokite and birnessite are much less abundant than X-ray amorphous shells but are of special interest because they contain the greatest concentrations of Ni, Cu, and Mn. Textural and mineralogical evidence suggests a colloidal origin for both types of shell material.

Five distinctive textural patterns called zones are recognized in the sequences of shells. Zones are designated massive, mottled, compact, columnar, and laminated and differ in composition, texture and homogeneity. The massive and mottle zones contain the highest concentrations of Mn, Cu, Ni, and K, while the columnar, laminated and compact zones contain the greatest concentrations of Fe, Ti, Ca, and Si. The mottled and columnar zones are the most abundant.

Each zone type evidently forms during a period characterized by a relatively stable and unique sea-floor environment. Most nodules show a succession of zone types indicating that major environmental changes took place during growth. Minor textural differences between nodules suggests that local fluctuations in the depositional environment occurred. Environmental factors involved probably include fluctuations in Eh, pH, ion concentration of the sea-water and substrate pore water and the relationship of each nodule to the sea-floor sediment-water interface.

Ocean bottom photographs indicate that opposite sides of a nodule are exposed to different depositional environments; namely, the sea-floor sediment and the ocean bottom water. Textural evidence indicates that nodule growth occurs on both sides of the interface and that certain zone types are formed in each environment. Formation in contact with the sediment is suggested for the mottled, columnar and laminated zones. The massive and compact zones are thought to grow in the sea-water environment. For a given period of time, greatest thicknesses of nodule material appear to accumulate on the side of the nodule exposed to the sediment.

Many concentric growth shells appear to have undergone "diagenetic" changes after burial under succeeding layers. The "diagenetic" processes involved are:

1. filling of porespace with Mn—Fe-rich oxides.
2. replacement of clay and foreign inclusions by Mn—Fe-rich oxides.
3. minor replacement reactions between different species of opaque, X-ray amorphous materials.
4. replacement of fossil tests by todorokite and birnessite.
5. recrystallization of oxide material, especially in older portions of a nodule.

The rate and extent of these "diagenetic" changes is probably enhanced by the great porosity and permeability of the nodules.

Physical forces affect nodule development as well. Periodic overturn of nodules is indicated by zonal sequences displaying alternating zone types characteristic of different depositional environments. Movement may result from the activity of benthonic organisms, water or bottom movement, imbalance and toppling due to irregular growth, or other unknown forces. Abrupt interruptions of nodule growth, as recorded by nodule fragment cores, indicate past episodes of nodule shattering. Textural evidence suggests that internal forces cause nodule breakage.

This study of whole nodule textural and chemical relationships reveals that nodule formation is a much more complex process than most investigators have indicated. Discrete nodule growth shells, if treated as stratigraphic units, reveal

a detailed history of nodule growth. If present estimates of rate of nodule accretion are correct, the nodules studied display a record of environmental changes on or near the sea floor during the past several million years.

The final paper of the session was by DR. RONALD H. FEWKES, also of Washington State University, on *Conglomerate manganese nodules from the Drake Passage,* the abstract of which follows.

Marine manganese nodules from the Drake Passage area formed in an environment characterized by abundant terrestrially derived detritus. A textural study of twelve polished nodule sections reveals complex growth relationships between the detritus and the oxide minerals found in the nodules. Nodule growth can be attributed to the accumulation of clastic material, iron and manganese oxides, and microscopic fragment-rimmed pods.

The incorporation of detrital material in Drake Passage nodules is an important mechanism of growth. The size of the individual fragments varies, but it is estimated that at least 80 percent are less than 100 microns. The fraction less than 100 microns is composed of detrital quartz and feldspar with a scattering of other minerals and organic debris. The other 20 percent of the detrital material is made up of rounded rock fragments as large as one centimeter in diameter. Typical Drake Passage nodules consist of a rock core surrounded by accumulations of angular clastic debris, with a matrix or cement of iron and manganese oxides. The contact between the individual fragments and the oxides is sharp and distinct. Where several large rock fragments are found in the interior of the nodules, the oxides appear as distinct layers only on the side of the fragments away from the nodule core. Fragments on the outer edges of the nodules are generally enclosed by oxides, but many have prominent oxide accumulations on their exterior sides, with the thickest oxide layers concentrated around the sharpest points of the fragments. Where detrital material is minimal, oxide minerals occur in colloform layers which in some nodules form columnlike structures. These structures consist of alternating bright (highly reflecting) and dark laminae. The highly reflecting layers contain chiefly oxide minerals while the darker layers are detritusrich. Nodules with an abundance of detrital material or an abundance of microscopic fragment-rimmed pods have few well-developed columnar structures.

The microscopic pods found in the nodules are roughly circular in form and consist of a nucleus surrounded by angular clastic fragments. The nucleus is very fine-grained and non-opaque and has the appearance of clay. The surrounding fragments are detrital quartz or devitrified glass shards. Pod diameter is generally less than 200 microns. The origin of these pods remains a mystery but possible organic and inorganic modes of origin are suggested.

The textural features of Drake Passage nodules may be characteristic of nodule growth in an environment where abundant wind, water, and ice transported material is accumulating. The contrast with nodules of the open ocean where low sedimentation rates prevail is striking.

The first paper of the August 25 session was by DR. IGOR M. VARENTSOV of Geological Institute, Academy of Sciences, Moscow, USSR, our Secretary, and N. V. PRONINA of the same Institution. The result of experiments on *The study of sorption by natural iron-manganese oxides from seawater in the presence of complex-forming compounds* was reported.

Highly selective sorption of Ni and Co was observed. In the runs with biogenic

forms of these metals, after 20 days as much as 77.8 percent Ni was removed from the seawater and complete extraction of Co took place. The range of concentration of these metals in solution was 10 to 100 ppb. The character of isotherms of the Ni and Co sorption from seawater in the presence of complex-forming agents citric acid give evidence that, even at the high amounts of sorbed metals (10 to 40 weight percent), there is no tendency for reaching the limits of sorption capacity.

The experiments on desorption showed that the initial stages of the process are of ion-exchange character, mainly for Ni, to a lesser extent for Co. In the later stages, the formation of nonexchangeable, firmly fixed forms of Co and Ni takes place. These forms are hydroxides of Ni and Co. Chemosorption plays the leading role, with an autocatalytic oxidation process of accumulation of these metals. The newly formed phases act in the future cycles of interactions as active sorbents.

This paper was followed by one by DR. D. A. CRERAR, R. K. CORMICK, and H. L. BARNES of Pennsylvania State University, USA, on *Organic controls on the sedimentary geochemistry of manganese,* printed elsewhere in this volume.

An interesting newly discovered and very large deposit of manganese carbonate in Mexico, the *Molango manganese deposit, Hidalgo, Mexico,* was described by INGS. E. TAVERA and R. ALEXANDRI, with ING. ALEXANDRI delivering the paper.

These manganese deposits are in the Upper Jurassic Taman formation, and the manganiferous limestone ranges from 5 to 30 percent Mn over a thickness of about 25 meters, with the higher values concentrated in a range of 5 to 10 meters near the base of the unit. The manganiferous limestone has been traced in outcrop over an area some 50 km in north-south extension and 25 km in east-west direction. It is included in a thick sequence of Lower Permian and Mesozoic sedimentary rocks that unconformably overlies a Precambrian metamorphic complex and is unconformably overlain by Tertiary basalts. The area is in the southern part of the Sierra Madre Oriental and occurs within one of the major anticlinal structures of that range.

The syngenetic manganese deposits are primary manganese carbonates amenable to calcination, producing a clinker containing over 40 percent Mn. The manganese occurs as kutnahorite and rhodochrosite, which are distributed in thin bands rhymically distributed in the manganiferous unit. Pyrite and organic carbon also are found in this portion of the Taman Formation, as well as clay bands. The manganese was deposited in a transgressive and strongly reducing marine environment.

It has been calculated that, although at least half the manganiferous zone of the Taman Formation has been removed by erosion, the remaining part contains about 1,350 million tons of manganese metal. Much of this is in rock now too low grade to be economically extractable, but the concentration of manganese is, from a geologic viewpoint, noteworthy. No apparent source for this quantity of manganese is now known and it must be presumed that the metal was derived by the weathering of continental rocks and transported to the depositional area by surface waters. No contemporary volcanic action in the region, either submarine or terrestrial, is known.

Epigenetic deposits of manganese oxide, some of battery grade, were formed by weathering of the syngenetic carbonate and are also being exploited. Owing to

the extreme relief in the area and the consequent rapid erosion, these are small and pockety, being controlled by topographic and structural features which permitted local accumulation of the weathering products.

The final paper on the scientific program was *Manganese deposits of South Korea,* presented by PROF. SOO JIN KIM. The paper is printed elsewhere in this volume.

REPORT ON THE BUSINESS MEETING OF THE WORKING GROUP ON MANGANESE FORMATION (NOW COMMISSION ON MANGANESE)

August 24, Montreal, Canada

DR. JOHN VAN N. DORR II
Vice-President

DR. I. M. VARENTSOV
Secretary

PROF. DR. GY. GRASSELLY
President

The technical session and a business meeting of the Working Group on Manganese Formation were held in conjunction with the XXIV International Geological Congress. The business session was held August 24 and was followed by a 45 minute presentation on prospecting for and exploiting deep sea manganese nodules by officers of Deepsea Ventures, Inc. The technical sessions and the business meeting were chaired by Vice-President DR. JOHN VAN N. DORR II at the request of PROF. GRASSELLY and were attended by more than 50 geologists. About 20 persons attended the business meeting.

The business meeting was addressed by PROF. GRASSELLY, President, on the history of the WGMF. DR. VARENTSOV, Secretary, discussed results of past activity and the present situation of the WGMF. Both emphasized the necessity for fuller cooperation from country representatives and for fuller representation from the rest of the world.

Till now the following countries are represented in the WGMF: Bulgaria, Czechoslovakia, Hungary, India, Japan, Korea, Romania, Soviet Union, United Arab Republic, United States of America, Yugoslavia. DR. LOUIS DOYEN of Belgium (Louis Doyen, Licencié en Sciences Géologiques et Minéralogiques, Assistant a l'Université, 14—18, Rue des Pavots, Bruxelles 3, Belgium), DR. HUBERT PÉLISSONNIER (Professeur a l'École des Mines, 60 Boulevard Saint-Michel, Paris VI, France), PROF. EVARISTO RIBEIRO FILHO (Geologo, Professor Livre Docente, Instituto de Geociências, Universidade de São Paulo, Depto. de Geologia Econômica, Rua Iraci, 590, 01457, São Paulo, Brazil) agreed to serve as national representatives for their countries. DR. HANSJUST W. WALTHER, Wissenschaftlicher Direktor in der Bundesanstalt für Bodenforschung (3 Hannover-Buchholz, Alfred-Bentz-Haus, FRG) and ING. GEOL. RAFAEL ALEXANDRI R. (Sociedad Exploradora Minera, S. A. de C. V., Viena 4, 3er piso, Mexico 6, D. F., Mexico) promised that in the near future they will give personal proposals for reprezentation of the Federal Republic Germany and Mexico, respectively. Naturally, it would be successful to have national representatives for Australia, Cuba, China, Ghana, Indonesia, Morocco, Pakistan, South Africa, too. The WGMF will request the Geological Surveys of these countries to propose proper experts to fullfil this duty.

A change in the name and status of the Working Group on Manganese Formation to Commission on Manganese was proposed and approved. The Council of IAGOD was requested to approve this change, which was done on August 25.

The next technical sessions and business meeting of the Commission on Manganese will be held during the IAGOD Symposium in Varna, Bulgaria, in 1974 and the dates September 19—21 were selected. About 20 technical papers are hoped for in the first and last of these dates and the agenda for the business meeting on September 20 was discussed and approved. The agenda of the business meeting: *a)* Report on the activity of the Commission on Manganese; *b)* Preparation of the International Symposium on Manganese at the XXV IGC, 1976, Australia and discussion of the progress made in the last two years; *c)* Election of officers of the Commission on Manganese for four-year period according to the IAGOD Statutes.

The Commission on Manganese (former Working Group on Manganese Formation), an affiliate of IAGOD, has as its purpose the promotion of international cooperation in advancing knowledge of this essential element to our civilization. To this end, *it is proposed that a symposium be organized as part of the XXV International Geological Congress to be held in 1976.*

The proposed symposium will try to assemble in one publication our present knowledge on the geochemistry, mineralogy, geologic associations, occurrence, and distribution of manganese in earth's crust and oceans. During the last two decades, powerful new tools have extended scientific knowledge of the habits of manganese, great new deposits have been found and developed, much new and important information has been secured on previously known deposits, the potential of the sea floor nodules recognized. An updating of the excellent Symposium on Manganese held at the XX IGC in Mexico, 1956, will be of great benefit to the profession and to society. The symposium hopes to illuminate the relation between scientific investigation and practical development.

The general organization of the XX IGC Symposium would be followed. General papers, as outlined below, will be invited on the broader aspects of manganese geology, investigation, and resources. Individual countries, through their Geological Surveys or other appropriate agencies, will be invited to contribute papers on the occurrence and resources of manganese within their borders. These will be grouped by continents and, if appropriate, a summary by continents prepared. *At the Congress itself, the general papers will be presented; there would not be time for presentation of all the detailed papers on individual countries. These, with the general papers, would be published in a multivolume monograph, in English.*

The proposed general organization of the symposium is as follows:

I GENERAL PROBLEMS

a) Classification of manganese deposits
b) Patterns of distribution of manganese in the earth's crust in space and time. Relation to tectonic plates
c) Problems of manganese mineralogy
d) Problems of manganese geochemistry
e) Manganese ore deposition in recent basins
f) Microbiological aspects of manganese ore deposition
g) Problems of beneficiation of manganese ores

II PHYSICAL AND CHEMICAL METHODS OF INVESTIGATION OF MANGANESE ORES

Review of modern methods of chemical and physical analysis of solids as applied to manganese ores

III GEOLOGY OF MANGANESE DEPOSITS

a) Western Hemisphere
b) Africa.
c) Europe, including the USSR
d) Asia
e) Australia and Oceania
f) Ocean basins, lakes, and mediterranean seas

In order to give coherence to the papers on the manganese deposits in individual countries, the following outline is suggested to contributors to Section III.

1. Name, geographical and climatological relations, short statement on general geology as significant to manganese deposition.
2. History of production, with grade and tonnage broken down, if appropriate, by districts and major deposits.
3. Types of deposits represented in the country, with relative importance, grades, and productivity.
4. Geology of major deposits or districts, with particular attention to primary, metamorphic, and supergene mineralogy; structural and stratigraphic relations; wall rocks and wall rock alteration, age, and metamorphic grade; analyses of ores and protores and wall rocks, including minor and trace elements; ore controls; present and, if known, past climatic regimes; physiographic setting; depth and effects of weathering and supergene action; environment of sedimentation (if sedimentary), deduced temperature environment and associated metals (if hydrothermal), nature of and relations with associated volcanic rocks (if volcanogene); relations, if any, with iron-formation; sources of manganese in the deposits. (Geologic maps and sections as appropriate.)
5. Reserves, with estimated tonnage and grade in as much detail as seems appropriate. Identified resources.
6. Possibility of undiscovered reserves and resources.
7. Mining and beneficiation methods used (short and general).
8. Special problems relating to manganese mining in the country.

Most of the papers on individual countries could be short and succinct because few countries possess large reserves of manganese ores. In the case of countries such as Australia, the USSR, South Africa, Brazil and some others with very large or newly developed reserves, more extended papers would be justified and needed. Emphasis on new information and facts would be requested, with special attention to possibilities opened by modern technology in transport, beneficiation, and mining.

The Symposium on Manganese published by the XX IGC in 1956 consisted of five volumes totaling about 1600 pages. This was large type and small pages. Using smaller type and perhaps larger pages, the proposed publication might involve approximate the same number of pages or possibly a relative small percentage more.

We hope that all countries interested in manganese research will contribute. The focus of the IIIrd section of the symposium should be on new information.

Concerning *the preparation of the monograph* on manganese on a world-wide basis, with the suggested structure, among myriad others, two principal problems are now paramount: *1)* to identify an active group of contributors to cover the indicated subjects; *2)* to secure backing for the publication of such a large enterprise.

The effectively attack problem 1, the cooperation not only of individuals but of Governmental, University, and private organizations throughout the world will be essential. Various suggestions, many very constructive, were made to solve problem 2, but no decisions were reached. These suggestions will be explored in the immediate future and any solution found will be announced as soon as possible.

The basic outlines of the proposed symposium as prepared by the officers of the Commission on Manganese follow; suggestions as to improvment or modifications or deletions would be greatly appreciated. Correspondence on this subject should be addressed to Prof. Grasselly or to the other officers as convenient.

DR. I. M. VARENTSOV
Secretary
Geological Institute of the Academy
of Sci. of USSR
Pyzhevsky pereulok 7,
Moscow Zh-17, USSR

DR. JOHN VAN N. DORR II
Vice-President
US Geological Survey, Washington,
D. C. 20242, USA

PROF. DR. GY. GRASSELLY
President
Inst. of Mineralogy, Geochemistry
and Petrography,
University of Szeged
Táncsics M. u. 2., Szeged, Hungary

CONTENTS